

https://dspace.org/

Sedimentology and taphonomy of a tetrapod fossil accumulation in the Triassic Burgersdorp Formation of the Karoo Basin

Wolvaardt, Frederik Petrus

2021

https://hdl.handle.net/10539/33141

Downloaded from a DSpace repository. https://dspace.org/



SEDIMENTOLOGY AND TAPHONOMY OF A TETRAPOD FOSSIL ACCUMULATION IN THE TRIASSIC BURGERSDORP FORMATION OF THE KAROO BASIN

Dr Frederik Petrus Wolvaardt
ORCID Number: 0000-0001-8117-558X

A dissertation submitted to the Faculty of Science, University of the Witwatersrand, Johannesburg, in fulfilment of the requirements for the degree of Master of Science.

Cape Town, 2021

DECLARATION

I declare that this dissertation is my own, unaided work. It is being submitted for the Degree of Master of Science at the University of the Witwatersrand, Johannesburg. It has not been submitted before for any degree or examination at any other University.



F. P. Wolvaardt

On this 12th day of August 2021 at Cape Town.

ABSTRACT

Field investigations of a rare accumulation of tetrapod fossils in the Triassic Burgersdorp Formation of the Karoo Basin reveal the palaeoenvironmental and behavioural mechanisms that led to its genesis. A total of 140 skulls and skeletons of seven tetrapod taxa and samples of three burrow cast geometries were collected with details of their depositional environment setting. These data are interpreted and integrated to reconstruct the palaeoenvironment and taphonomic pathways leading to accumulation, burial and preservation of this anomalous occurrence. The sedimentological facies analysis reveals a high sinuosity meandering river and floodplain setting. A semi-arid climate, with seasonal rainfall caused periodic rise and fall of the water table and floodplain ponds. Herbivorous tetrapods dominated by procolophonids, with dentitions adapted to browse fibrous reedbeds, congregated around pond margins. The animals scratch-burrowed in the floodplain surface for thermo-regulation and possibly estivation. Combined physical and behavioural factors caused the higher-than-average probability of tetrapod death, burial and preservation at this site.

In memory of the two people who introduced me to the wonderful world of fossils.

My father
George Sebastiaan Wolvaardt

1938 to 2012

and world-renowned fossil-finder

James William Kitching
1922 to 2003.

ACKNOWLEDGEMENTS

During the course of this study, I have become deeply indebted to many individuals. My gratitude is therefore extended to the following persons and Institutes for their hospitality and help in various ways:

To my supervisors Prof. Roger Smith and Prof. John Hancox for their many inputs, enthusiasm, support, critical counsel and encouragement during this work. I am particularly grateful to have been part of Prof. Smith's Karoo field team since 2003 and his continuous motivation for me to become a palaeontologist. During these field trips I learned a great deal about palaeontology. Prof. Bruce Rubidge is thanked for his support of this project. I am indebted to the late Prof. James Kitching for first pointing out the Lemoenfontein locality to me in 1976.

To my friend Dr Michael Strong for the many hours of debate about rocks and fossils during field trips to the Karoo.

To Mr André van der Walt of the farm Lemoenfontein for permission to work on the farm over many years and his interest in fossils.

To numerous colleagues and members of staff at the Evolutionary Studies Institute at University of the Witwatersrand. To the Iziko South African Museum for curating, preparing and providing access to the Lemoenfontein fossil collection. I am grateful for the many hours of laboratory and field work support from Ms Claire Browning and her interest in the project. I would also like to thank Ms Zaituna Skosan, Ms Tiffany-Lea Van Zyl and Mr Sibusiso Mtungata for the excellent preparation of the Lemoenfontein fossils and for making access to the collection possible.

To my sister Léta for hosting my field camps on the family farm, Gladde Grond, and my brother Wimpie for always being on the lookout for new fossil localities. To my mother Alta for being the *de facto* curator of the initial Lemoenfontein fossils until 2003. Last but not least, to my wife Jessie and my children Laura and Luca, for giving up many potential family holidays while I was camping in the Karoo.

TABLE OF CONTENTS

1. INTRODUCTION 1

1.1 Hypotheses tested 4

1.2 Objectives 4

1.3 Aims 5

1.4 Dissertation overview 6

2. MATERIALS AND METHODS 10

2.1 Field Based Observations 10

2.2 Laboratory and collections-based data capture 11

2.3 Analyses 12

3. SEDIMENTOLOGY AND LITHOSTRATIGRAPHY OF LEMOENFONTEIN 16

3.1 Overview of the lithostratigraphy of the main Karoo Basin 16

3.2 Lemoenfontein fossil site: geological setting 19

3.3 Basis for facies sequence description 23

3.4 Description of the Lemoenfontein facies sequences 29

Cycle 0 29

Cycle 1 30

Cycle 2 32

Cycle 3 32

Cycle 4 33

Cycle 5 34

Cycle 6 35

Cycle 7 35

Cycle 8 36

Bamboesberg Member 36

3.5 Detailed description and interpretation of the bonebed interval of Cycles 0 and 1 39

3.6 Interpretation of depositional environment 63

4. BURROW CAST ICHNOLOGY OF LEMOENFONTEIN 66

4.1 Background information on Triassic burrow casts 66

4.2 Lemoenfontein burrow casts 71

4.3 Reniform burrow casts 73

Reniform burrow architecture 73
Surficial morphology of reniform burrow casts 75
Reniform burrow fills 76
4.4 Lemoenfontein sub-circular burrow casts 76
Sub-circular burrow architecture 76
Surficial morphology of sub-circular burrow casts 77
Burrow fill 79
4.5 Qualitative analysis of Lemoenfontein burrow casts 81
4.6 Reniform burrow discussion 85
4.7 Sub-circular burrow discussion 90
4.8 Potential burrow-makers 92
Lemoenfontein reniform burrow trace makers 92
Lemoenfontein sub-circular burrow trace makers 98
Palaeoenvironmental significance of crayfish burrows 102
4.9 Putative *Langbergia* burrow cast and its biostratigraphic significance 104
5. CREVASSE SPLAY SURFACE ICHNOLOGY OF LEMOENFONTEIN 108
5.1 General description 108
5.2 Current crescents 110
5.3 Scratch-digging traces 115
5.4 *Scoyenia* ichnofacies 122
5.5 Sequence of deposition and trace events 123
6. VERTEBRATE TAPHONOMY OF LEMOENFONTEIN 125
6.1 Literature review of studies relevant to the taphonomic analysis of the Lemoenfontein bonebed 125
6.2 Lemoenfontein: Spatial and stratigraphic distribution of fossil bones 130
6.3 Lemoenfontein: Taphonomic analysis of fossil bones 132
Taphonomic data recorded 132
Lemoenfontein Taphonomic classes 132
Physical characteristics descriptors 133
Interpretation descriptors 134
Perimineralisation and nodule formation 137

6.4 Taphonomy of tetrapod fossils in Gully 1 139
Teratophon SAM-PK-K10174 (Field number 117) 139
Teratophon SAM-PK-K011599 (Field number L18-2) 140
Teratophon Field number L18-1 147
Teratophon Field number L19-1 147
Teratophon Field number L20-10 148
Procolophonid SAM-PK-K10171 150
6.5 Taphonomy of tetrapod fossils in Bonebed 1: 150
Taphonomic Group 1: Isolated skull with articulated lower jaw 151
Taphonomic Group 2: Articulated skeletons encased in nodules that take the shape of the carcass 152
Taphonomic Group 3: Articulated skeletons curled up in a 3-D spiral, encased in nodules 156
Taphonomic Group 4: Isolated skulls and articulated postcranial elements SAM-PK-10201 (Field numbers 122 A/B, and L19-2 to L19-8) 157
6.6 Taphonomy of tetrapod fossils in Gullies 2 and 3: 160
Trirachodon SAM-PK-K10163 (Field number 98) 160
6.7 Taphonomic insights 162
7. VERTEBRATE PALAEONTOLOGY OF LEMOENFONTEIN 169
7.1 Overview of the *Cynognathus* AZ biostratigraphy 169
Lower *Cynognathus* AZ (*Langbergia-Garjainia* Subzone) (Olenekian) 170
Middle *Cynognathus* AZ (*Trirachodon-Kannemeyeria* Subzone) (Early Anisian) 170
Uppermost *Cynognathus* AZ (*Cricodon-Ufudocyclops* Subzone) (Late Anisian) 171
7.2 Systematics of the Lemoenfontein fauna 173
7.3 Discussion of the Lemoenfontein fauna 189
8. LEMOENFONTEIN PALAEOENVIRONMENTAL RECONSTRUCTION AND THE ORIGIN OF BONE ACCUMULATION 193
8.1 Overview of bonebed definition, classification, and genesis. 193
8.2 Triassic Karoo Bone Accumulations 198
Literature review of studies relevant to the sedimentologic and taphonomic analyses of the Lemoenfontein bone accumulation. 198
8.3 Lemoenfontein fossil accumulation 203

8.4 Reconstruction of the once living *Cynognathus* AZ *T-K* Subzone ecosystem 205
Sedimentological interpretations 205
Crevasse splay sole surface interpretations 205
Burrow cast interpretations 206
Taphonomic interpretation of the bone accumulation 207
Faunal community interpretations 208
Palaeoenvironmental reconstruction 209
8.5 Origin of bone accumulations at Lemoenfontein 213
8.6 Comparison to other bone accumulations in the Triassic strata of the Karoo Basin 216
8.7 Comparison to the Lifua Member of Tanzania and the Santa Maria Formation of Brazil 218
9. CONCLUSIONS 220
REFERENCES 223
APPENDIX A: LITHOSTRATIGRAPHIC LOG 246
A.1 Legend 246
A.2 Lithostratigraphic log 247
APPENDIX B: TETRAPOD FOSSIL DATABASE 252
APPENDIX C: BURROW CAST DATA 263

LIST OF FIGURES

Figure 3.1:	Geographic location of the Lemoenfontein bone accumulation site.	21
Figure 3.2:	Google Earth Image of the locality and the measured section. The Lemoenfontein hill is in the foreground. This section crosses eight ledge forming sandstones each of which represents the base of a fining-upward third order cycle. The dashed lines show the path of the measured section from the channel of the spruit to the top of the hill and its extension from the second ledge forming sandstone (the stratigraphic equivalent of the top of the sandstone cap on the hill) up to the Bamboesberg Member. The final one being the Bamboesberg Member. The beds containing the bone accumulation are indicated in light yellow. Note that although the green portion of the section is following the downstream direction in the spruit, it is traversing upwards strategraphically due to the dip of the beds towards the southeast.	22
Figure 3.3:	Condensed stratigraphic section showing the third order cycles, lithofacies codes, interpreted facies associations, depositional environments, and depositional system. The lithofacies codes, overbank facies associations and channel facies associations used to characterize the beds are provided in Table 3.1, Table 3.2 and Table 3.3, respectively. The legend for the sedimentary structures is provided in Appendix A.	38
Figure 3.4:	Stratigraphic section of the beds that host the vertebrate fossil and burrow accumulation (-12 m to 26 m). Expanded sections provide an interpretation of the pedogenic sedimentary structures, the seasonal water table variation and the stratigraphical exten of the two types of burrow casts in the fossil hosting beds. The legend for the sedimentary structures is provided in Appendix A.	42
Figure 3.5:	(A) BCk-horizon consisting of massive mudstone. Measuring staff = 1 m. (B) *Skolithos* bioturbation of surface (multiple light-grey disks, < 0.5 cm diameter, two examples arrowed). (C) Discrete Stage II calcareous nodules. Scale bars = 5 cm	44
Figure 3.6:	(A) Strongly developed structural Bg-horizon consisting of prismatic peds and BCss-horizon with slickensides. Note the modern alluvium consisting of A, B and C soil horizons overlying the ancient palaeosols. (B) Calcified rootlets. (C) Mottling. Scale bar in B = 5 cm. Ruler in C = 10 cm x 10 cm.	46
Figure 3.7:	Claystone coated slickensides in massively bedded silty mudstone. These pedogenic slickensides are convex-concave slip surfaces that form during expansion/contraction in expansive clay soils such as vertisols. Scale bar = 10 cm.	47

Figure 3.8: (A) BCk-, BCt- and calcareous nodular horizon, k. (B) Embedded procolophonid skull in nodular horizon (white arrow = snout, black arrow = back of skull). (C) Reniform burrow penetrating nodular horizon. Ruler in C = 10 cm x 10 cm, scale bar in B = 3cm. 51

Figure 3.9: (A), (B) Sandstone sheet, SS (arrowed), above calcareous horizon, BCk. (C) Dish- shaped sandstone lens (1–2 m diameter). Scale bar in B and C = 20 cm. 52

Figure 3.10: (A) Structural Bg-horizon containing numerous isolated, reworked and articulated procolophonid skulls and postcranial elements (B) and (C). White arrows = snouts of two skulls in dorsal view, red arrow = small skull in lateral view with teeth visible. Scale bars in B and C = 2 cm. 54

Figure 3.11: Crevasse splay sandstone at Lemoenfontein locality. (A) View of crevasse splay sandstone outcrop. (B) Circular current crescent casts on sole surface. (C) Casts of interpreted vertebrate scratch digging activity (arrowed) on sole surface. Ruler in A = 10 cm x 10 cm, Scale bar in B and C = 5 cm. 55

Figure 3.12: Schematic diagram showing the vertical stratigraphic position of the different types of soil horizons and the relative position of pedogenic and diagenetic carbonate formation within these. Also shown is the region where ground water influenced the formation of pedogenic calcrete. The rooted horsetail stands are not to scale and have been enlarged for clarity. (Diagram modified from Figure 4 in Tabor and Myers (2015)). 60

Figure 4.1: Reniform burrow casts. (A) B19-5, gently curving inclined burrow cast showing chevron pattern of ridges (Note the penetration by secondary smaller burrow). (B) B19-2, bilobed cross-section. (C) Sets of narrow oblique ridges on the latero-ventral surface of the B19-5 burrow cast. Two types of these sets are highlighted according to their angle with respect to the long axis of the burrow cast (Low angle: yellow dashed lines and arrows. High angle: red dashed lines). Ruler in A = 10 cm x 10 cm, scale bar in B and C = 2 cm. 74

Figure 4.2: Sub-circular burrow casts: (A) Burrow B19.7-2 with enlargement chamber near the top (total excavated length 80 cm). (B) Cross-section showing a diagenetic colour alteration halo. (C) Knobby and hummocky surficial morphology over printing sub-horizontal scrape marks (selected examples highlighted with yellow dashed lines). (D) Knobby and hummocky surficial burrow morphology from Hasiotis and Mitchell (1993, Fig. 6-E). Scale bar in B and C = 5 cm. 78

Figure 4.3:	Sub-circular burrow casts. (A) Burrow B19-10 with less prominent surface scrape marks or ridges transverse to the burrow axis (selected examples highlighted with white dashed lines). (B) Surficial burrow morphology from Hasiotis and Mitchell (1993 Fig. 6-B). Scale bar = 2 cm.	80
Figure 4.4:	(A) Plot of horizontal to vertical diameter. (B) Comparison of diameter ratios for the two types of burrows.	82
Figure 4.5:	(A) Comparing ramp angles for the two types of burrows. (B) Plot of Ramp angle as a function of diameter ratio. (C) Plot of ramp angle versus burrow size. (D) Comparing burrow sizes for the two types of burrows.	83
Figure 4.6:	*Microgomphodon* in the burrow terminal chamber (pictures provided by V. Fernandez, August 2019). (A) Burrow chamber surface showing scratch marks (arrowed). (B) Micro CT scan showing the articulated *Microgomphodon* skeleton. Scale bar = 10 cm.	94
Figure 4.7:	(A) Giant reniform burrow terminal chamber from the study locality. (B) Distinct reniform cross-section (width = 15 cm, mid-level height = 7.5 cm, maximum height 12.5 cm). Scale bar = 5 cm.	96
Figure 4.8:	Schematic model of continental freshwater crayfish burrowing near a water source where there is a seasonal variation in the ground water table (based on Abouessa et al., 2015, Fig. 8). (A) Mid-season water level and burrow depth; (B) Dry season water level, older burrows are extended down to the new water level and new burrows are excavated all the way to the lowered water level, note the change in the burrow orientation from sub-vertical to oblique below the mid-level enlargements; (C) Wet-season water level, older burrows are partially filled in with mud or sand and can get penetrated by smaller new burrows. (This is a diagrammatic representation and the burrows and reedbeds are not to scale, the former have been enlarged for clarity).	103
Figure 4.9:	Large reniform burrow cast at 1 m of the Lemoenfontein stratigraphic section. (A) location in siltstone cliff face (arrowed). (B) View showing T-junction. Hammer length = 33 cm (arrowed). (C) Left shaft and terminal chamber. (D) Right shaft and terminal chamber. Ruler = 10 cm.	105
Figure 4.10:	Comparison of the Lemoenfontein bifurcating burrow cast (A) with the *Langbergia* burrow casts (B) and palaeoenvironmental reconstruction (C.) B and C are Figures 6 and 13 of Groenewald et al. (2001). Hammer length in A = 33 cm. Scale bar in B = 15 cm.	106
Figure 5.1:	(A) View of tabular crevasse splay sandstone that crops out at the Lemoenfontein study site. (B) *Skolithos* vertical burrows opening onto sharp top surface of crevasse splay sandstone. Examples arrowed. Ruler in (A) = 10 x 10 cm, Scale bar in (B) = 15 cm.	109

Figure 5.2: (A) Cluster of aligned current crescents. Note *Cynodontipus* traces in the foreground. (B) Desiccation crack dissecting current crescents. Foreground scale bar in A = 15 cm, Scale bar in B = 5 cm. 111

Figure 5.3: (A) Stem casts preserved in 3-D. (B) Horizontal stem compressions on top surface of crevasse splay sandstone (arrowed). (C) Pith casts preserved as the central peg in each crescent. (D) Vertically preserved stem cast showing horizontal nodes and vertical ridges around the stem. Scale bar in A = 5 cm, scale bar in B = 10 cm, Scale bar in C= 4 cm, scale bar in D = 3 cm. 112

Figure 5.4: Typical examples of Horseshoe Vortex simulation and experimental results. Diagrams from (A) Jahangirzadeh et al. (2014), (B) Zhao et al. (2010), (C) Yagci et al. (2017). (D) Modern example of a scour around a sub-round pebble (picture taken after an overbank flood at the Lemoenfontein locality). Ruler in D = 10x10 cm. 113

Figure 5.5: Lemoenfontein scratch-like traces. (A) Slab containing an elongated trace and a single crescentic trace (arrowed in black) and a possible *Rhynchosauroides* footprint (arrowed in white). (B) Elongated trace showing a bilobed architecture. (C) Crescentic trace showing opposing scrapes. (D) Cluster of three crescentic traces. Scale bars = 5 cm. 117

Figure 5.6: Examples of *Cynodontipus* terminal burrow traces from Olsen et al. (2020), Figure 23. Scale bar = 1 cm. 118

Figure 5.7: (A) Example of crescentic scrape marks from Lemoenfontein (B) Colour coded traces of scrape marks that occur in sets with four to five subparallel scrapes with the same direction, depth, and length, this being indicative of the number of claws on a tetrapod manus or pedes. Scale bar = 1 cm. 118

Figure 5.8: (A) Trace of the rhynchosaur manus (SAM-PK10180). (B) Superposition of this trace on a *Cynodontipus* specimen from Lemoenfontein. (C) and (D) Superposition of this trace on a possible *Rhynchosauroides* print from Lemoenfontein. Scale bars = 1 cm. 121

Figure 5.9: Scoyenia ichnofacies. (A) Narrow softground meniscate feeding trace (arrowed). (B) Wide firmground striated meniscate traces. Scale bars = 1 cm. 122

Figure 5.10: Sequence of events that allowed the *Cynodontipus, Scoyenia*, and *Rhynchosauroides* traces to be made on the mud surface as well as the preservation of Sphenophyte stem casts. Drawing by Claire Browning (2021). 123

Figure 6.1: Drone image showing the Lemoenfontein hill in the foreground with the three exposures of the fossiliferous beds, Gully 1, Bonebed 1, and Gullies 2 and 3 in the distance. 131

Figure 6.2: *Teratophon* (SAM-PK-K10174). (A) In-situ during excavation, showing association with *Reniformichnus*, and vertical position relative to the calcareous horizon. (B) Specimen post-excavation showing calcium carbonate surface coating. (C) Specimen post-preparation. Scale bar = 5 cm. 140

Figure 6.3: (A) L18-2 lying in the base of erosion gully in the orientation and attitude that it was found, which although apparently ex-situ it is still considered to be in its original stratigraphic position. Note the association with *Reniformichnus* and its stratigraphic level relative to the calcareous horizon. (B) L18-2 before preparation showing the detached skull block and colour mottling attributed to hydromorphic gleying of the mudrock surrounding the specimen. (C) Specimen after mechanical preparation showing the presence of 2 fully articulated curled-up *Teratophon* skeletons, one on top of the other. Top arrow indicates position of the second skull. Dashed line traces the inferred still-covered articulated spine, and the bottom arrow indicates the string of articulated caudal vertebra attributed to the second specimen. (D) Lateral view of second *Teratophon* skull lying dorsal-up beneath the still articulated, but slightly dislodged, thoracic ribs of the top specimen. Note the position of two gastralia ribs (arrowed) that had also become slightly dislodged from the top specimen. This taphonomic style suggests that the two sub-adult *Teratophon* had their skin intact when they became arranged into this configuration, and that they were most likely both alive. An underground burrow setting is therefore the most likely scenario. (E) Right lateral view of uppermost specimen. The two skulls have small differences in shape and size that may be attributed to ontogeny or sexual dimorphism. All scale bars = 5cm. 146

Figure 6.4: (A) *Teratophon* (L18-1), skull embedded in calcareous nodular horizon. (B) L18-1 Specimen afer preparation. (C) L19-1 *Teratophon* lower jaw embedded in calcareous nodular horizon. (D) L19-1 *Teratophon* lower jaw after preparation. (E) *In-situ Teratophon* articulated skeleton (L20-10) coated in cemented mudstone. Identification based on triangular shape of skull (arrowed). Scale bars in A = 3 cm and B = 4 cm, scale bar in C and D = 2 cm, scale bar in E = 10 cm. 149

Figure 6.5: Examples of Taphonomic Group 1: Isolated skull with articulated lower jaw. (A) and (B) M*icrogomphodon* skull (L20-3), encased in carbonate nodule as found in the field. (B) *Trirachodon* skull (L19-17) encased in carbonate nodule as found in the field. (D) Very rare *Lumkuia* skull (L19-19) encased in carbonate nodule as found in the field. Scale bar in A, B and C = 3 cm, scale bar in D = 2 cm. 152

Figure 6.6: Examples of Taphonomic Group 2: Articulated skeletons encased in nodules that take the shape of the carcass. (A) *Microgomphodon* (SAM-PK-K11601), skeleton encased in carbonate nodule that takes the shape of the carcass. This is the first *Microgomphodon* specimen with a fully articulated skeleton attached to the skull. (B) Left lateral view of SAM-PK-K11601 skull, showing possible preburial damage (arrowed) and excellent preservation quality of the bone. (C) *Microgomphodon oligocynus* (SAM-PK-K10160), skull with articulating cervical vertebrae and manus encased in carbonate nodule (articulated manus removed from nodule during preparation). (D) *Eohyosaurus wolvaardti*, SAM-PK-K10180, skull was encased in carbonate nodule before preparation. Note articulated right manus on temporal region. Scale bar in A = 15 cm, scale bar in B = 3 cm, scale bar in C and D = 2 cm. 155

Figure 6.7: (A) Examples of juvenile *Teratophon* articulated skeletons tightly curled-up and encased in carbonate nodules. (A) and (B) L18-5 dorsal and lateral views. (C) *Teratophon* (L19-21), note the position of the manus beneath the skull and 3-dimensional preservation of the articulated ribs in life position. (D) *Teratophon* (L19-23B), articulated juvenile skeleton. Scale bars = 3 cm. 157

Figure 6.8: (A) Structural Bg-horizon, source of numerous isolated, reworked, and articulated skulls and postcranial elements. (B) Procolophonid skull, SAM-PK-K10208. (C) *Trirachodon* skull SAM-PK-K10207, note evidence of reworking in that the snout has been weathered off and "re-sealed" after final burial with an iron-rich crust. (D) semi-articulated postcranial elements. Scale bars = 3 cm. 158

Figure 6.9: *Trirachodon* SAM-PK-K10163 (A) Ventral view of the anterior half of the burrow tunnel-shaped nodule containing skull and skeleton showing the orientation of the skull that is downwards and to the right. Note the presence of the maxillary platform that is characteristic of *Trirachodon*. (B) Dorsal view of the cylindrical nodule as found in the field (left squamosal arrowed). (C) Dorsal view of skull. Scale bars = 3 cm. 161

Figure 7.1: (A) Right lateral and (B) left lateral views of the rhynchosaur, *Eohyosaurus wolvaardti*, SAM-PK-K10159, (holotype, from Butler et al., 2015). Right lateral (C), dorsal (D) and left lateral (E) photos of prepared skull of SAM-PK10180, *Eohyosaurus wolvaardti*. Note articulated right manus lying across the temporal fenestra on the right side. Scale bars = 2 cm. 174

Figure 7.2: (A) Right lateral, (B) dorsal and (C) left lateral photos of prepared skull of SAM-PK-K10762, *Trirachodon berryi* from the Lemoenfontein locality. Note prominent maxillary platform (arrowed). Scale bar = 2 cm. 176

Figure 7.3: (A) Ventral view of *Langbergia modisei*, holotype specimen NMQR 3255 (from Abdala et al., 2006). Note the absence of a prominent maxillary platform (arrowed). (B) Ventral view of partially prepared skull of L19-17, *Trirachodon* and (C) ventral view of prepared skull of SAM-PK10762, *Trirachodon berryi* from the Lemoenfontein locality. Note prominent maxillary platforms in B and C (arrowed). (D) Lateral view of L20-12, *Cricodon*, showing sectorial postcanines (arrowed). Scale bar = 2 cm. 178

Figure 7.4: (A) and (B) Right lateral views of the prepared skull of the holotype of *Lumkuia fuzzi*, Specimen BP/1/2669 (Picture in A by C. Kammerer (2018), drawing in B from Hopson and Kitching, 2001). (C) Dorsal view showing possible parietal foramen endocast (arrowed), (D) right lateral view and (E) left lateral view of the new prepared skull of *Lumkuia*, Specimen L19-19. Scale bar = 2 cm. 179

Figure 7.5: (A) *Microgomphodon oligocynus* (SAM-PK-K10160), dorsal, left lateral and ventral views of the skull with articulating cervical vertebrae and manus that was encased in carbonate nodule (articulated manus removed from nodule during preparation), Image from (Abdala et al., 2014). (A) *Microgomphodon* (SAM-PK-K11601), skeleton encased in carbonate nodule that takes the shape of the carcass. This exceptional specimen is the first *Microgomphodon* specimen with a fully articulated skeleton attached to the skull. (C) Dorsal view of its skull. (D) Right lateral view of its skull. Scale in A bar = 1 cm, Scale bars in B, C and D = 3 cm. 181

Figure 7.6: (A) *Teratophon spinigenis* (SAM-PK-K010174). (B) Dorsal and right lateral view of *Teratophon spinigenus* (skull of L18-2). (C) Dorsal and left lateral views of the holotype of *Thelerpeton oppressus* (BP/1/4538, from Modesto and Damiani (2003)). Scale bar = 2 cm. 183

Figure 7.7: Ontogenetic range of *Teratophon* skull sizes from Lemoenfontein. (A) Juvenile (SAM-PK-K10190). (B) Sub-adult (SAM-PK-K011599, L18-2). (C) Adult (SAM-PK-K010174). Scale bars = 4 cm. 184

Figure 7.8: Comparison of juvenile *Teratophon* to *Thelerpeton*. (A) and (B) *Thelerpeton* paratype (BP/1/4586), dorsal and right-lateral views, respectively. (C) and (D) Juvenile *Teratophon* (SAM-PK-K10190), dorsal and right-lateral views, respectively. Scale bars = 4 cm. 185

Figure 7.9 (A) *Teratophon* specimen 18-1 showing prominent right quadratojugal horn after preparation. (B) *Thelephon* specimen SAM-PK-K10172. Scale bars = 4 cm. 187

Figure 7.10: (A) Dorsal view, (B) left lateral view, and (C) right lateral views of *Thelephon contritus* (PK-K010162). Note the expanded marginal teeth in B and C (arrowed). Scale bar = 2 cm. 188

Figure 7.11: Relative frequency of the fossils of different genera collected from the Lemoenfontein locality. 189

Figure 8.1: (A) Spatial abundance of tetrapod fossils in Bonebed 1. The size of each circle correlates to the number of specimens assigned to the same GPS coordinate. (B) Spatial distribution of tetrapod fossils covering Gully 1, Bonebed 1 and Gullies 2 and 3. Each white dot represents an individual specimen (Black rectangle corresponds to the area in (A)). 204

Figure 8.2: Schematic palaeoenvironmental reconstruction of the once-living ecosystem at the base of the *Cynognathus* AZ T-K Subzone at the Lemoenfontein locality. The landscape was dominated by a floodplain dotted with seeps and standing water bodies that became the preferred habitat of small herbivorous and carnivorous cynodonts, archosaurs, therocephalians and procolophonids. These semi-permanent ponds were surrounded by sphenophyte reed beds that acted as source of food. The stratigraphic sequence has been simplified from that of Lemoenfontein. Active and older buried burrows and bones are indicated. Also, areas of down wasting of the floodplain following the abandonment of previously active channels as well as areas of floodplain deposition due to sediment laden overbank flood events is also presented schematically. 212

LIST OF TABLES

Table 2.1:	Data collection and analysis process. Columns identify the main elements of the study and their progression from left to right delineates the data collected and methods used to obtain the partial and final interpretations. These steps were applied for each of the main aspects of the study i.e., sedimentology, vertebrate fossils, and trace fossils. The insights from these topics combine for an integrated interpretation.	15
Table 3.1:	Lithofacies Classification	23
Table 3.2:	Overbank facies associations (adapted from Colombera et al., 2013)	24
Table 3.3:	Channel Facies Associations (adapted from Colombera et al., 2013)	25
Table 4.1:	Lemoenfontein burrow casts - basic dimensions	75
Table 4.2:	Lemoenfontein burrow casts characteristics and comparison to similar burrow casts	87
Table 4.3:	Skull width of the possible burrow makers	94
Table 6.1:	Taphonomic classes with characteristic descriptors (adapted from Smith, 1989)	136
Table 8.1:	Summary of the various biogenic and physical bone accumulation mechanisms. Specific examples and influencing factors of these mechanisms are also provided. Summary based on Rogers et al., 2007.	196
Table 8.2:	Summary of the possible post concentration taphonomic pathways and their resultant signatures. Summary based on Rogers et al., 2007.	197

1. INTRODUCTION

The main Karoo Basin of South Africa is infilled with a near-continuous sequence of sedimentary rocks deposited over a period of almost 120 million years (Catuneanu et al., 2005). The rocks accumulated in a retro-foreland basin (Catuneanu et al., 1998) in southwestern Gondwana from the Late Carboniferous (300 Ma) to the Early Jurassic (183 Ma) (Duncan et al., 1997). Karoo Supergroup strata cover two thirds of the surface area of South Africa, although much of this is sub-outcrop that is covered by Cenozoic deposits. Based on their lithological and sedimentological characteristics, several groups can be defined within the Karoo Supergroup. From oldest to youngest, these are Dwyka, Ecca, Beaufort, Stormberg and Drakensberg groups (Johnson, 1976; SACS, 1980). Deposition of the Karoo succession began during the melt-out stages of the Late Carboniferous Gondwanan glaciation and terminated with the early stages of breakup recorded by the vast basaltic flows that form the bulk of the Drakensberg Group (Duncan et al., 1997). The main Karoo Basin is the largest and deepest (5 km at its maximum in the southern foreland trough) of several connected or partially connected basins on Gondwana (Hancox, 1998; Catuneanu et al., 2005; Scheiber-Enslin et al., 2015). The succession thins significantly towards the north, where it rests on the stable margin of the basin and against the upwarping forebulge (Catuneanu et al., 2005; Rutherford et. al, 2015).

The Beaufort Group is divided into a lower Adelaide Subgroup and an upper Tarkastad Subgroup (SACS, 1980; Catuneanu et al., 2005). These dominantly fluvial deposits are made up of fining-upward cycles of sandstones, siltstones, and mudstones (Catuneanu et al., 2005). The Tarkastad Subgroup can be distinguished by its greater sandstone-to-mudstone ratio (Rutherford et al., 2015).

The Burgersdorp Formation is the final depositional episode of the Beaufort Group. It is paraconformably overlain by the Molteno Formation, which is the basal unit of the Stormberg Group. The Burgersdorp Formation consists mainly of mudrocks with inter-bedded sandstones in fining-upward cycles of a few metres to tens of metres in thickness, with a maximum thickness of 1000 metres in its southernmost outcrops (Johnson et al.,

2006). It is considered to be Early to Middle Triassic in age (Hancox, 1998, p. 11). Recent radiometric dates from biostratigraphic correlatives in South America suggest an early Late Triassic age (Marsicano et al., 2016; Ottone et al., 2014), however there is significant controversy regarding this interpretation (Kammerer and De los Angeles Ordoñez, 2021). An extensive study of the Burgersdorp Formation is reported by Hancox (1998) and other geological descriptions are provided by Karpeta and Johnson (1979), Dingle et al. (1983), Johnson (1976, 1984), Hiller and Stavrakis (1984), Johnson and Hiller (1990), Kitching (1995), Hancox (2000), Neveling et al. (2005) and Rutherford et al. (2015).

Burgersdorp Formation rocks consist of isolated, lenticular, feldspathic fine to medium-grained channel sandstones, common tabular fine-grained crevasse splay sandstones and argillaceous overbank mudrocks. The sandstones often overlay a basal lag consisting of reworked mudclast conglomerate (Hancox, 1998, p. 55). The common greyish-red (5R 4/2) to dusky-red (5R 3/4) massive overbank fines consist mainly of siltstones and mudstones and may contain sand-filled mudcracks and vertebrate and invertebrate burrows. Playa lake deposits are present in the form of well-laminated reddish mudrocks with pedocrete (cemented soil) horizons (Neveling, 2002; Hancox et al., 2010).

It is generally accepted that the Burgersdorp Formation mudrocks and sandstones were deposited by northwesterly flowing meandering rivers, during a warm, arid to semi-arid climatic interval (Hancox, 1998). These high sinuosity rivers transported a mixed sediment load and regularly flooded, resulting in overbank traction and suspended load deposition on the floodplain surface. Some granular sheetwash beds as well as shallow-ephemeral floodplain channel fills and bedload dominated braided river deposits are also present, particularly in the lower part of the Burgersdorp Formation. Lacustrine palaeoenvironments also occur in the lower Burgersdorp Formation in the northern part of the Karoo Basin (Groenewald, 1996; Hancox et al., 2010).

The rocks of the Beaufort Group preserve a rich tetrapod fossil record that has allowed for the establishment of seven assemblage zones, with nine subzones (Smith et al., 2020). Due to the abundance of body and trace fossils, their excellent preservation and their near-continuous temporal record, the biostratigraphy of the Beaufort Group has become a global

standard for the correlation of Middle Permian to Middle Triassic terrestrial sequences (Lucas, 1998; Hancox, 2000; Neveling et al., 2005).

The Triassic strata of the Beaufort Group consists of the Early Triassic *Lystrosaurus declivis* Assemblage Zone (AZ) and the Early to Middle-Triassic *Cynognathus* AZ (Rubidge et al., 1995; Botha and Smith, 2020; Hancox et al., 2020). The *Cynognathus* AZ corresponds lithostratigraphically to the Burgersdorp Formation. Although there are few lithostratigraphic marker horizons in the Burgersdorp Formation, the *Cynognathus* AZ has been subdivided into three subzones based on differences in stratigraphic (and likely temporal) distribution of fossil tetrapod taxa (Shishkin et al., 1995; Hancox et al., 1995; Hancox, 1998; Hancox et al. 2020). The exceptional fossil record of the Beaufort Group also provides extensive data for the study of terrestrial vertebrate evolution.

Studies on the taphonomy of Triassic bonebeds in the main Karoo Basin are few (Smith, 1980; Smith, 1989; Smith and Kitching, 1997). Kitching (1963) first drew attention to the occurrence of "bonebeds" in the Middle Triassic exposures in the Joe Gqabi (Burgersdorp) district, located on the farms Cragievar and Winnaarsbaken. The term "bonebed" has since been more rigidly defined (Rogers et al., 2007). Here, the term is used as a general term to reflect the anomalous accumulation of vertebrate fossils. Kitching also pointed out a locality on the farm, Lemoenfontein, in the Xhariep (Rouxville) district, where he found what he interpreted to be cynodont burrow casts and a few *Trirachodon* and procolophonid skulls (pers. comm., 1976). Subsequent exploration of this locality, first in my personal capacity and then followed by a formal field trip to the locality in 2003 accompanied by Dr Smith (then curator of Karoo Palaeontology at Iziko SA Museum, Cape Town) resulted in the discovery of a variety of well-preserved fossils of several different taxa and the identification of this locality as a potential bonebed. The Lemoenfontein locality has so far delivered over 140 identifiable skulls of at least six different taxa, many attached to articulated skeletons. The taxa from this bonebed have several unique features in common, such as herbivory, small body size and a high degree of articulation. To date, the collection includes two holotypes and one potential paratype. Along with the body fossils at least three different types of interpreted burrow cast geometries have also been identified at this field site.

1.1 Hypotheses tested

Based on the information collected during this study five different hypotheses were tested.

- The sedimentology and taphonomy of the locality indicate a floodplain lake or pond margin paleoenvironment, colonised in the long term by a diversity of taxa and supporting abundant vegetation in the wet season.
- The changing water table (calcareous nodular horizon), sheet wash burrow fill, slickensides, textural B horizons, pedogenesis and mud crack casts point to seasonal variation in rainfall (and possibly to periods of drought).
- The bone accumulation mechanism at this locality is a combination of intrinsic biogenic and physical concentration agents. Climatic rather than tectonic factors were the overriding influence on accumulation of sediments and bones at this site.
- The sedimentary strata hosting the Lemoenfontein bonebed are at the transition between the *Cynognathus* AZ *Langbergia-Garjainia (L-G)* Subzone and the *Trirachodon-Kannemeyeria (T-K)* Subzone.
- Procolophonids dug underground burrows or scratched-out near surface holes in the floodplain soils surrounding ponds and lakes.

1.2 Objectives

The main purpose of this study is to identify the palaeoenvironmental and behavioural mechanisms that led to the accumulation of tetrapod fossils at the Lemoenfontein locality. Firstly, field data were gathered by studying the Lemoenfontein sedimentology, the burrow casts, other traces, and the tetrapod fossil faunal diversity and taphonomy. Secondly, these data were integrated and interpreted to reconstruct the palaeoenvironment and taphonomic pathways that explain the anomalous accumulation of tetrapod fossils.

As a secondary objective, it is intended that this detailed investigation of the Lemoenfontein concentration of fossil bones will make important contributions to our understanding of the bone accumulation mechanisms, and in doing so, generate information that will help to reconstruct the palaeoenvironments and palaeoecology of Middle Triassic tetrapods in the main Karoo Basin of South Africa more accurately.

It has been observed that procolophonid fossils often occur in clusters in Triassic Karoo sedimentary rocks and it has been postulated that they were burrowing animals (Colbert and Kitching, 1975; Sidor et al., 2008; Bordy and Krummeck, 2016; deBraga, 2003). Many of these citations referred to Kitching's verbal communication as reported by Groenewald (1991) about possible procolophonid fossil remains in a burrow. No formal study to test the validity of these observations has been done to date, and this is one aspect that the present study aims to address.

1.3 Aims

To gain an understanding of the bone accumulation mechanisms and generate information to reconstruct the palaeoenvironments, this study adopted several aims.

- A systematic search of the locality to collect remaining skulls and skeletons in *ex-situ* calcareous nodules within the surface "float", as well as those still embedded in the mudstone or preserved in burrow casts.
- Preparation of a representative sample of the fossils from this locality and with the help of experts in the taxonomy of the various groups, achieve a positive identification to species level, if possible.
- Search the collections of the Evolutionary Studies Institute, Iziko South African Museum and National Museum to include all previously collected fossils from this locality in the database.
- Analyse and describe the biodiversity of the tetrapod assemblage at the bonebed locality.
- Identify and describe the different taphonomic styles of fossilization at the locality.

- Sample and log the different types of burrow casts from the locality. Use the systematic methods of Miller et al. (2001) to identify and classify the burrow casts and to identify the possible burrow producers.
- Measure and sample a detailed sedimentological section from the lowest mudrock exposures below the bonebed locality up to the base of the Bamboesberg Member of the Molteno Formation and plot the occurrence of the fossils and the burrow casts on this log. Locate existing fossils and burrows relative to the B horizon and calcareous nodular horizon that demarcate the fossiliferous beds at this locality and make informed interpretations about the trace makers, their reasons for burrowing and the possibility that burrows are terminated just above the ancient water table.
- Based on the insights from sedimentology and taphonomy, propose a mechanism that explains the anomalous accumulation of bones at the locality and derive conclusions about the ancient floodplain processes, depositional environments and climate.

1.4 Dissertation overview

An extensive literature survey was performed at the beginning of this study. This survey interrogated relevant studies on the Triassic aged strata in the main Karoo Basin, with particular focus on the Burgersdorp Formation. The results of the literature survey are presented as an introduction to each of the core chapters of this dissertation according to the main topic under investigation in that chapter.

The methods and materials used for field, laboratory and collections-based data capture are described in Chapter 2. It also contains a description of the approach used to analyse and interpret this information.

The sedimentology and lithostratigraphy of Lemoenfontein are described in Chapter 3. First, the results of the literature survey of these aspects within the main Karoo Basin, with emphasis on the Burgersdorp Formation are provided. This is followed by a description of the

geographical and geological setting. The third-order upward-fining facies sequences that extend from the informal Eldorado marker up to the Bamboesberg Member are described, along with a detailed analysis of the beds hosting the bone accumulation in the first cycle. Chapter 3 concludes with an interpretation of the depositional environment.

Chapter 4 presents a full analysis of the burrow cast ichnology of the Lemoenfontein site. The chapter starts with the results of the literature survey of Triassic burrow casts. An overall description of the burrow casts is then provided. The results of the detailed analysis of the reniform and sub-circular burrow casts that considered burrow architecture, surficial morphology, burrow fill and characteristic burrow measurements are presented. The chapter concludes with a discussion of the potential burrow-makers and the palaeoenvironmental significance of these burrows.

The ichnology of the crevasse splay sole surface is presented in Chapter 5. A general description of the sandstone is provided, followed by a discussion of the flow induced current crescents, casts and imprints of sphenophyte stems, desiccation cracks, various worm, insect, and arthropod traces, as well as tetrapod scratch-digging traces. A discussion of its similarity to the *Scoyenia* ichnofacies is followed by an interpretation of the palaeoenvironmental significance of these traces.

The taphonomy of the tetrapod fossils is addressed in Chapter 6. This chapter starts with the results of the literature survey of the vertebrate taphonomy in the Karoo Basin, followed by an introduction to the spatial and stratigraphic distribution of the fossil bones on Lemoenfontein. Descriptors for the observable taphonomic characteristics and the interpretation of these characteristics are introduced. These descriptors are then used to identify taphonomic groups to which a representative sample of the fossils could be assigned in a systematic way. Based on this analysis, insights are derived about the palaeoenvironment and the animal behaviour.

A systematic description of the Lemoenfontein tetrapod fauna is presented in Chapter 7. The chapter starts with an overview of the *Cynognathus* AZ biostratigraphy. Seven different faunal types from the main families that are present: Rhynchosauria (one genus), Cynodontia (three genera), Therocephalia (one genus), and Procolophonidae (two genera) are identified at genus and species level. The relative frequency of occurrence of the taxa is calculated and presented in graphic form. Key aspects of these taxa, with a focus on dentition, are described and analysed. The insights gained from this assessment are then used to interpret the palaeobehaviour of the fauna as well as to identify the biostratigraphic position of the Lemoenfontein site.

In Chapter 8 the insights gained from the investigation of the Lemoenfontein sedimentology, the crevasse splay sole surface, the burrow casts, the taphonomy, and the fauna are summarised and combined to interpret how palaeoenvironmental and behavioural factors contributed to the concentration of tetrapod fossils at the Lemoenfontein locality. The chapter starts with a description of a generic conceptual framework for the genesis and analysis of vertebrate skeletal concentrations, as well as the results of the literature survey of Triassic Karoo Basin bone accumulations. The accumulation of fossil skulls and skeletons at Lemoenfontein is described and each occurrence is plotted on aerial photographs of the site. The palaeoenvironment and once-living ecosystem at the base of the *Cynognathus* AZ *T-K* Subzone is then reconstructed by integrating the evidence from the various investigations. A schematic illustration of this palaeoenvironment is provided. This reconstruction is then used to develop the most parsimonious explanation for the origin of the concentration of fossil bones at Lemoenfontein. The chapter concludes by comparing the Lemoenfontein accumulation to other bone accumulations in the Triassic strata of the Karoo Basin, as well as to bone accumulations in the Lifua Member of Tanzania and the Santa Maria Formation of Brazil.

A final summary of the key insights and conclusions is provided in Chapter 9. These conclusions are presented in a way that is consistent with the main aims and objectives as set out above in this introduction.

Appendix A contains the full stratigraphic log from the informal Eldorado marker up to the base of the Bamboesberg Member of the Molteno Formation. Appendix B contains the database of all the tetrapod fossil specimens that were collected and considered as part of this study. Appendix C contains the basic burrow cast parameters as recorded in the field and in the laboratory. The dissertation is concluded with the full list of references in the Reference List.

2. MATERIALS AND METHODS

2.1 Field Based Observations

The field work for this study was conducted over two ten-day fieldtrips in April 2019 and September 2020. It was mainly focused on the bone accumulation site on the farm Lemoenfontein (44) in the Xhariep (Rouxville) district on the road between Aliwal North and Bethulie. Additional bonebed localities on the farms Winnaarsbaken and Cragievar in the Joe Gqabi (Burgersdorp) district (Kitching, 1963) were surveyed for comparative purposes. A stratigraphic section was logged through the Burgersdorp Formation strata from the informal Eldorado marker exposures below the locality up to the Bamboesberg Member of the Molteno Formation. The strata at this locality are mostly horizontal and, in some cases, slightly tilted from the horizontal, dipping towards the southeast. A Jacob staff with Abney level, tape measure, a handheld Global Positioning System (GPS) device and compass were used to measure the vertical sedimentological sections and record palaeocurrent directions. Lithological textures and rock colours were noted during logging. Samples of the various silt- and mudstones, crevasse splay sandstones, crevasse channel sandstones, palaeosols and calcareous nodules were collected for study and reference.

A systematic search for vertebrate and invertebrate body fossils, coprolites, burrow casts, trackways and other traces was performed during two field trips to the locality. The GPS coordinates of each *in-situ* fossil were logged. The lithology (mudstone, siltstone, sandstone) and other sedimentary structures of the host matrix were recorded along with its colour using a Munsell Soil Color Chart (1975 edition). Photographs of embedded fossils were taken. Following the taphonomic methods of Smith (1989), the attitude (dorsal up, ventral up, lateral up etc.), degree of articulation, pre-burial weathering or breakage and evidence of perimineralisation were recorded for each fossil. Drone-sourced aerial photographs of the locality were also taken to provide an up-to-date base map for accurate positioning of fossils and sample localities.

The methods of Miller et al. (2001) and Bordy and Krummeck (2016) were used to record the following measurable parameters that characterise burrows: diameter, width/height ratio,

architecture, branching, penetration depth and angle, surface markings, burrow lining (mud chips), producer in burrow and occurrence density (per square meter of outcrop). Samples of the burrow casts were collected.

The study area contains a distal crevasse splay sandstone with a sole surface that has preserved in minute detail the surface features of the underlying mudrock palaeosurface. A 20 m x 2 m strip of the sandstone bed was lifted in slabs to expose the casts of invertebrate and vertebrate activity as well other flow-induced features on the basal surface of this sandstone. Samples were collected, photographed and the presence of various biogenic and current induced markings were recorded.

2.2 Laboratory and collections-based data capture

The Karoo fossil databases of the Evolutionary Studies Institute at the University of the Witwatersrand in Johannesburg, the Iziko South African Museum in Cape Town, as well as the National Museum in Bloemfontein were interrogated for additional records of fossils and burrow casts from the Lemoenfontein locality. These specimens were incorporated into the analyses.

A selection of the fossils in these collections as well as a representative sample of new specimens recovered during fieldwork for this project were prepared using pneumatic percussion drills up to a degree of completion that allowed positive identification to species level. Preparators were assigned at the Iziko South African Museum and at an external independent preparation laboratory under the supervision of Professor Smith. To reduce the likelihood of fruitless hours of preparation with no positive identification, arrangements were made at the start of this study for several of the specimens to undergo micro-CT scanning and rendering to 3-D models. However, due to the 2020 COVID19 lockdown restrictions in South Africa, access to these facilities was not possible. Therefore, only the mechanically prepared specimens were identified to the taxonomic level of genus and species. High resolution photographs were taken under controlled conditions.

All fossils were allocated a taphonomic class based on the scheme devised by Behrensmeyer (1978) and Smith (1989) and as extended in this study. Using the taphonomic classes that were retained for this locality, information was derived about the depositional environment and climate during deposition of the sediments at this locality.

A generic conceptual framework for the genesis and analysis of vertebrate skeletal concentrations is provided by Rogers and Kidwell (2007). This framework was utilised to categorise the bonebeds genetically and to derive insights about the biogenic mechanisms (intrinsic versus extrinsic) or the physical agents that led to the bone accumulations.

Using the systematic approach for characterizing burrows developed by Miller et al. (2001) and implemented by Bordy and Krummeck (2016), the measured burrow parameters were used to allocate burrows to an ichnotaxon and to identify possible burrow producers.

2.3 Analyses

The lithology of the of the rocks that make up the stratigraphic section were analysed by recording the physical characteristics such as colour, texture, grain size and composition of the collected samples. Age data were obtained by relative dating using biostratigraphic correlation of tetrapod taxa.

Miall (1985, 1996) defined a systematic nomenclature for lithofacies codes and fluvial architectural elements and Hancox (1998) applied these to the Burgersdorp Formation. These codes were adapted and used to interpret the sedimentological information recorded during the logging of the vertical stratigraphic section. The data generated for the beds containing the tetrapod bone accumulations was correlated with the interpretations derived from the overall lithological and sedimentological analyses.

The GPS coordinates of fossils and ichnofossils were plotted on a Google Map image that was overlaid with a high-definition drone-captured aerial image of the area. Clustering and other

characteristics were noted. The fossil occurrences were recorded in a database and relative frequencies were then calculated.

The taphonomy of the tetrapod bone accumulation was analysed by extending the methods of Behrensmeyer (1978) and Smith (1989), with consideration given to factors such as the taxa present, degree of articulation, pre-burial weathering, breakage, or perimineralisation. Representative taphonomic styles were defined and the specimens were assigned accordingly.

Using the outcome of the systematic approach for characterizing burrows (Miller et al., 2001), interpretations were derived about the social behaviour and lifestyle of the possible burrow producers.

The insights gained from the lithology, sedimentology, taphonomy, fossil taxa, ichnofossils and burrow analyses were used to reconstruct the palaeoenvironment that existed during the deposition of the sediments as well as to identify the mechanisms or combinations thereof that led to the bone accumulations. The sedimentological and taphonomic data are integrated into a taphonomic pathway description.

The analyses were concluded by a discussion of the palaeoclimatic and/or tectonic drivers of environmental conditions that led to the bone accumulation. A reconstruction of the once living *Cynognathus* AZ ecosystem at the base of the *T-K* Subzone at this locality was provided, along with an interpretation of the floodplain processes and tetrapod community behaviours.

Comparisons of the Lemoenfontein sedimentology, taphonomy and faunal composition were made with similar-aged bone accumulation sites in the Manda Beds of Tanzania (Smith et al., 2017) and the Middle Triassic Santa Maria Formation of Brazil (Bertoni-Machado and Holz,

2006). Based on these, the biostratigraphic correlation and robustness of the interface of the *L-G* and *T-K* Subzones was confirmed.

The process of analysis followed during this study is illustrated in Table 1.1. The columns identify the major steps taken during the study and the progression from left to right identifies the data collected and methods used to obtain the partial and final interpretations. These steps were applied for each of the main aspects of the study i.e., sedimentology, vertebrate fossils, and trace fossils. The insights from these topics combined for an integrated interpretation.

Table 2.1: Data collection and analysis process. Columns identify the main elements of the study and their progression from left to right delineates the data collected and methods used to obtain the partial and final interpretations. These steps were applied for each of the main aspects of the study i.e., sedimentology, vertebrate fossils, and trace fossils. The insights from these topics combine for an integrated interpretation.

Aspect	Field Methods	Data Collection	Lab Methods/Analyses	Interpretative parameters	Integrated Interpretation
Sedimentology	Measure stratigraphic section. Locate fossils on section. Photographs of fossiliferous beds.	Lithology. Sedimentary structures. Pedogenesis. Colours. Palaeocurrents.	Confirmation of lithology based on samples. Transcription of field records. Assignment of lithofacies codes and fluvial architectural elements.	Depositional environment and timing.	Derivation of conclusions about the ancient floodplain processes, depositional environment, and climate. Derivations of conclusions about the behaviour of the animals that colonized the site. Proposal of a mechanism that explains the anomalous accumulation of bones.
Vertebrate fossils	Systematic search and collection. Excavation. Encasement in plaster jackets. Photographs of in situ fossils. Drone based aerial photographs.	GPS coordinates. Taphonomic parameters. Host matrix. Preliminary taxonomic identification.	Fossil preparation. Taxonomic identification. Taphonomic modes definition. Characterisation of the bone accumulation. Museum data base search. High resolution photographs of specimens.	Animal behaviour. Taphonomic pathway.	
Ichnofossils	Systematic search and collection. Excavation. Photographs of in situ burrow casts and traces. Record characteristics (architecture, surficial morphology).	Burrow cast data: Ramp angle. Architecture and morphology. Vertical and horizontal diameter. Penetration depth. Palaeosurface physical and biological traces.	Measure burrow characteristics. Record surficial morphology and burrow architecture. Systematic classification. Identification of burrow-makers. High resolution photographs of specimens.	Animal behaviour. Depositional environment.	

3. SEDIMENTOLOGY AND LITHOSTRATIGRAPHY OF LEMOENFONTEIN

3.1 Overview of the lithostratigraphy of the main Karoo Basin

The main Karoo Basin (MKB) of South Africa represents a near continuous sequence of sediment deposition over a period of almost 120 million years (Catuneanu et al., 2005). Up to 8 km of basin-fill sediments accumulated in a broadly east-west trending foreland basin (de Wit, 1992, Catuneanu, 2005) in southwestern Gondwana from the Late Carboniferous (300 Ma; Visser and Dukas, 1979) to the Middle Jurassic (183 Ma; Duncan et al., 1997). The Karoo sequence of sedimentary rocks has the lithostratigraphic rank of Supergroup and its outcrops (and sub-outcrops) cover two thirds of South Africa. Based on sedimentological characteristics, several groups can be defined within the Karoo Supergroup. Starting with the oldest, these are named the Dwyka, Ecca, Beaufort, Stormberg and Drakensberg groups (SACS, 1980; Catuneanu et al., 2005; Johnson et al., 2006). Karoo sediment accumulation began at the end of the Carboniferous as the super continent emerged from an extended glaciation and continued relatively uninterrupted until the beginning of the breakup of Gondwana, heralded by the vast magma flows that form the Drakensberg Group (Duncan et al., 1997). The Main Karoo Basin is the largest and deepest of several connected or partially connected basins across southern Gondwana (Hancox, 1998). The thickest deposits in the main Karoo Basin occur in the southeast, proximal to the Cape Fold Belt where they reach a maximum of 5 km (Scheiber-Enslin et al., 2015). Most of the formations thin significantly to the distal northeast (Rutherford et al., 2015), however reciprocal flexure of the crust has created some areas of overthickening and removal/non-deposition in the central and northern areas (Bordy et al., 2004; Catuneanu et al., 2005). In the southern Karoo Basin, the Dwyka Group (320-280 Ma) glaciogenic deposits accumulated subaqueously mainly from floating ice and outwash from retreating glaciers. The confined post-glacial meltwaters resulted in Ecca Group marine and deltaic strata that conformably overlie the Dwyka Group. These are followed by the non-marine Beaufort Group and after a five-to-ten-million-year hiatus, the Stormberg Group.

The Beaufort Group is divided into a lower Adelaide Subgroup (Middle-Late Permian Koonap-Middleton, and Balfour formations) and upper Tarkastad Subgroup (Early to Middle Triassic Katberg and Burgersdorp formations) (SACS, 1980; Catuneanu et al., 2005). These alluvial successions are made up of stacked fining-upward cycles of various scales and complexity but with similar sandstone, siltstone, and mudstone lithologies. (Catuneanu et al., 2005). The Tarkastad Subgroup overall has a greater sandstone-to-mudstone ratio than the Adelaide Subgroup (Johnson, 1976, page 243).

The Stormberg Group overlies the Beaufort Group. It is made up of the Late Triassic Molteno formation, the Triassic-Jurassic Elliot Formation and the Jurassic Clarens Formation. There is a stratigraphic hiatus between the Burgersdorp Formation and the Molteno Formation (Hancox 1998, Catuneanu et al., 2005) as well as at the lower and upper contacts of the Lower Elliot Formation (Bordy et al., 2004). The Molteno Formation consists of the upward-coarsening Bamboesberg and Indwe members (Hancox, 1998) and the informally named Tsqima succession (Bordy et al., 2005).

The Beaufort Group fill of the Karoo Basin was controlled by pulsed orogenesis of the Cape Fold Belt (CFB) resulting from subduction of the Palaeo-Pacific plate beneath the Gondwana plate (Hancox, 1998; Catuneanu et al., 1998; Catuneanu et al., 2005). This tectonic activity created the reciprocal flexural profile of the Karoo Basin with a deep retro-foreland basin proximal to the orogenic load and a peripheral bulge distal to the load (Catuneanu et al., 1997; Catuneanu et al., 1998). During a loading event the proximal foreland undergoes subsidence, and the peripheral bulge undergoes uplift. This creates accommodation space in the foreland, which in turn leads to retrogradation of coarse sediments. During the unloading that follows the opposite occurs, i.e., uplift of the proximal foreland and subsistence of the distal foreland, leading to a progradation of coarse sediments. The response of coarse clastic deposition is therefore 180 degrees out of phase with the tectonic pulse events (Hancox 1998).

Hancox (1998) was able to correlate the deposition of the arenaceous Katberg and Molteno formations to periods of orogenic unloading that resulted in progradation of coarse clastic wedges into the basin. Similarly, the deposition of the predominantly argillaceous Balfour and

Burgersdorp formations was correlated to orogenic loading tectonism leading to retrograde deposition of coarse sediments confined to the southern margin of the basin. Thus, the deposition of Triassic sediments in the Karoo retro-foreland basin was controlled by periods of limited or no tectonic activity during which channel-dominated fluvial systems prograded (basinward), followed by periods of pulsed tectonism in the CFB, creating accommodation space and leading to sourceward retrogradation of the channel-dominated systems. This model for deposition control is out of phase with the previous sedimentary model of Hancox and Rubidge (1998) and the tectonostratigraphic model of Groenewald (1996).

The Burgersdorp Formation is the final depositional episode of the Beaufort Group. As described above, it is para- to un-conformably overlain by the Molteno Formation of the Stormberg Group. It is of Early to Middle Triassic age with an overall thickness of up to 1000 metres in its southern parts (Johnson et al., 2006) and consists of mudrocks with inter-bedded sandstones in upward-fining cycles of a few meters to tens of meters thick. An extensive study of the Burgersdorp Formation is reported in Hancox (1998). Other geological descriptions are provided by Karpeta and Johnson (1979), Dingle et al. (1983), Johnson (1976, 1984), Hiller and Stavrakis (1984), Johnson and Hiller (1990), Kitching (1995) and Hancox (2000), Neveling et al. (2005), and Rutherford et al. (2015).

Most of the Burgersdorp Formation was deposited by northwesterly flowing meandering rivers during a warm, arid to semi-arid climatic interval (Hancox, 1998). These rivers formed a high sinuosity, mixed-load fluvial system. Suspension-load dominated deposition occurred on the floodplains during and following overbank flood events. Some sheetwash, shallow-ephemeral and bedload-dominated sand sheets deposited by low-sinuosity and possibly braided rivers are also present, particularly in the lower part of the Burgersdorp Formation (Hancox, 1998). This depositional scenario resulted in a succession of isolated, lenticular, feldspathic channel sandstone bodies, common tabular crevasse splay sandstone sheets and thick tabular beds of pedogenically-modified overbank mudrocks. The channel sandstone bodies invariably overlay an eroded surface commonly marked with patches of intraformational basal lag conglomerate consisting of reworked mudclasts and calcareous nodules. The thick beds of massive greyish-red (5R 4/2) to dusky-red (5R 3/4) overbank fines

consist mainly of siltstones and mudstones and contain some sand-filled mudcracks, vertebrate and invertebrate burrows and vertebrate body fossils. Playa-lake deposits are present in the form of well-laminated greyish-red (10R 4/2) mudrocks with pedocrete (cemented soil) horizons. Lacustrine laminated mudrocks also occur in the lower Burgersdorp Formation in the northern part of the Karoo Basin (Groenewald, 1996; Hancox et al., 2010).

3.2 Lemoenfontein fossil site: geological setting

The farm Lemoenfontein (44) is situated in the Southern Free State, 14 km to the northwest of the town of Aliwal North on the road to Bethulie. It is one of several farms (Gladde Grond, Betjies Kraal, Blom and Mooiplaas) that lie in a wide semi-circular valley that opens towards the southwest with the Orange River forming the southern boundary (Figure 3.1). The northern, eastern, and western flanks of the valley are formed predominantly by mudrock exposures, up to 160 m in height, of the Early (Scythian) to Middle (Anisian) Triassic Burgersdorp Formation. These exposures correspond biostratigraphically to the *Trirachodon-Kannemeyeria* (*T-K*) Subzone of the *Cynognathus* AZ, (Smith et al., 2020). The mudrock exposures are capped at 1479 m in the north and northwest by the prominent Bamboesberg Member sandstone that forms the lower part of the Molteno Formation (Hancox 1998, pp. 158-159). The mid-valley elevation is at 1303 m. The valley is bisected by a large ephemeral erosion “sluit” or “spruit” that runs from north to south towards the Orange River. Water from the catchment area in the north flows to the Orange River via this spruit resulting in numerous shallow gullies eroded into fossil-bearing mudrocks.

The bonebed under investigation occurs in dark reddish-brown (5YR 4/3) mudrock exposures around and to the north of an isolated hill on the farm Lemoenfontein. This hill is situated to the west of the erosion spruit and southeast of the main homestead on the farm (Figure 3.1). The Lemoenfontein hill forms the southernmost and lowermost of eight stepped plateaus that extend into the valley from the base of “Vaalkop”, the prominent hill on the highest of these plateaus that is capped by a sandstone that forms the base of the Indwe Member (middle Molteno Formation). Stratigraphically these steps extend from the Bamboesberg Member (basal Molteno Formation) in the north down towards the south on the western

side of the spruit (see Figures 3.1 and 3.2) to some 25 m above the informally named Eldorado marker (Neveling, 2004) or “middle marker” (Hancox, 1998). The plateaus, including Lemoenfontein hill are topped by erosion- resistant sandstones with the more easily- eroded mudrocks forming slopes that steepen with increased elevation up to the Bamboesberg Member.

The fossil-rich Lemoenfontein hill is topped by a 2.8 m thick multi-storied sandstone that has been erosively separated from the sandstone body that forms the lowest of the stepped plateaus, and it is now linked by a mudrock-dominated saddle exposure. The sandstone capping the lowest plateau is a 1 m thick tabular sandstone and it is likely to have originally been connected with the sandstone capping the Lemoenfontein hill. The basal surface of this sandstone corresponds stratigraphically (and in elevation) with the top surface of the sandstone that caps the hill. The interlinking saddle contains the main fossil-bearing dark reddish-brown (5YR 4/3) mudstone exposures, and there are parallel erosion gullies (depth of approximately 1 m – 1.5 m) on both east and west sides of the saddle. Similar erosion gullies exposing fossil-bearing reddish-brown (5YR 4/3) mudstones occur on the eastern flank of the main body of the ridge. The exposed mudrock slopes and surfaces are densely covered by a float of small to medium sized (3 to 15 cm) smooth-surfaced brown-weathering, ellipsoidal, calcareous nodules, and irregularly shaped sandstone slabs.

A sedimentological log of approximately 175 metres was measured through eight 3rd-order fining-upward cycles (Hancox, 1998; Miall, 2014) from the bed of the spruit up to the top of the first prominent sandstone of the Bamboesberg Member (Figure 3.2). Standard field methods, including Jacob’s staff and sight level as well as a Munsell geological rock-colour chart (2009 revision) were used to record a stratigraphic log to an accuracy of 5 cm (see Appendix A for the full log). The sedimentary rocks of this section are typical of the *T-K* Subzone of the *Cynognathus* AZ and consist mainly of massive or horizontally stratified mudrocks with inter-bedded sandstones in cycles of a few meters to tens of metres in thickness. The stratigraphic positions of all *in-situ* vertebrate fossils, burrow casts, fossil-bearing conglomerates and coprolites were mapped onto the log.

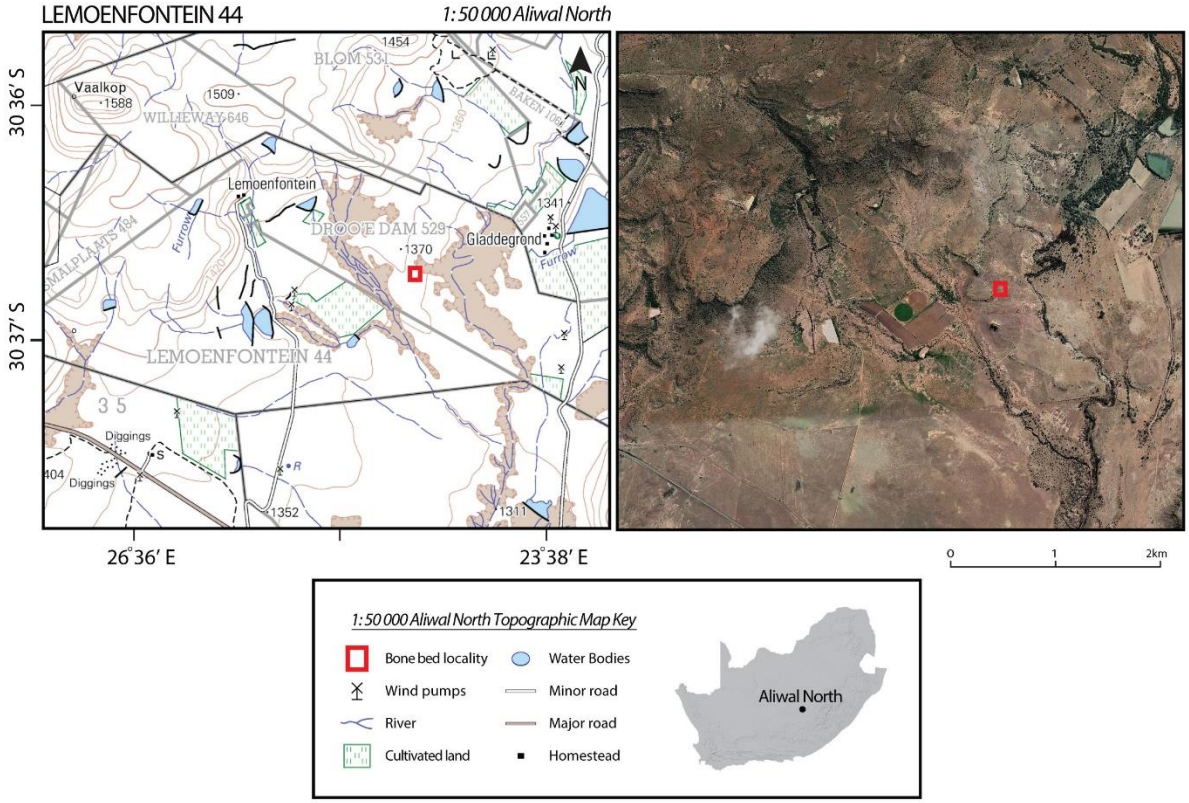


Figure 3.1: Geographic location of the Lemoenfontein bone accumulation site.

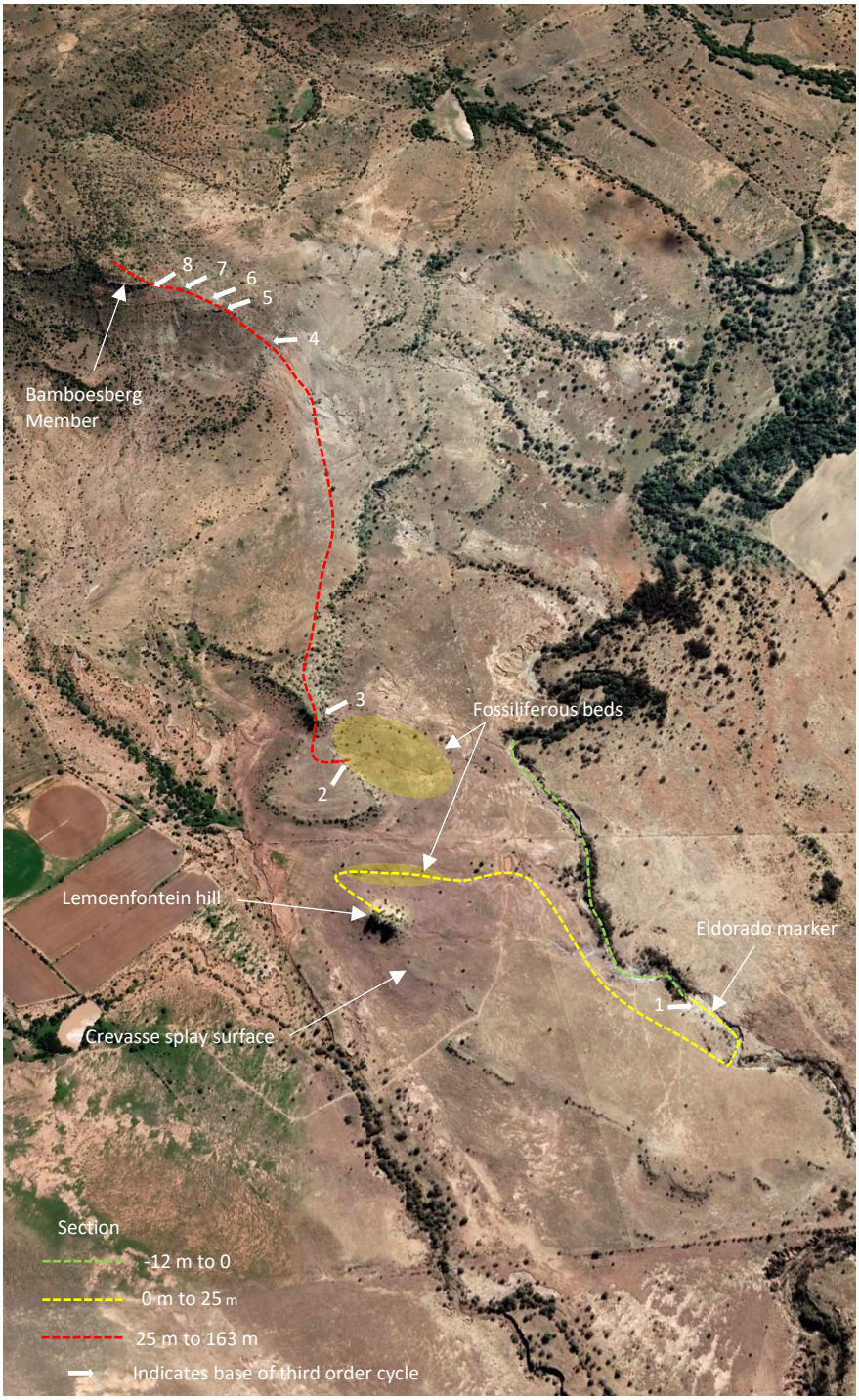


Figure 3.2: Google Earth Image of the locality and the measured section. The Lemoenfontein hill is in the foreground. This section crosses eight ledge forming sandstones each of which represents the base of a fining-upward third order cycle. The dashed lines show the path of the measured section from the channel of the spruit to the top of the hill and its extension from the second ledge forming sandstone (the stratigraphic equivalent of the top of the sandstone cap on the hill) up to the Bamboesberg Member. The final one being the Bamboesberg Member. The beds containing the bone accumulation are indicated in light yellow. Note that although the green portion of the section is following the downstream direction in the spruit, it is traversing upwards strategraphically due to the dip of the beds towards the southeast.

3.3 Basis for facies sequence description

The lithofacies codes, overbank facies associations and channel facies associations used to characterize the Lemoenfontein beds are provided in Table 3.1, Table 3.2, and Table 3.3, respectively.

Table 3.1: Lithofacies Classification

Facies Code	Lithofacies	Sedimentary Structure	Description*
Sp	Sandstone	Horizontal, parallel, planar stratification	Parallel and non-inclined (upper-phase plane bed high velocity laminar flow).
Sm	Sandstone	Massive	Crevasse splay.
St	Sandstone	Trough cross-stratification	Sets of arcuate foresets with curved bounding surface resulting from, downstream migration of 3-D bedforms over an uneven channel floor with scour depressions under moderate to high energy turbulent flow.
Ss	Sandstone	Scoured surface	Channel bottom, erosional bounding surface, commonly elongate depressions parallel to flow overlain with mud clast gravel lags resulting from high energy turbulent flow in channel thalweg.
Sl	Sandstone	Lenticular	Floodplain depressions and distributary channels.
Sr	Sandstone	Ripple cross-stratification	Moderate turbulent flow over rough sandy beds form downstream migrating ripples. With abundant sediment supply the migration of one ripple on the stoss side of another results in climbing ripple cross-stratification.
Spcb	Sandstone	Planar cross-stratification	Parallel, inclined planar foresets dipping in a single direction resulting from downstream migration of straight- crested bar forms on a flat surface.
Se_i	Sandstone	Massive to cross-stratified, fine to medium grained sandstone, containing intra formational clasts.	Clasts are predominantly mud- and siltstone, with varying amounts of intra-formational debris including fossil bone, coprolites and fragmented and particulate plant material. This facies is further characterised by the total absence of extra formational clasts. (Hancox, 1998).
SSp	Siltstone	Horizontal, parallel, planar stratification and lamination.	Parallel and non-inclined thin planar beds resulting from sedimentation of suspended silt during waning phase of unconfined overbank flows.
Mp	Mudstone	Horizontal, parallel, planar stratification and lamination	Parallel and non-inclined laminated thin beds that result from suspension settling of fine-size sediment or precipitation from solution, low energy-slack-water pools, ponds and lakes.
Mm	Mudstone or Claystone	Massive	Contain few or no visible internal lamina, overbank or abandoned channel deposits
Cc	Calcium carbonate - limestone	Nodules	Pedogenic or early diagenetic in origin

* Adapted for the Burgersdorp Formation from Li and Zhang (2017).

Table 3.2: Overbank facies associations (adapted from Colombera et al., 2013)

Overbank Facies Associations	Notation	Key Characteristic	Corresponding Subenvironment
Levee	LV	Levee elements typically take the form of tapering wedges that thin away from channel-belt margins and are slightly elevated above the rest of the floodplain; their base may be poorly defined, and internal accretion surfaces may offlap and/or downlap, showing dip angles up to 10°, although 2 to 5° are more common, associated with the sloping topography bordering channels; (palaeo) flow direction is usually oriented at high angle with the channel border. They have distinctive internal erosion surfaces.	Although levees may develop at smaller scales (for example, crevasse channel levees), LV elements usually represent the sedimentary and geomorphic expression of the most proximal over-bank deposition next to channel-belt margins. Smith (1990) distinguished inner- from outer -bank levees based on their facies sequence and the fact that outer-bank levees have more deeply incised scour surfaces
Crevasse splay	CS	These elements are tongue-shaped sandstone bodies bordering channel-belt margins. These bodies thin away from the channel margins, as they interfinger or grade laterally into other elements, and they tend to have flat, sharp, and slightly erosive bases although tabular stratification is common, internal accretion surfaces usually downlap, dipping at low angle to angle of repose, as they record the progradation of the splay onto the floodplain or into standing bodies of water. Upper surfaces are sharp and scoured by runoff channels in the proximal part and more interdigitating with mudrock distally.	These elements represent the sedimentary and geomorphic product of splay progradation and aggradation through the periodic unconfined flow from crevasse channels tapping discharge from the channel-belts during floods.
Distal overbank fines/ floodplain lake	DF	Interbedded thinning upwards fine sandstone-siltstone cycles and horizontally stratified fine-grained sandstones and contains thin siltstone lenses.	These elements are interpreted to be distal floodplain deposits, typically around the margins of distal floodplain lakes.
Proximal overbank fines	PF	These elements consist of tabular or prismatic siltstone bodies in which laterally persistent depositional increments tend to be vertically stacked and bounded by planar surfaces, demonstrating an overall aggradational character. Pedogenic alteration is common. Isolated calcareous nodules and nodular horizons are common. The presence of slickensides in the siltstone results in a crumbly weathering pattern. Well-developed B-horizons are present (Smith, 1990).	These elements are the sedimentary expression of vertically aggrading floodbasins, in which traction and suspension settling from episodic subaerial unconfined flows with a high sediment load is the dominant process; bedload deposition of mud- aggregates on the floodplain can also produce fine-grained floodplain units (Rust and Nanson, 1989).

Table 3.3: Channel Facies Associations (adapted from Colombera et al., 2013)

Channel Facies Associations	Notation	Key Characteristic	Corresponding Subenvironment
Vertically aggraded channel-fill	CHv	These elements are characterized by downstream-elongated incisional concave-upward bases, on which depositional increments are overall vertically-stacked, either concentrically or onlapping the channel margin, resulting in the dominantly horizontal orientation of planar, undulating or scour-like internal second and third order bounding surfaces. Although CH elements may be locally composed of small-scale downstream, oblique, lateral or upstream-accretion increments, they significantly lack the laterally persistent inclined accretion foresets that is typical of barform deposits.	These elements generally represent the overall aggradational infill of active low sinuosity and anastomosing channels.
Lateral accretion barform	CHl	These elements are characterized by sharp, sub-horizontal to slightly concave-upward, and often erosional bases, on which depositional increments are laterally stacked, with dip direction at high angle with respect to the palaeoflow direction, and dip angle up to 25°, generally showing off-lapped upper terminations and interdigitations with mudrocks of the levee facies.	These elements represent the infill of active channel belts by inner bank attached, laterally expanding and downstream migrating bars, most commonly typified by meander point bars.
Downstream accretion barform	DA	These elements are characterized by sub-horizontal to slightly concave-upward and often erosional bases, on which depositional increments are stacked at low angle with respect to palaeoflow, determining a dominance of low-angle downstream-dipping second and third-order bounding surfaces. DA elements may be locally composed of oblique, lateral, or upstream accretion increments, but the overall preponderance of downstream growth is their key character.	These elements represent the infill of active channel-belts by downstream-migrating bars typical of braided channel systems.
Chute channel fill	HO	This element type encompasses major scour-hollow fills, characterized by incisional concave-upward scoop-shaped bases, and by infill through accretion on inclined or horizontal surfaces or on a combination of both	These elements represent the infill of deeply incised trough shaped scours within channel belts, for example by the migration of mouth-bars into deep confluence scours or by infilling of flood-related scours during waning-flood stage. This is typical of an abandoned channel-fill common in meander cut-offs (ox bow lakes) and chute channels.

The description of the sedimentary rocks in the Lemoenfontein succession is based on the hierarchy of sedimentological cycles on the fluvial floodplain as defined by Miall (2014) as a framework. These cycles can briefly be summarised.

- First order cycles are formed by allogenic causes and typically represent the entire succession of gradual upward-fining deposition following an initial orogenic up-lift or unloading event. In the context of this study an example of a first order cycle is represented by the the deposition of Triassic sediments in the Karoo retro-foreland basin during periods of limited or no tectonic activity when the facies prograded basinward and resulted in the succession from the base of the Katberg Formation to the base of the Bamboesberg member of the Molteno Formation.
- Second order allogenic cycles reflect isostatic adjustments or major climate change events. Isostatic adjustments can occur due to major erosion and deposition events that leads to secondary loading or unloading in different parts of the floodplain. The paraconformable contact between the Burgersdorp and Molteno formations as evidenced on Lemoenfontein is a result of such a second order erosional cycle.
- Third order cycles are autogenetic to the fluvial system and refer to rapidly changing events that occur when geomorphic thresholds are exceeded after periods of metastable equilibrium. Such events are represented in the Burgersdorp Formation sedimentary rocks by the arrival, migration or abandonment of fluvial channels or avulsions that lead to rapid truncation of a particular mode of deposition on the floodplain. The third order fining upward cycles at Lemoenfontein will be used as the main framework for this facies description.
- Fourth order cycles are caused by periodic erosion or other detailed responses of the fluvial system to the changes brought about by the first to third order cycles. For example, these are represented by the various erosional surfaces in the rocks on Lemoenfontein.
- Fifth order cycles relate to seasonal variations such as rainfall or temperature and encompass other significant non-seasonal hydrological events such as major floods that occur significant time periods apart. The consequence of seasonality is present on Lemoenfontein in the form of evidence for seasonal variation of the groundwater table, rapid sediment deposition or long-term floodplain depositional stasis.

Interpretation of the palaeoenvironments and sub-environments is made for each cycle through the logged section. Specifically, lithofacies codes (Miall, 1985, Li and Zhang, 2017) are assigned to the third order sedimentary strata in the section. Using this lithofacies classification and the guidance provided in Smith (1990), the depositional facies are assigned to four facies associations (architectural elements as per Miall (1985)).

- Channel (CH) – Typical features are sandstone bodies with concave-up erosional bases, comprising variety of stacked bar complexes, single or multistoried accretion units, fingers, or lenses. Vertebrate fossils are rare and typically confined to basal lag conglomerates.
- Levee/Channel-Bank (CB) – Typically consists of rapidly alternating fine sandstone and siltstone beds overlying simple or multi-storied channel sandstones. Small scale scour surfaces overlain with lenticular sandstones frequently occur. Thin mudstone veneers cap siltstone and sandstone beds and record features such as rippled surfaces, run-off rills or sand-filled desiccation cracks. Fossils are common but are usually disarticulated single elements such as skulls or lower jaws.
- Proximal Floodbasin (PF) – Accumulated from the base of the meanderbelt slope on level areas of the floodplain. Consists of massive siltstones and minor mudstones that are horizontally or climbing ripple cross-stratified. Are frequently interrupted by thick (>1 m) crevasse splay sandstones with sharp non-erosional bases. Mudstone veneers may occur with run-off rills and sand-filled desiccation cracks. Isolated calcareous nodules and nodular horizons are common. The presence of slickensides in the siltstone results in a crumbly weather pattern. Well-developed B-horizons are present. Fossil skulls with and without articulated lower jaws are common and articulated skeletons within burrows can occur. Carbonate precipitation around fossil bones is common.
- Distal Floodbasin (DF) – These low accretion rate deposits occur in depressions far away from the main channel. These deposits consist mainly of thinly-bedded mudstones interbedded with thin siltstone and sandstone beds. Desiccation cracks are common, but calcareous nodules are rare. Vertebrate fossils are rare and consist of small, isolated elements. Soil formation is usually inhibited by a water table that is near the surface (Smith, 1990).

A similar definition is provided by Zwoliński (1992). Four distinct floodplain zones are introduced. Zone 1 is immediately adjacent to the river channel and shows the most varied lithology and morphology. Zone 2 consists mainly of clays and muds and covers most of the proximal side of the floodplain. Zone 3 corresponds to the distal part and contains very little depositional material. Zone 4 corresponds to higher valley walls or higher floodplain surfaces that only get inundated in the most severe of overbank floods. Also overbank flood events on a lowland meandering river floodplain are categorized into 6 distinct phases as follows:

- Phase 1 – Rising of water and bank modification stage;
- Phase 2 – Floodplain inundation and initial deposition;
- Phase 3 – Flood peaks and widespread transport and deposition;
- Phase 4 – Falling of water stages and high intensity deposition;
- Phase 5 – Cessation of overbank flow and final deposition; and
- Phase 6 – Post-flood transformation of overbank forms and deposits.

These definitions are very useful for the interpretation of the sedimentary rocks in the Lemoenfontein stratigraphic section, particularly for the detailed description of Cycles 0 and 1.

3.4 Description of the Lemoenfontein facies sequences

The detailed description of the sedimentary rocks in the Lemoenfontein succession that follows is based on the framework described above. The interpretation of the Lemoenfontein palaeoenvironments and sub-environments derived from this description is schematically presented in Figure 3.3 for the entire 175 m of the stratigraphic log.

Cycle 0

The entire Cycle 0 is exposed in the stream bed and banks of the Lemoenfontein spruit. The base of the incomplete Cycle 0 is covered in river sand and the section extends from the - 12 m to - 5 m in the measured section. The beds that make up this cycle are tilted due to a dolerite dyke intrusion. This dip is 9° with a strike of 115° (southeast). Therefore, to log this part of the stratigraphic section, measurements were taken in the downstream direction of the spruit (green dashed line in Figure 3.2). The lower 1.5 m consists of massively bedded siltstone. The light-grey (5Y 7/1) bottom half of this siltstone consists of 12 to 20 cm thick beds with clay veneered surfaces. In the pale-olive (5Y6/3) top half these surfaces become irregular and hummocky with a pustular matted texture. Continuing up section a 1 m thick light-grey (5Y 7/1) blocky-weathering fine siltstone contains a single reniform burrow cast followed by 50 cm of pale-olive (5Y 6/3) blocky-weathering coarse siltstone that contains one subcircular burrow cast that extends into the fine siltstone below. This is overlain with an upward-fining light-grey (5Y 7/1) siltstone (1.4 m thick) with two horizons of elongated prismatic peds 15 cm apart and an 80 cm thick reddish-brown (5YR 4/3) massive mudstone with rootlets and isolated calcareous nodules that are approximately 4 cm in diameter. Its top surface is bioturbated by numerous vertical *Skolithos* burrows, 5 to 9 mm in diameter. Directly above this mudstone is a strongly developed 20 cm thick, mottled silty mudstone bed consisting of elongated prismatic peds overlain by 1 m thick massively bedded reddish-brown (5YR 4/3) silty mudstone. The massive mudstone features abundant near vertical striated slip surfaces or slickensides that are randomly orientated. The beds containing the nodules and peds have undergone pedogenesis and are like those in Cycle 1 that host the tetrapod body fossils and burrow casts. An interpretation of these pedogenic features is provided in Section 3.4 below. The evidence of pedogenesis and seasonal water table variation (peds,

slickensides, calcareous nodules) leads to the interpretation that these mudrocks were deposited in a proximal overbank floodplain setting (PF facies association).

Cycle 1

Cycle 1 extends from the -5 m level up to the base of the second major sandstone ledge at 23.5 m (yellow dashed line in Figure 3.2). The base of Cycle 1 consists of a fine-grained, light-grey (5Y 7/1), multi-storied sandstone that extends from -4.4 m to 0 m. The first storey is 40 cm thick and horizontally (parallel) stratified. This storey overlies a pale-olive (5Y 6/3), 30 cm thick siltstone with a ped horizon at its base. The second 1 m thick storey is trough cross-stratified. The large (8 m wide, 50 cm deep) elongated trough cross-beds that occur lower down in this storey reduce in size near its top (4 m wide, 25 cm deep). Some horizontal plant stem compressions are also preserved on this surface. The third storey is 1.9 m thick. Its first 50 cm contains thin horizontal stratification and laminae. This is followed by thicker stratification and laminae in the next 25 cm. The top surface of this bed is bioturbated by *Skolithos.* This is followed by another 75 cm and 40 cm thick horizontally and thinly bedded elements topped by relatively large wavelength, low amplitude ("washed-out") mega ripples. The final storey is 1.23 m thick and is also horizontally stratified. This multi-storied sandstone (-4.4 m to 0 m) is interpreted to be the Eldorado marker of Neveling (2004). The justification of this interpretation and the biostratigraphic significance of this marker is explained Chapters 4 and 7. This sandstone complex is interpreted as the result of high energy in-channel sedimentation in a low- to medium-sinuosity river, and is assigned to the CH facies association.

A 60 cm pale-olive (5Y 6/3) siltstone bed showing blocky weathering occurs directly on top of the Eldorado marker. This is followed by a 1.2 m thick light-grey (5Y 7/1) sandy-siltstone. This bed hosts a large bifurcating reniform burrow cast (horizontal diameter = 16 cm and vertical diameter 11 cm). Above this bed is a 50 cm thick pale-olive (5Y 6/3) mudstone bed that contains slickensides. It is initially massively bedded but incipient horizontal stratification occurs towards its top. A 25 cm thick horizontally stratified light-grey (5Y 7/1) fine sandstone follows, which in turn is overlain with a 40 cm thick pale-olive (5Y 6/3) siltstone. Above this

siltstone is a 20 cm thick sandstone with an erosional base with runnels. This is followed by two sets of 60 cm thick siltstone/sandstone couples.

The rest of the Cycle 1 sedimentary succession is dominated by tabular massive dull reddish-brown (2.5YR 5/4) and greyish-red (5R 4/2) mudstone beds between 20 – 40 cm thick interbedded with a single yellowish-grey (5Y 7/2) 10 cm thick fine-grained sandstone of (interpreted to be a crevasse splay sandstone, CS, at 13 m of Figure 3.3). The mudstone beds display evidence of pedogenesis suggesting seasonal ground water level fluctuations. This is interpreted from the structure of the mature textural B-horizon, two well-developed calcareous nodular horizons, slickensides and cutan formation. Sandstone-filled desiccation cracks penetrating the massive mudstone are present at 9.5 m and 13 m. It is interpreted that the stacked mudstone beds were deposited rapidly in overbank traction and suspended load deposition from sediment-laden overbank floods, but the mature B-horizon and calcareous nodular horizons point to long periods of floodplain stasis with little or no sediment accumulation. The mudstones are very rich in tetrapod fossils. These fossils are predominantly articulated skulls with skeletons and isolated skulls with articulated lower jaws and are frequently coated in thin to thick calcareous skins. The mudstones also host tetrapod and other burrow casts. Based on the massive nature of the mudrocks, these are assigned the lithofacies code Mm. The presence of a crevasse splay sandstone, the evidence of pedogenesis and seasonal water table variation, and the other factors mentioned above, leads to the interpretation that these mudrocks have been deposited in a proximal overbank floodplain setting (PF facies association). Cycle 1 is the host of the bone accumulation that forms the focus of this study and is therefore discussed in detail in Section 3.4 where fourth and fifth order cycles are also considered. These mudstone beds are anomalously thick. To account for this, a possible mud aggregate depositional mechanism is explored further in the detailed description of Cycle 1 in Section 3.4.

Cycle 2

Cycle 2 extends from the base of the fine-grained horizontally (parallel) stratified sandstone at 23.5 m up to the base of the sandstone that forms the third significant ledge at 38 m. (Figure 3.*2*). This yellowish-grey (5Y 7/2) channel sandstone has an erosional base (with runnels) and consists of two storeys. There is a thin clay pebble conglomerate at the contact between the two storeys. The top surfaces show parting lineation. The uppermost storey contains large concave-up erosional channel surfaces which are filled with horizontally-stratified sandstone (lithofacies code Sp, see Figure 3.3). This sandstone complex is interpreted as the result of high energy in-channel sedimentation in a low- to medium-sinuosity river and assigned the CH facies association.

A 1 m thick, horizontally-stratified, fine-grained olive-grey (5Y 3/2) tabular sandstone (lithofacies code Sp) follows directly above the stratigraphic level of the channel sandstone. This interpreted crevasse splay sandstone has runnels and current crescents at its generally sharp base and *Skolithos* on its upper surface. By its nature, this sandstone is proximal overbank and assigned to the PF facies association.

The crevasse splay sandstone is followed by a 10 m thick interval of horizontally stratified dusky-red (5R 3/4) to olive-grey (5Y 3/2) mudstone beds (lithofacies code Mp). The lower 2 m hosts isolated oblate and irregular-shaped calcareous nodules. Due to its vertical superposition on a crevasse splay sandstone, as well as the evidence for pedogenesis, this mudstone interval is interpreted to be deposited in a proximal overbank environment and assigned PF facies association. No vertebrate fossils were found in Cycle 2.

Cycle 3

Cycle 3 extends from 38 m to about 55 m up to the base of the sandstone assembly that form the fourth prominent ledge in the succession. The base of Cycle 3 consists of a 2.8 m thick, olive-coloured (5Y 5/4), fine-grained sandstone that is multi-storied. The different storeys have different structures and textures; from the bottom up – mudstone flakes, a prominent

concave-up erosional channel surface which is filled with planar stratified sandstone, trough cross-stratification, diagenetic concretions, erosional contact surfaces, rib and furrow structures with a final transition from horizontal to massive stratification near its top (assigned to the lithofacies codes St, Sp, Sm and Ss). This sandstone is interpreted to be part of a medium- to high-sinuosity channel facies assemblage (CH).

This channel assemblage is followed by a 14 m thick mudrock interval that is dominated by olive-coloured (5Y 5/4) mudstone beds. Interbedded in this mudstone units are two crevasse splay sandstones (one planar- and one massively-bedded) and a single siltstone bed showing blocky weathering (lithofacies codes Sp, Mp, SSp and Sm.) The mudstone is thickly-bedded (10 - 30 cm thick tabular units) and contains features such as slickensides, colour mottling and calcified fissures. This mudstone interval is interpreted to have been deposited in the proximal floodplain environment and assigned the PF facies association. No tetrapod or other body fossils have been found. *Skolithos* is the only trace fossil recorded.

Cycle 4

Cycle 4 extends from 55 m up to the base of the fifth prominent ledge-forming sandstone at 105 m. The base of cycle 4 consists of an 8.5 m thick, olive (5Y 5/4) to olive-green coloured (5GY 3/2), five storied fine-grained sandstone body, see Figure 3.3 for a schematic representation (the full stratigraphic log in Appendix A shows each bed individually). The lower three stories are horizontally stratified, ripple cross-stratified and horizontally/massively stratified, respectively. The fourth storey is horizontally stratified with prominent scours (containing mudrock pebbles) at the base abruptly changing to trough cross-stratification near the top. The fifth sandstone storey in this complex is massively-stratified. This multi-storied sandstone contains the lithofacies Sp, Sr, Sm, Ss and St and is interpreted to be the in-channel deposits of a vertically accreted low sinuosity river and thus assigned to the CH facies association.

This channel sandstone complex is overlain by 6.5 m of olive-green (5GY 3/2) and red (5R 3/4) thickly bedded siltstone. This siltstone contains several fine sandstone lenses and a

prominent concave-up scour surface that is filled with massively bedded siltstone (lithofacies codes SSp, Sl, Sp). Near the top it undergoes blocky-weathering, and it is capped by a 10 cm thick fine-grained sandstone displaying vertical root moulds. This interval has yielded some medium-sized dicynodont vertebra. Considering that the siltstone and fine sandstone beds overlay a multi-storied channel sandstone, the presence of a scour surface overlain with lenticular sandstones and the presence of disarticulated single element tetrapod fossils, this architectural element is interpreted to be levee/channel-bank deposits of the LV facies association.

The measured section from 70 m up to 105 m consists largely of thickly bedded mudstone. Up to the 82.5 m mark, the colour alternates between olive-green (5GY 3/2), medium-grey (N 5), red (5R 3/4) and olive (5Y 5/4). Colour mottling is also present. The mudstone contains an amalgamated calcareous nodular horizon (at 76.8 m Figure 3.3 and Appendix A), desiccation fissures, slickensides and is interbedded with some thin (<15 cm thick) tabular sandstone beds. This interval is lithofacies codes Cc, Mp and Sp and interpreted to have been deposited on the proximal floodplain and is here included in the PF facies association. Above 82.5 m the mudstone varies in colour from olive (5Y 5/4), red (5R 3/4), light-grey (N 7), reddish-brown (10R 4/3) and greyish-olive (10Y 4/2). It is interbedded with several thinning upwards sandstone-siltstone cycles and horizontally stratified fine-grained sandstones and contains thin siltstone lenses at the top (lithofacies codes Mp, SSp and Sp). These mudstone beds also delivered several isolated tetrapod skulls and disseminated fish scales and bones. Based on these characteristics, this section is interpreted to be distal floodplain deposits and grouped into the DF facies association.

Cycle 5

Cycle 5 extends from the base of the fifth ledge at 105 m (see Figure 3.3) up to the base of the next prominent ledge-forming sandstone at 110 m. The lower most unit in this short 5m thick cycle is a 1.5 m thick light-grey (N 7) sandstone bed that fines upward from a conglomeratic erosive base to a fine-grained sandstone with a sharp top surface. The sandstone is trough cross-stratified and contains dispersed pebbles (lithofacies codes St and

Sr). The clay pebble conglomerate at the base thickens in the deeper scours and contains scattered temnospondyl dermal bones. The sandstone body is topped by a 25 cm thick, yellow (5Y 6/4), ripple cross-stratified sandstone. This facies association is interpreted to be a single storey high sinuosity channel deposit (CH). The sandstone is followed by a thickly-bedded red (5R 3/4) mudstone bed (Mp), 3.2 m thick. This bed is interpreted as due to proximal floodplain deposits and assigned to the PF facies association.

Cycle 6

Cycle 6 extends from the base (110 m) of the sixth ledge forming sandstone up to the next sandstone (126.4 m). The first 10.6 m of this succession consists of a complex succession of various sandstone geometries. The first 2.2 m thick yellow (5Y 6/4) fine-grained sandstone is trough cross-bedded and has an erosional basal surface overlain by a cobble-sized mud clast conglomerate that contains temnospondyl bones. This sandstone is followed by a double set of stacked, massive, tabular sandstone beds, a rooted sandstone bed, a second intraformational claystone conglomerate, two sets of thin trough cross-bedded olive-grey (5Y 4/1) crevasse splay beds, two ripple cross-stratified sandstones (containing mud clasts), several stacked medium grained conglomeratic sheet flood deposits, a red (5R 3/4) siltstone bed containing mud flakes, and finally topped with a trough cross-bedded sandstone bed. This succession of St, Sr and SSp lithofacies is interpreted to be a complex interdigitation of in-channel, levee and proximal overbank deposits and is assigned to the levee/channel-bank (LV) lithofacies association.

The cycle is completed by a 5.8 m thickly-bedded red (5R 3/4) mudstone (Mp) considered to be part of the proximal floodplain facies association (PF).

Cycle 7

Cycle 7 extends from the base of the first medium-grained sandstone at 126.5 m up to the base of the final ledge forming sandstone assembly in the succession at 150 m. The basal sandstone does not form a prominent ledge, but since it is the first medium-grained

sandstone, it represents a noteworthy change in fluvial style. This light-grey (N 7) sandstone (1 m thick) has an erosional base and is trough cross-bedded (St). It is overlain by a horizontally-stratified medium sandstone (Sp) with an undulating top surface. This set of sandstones is interpreted as the in-channel deposits of a low-sinuosity river (CH).

The remainder of cycle 7 consists of red (5R 3/4) to olive (5Y 5/4) thickly-bedded mudstones. Interbedded with the mudstone is a 0.5 m thick fine sandstone bed, a horizon containing fine sandstone lenses (Mp, Sl and SS), and a 0.5 m thick rooted siltstone B-horizon. This association of mudrock facies is interpreted as having accumulated in the proximal floodplain environment (PF).

Cycle 8

Cycle 8 is incomplete and is made up of an upward-coarsening succession of thickly-stacked sandstone beds extending from 150 m up to the base of the first Bamboesberg Member sandstone at 154 m (Figure 3.3). The set of stacked sandstones is light-grey coloured (N 7) and fine-grained and consists of alternating horizontally and massively stratified sandstones (Sm and Sp). There is a mudstone cobble conglomerate at the base of the first of these with conspicuous iron-manganese secondary mineralization. These strata are interpreted as the in-channel deposits of a low-sinuosity river, possibly braided in places, and thus assigned to the CH facies association.

Bamboesberg Member

The first Bamboesberg Member sandstone occurs at 154 m. Up to 158 m, it consists of light-grey (N 7) medium-grained sandstone beds, two beds of trough cross-bedded sandstones (the cross-stratification is open and large in the lowest of these), with iron/manganese staining and two beds of massively bedded sandstone (St and Sm). The next sandstone bed above 158 m is 2 m thick, olive coloured (5Y 5/4) and coarse-grained. It is massively stratified (Sm) with a scoured lower surface and contains isolated mudstone pebbles. The sandstone is wacky, dirty and contains opaque minerals. These beds record a change in depositional style

as reflected in the large size of the trough cross-stratification and the coarseness of the grains. This is again interpreted to be in-channel longitudinal barforms of a low sinuosity river and assigned to CH facies association.

At 160 m (see Figure 3.3) the sandstones record a distinct change in lithology and texture. The uppermost part of the measured section comprises two coarse-grained yellow (5Y 6/4) sandstone beds. The first 1.5 m is planar cross-stratified (Spcb) with 1.5 m thick foresets and it has a pebble conglomerate top surface. The second is medium grained, trough cross-bedded (St), and yellow (5Y 6/4) in colour. Its top is capped with a pebble clast conglomerate heavily cemented in iron/manganese.

The abrupt transition at 154 m from fine-grained to medium-grained sandstones (followed by coarse-grained sandstone above 160 m) marks the paraconformable contact between the Burgersdorp and Molteno formations. The sandstone beds recorded above 154 m on the measured section are therefore at the base of the Stormberg Group. The sandstone facies association is clearly in–channel (CH and DA) however the para-unconformity is also coincident with a subtle but significant change in interpreted fluvial style from low sinuosity to braided river channel morphology.

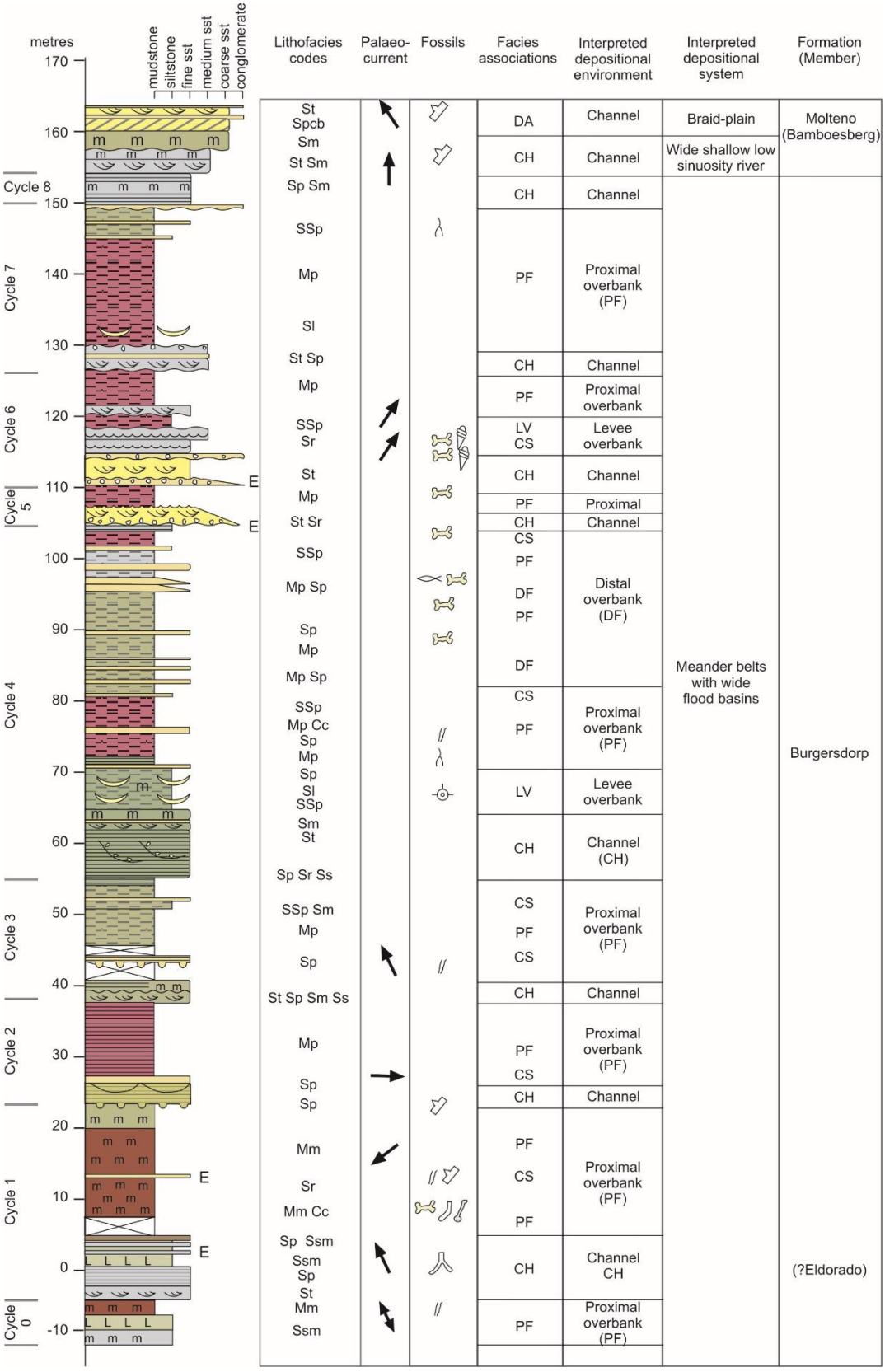


Figure 3.3: Condensed stratigraphic section showing the third order cycles, lithofacies codes, interpreted facies associations, depositional environments, and depositional system. The lithofacies codes, overbank facies associations and channel facies associations used to characterize the beds are provided in Table 3.1, Table 3.2 and Table 3.3, respectively. The legend for the sedimentary structures is provided in Appendix A.

3.5 Detailed description and interpretation of the bonebed interval of Cycles 0 and 1

The massive mudstone beds in Cycle 1 host the anomalously rich accumulation of tetrapod fossils and burrow casts that are the focus of this study. The detailed sedimentological, palaeopedological, ichnological and taphonomic observations of these beds presented here provide insights and conclusions about the palaeoenvironment and other conditions that led to the genesis of the bone accumulation. The stratigraphic log in Figure 3.4 was measured to an accuracy of 5 cm and contains two expanded sections and palaeoenvironmental interpretations. The first interval extends from -12 m to -5 m (Cycle 0) and the second is an 8 m interval that extends from about 1 m below the first occurrence of tetrapod fossils to 2 m above the last (part of Cycle 1).

The mudrock and sandstone beds that host the fossil accumulation show distinct signs of having undergone pedogenesis on the floodplain under conditions of seasonal variation in rainfall and groundwater level. The features recorded in the rocks include structural B-horizons, C-horizons, calcareous nodular horizons, slickensides, cutans, peds, bioturbation and evidence of flash flood and sheetwash events. The description of these beds lays emphasis on these palaeosol features and therefore a brief description of each is appropriate.

Soil formation or pedogenesis is the modification of newly deposited sedimentary strata by various processes such as bioturbation by plant roots or animal/insects burrowing, the preservation of these bioturbation structures, the eluviation or leaching of clays from the upper horizons, resultant clay accumulation in lower horizons and the formation of calcium carbonate nodules or horizons and the final preservation as a palaeosol (Retallack, 1988; Alonzo-Zarza, 2002; Tabor and Myers, 2015; Tabor et al., 2017). Typical modern soil profiles consist of (from the top down).

- A-horizons are uppermost and are zones of accumulation of organic material that originates from the decomposition of plants and plant roots. A-horizons are often removed by erosion before preservation in the palaeosol profile. A-horizons undergo

leaching or eluviation of material such as clays or organic colloids that relocate and accumulate in lower horizons.

- B-horizons are zones of accumulation of material (illuvial clay, calcium carbonate) leached from the A-horizon and/or the development of ped structures. The development of ped structures usually replaces the structure of the original parent material. Transitional horizons can also exist. BA-horizons are transitional between A and B but more like B- and BC-horizons are transitional between the B-horizon and the C-horizon. In this case the parent material of the B-horizon resembles the C-horizon material (Tabor et al., 2017). Peds are the stable structures of soil material that are bordered by cracks or voids (Retallack, 1988). These voids are often filled and lined by clays that have washed down from the A-horizon to form cutans (clay skins). The voids are formed by shrinking and swelling of clays during seasonal variation of soil humidity. Several different ped structures have been identified (Retallack, 1988), but the most relevant form for this study is prismatic (elongate, flat top, with vertical cutans).
- C-horizons consists of the originally deposited material that is not significantly weathered. It is a zone of incipient pedogenesis. It may or may not resemble the original sediments that form the parent material for A-, B- and C-horizons. C-horizons typically occur under B-horizons and can have calcium carbonate accumulations (nodular horizons).

More complex stacking patterns can develop depending on soil aggregation rates and truncation events (Marriot and Wright, 1993; Tabor and Myers, 2015). *Simple* profiles develop when A-horizons are situated on top of B-horizons during periods of no or very slow deposition. This is typical in avulsion belts where deposition events are rare. *Compound* profiles are similar, but with stacked A and B profiles interrupted by thin un-weathered material (C profiles). This happens when long periods of slow or non-deposition are interrupted by short periods of fast aggregation. *Composite* profiles occur when the B-horizon of the upper profile directly overlaps with the A or B profile of the underlying profile with little or no material in between. *Cumulate* profiles occur when there is continuous, slow

aggradation resulting in thick B-horizons that overprint the characteristics of the overlying A-horizon. This is typical of overbank deposits in floodplain environments.

The structure, morphology and chemical composition of these palaeosols can be used as proxies for the palaeoclimate (Marriot and Wright, 1993; Tabor and Myers, 2015). The presence of calcareous nodular horizons are important indicators of seasonality in the palaeoenvironment, seasonal variation in rainfall and groundwater table (Marriot and Wright, 1993; Alonzo-Zarza, 2002; Tabor and Myers, 2015) as well as the rates of sediment accretion (Wright, 1990; Marriot and Wright, 1993). It is therefore important to accurately record the maturity/size and depth of these horizons.

Shrink-swell features such as slickensides, desiccation cracks and cutans, are important indicators of seasonal variation in rainfall and soil humidity. The depth of desiccation cracks and the depth of slickenside horizons are indicators of climate, with palaeoenvironments with higher rainfall and seasonality leading to deeper development of slickensides (Tabor and Myers, 2015).

Other factors such as type and depth of rooting, palaeosol maturity, clay mineralogy, stable isotope geochemistry, etc. also provide insights into the palaeoenvironment (Tabor and Myers, 2015, and the references therein).

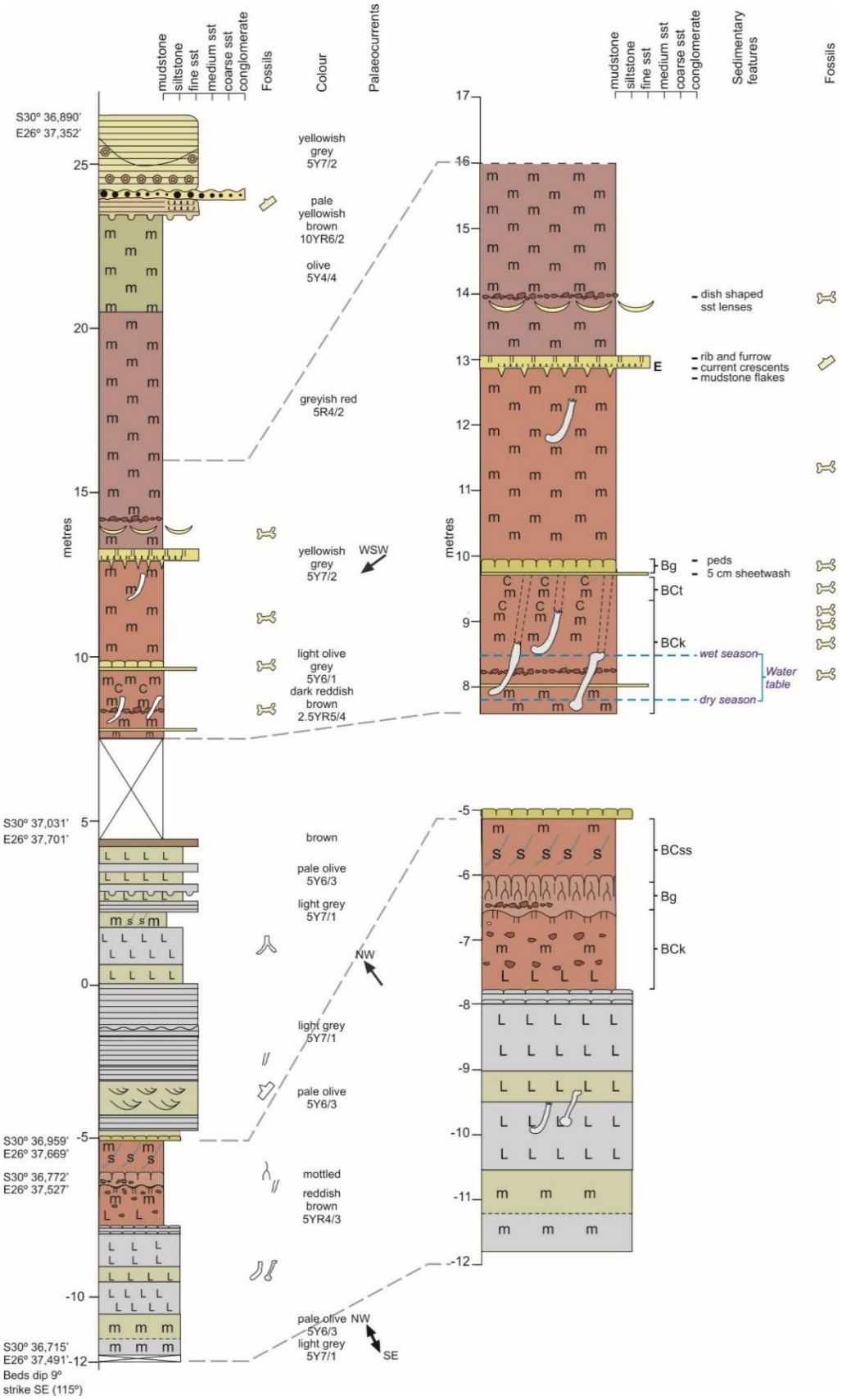


Figure 3.4: Stratigraphic section of the beds that host the vertebrate fossil and burrow accumulation (-12 m to 26 m). Expanded sections provide an interpretation of the pedogenic sedimentary structures, the seasonal water table variation and the stratigraphical extent of the two types of burrow casts in the fossil hosting beds. The legend for the sedimentary structures is provided in Appendix A.

The detailed description of the Lemoenfontein stratigraphic section starts in the channel of the spruit (from -8 m to -5 m, Figure 3.5). The first bed is an 80 cm thick reddish-brown (5YR 4/3) massive mudstone that is bioturbated by rootlets and it contains isolated calcareous nodules that are approximately 4 cm in diameter. Some thin claystone horizons are interbedded in this mudstone and its top surface is bioturbated by *Skolithos* burrows, 5 to 9 mm in diameter (Figure 3.5 B). This massive mudstone bed is interpreted as having been deposited by periodic overbank flood events in a proximal floodplain setting. During each periodic inundation, the mudstone was deposited during the Phase 4 "Falling water stages and high intensity deposition" (Zwoliński, 1991) followed by the finer claystone deposition during Phase 5 "Cessation of overbank flow and final deposition" (Zwoliński, 1991). The palaeosurface then became bioturbated by infaunal vertical burrowing invertebrates – likely suspension feeding worms – to leave behind the unlined shallow *Skolithos* tubes. As discussed below, this bed underlies a mature structural B-horizon and consists of material resembling the original C-horizon material and is therefore interpreted as a BC-horizon that has developed a Stage II palaeocalcrete i.e., discrete well-cemented nodules (Gile et al., 1965; Machette, 1985; Retallack, 1988; Wright, 1990; Tabor and Myers, 2015). The master horizon descriptor for a horizon that contains carbonate nodules or concretions can be modified using the "k" modifier (Tabor et al., 2017). This horizon is assigned the horizon description BCk (Tabor et al., 2017).

Directly above this mudstone is a strongly developed 20 cm thick, silty mudstone bed (Figure 3.6) consisting of elongated prismatic peds interpreted as a palaeovertisol (Tabor et al., 2017). This horizon is strongly mottled. The dominant matrix is weak-red (10R 4/3) while the mottling is greyish-blue (5PB 7/2) and light-grey (N 7). This type of low chroma mottling is consistent with a reduction of and removal of iron or manganese through gleying. Gleying is caused by seasonal variation in soil water content with alternate periods of saturation and drying leading to reduction and oxidation, respectively. There is a correlation between the degree of mottling and the intensity of this seasonal variation in water saturation (Tabor et al., 2017). Using the criteria of Retallack (1988) the mottling can be classified as follows: Contrast = Prominent; Abundance = Common; and Size = Medium to coarse.



Figure 3.5: (A) BCk-horizon consisting of massive mudstone. Measuring staff = 1 m. (B) Skolithos *bioturbation of surface (multiple light-grey disks, < 0.5 cm diameter, two examples arrowed). (C) Discrete Stage II calcareous nodules. Scale bars = 5 cm.*

This bed is interpreted to be a structural B-horizon of a palaeovertisol with a well-developed prismatic structure (Retallack, 1988, Tabor et al., 2017). The horizon description modifier “g” is used for horizons that have undergone gleying leading to mottles, this horizon is assigned to the horizon descriptor Bg (Tabor et al., 2017). The peds were formed by shrinking and swelling of clays during seasonal variation of soil humidity. The top surfaces of the peds are bioturbated by fine calcified rootlet rhizoliths. The original A-horizon that existed above this B-horizon has been eroded.

A 1 m thick reddish-brown (5YR 4/3) silty mudstone that is massively bedded overlays the textural B-horizon (Figure 3.6). The structure of this bed features abundant smooth, striated slip surfaces or slickensides that are randomly orientated (Figure 3.7). Slip surfaces can be caused by shrink and swell processes due to seasonal variation in rainfall (Retallack, 1988; Tabor and Myers, 2015) or can also result from tectonic activity. Due to the random orientation of the slickensides in this bed, as opposed to being aligned in a preferred attitude, and the fact that they are lined with a thin veneer of claystone, it is concluded that they have however been caused by ancient shrink and swell processes. The depth of slickenside horizons below the palaeosurface can be an indication of the palaeoclimate i.e., palaeoenvironments with higher rainfall and seasonality lead to deeper development of slickensides (Tabor and Myers, 2015). In this case the top of the bed is overlain with alluvium and the slickensides occur mostly about 0.5 m below the top surface. These slickensides were formed in a clay-rich alluvium with a shallow water table. Due to the presence of the slickensides, this bed is interpreted to be a BC transitional horizon. BC-horizons are transitional between the B-horizon and the C-horizon (with the B-horizon material resembling the material of the C-horizon). A C-horizon with slickensides is usually described as a Css-horizon (Tabor et al., 2017) so in this case the notation BCss is adopted.

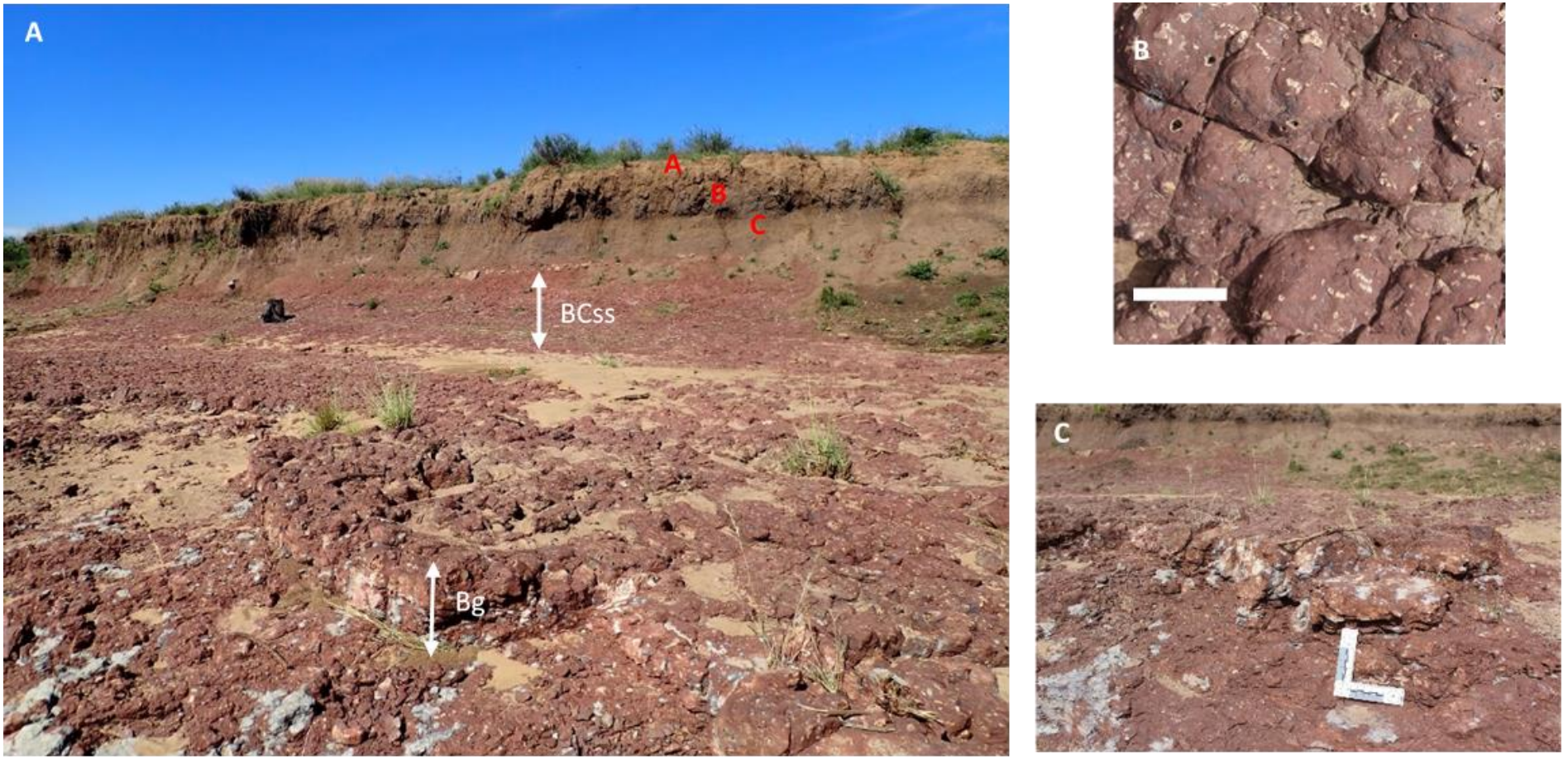


*Figure 3.6. (A) Strongly developed structural Bg-horizon consisting of prismatic peds and BCss-horizon with slickensides. Note the modern alluvium consisting of **A**, **B** and **C** soil horizons overlying the ancient palaeosols. (B) Calcified rootlets. (C) Mottling. Scale bar in B = 5 cm. Ruler in C = 10 cm x 10 cm.*

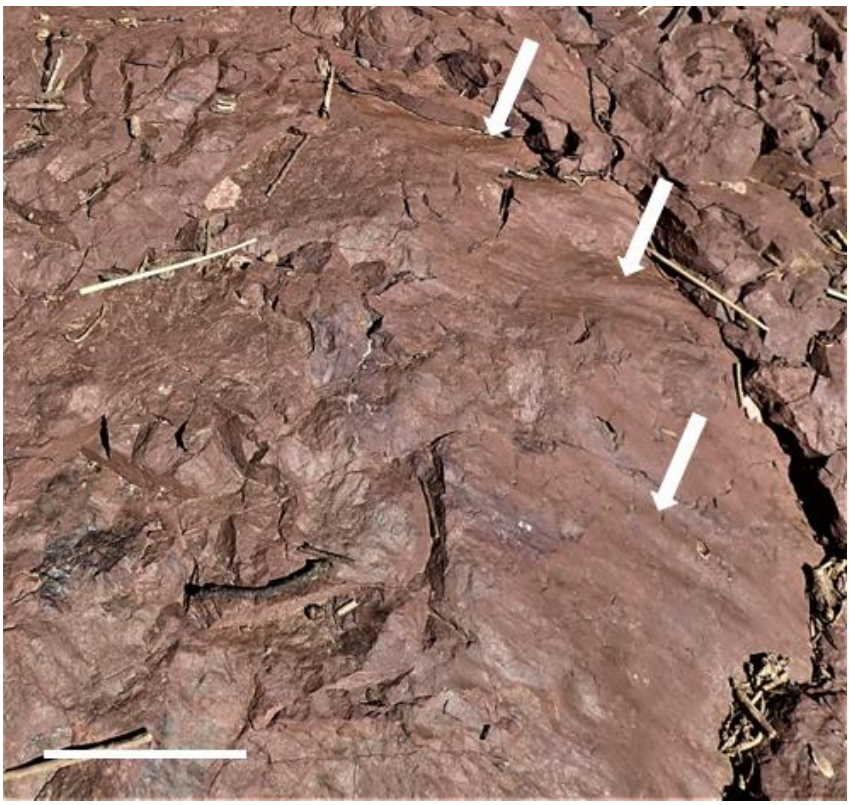


Figure 3.7: Claystone coated slickensides in massively bedded silty mudstone. These pedogenic slickensides are convex-concave slip surfaces that form during expansion/contraction in expansive clay soils such as vertisols. Scale bar = 10 cm.

The stacking pattern of this 2 m thick sequence of pedogenic horizons is from the top down (Figure 3.5):

- BC transitional horizon with slickensides (BCss);
- B-horizon with well-developed prismatic peds (Bg); and
- C-horizon that contains Stage II calcareous nodules (BCk).

This type of stacking corresponds to a *Compound* profile except that the A-horizon has not been preserved and that the B-horizons are interrupted by *thick* (instead of thin) un-weathered material (C profiles). The structural features such as peds form relatively quickly in vertic soils (5-200 years), while Stage II carbonate nodules (cm scale) require hundreds to thousands of years to form (Marriot and Wright, 1993). This in turn implies that the accumulation rate of sediments must have undergone long periods of stasis or slow accumulation. Slickensides can form when floodplain accumulation rates are 2 mm to 5 mm

per year, while the formation of carbonate nodules requires rates less than 2 mm per year (Marriot and Wright, 1993). The following depositional history can be reconstructed for this 2 m thick palaeosol interval beds.

- The mud and clay sediments that make up the lower B-horizon and the C-horizon below were deposited rapidly by periodic overbank floods (5^{th} order events) in a proximal floodplain setting during the waning (Phase 4 and Phase 5 of Zwoliński, 1991) of each flood event. In particularly severe flood events, significant amounts of sediments can be deposited (of the order of 1 m) (Retallack, 1988).
- Following deposition, a long period of hundreds to thousands of years followed when sediment accumulation was less than 2 mm per year. This period of stasis allowed the formation of cm scale Stage II carbonate nodules in the BCk-horizon and the formation of the strongly developed overlying Bg-horizon (Marriot and Wright, 1993). Such interruptions of deposition can result from avulsion events where the course of the river flow is dramatically redirected on another part of the floodplain and essentially change the areas undergoing proximal deposition into distal zones that undergo very slow deposition (Zwoliński, 1991; Tabor and Myers, 2015).
- The final deposition of the BC-horizon recorded in this part of the section also occurred rapidly by periodic overbank flood events in a proximal floodplain setting. The presence of slickensides indicates that this period of fast deposition was followed by 5 to 200 years of deposition at rates below 5 mm per year (Marriot and Wright, 1993) with significant seasonal variation in rainfall.

Next, the discussion considers the sedimentary rock deposits some 13 m above this palaeovertisol that host the tetrapod body and trace fossils that form the focus of this investigation (Figure 3.4 and Figure 3.8). The interval of Cycle 1 from 7.5 m to 23.5 m (just below the prominent channel sandstones forming the base of Cycle 2) consists of massively bedded dull reddish-brown (2.5YR 5/4) mudstone (7.6 m to 9.2 m) and greyish-red (5R 4/2) silty mudstone (9.2 m to 23.5 m). This argillacous interval is interpreted as having been deposited by periodic overbank flood events in a proximal floodplain setting during the waning (Phase 4 and Phase 5 of Zwoliński, 1991) of each flood event. However, this interpretation does not fully explain the anomalously thick nature of the mudstone beds.

Mudstone deposits in the distal region of a floodplain are usually thinly bedded and occur as minor beds in the proximal region that is usually dominated by massive siltstone beds (Smith, 1989). Rust and Nanson (1989) provide a plausible explanation. Pedogenically modified, sand-sized mud aggregates can form on clay-rich alluvial floodplains that are subjected to seasonal drying. The alternating wet-dry seasons cause shrinking and swelling of clays leading to vertisol formation. The mud aggregates are formed as a direct result of the pressures created by shrinking clay when drying. The mud aggregates are then available for transport as bedload from regions of the floodplain undergoing down wasting, which in turn leads to sheet flood deposits on braid plains. The interpretation is made here that similar sheet flood deposits of mud aggregates can occur on proximal floodplain regions during frequent overbank flood events. Under these circumstances, thick clay-rich mud beds are formed. After deposition, compaction and the addition of suspended clay, quickly destroys the aggregate structure of the sediments (Rust and Nanson, 1989). As discussed below, there is also evidence of floodplain down wasting recorded in the sedimentary rocks in the stratigraphic section under consideration here section (eroded A-horizon, eroded top surface of B-horizon, long periods of no floodplain deposition).

At 7.8 m a thin (2 to 3-cm thick) light olive-grey (5Y 6/1) fine-grained sandstone sheet occurs at the base of which there are some vertical fissures that are also in-filled with the same sandstone to form very thin (< 1 cm thick) vertical sheets of sandstone. These fissures are aligned parallel to each other and do not appear to form polygonal patterns. They are thus suspected as having been tectonically induced.

A continuous greyish-red (5R 4/2) carbonate horizon consisting of coalescing nodules, considered to be Stage III palaeocalcrete, following Machette (1985), Retallack (1988), Wright (1990) and Tabor and Myers (2015), occurs at 8.2 m, Figure 3.8. The nodules in this horizon are less than 8 cm in diameter and although they coalesce, they do not yet form a fully cemented sheet. The host matrix of this nodular horizon is largely unmodified or weathered and would usually be considered a C-horizon. However, since it contains the nodules, it is considered to be a transitional B-horizon consisting mostly of the C-horizon parent matrix. As discussed above, in this case a BC label can be adopted (Tabor et al., 2017). The master

horizon descriptor with for a horizon that contains carbonate nodules or concretions can be modified using the “k” modifier (Tabor et al., 2017). Therefore, the notation BCk is adopted to describe the host matrix of the carbonate horizon. This calcareous nodular horizon hosts the first *in-situ f*ossils in the section and marks the base of the bonebed (see Figure 3.4). These fossils occur as skulls with articulated lower jaws as well as skulls attached to partially- and fully- articulated skeletons. Many vertebrate burrow casts originate from the mudrocks immediately above this nodular horizon and appear to terminate just below it. Two types of burrow casts occur here; the first has a bi-lobed, reniform cross-section with characteristic linear surface ridges (interpreted scratch marks) and the second type has a sub-circular cross-section and displays a knobby outer surface texture. From about 9.2 m to 9.7 m the mudstone is replaced by a silty-mudstone that contains claystone-lined cutans characteristic of the textural BC transitional horizon of a palaeovertisol (Tabor et al., 2017). The horizon description modifier “t” is used for B-horizons within which clay-sized materials have accumulated and so the descriptor BCt is adopted (Tabor et al., 2017).

A light olive-grey (5Y 3/2) fine sandstone sheet (5 cm thick) occurs at 1.5 m above the calcareous nodular horizon at 9.7 m (Figure 3.9). It displays very thin, muddy horizons and has vertical desiccation cracks at its base. The burrows and cracks are filled with the same fine olive-grey (5Y 6/1) sandstone, and it is likely that the same sheet flood event that deposited the sandstone sheet also in-filled the burrows.

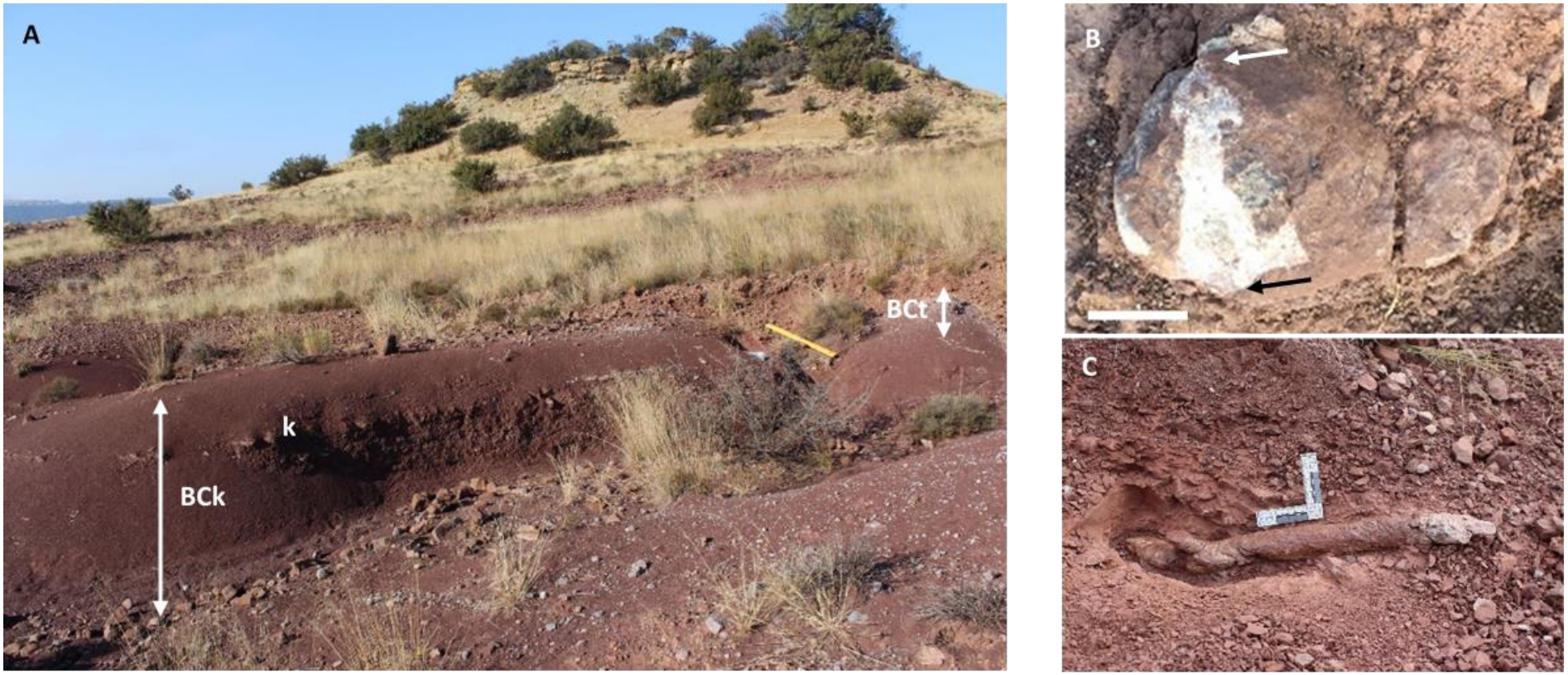


Figure 3.8: (A) BCk-, BCt- and calcareous nodular horizon, k. (B) Embedded procolophonid skull in nodular horizon (white arrow = snout, black arrow = back of skull). (C) Reniform burrow penetrating nodular horizon. Ruler in C = 10 cm x 10 cm, scale bar in B = 3cm.



Figure 3.9: (A), (B) Sandstone sheet, SS (arrowed), above calcareous horizon, BCk. (C) Dish- shaped sandstone lens (1–2 m diameter). Scale bar in B and C = 20 cm.

About 20 cm above this sandstone (at 9.9 m) a strongly developed but thin (10 to 15 cm) silty mudstone bed occurs that consists of elongated prismatic peds (Figure 3.10). The top surface of this bed has been eroded and does not show significant evidence of calcified rootlets or rhizoliths. This horizon has undergone a significant degree of gleying. The original colour of the parent matrix has entirely been removed leaving only the low chroma mottling (mostly light olive-grey (5Y 6/1) with some light brownish-grey (5YR 6/1)) that is consistent with a complete reduction of and removal of iron or manganese (Tabor et al., 2017). As discussed before, gleying is caused by seasonal variation in soil water content with alternate periods of saturation and drying leading to reduction and oxidation respectively. There is a correlation between the degree of mottling and the intensity of this seasonal variation in water saturation (Tabor et al., 2017). Using the criteria of Retallack (1988) the mottling can be classified as follows: Contrast = Prominent; Abundance = Many; and Size = Coarse. The erosion of the top surface and the extensive degree of gleying suggest that the surface must have remained subaerially exposed for a significant time during which there was down wasting of the floodplain. This bed is interpreted to be a structural B-horizon of a vertisol with a well-developed prismatic structure (Retallack, 1988, Tabor et al., 2017). The horizon description modifier “g” is used for horizons that have undergone gleying leading to mottles (Tabor et al., 2017); this this horizon is taken to be Bg. This horizon is also the host for numerous reworked tetrapod skulls and postcranial elements. The interpretation of the origin of this rich occurrence of tetrapod fossils is presented in the taphonomy discussion of Chapter 6. Consistent with the eroded surface of this Bg-horizon, the original A-horizon above it has also been eroded and is not preserved at all.

The dominant massively bedded silty-mudstone continues all the way to the base of the channel sandstone marking the end of Cycle 1. At 12.9 m it is interrupted by a laterally extensive yellowish-grey (5Y 7/2) fine-grained sandstone (Figure 3.11). This sandstone is about 10 cm thick and is ripple cross stratified to massively bedded and has rib and furrow features on its top surface. The sole surface of this sandstone records several features of the underlying mudstone palaeosurface such as current crescents, desiccation cracks, vertebrate scratch digging traces and other traces. It is interpreted as a crevasse splay sand sheet and a detailed interpretation of these features is provided in Chapter 5.



Figure 3.10: (A) Structural Bg-horizon containing numerous isolated, reworked and articulated procolophonid skulls and postcranial elements (B) and (C). White arrows = snouts of two skulls in dorsal view, red arrow = small skull in lateral view with teeth visible. Scale bars in B and C = 2 cm.



Figure 3.11: Crevasse splay sandstone at Lemoenfontein locality. (A) View of crevasse splay sandstone outcrop. (B) Circular current crescent casts on sole surface. (C) Casts of interpreted vertebrate scratch digging activity (arrowed) on sole surface. Ruler in A = 10 cm x 10 cm, Scale bar in B and C = 5 cm.

Several dish-shaped fine-grained sandstone lenses, 1 to 2 m in diameter, occur higher up at 13.8 m (Figure 3.9 C). These sandstone lenses are horizontally laminated, pale reddish-brown (10R 5/4), and are interpreted to be sand-filled depressions on the ancient floodplain most likely filled with windblown rather than water laid sand. Another horizon of greyish-red (5R 4/2) coalescing calcareous nodules occurs 10 cm above these lenticular sandstone dishes. This horizon is 5 cm thick, Stage III (Machette, 1985; Retallack, 1988) and is the source of some small isolated but complete procolophonid skulls. There are no additional distinguishing features in the massively-bedded silty-mudstone above this level. The last few metres below the channel sandstone are covered in colluvium from these sandstones.

The beds from 8.2 m to 9.9 m (transitional BC-horizon with calcareous nodular horizon, transitional BC-horizon with cutans, structural B-horizon) host the unusual bone accumulation and the burrow casts that are the focus of this study. The stacking pattern of this 2.3 m thick 3rd to 5th order cycle is from the top down:

- B-horizon with well-developed prismatic peds (Bg);
- BC transitional horizon with cutans (BCt); and
- BC-horizon that contains Stage III calcareous nodules (BCk).

As discussed above, this type of stacking corresponds to a *Compound* profile except that the A-horizon has not been preserved and that the B-horizons are interrupted by *thick* (instead of thin) un-weathered material (C-profiles). Although structural features such as the peds in the B-horizon formed relatively quickly (5-200 years), the Stage III carbonate nodules (cm scale) require thousands of years to form (Marriot and Wright, 1993). The eroded top of the structural B-horizon and its extensive degree of gleying and the formation of a Stage III calcareous horizon 1.7 m below the B-horizon, indicate that the accumulation of sediments on the floodplain was interrupted for thousands of years and that down wasting of the floodplain palaeosurface occurred. The following interpretation can be made for this assembly of beds.

- The parent mud and clay sediments were deposited rapidly by periodic overbank flood events (5th order events) in a proximal floodplain setting during Phase 5 of each flood event (Zwoliński, 1991). It is usually during Phase 5 events that the fine muds

and clays are deposited. In particularly severe flood events, significant amounts of sediments can be deposited (of the order of 1 m) (Retallack, 1988). It is also during these frequent periodic flood events that the tetrapod skeletons were embedded in the mud and the burrows were filled in. Note that there is a preservation bias towards burrows filled in with the fine sandstone sheetwash at this locality as opposed to burrows filled by clay or mud.

- At the end of this deposition, a long period of several thousands of years followed with no significant sedimentation (Marriot and Wright, 1993). This period of stasis allowed the formation of cm scale Stage III carbonate nodules within the BC-horizon and the formation of the strongly developed B-horizon. Since the formation of the Stage III calcareous horizon takes an order of magnitude longer than the formation of the peds in the B-horizon, the peds underwent erosion during the period of non-deposition on the soil surface. Such interruptions of sediment accumulation can occur when the contributing river avulses, usually in response to a major flood event that permanently redirects the main channel discharge out through a crevasse splay, which causes the abandonment of the former downstream channel and associated floodplain (Zwoliński, 1991; Tabor and Myers, 2015).
- During this period of erosion, the parent material in the C-horizon, below the B-horizon, became overprinted with material eluviated from the B-horizon to form a BC-horizon that is transitional between the B-horizon and the C-horizon. Voids formed in the C-horizon by shrinking and swelling of clays during seasonal variation of soil humidity. These voids were then filled and lined by clays that have washed down from the B-horizon to form cutans (clay skins).

The occurrence of calcareous nodular horizons are important indicators of palaeoclimate conditions both subaerial and subterranean. The depth under the surface and stage of development provides valuable insights (Retallack, 1988; Marriot and Wright, 1993; Tabor and Myers, 2015). Li et al. (2018) performed an extensive literature survey on the formation of calcareous nodules in loess-palaeosol sequences. The formation of calcareous nodules is a common occurrence where there is seasonal variation in groundwater level. Li et al. (2018)

considered two mechanisms for the formation of calcareous nodules: per descendum and per ascendum models. Both refer to the dominant groundwater movement.

Per descendum model: In this model, biological activities in the soil generate CO_2 that gets trapped in the intergranular spaces. This CO_2 is then dissolved in rainwater moving downward through the soil, creating more acidic conditions. Calcium minerals (calcite) are leached out of the soil by the more acidic water (carbonic acid). Calcium carbonate, $CaCO_3$, reacts with water that is saturated with carbon dioxide to form the soluble Calcium bicarbonate $CA(HCO_3)_2$. The solution continues to migrate downwards through the soil and eventually gets super saturated with $CaCO_3$. Finally, the $CaCO_3$ gets precipitated at a specific depth in the soil caused by pH variations, a decrease of CO_2 partial pressure, and reduction of solvent water. However, Li et al. (2018) find that these causative factors do not completely explain the supersaturation of the solvent water with $CaCO_3$.

Per ascendum model: in this model calcium bicarbonate also enters into a solution due to the downward movement of CO_2 laden rainwater. However, in dry seasons, ground water evaporation occurs, and capillary pull causes the solution containing calcium bicarbonate to rise in the soil and become supersaturated due to the loss of the free H_2O and as a result the $CaCO_3$ precipitates. Three conditions are required: capillary pores, a source of a $Ca(HCO_3)_2$ solution and strong evaporation. This model explains the formation of regular shaped (ellipsoid) calcareous nodules along *narrow* horizons such as the case under consideration here.

A seasonal variation in the water table and the depth at which it occurs is an important factor in the formation of calcrete in soils. It is therefore important to distinguish between pedogenic calcretes and diagenetic (groundwater) calcretes (as well as palustrine carbonates) (Alonso-Zarza, 2003). Pedogenic calcretes form in well drained soils above the water table in the vadose zone and can be affected by capillary rise from the water table. These calcretes can be formed in various types of horizons (Chalky, Platy, Hardpan etc.), but importantly for this study they can take the form of a nodular horizon. Sub-aerial exposure for hundreds to

thousands of years is required to form pedogenic calcretes. Pedogenic calcretes typically form well developed profiles (one to several meters thick) with calcareous nodular horizons showing diffuse upper and lower boundaries (Wright, 1990; Alonso-Zarza, 2003).

Diagenetic calcretes form in phreatic zone below the water table. These calcretes do not have any root traces or peds, are usually massive bodies and are not overlain with B-horizons or eluviated clays (Alonso-Zarza, 2003). Thin developments of groundwater nodules are also possible (Arakel and McConchie, 1992). Groundwater calcretes typically have sharp top and bottom surface contacts. Near lakes or ponds on the floodplain, the groundwater depth is shallower. In these zones there is overlap between the formation of pedogenic (vadose) calcretes and diagenetic (phreatic) calcretes (Alonso-Zarza, 2003). This overlap occurs typically in the capillary fringe zone and leads to *thin* calcrete horizons with sharp bases overlain by calcrete nodules (Mack et al, 2000). Mudstones and siltstones that contain peds and slickensides, often host carbonate nodules 2 – 10 cm in diameter (Mack et al., 2000) that are either isolated or coalescing and are elongated parallel to the bedding plains. These nodules are pedogenic in origin, but if the mudrocks show colour mottling (gleying), and the nodules are elongated parallel to the bedding plane, it is likely that their formation was influenced by through-flowing fluctuating ground water. Such mudrocks may be described as hydromorphic palaeosols (Mack et al., 2000).

Palustrine calcretes form when the water table extends above the soil in the form of lakes followed by periods of desiccation and sub-aerial exposure. This results in the formation of palustrine limestone.

Based on this distinction, the three *narrow* horizons consisting of *ellipsoid* calcareous *nodules* that occur below, in and above the Lemoenfontein bonebed are interpreted to be pedogenic in origin and by definition formed above the water table in the vadose zone, with significant capillary influence from below (Alonso-Zarza, 2003; Li et al., 2018). Specifically, the water table at the bonebed locality was below the nodular horizon, but due to seasonal variations, either affected the calcrete formation through capillary action or by rising above the horizon.

This interpretation also requires that the calcrete formation occurred near a water body on the floodplain where the water table was shallow. This process is schematically presented in Figure 3.12 (modified from Figure 4 in Tabor and Myers (2015)). This issue is explored further in the context of the vertical stratigraphic extend of the burrow casts in the section of this study dealing with the burrows (Chapter 4).

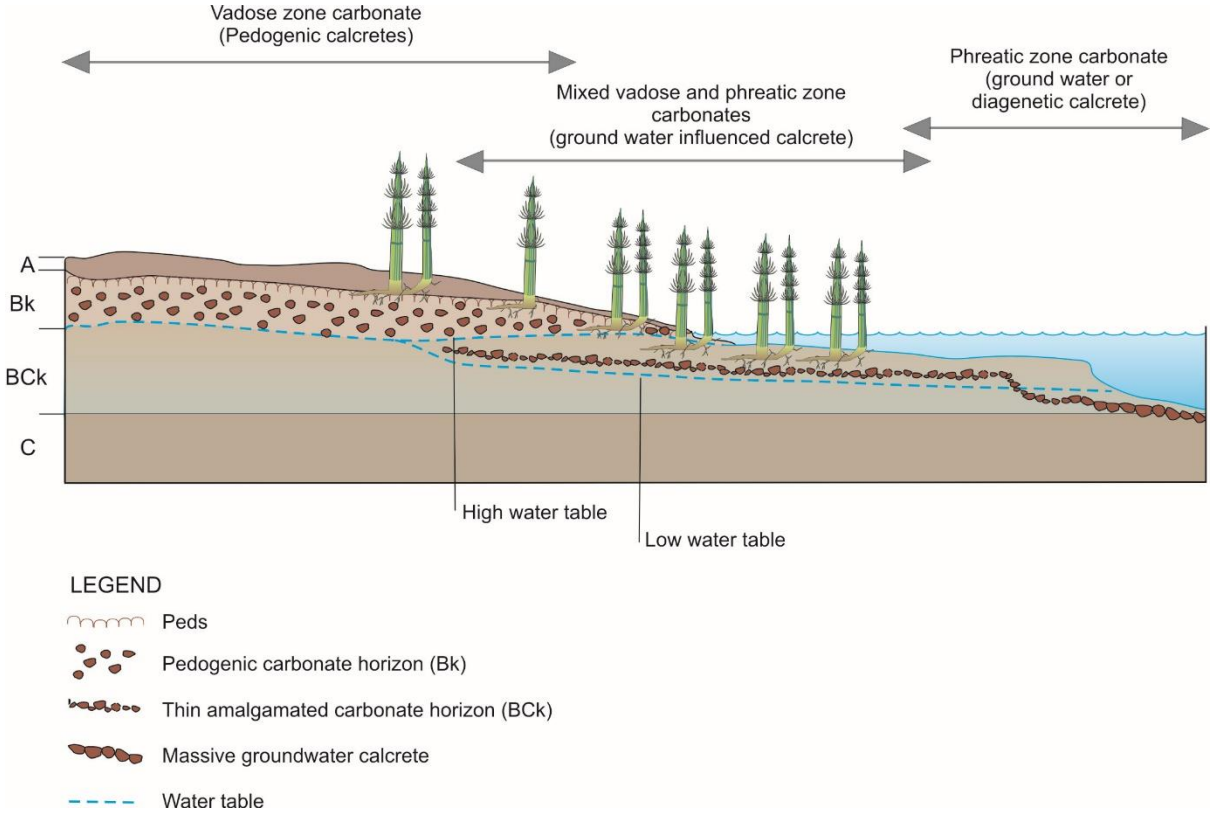


Figure 3.12: Schematic diagram showing the vertical stratigraphic position of the different types of soil horizons and the relative position of pedogenic and diagenetic carbonate formation within these. Also shown is the region where ground water influenced the formation of pedogenic calcrete. The rooted horsetail stands are not to scale and have been enlarged for clarity. (Diagram modified from Figure 4 in Tabor and Myers (2015)).

The calcareous nodular horizons are located 1.7 m below the structural B-horizon at the elevation of the bonebed and 20 cm below the surface at the elevation of the spruit. The depth of these horizons reflects the depth of soil wetting by the ground water (Retallack, 2000). In dry regions, these horizons are closer to the surface than in wet regions. A climofunction correlation between mean annual rainfall in mm and the depth in the soil of the Bk-horizon was developed by Retallack (1994) and later updated with additional data (Retallack, 2005; Tabor and Myers, 2015).

$$MAP = 137.2 + 6.45D - 0.013D^2$$

MAP = mean annual precipitation in mm/year

D = depth of the carbonate horizon below the soil in cm.

Correlation coefficient R^2 = 0.52, standard error ± 147 mm

This relationship applies to soils with Stage II or less developed calcareous nodules (Retallack, 1994; Alonso-Zarza, 2003) in unconsolidated alluvium. It is not valid for soils with well-developed carbonate layers (Retallack, 2000; Alonso-Zarza, 2003). However, it can also be applied to regions with seasonal warm climates provided the depth is measured to a well-developed (Stage III or more) horizons (Retallack, 2000). This would give a precipitation of 263 mm/y for the first Stage II calcareous horizon in the spruit and 858 mm/year the second Stage III horizon. The upper limit of mean annual rainfall that allows for calcrete formation is 600 to 1000 mm/year with lower limits as low as 50 mm/year (Mack and James, 1994; Alonso-Zarza, 2003) so the results obtained here are consistent. There is no general agreement on the validity of this equation (Alonso-Zarza, 2003). Erosion of the surface, compaction, unusually high level of atmospheric CO_2 (only under severe greenhouse conditions) and seasonal floods can affect the results (Retallack, 2000). However, Royer (1999) found a significant correlation for the occurrence of calcareous horizons and precipitation below 760 mm. Stiles et al. (2001) also found a strong linear correlation between the depth of carbonate enriched horizons and the average annual precipitation in Texan vertisols. Finally, Retallack (2005) added additional soils to the existing data, expanding the number of soils in the database from 675 to 807 and confirmed that the relationship remains valid. Calcareous horizons form in soils with a net moisture deficit. Under these conditions the carbonate that is precipitated in the dry season is not leached away during the wet season. Modern day carbonate precipitation occurs in regions with warm to hot annual average temperatures (16 to 20 °C) and low seasonal rainfall (Goudie, 1983).

A recent study (Retallack, 2021), of the palaeoenvironmental interpretation of palaeosols that occur below and above the level of the Permian-Triassic extinction in the main Karoo Basin, extended from the base of the Elandsberg Member in the Balfour Formation (corresponding biostratigraphically to the base of the *Daptochephalus* AZ) up to the top of

the “Lower Member” of the Burgersdorp Formation (corresponding biostratigrapically to the top of the *L-G* Subzone of the *Cynognathus* AZ). One of the objectives of this study was to measure the depth and thickness of pedogenic carbonates in the Bk-horizons of these palaeosols. The climofunction correlation between mean annual rainfall in mm and the depth in the soil of the Bk-horizon was used to calculate the mean annual precipitation (MAP). This study finds that at the top of their “Lower Member” the depth to the Bk-horizon is approximately 60 cm translating in a sharp increase in MAP to just below 800 mm with a mean annual range of 50 mm. Retallack (2021) concluded that there was significant seasonal fluctuation in precipitation. These results are largely consistent with those of the present study reported above i.e., 263 mm/year for the first Stage II calcareous horizon in the spruit (below the top of their “Lower Member”) and 858 mm/year the second Stage III horizon (above the top of their “Lower Member”).

Retallack (2005) also presents a correlation between calcareous nodule size and age as determined from radiocarbon dating of pedogenic carbonate nodules from the Desert Project in New Mexico (Gile et al., 1981). According to this correlation, the isolated 4 cm nodules from the first nodular horizon may take as long as 6000 years to form. Nodules of around 8 cm in diameter as in the second nodular horizon can take up 8000 years to form, while a fully developed tabular horizon formed by coalescing nodules can take 12 000 years to form.

3.6 Interpretation of depositional environment

Figure 3.4 records an expanded view of the beds that host the tetrapod fossils and burrow casts. This is ranked as a 3rd order cycle (Cycle 1) and consists almost entirely of stacked beds of massively bedded (structureless) mudstone interpreted as having accumulated on the proximal parts of a seasonally flooded floodplain during the waning phase after overbank flooding from the main channel. These deposits consisted of sand-sized mud aggregates. Following deposition, compaction removed the aggregate structure resulting in thick massively bedded mudstone beds. Such overbank flood outs would correspond to 5th order cyclic events. The anomalously thick mudstone bed contains three calcareous nodular horizons, the first consist of isolated nodules (Stage II) and the second two experienced coalescence (Stage III). The first two of these nodular horizons are associated with an overlying well-developed structural B-horizon. These calcareous and nodular horizons indicate that sediment accumulation slowed or ceased on the floodplain for extensive periods of time that allowed the pedogenic nodular and B-horizons to form. These interruptions are likely due to avulsions of the associated meandering river. The first period of stasis corresponds to a duration of approximately 6000 years while the second to about 8000 years. The MAP was 263 mm/year for the first period of pedogenesis and 858 mm/year during the second. During the second period of depositional stasis and pedogenesis, parts of the floodplain were abandoned, and some down wasting of the surface (A-horizon) occurred. Since some removal of sediment has occurred, the MAP provided by the correlation is likely to be somewhat underestimated. It is proposed that the down wasting reached the top surface of the B-horizon and in the process many previously buried procolophonid skulls and articulated skeletons were exhumed and became concentrated on this horizon. However, since a Stage III calcrete horizon developed during this period of depositional stasis, the extend of the erosion was not enough to inhibit the formation of the calcrete horizon or the erosion occurred after the B-horizon, and the nodules were fully developed. The palaeosols indicate a semi-arid, warm to hot climate with strong seasonal variation in precipitation.

The burrow casts at this locality originate below the structural B-horizon and are hosted within the palaeosol BC-horizon. The best-preserved burrows are in-filled with fine

sandstone, and it is likely that the same sheet flood event that deposited the sandstone sheet (1.5 m above the calcrete horizon) also in-filled the burrows. This suggests that the original burrow entrances, and by implication the floodplain surface at the time of burrowing, corresponded with the horizon represented by the contact of the massive mudstone with the overlying sandstone sheet. Some burrows in-filled with mudstone were observed in the field, but these generally blend in with the host matrix and are not very distinct. Although the burrow entrances are not preserved, no burrow shaft casts were found above the B-horizon. The burrows penetrate through the mudstone and the calcareous nodular horizon and then apparently terminate. This calcrete horizon is pedogenic in origin and was formed in the vadose zone above the average seasonal water table. For this reason, the interpretation is made that the reniform burrows (identified to be tetrapod in origin in Chapter 4) terminate above the water table, while the subcircular burrows (identified to be crayfish in origin in Chapter 4) terminate in the phreatic zone below the water table (Figure 3.4). Smith (1989) uses a similar argument to determine the minimum depth to a palaeosol water table based on the depth of burrow terminal chambers.

The tetrapod fossils from this bonebed locality originate from within the structural B-horizon, the calcareous nodular horizon and the mudstone that is interbedded between these two horizons. No tetrapod fossils encased in calcium carbonate nodules were recovered below the calcrete horizon within the phreatic zone. This is consistent with the absence of pedogenic calcrete in this zone. The taphonomic processes that resulted in the preservation style present here are explored further in the taphonomy part of this study (Chapter 6).

Based on the interpretation of the sedimentary rocks present at this locality several mechanisms contributed to the unique features of bone accumulation at this locality.

- *Overbank flooding increased in frequency*: The palaeoclimate also resulted in seasonal overbank flood events that led to the rapid deposition of fines on the floodplain.
- *Avulsion events increased in frequency*: When hydraulic limits were exceeded on the floodplain (3rd order cycle events), the course of the meandering river flow changed, changing proximal floodplain settings into distal settings with little or no floodplain

deposition for long periods of time. The pedogenic B-, C-, Bk- and BCk-horizons formed during these periods of stasis.

- *Vegetation, soils, and fauna responded to increased seasonality:* The palaeoclimate was semi-arid, with strong seasonal variation in rainfall, and warm to hot average annual temperature. Such conditions resulted in the confinement of perennial vegetation to the areas surrounding permanent and semi-permanent water bodies on the floodplains, an increase in the seasonal fluctuation of the depth to water table, and the formation of strong Bk- and BCk-horizons. The fluctuating temperature and rainfall regimes also encouraged underground burrowing by both vertebrates and invertebrates at this time.

These conclusions from the sedimentological analysis form the foundation for the following taphonomic analysis of the bonebed to reconstruct the taphonomic pathways that led to the preservation of this anomalously rich fossil bone accumulation at this site.

4. BURROW CAST ICHNOLOGY OF LEMOENFONTEIN

4.1 Background information on Triassic burrow casts

Shone (1978) first published on Triassic-aged burrows in the Burgersdorp Formation in a paper titled "Giant *Cruziana* from the Beaufort Group". This study reported on large burrows casts or tracks found in sedimentary rocks in the town of Burgersdorp in the Eastern Cape. The tracks were described as two parallel elongated furrows separated by a median ridge. Based on the V-shaped scratch marks on the burrow surfaces, the origin of the tracks or burrows was assigned to large trilobite-like arthropods. Stanistreet and Turner (1979) agreed with the assignment of these traces to the ichnotaxon *Cruziana* but disagreed that trilobites were the trace makers. Instead, they noted the similarity of the scratch marks to those on decline burrow casts in the Teekloof Formation that were assigned to tetrapods (also see Smith, 1987). In a more recent study using laser scans of the sole marks on the same sandstone block, Bordy et al. (2019) concluded that they are all tetrapod burrow casts.

The first in-depth study of vertebrate burrows in the Karoo was performed by Smith (1987). This ground-breaking paper documents large helical burrow casts from the Permian in the southwestern part of the main Karoo Basin. These burrows are the oldest and first helical pre-mammalian vertebrate burrows. Three of the burrow casts contained articulated skeletons of the dicynodont *Diictodon.* The outer surfaces of the tunnel and terminal chambers preserve scratch-digging marks made by the claws and possibly the beak of *Diictodon.* The sand infill of the burrows originated from episodic sheet floods and splay-fans in a proximal floodplain environment.

Groenewald (1991) studied five different types of burrows from various localities in the Early Triassic Katberg Formation. The burrow cast diameters vary from 10 to 50 cm and are associated with fossilised material of *Procolophon* and *Lystrosaurus*. This led Groenewald (1991) to conclude that *Procolophon* and *Lystrosaurus* were burrowing animals and, citing Kitching (pers. comm., 1990), this is the first formal reference that *Procolophon* was a

burrowing animal. These burrows also occur in association with casts of desiccation cracks in mudstone, leading to the conclusion that animals burrowed to survive harsh environmental conditions on distal floodplains and playa-lake environments.

Possible evidence that *Lystrosaurus* was a burrower is provided by a large burrow cast from the Lower Triassic strata of the Palingkloof Member of the Balfour Formation (basal portion of the *Lystrosaurus* AZ of South Africa (Modesto and Botha-Brink, 2010). This cast contains a partial disarticulated skeleton of a juvenile *Lystrosaurus.* However, the authors of this study concluded that the *Lystrosaurus* skeleton is too small to be the producer of the burrow and propose that a carnivorous tetrapod was responsible. The disarticulated state of the bones in the burrow led to the alternative interpretation that the *Lystrosaurus* was the prey of the burrow maker.

In another pioneering study Groenewald et al. (2001) describe vertebrate burrow complexes from the Early Triassic and attribute these to *Trirachodon* (note that the trirachodontid material from the *L-G* Subzone of the *Cynognathus* AZ has subsequently been recognized as the new taxon *Langbergia modisei* (Abdala et al., 2006; Smith et al., 2012)). The presence of several individuals in the end chamber of one of these localities suggest multiple cohabitation and complex social behaviour for *Trirachodon.* Groenewald et al. (2001) further suggest that the most likely advantage obtained by fossorial behaviour of *Trirachodon* is thermoregulation. Possible other advantages may include protection against predators, sites for reproduction and raising of young. A literature survey performed by Groenewald et al. (2001) suggests that terrestrial burrows provide seasonal or permanent shelters from extreme environmental conditions for both vertebrates as well as invertebrates. It is proposed that aridity and extreme day-night temperature fluctuation induced the social burrowing lifestyle of *Trirachodon*.

In a series of papers on Triassic burrows from Antarctica (Hasiotis et al., 1999; Miller et al. 2001; Sidor et al., 2008) several insights are gained that are relevant to burrows in the Triassic of the Karoo Basin.

Hasiotis et al. (1999) compares possible crayfish burrows from the Lower Triassic Fremouw Formation and Lower Permian Pagoda Formation in Antarctica to Permian and Triassic tetrapod burrows from South Africa (with reference to the work by Smith (1987)). By comparing the architecture and external surface morphologies of these burrows to Triassic crayfish burrows from Utah (USA), and by performing a statistical analysis of burrow diameters and diameter ratios, the conclusion is reached that the Antarctic burrows belong to therapsids instead of crayfish. The Antarctic burrows are shallow dipping tunnels (lateral or spiral) that contain longitudinal scratch marks and a longitudinal medial grove along the base. In current terminology these burrows would be described as having a bilobate cross-section (Krummeck and Bordy, 2016).

An important contribution to the identification and classification of burrow casts was made in a follow up study of burrows from the Lower Triassic Fremouw Formation, Shackleton Glacier area, Antarctica (Miller et al., 2001). Two non-overlapping size types of burrows are identified:

- Type G (giant) – 8 to 9 cm diameter, gently dipping, parallel to tangential scratch marks. Interpreted as tetrapod burrows by comparison to Permian burrows from South Africa;
- Type L (large) – 2 to 6.5 cm diameter, curved, limited branching, and parallel to tangential scratch marks. Interpreted as being produced by either tetrapods or crayfish.

The following measurable parameters are introduced to characterise the burrows: diameter, width/height ratio, architecture, branching, penetration depth, surface markings, burrow lining (mud chips), producer in burrow and occurrence density (per meter of outcrop). These characteristics are also used in a detailed comparison of burrows made by various possible producers: Permian lungfish, Triassic crayfish, Permian therapsid, and Triassic tetrapod. In this study, seven criteria that can be used for identifying producers of terrestrial burrows are introduced. These criteria allow identification within three levels of confidence: Most reliable, Less reliable, and Least reliable. This paper is very relevant for the present study. The parameters used to characterise burrows, the comparison of the characteristics due to different producers and the criteria for allocating possible producers to burrows are used.

Sidor et al. (2008) undertook further investigations on burrows from the Triassic of Antarctica. A giant terminal chamber from the lower Fremouw Formation (Lower Triassic) at Wahl Glacier (Beardmore Glacier region, central Transantarctic Mountains) is compared to a South African burrow chamber that contains the articulated skeleton of a *Thrinaxodon liorhinus.* The conclusion is reached that this burrow was created by a tetrapod of similar size to *Thrinaxodon.* They also studied several burrows from Member 'A' of the Lashly Formation (lower Middle Triassic). Again, by comparing the burrow characteristics to similar burrows from the Triassic in South Africa, procolophonids are identified as possible trace makers. However, this conclusion is speculative as no procolophonids have yet been found *in-situ* in any burrow and the morphological characteristics that could tie procolophonids to these types of burrows are not unique. This is a very relevant discussion for the current investigation in that the Lemoenfontein fossils contribute some pertinent information to help resolve the conundrum.

The burrow chamber containing the *Thrinaxodon* skeleton referred to by Sidor et al. (2008) in the discussion above is described in Damiani et al. (2003). It is the oldest cynodont burrow and occurs close to the Permian-Triassic Boundary (PTB) in the Karoo. This Early Triassic find, along with later evidence of burrow-making by *Trirachodon* (now *Langbergia*) (Groenewald et al., 2001), indicates that burrow-making by therapsids was a common occurrence. This behaviour is interpreted to be an adaptation in response to the environmental changes associated with the mass extinction event at the end of the Permian (Smith and Botha-Brink, 2009). The prevalence of burrowing behaviour among extant mammals implies that this adaptation provided a strong evolutionary advantage.

The conclusion that burrowing was widespread after the Permian-Triassic extinction event is corroborated by Bordy et al. (2011). In this study, very large (diameter of 30 to 35 cm) cylindrical burrows, found approximately 100 metres above the Permian-Triassic boundary in the Early Triassic Katberg Formation, are attributed to the therapsid *Lystrosaurus*. The conclusion is reached that these burrows were produced to serve as shelters in which a

stable micro-environment existed. This allowed the inhabitants to extend their survivability in conditions of periodic drought and extreme moisture and temperature fluctuations.

A recent analysis of an assembly of burrow casts (4 cm diameter) from the transition of the Katberg and Burgersdorp formations of the main Karoo Basin (Bordy and Krummeck, 2016), uses the set of burrow characteristics defined by Miller et al. (2001) to try and identify the burrow producers, their behaviour, and the depositional conditions in the Early Triassic of South Africa. The floodplain experienced periodic flooding, drying and pedogenesis when these burrows were formed. The burrow architecture and morphology differ from those that occur earlier and later in the Triassic of the Karoo. These burrows are simple vertical shafts with circular/elliptic cross-sections. Following the methods of Miller et al. (2001), a systematic comparison of the burrow characteristics of crayfish, lungfish and various tetrapods did not lead to a definitive conclusion about the burrow producers. However, the analysis confirms that terrestrial burrowing behaviour was common following the Permian-Triassic Extinction event in the Karoo Basin.

In a follow up study of several burrow specimens from the Lower Triassic Katberg Formation in the Karoo Basin, Krummeck and Bordy (2016) assign these specimens ichnotaxonomically to a new ichnogenus and ichnospecies, *Reniformichnus katikatii.* The holotype morphology resembles burrow casts from Antarctica as described by Sidor et al. (2008) and Miller et al. (2001). The holotype is described as follows: "*The holotype is an inclined, burrow cast with bilobate base and reniform cross-section. Its width ranges from 12.6 to 14.7 cm and its height is 5 to 7.4 cm resulting in an aspect ratio of 1.89 to 2.74. The surface preserves 70–180 mm long ridges running parallel to the long axis of the burrow on the upper parts of the walls and lower parts of the dorsum and shorter ridges (average length »27 mm) are preserved on the more ventral areas in two opposite orientations, cross-cutting each other in a rhomboid pattern.*" The burrows occur in fluvial floodplain mudrock deposits, are filled by coarser sandy sediments and occur as simple isolated inclined tunnels. The formal ichnotaxonomic naming of this style of burrow and its allocation to a tetrapod producer (therapsids, procolophonids) is an important contribution to the ichnology of the Early Triassic in the Karoo and in Antarctica. As part of the research for this study similar burrows have been discovered in the

Middle Triassic of the Karoo Supergroup (in Subzone *T-K* of the *Cynognathus* AZ) and therefore this it is a useful independent test of these findings.

4.2 Lemoenfontein burrow casts

The burrow casts described in this study were excavated, measured, photographed, and GPS logged during a field trip to the Lemoenfontein locality in April 2019. Representative samples were also obtained for further laboratory analysis. Two types of burrow casts were found. The first type has a bi-lobed, reniform cross-section with characteristic scratch marks like the recently named *Reniformichnus (*Krummeck and Bordy, 2018). The second type has a sub-circular cross-section and shows a knobby and hummocky outer surface. All burrows originate below the structural B-horizon and are hosted within the C-horizon as described in Chapter 3. The host matrix is a massive dark reddish-brown (2.5YR5/4) mudstone that shows claystone-lined pedogenic cutans, characteristic of the textural B-horizon of a palaeovertisol. Although the burrow entrances are not preserved, no burrow shaft casts were found above the B-horizon (only a single isolated very large bilobate burrow terminal chamber was found *ex-situ* some 3 m above it). The burrows penetrate through the mudstone and a calcareous nodular horizon, then apparently terminate. In one case, burrow B19-1, the burrow cast was exhumed down to its terminal chamber approximately 30 cm (vertically) below the nodular horizon. The calcareous nodular horizon is located 1.7 m below the structural B-horizon. There is also a light olive-grey (5Y 6/1) fine sandstone sheet 1.5 m above the calcareous nodular horizon. The burrows are filled with the same fine olive-grey sandstone, and it is likely that the same sheet flood event that deposited the sandstone also in-filled the burrows. This suggests that the original burrow entrances, and by implication the floodplain surface at the time of burrowing, closely corresponded with the contact between the massive mudstone host matrix and the overlying sandstone sheet. It is also worth noting that most of the tetrapod fossils from this bonebed locality originate in between the structural B-horizon and the calcareous nodular horizon, with several specimens occurring in the nodular horizon itself.

In the analysis of the Lemoenfontein burrow casts, the burrow architectural morphology, surficial morphology and burrow fill for each type were documented. The *architectural morphology* refers to the measurable characteristic parameters of the burrows such as the overall shape, the cross-sectional shape, the orientation and ramp angle in the host matrix, the presence or absence of original entrances, branching or chambers. The *surficial morphology* refers to the presence of structures on the surface of the burrow casts that originate from the activities of the burrow maker. They include scratch marks, striations, body impressions and other traces made by the burrower's appendages. The orientation of these bioturbation attributes, relative to the burrow axis and to each other, can provide information about the burrower's behaviour during both the burrow construction and its eventual use. The *burrow fill* refers to the sedimentary or other material that filled the burrow, allowing it to form a cast that records the architectural and surficial morphology of the burrow. The type of burrow fill can provide information about the behaviour of the burrow maker, as well as the movement of clastic sediments across the flood plain surface, and in some cases the preferential calcification and early lithification after infilling providing resistance to burial compaction.

4.3 Reniform burrow casts

Five burrow casts with a reniform cross-section have been excavated (Figure 4.1).

Reniform burrow architecture

The Lemoenfontein reniform burrows consist of simple, single decline shafts descending between 17° and 35° from horizontal and are at least 1 m long and between 6 to 8 cm wide. Their dorsal surfaces are convex and rounded while the ventral surfaces have two parallel furrows separated by a well-defined ridge that aligns with the burrow axis. Burrow entrances at the palaeo-floodplain surface are not preserved. In plan view the shafts curve in a slightly sinuous S-pattern. The burrows do not show evidence of branching. One burrow cast (B19-1) was excavated down to its termination chamber. This chamber is like the burrow terminal chamber description provided for the Tetrapod Ichnogenus B specimen (UWBM 88600) by Sidor et al. (2008). Like UWMB 88600, the top and bottom surfaces taper symmetrically towards each other distally, reducing the vertical diameter to about 66% of its value in the main shaft. Unlike UWMB 88600, the slight lateral widening is not present in B19-1.



Figure 4.1: Reniform burrow casts. (A) B19-5, gently curving inclined burrow cast showing chevron pattern of ridges (Note the penetration by secondary smaller burrow). (B) B19-2, bilobed cross-section. (C) Sets of narrow oblique ridges on the latero-ventral surface of the B19-5 burrow cast. Two types of these sets are highlighted according to their angle with respect to the long axis of the burrow cast (Low angle: yellow dashed lines and arrows. High angle: red dashed lines). Ruler in A = 10 cm x 10 cm, scale bar in B and C = 2 cm.

The basic dimensions, as recorded in the field and laboratory, are summarized in Table 4.1 (also see Appendix C). The shafts are at ramp angles that range from 17° to 35° (average 25°, SD 6°), as measured relative to the horizontal. The horizontal diameter (maximum width) of the burrow casts ranges from 6 to 8 cm (Average = 6.5 cm, SD = 0.8 cm). The vertical diameter (maximum height) ranges from 3 to 4 cm (Average of 3.5 cm, SD = 0.1 cm). The corresponding aspect ratio ranges from 1.6 to 2.3 (Average = 1.9, SD = 0.2). The height of the inverted trough or ridge that runs along the ventral surface of the burrow ranges from 0.3 cm to 1.5 cm (Average = 0.7 cm, SD = 0.4 cm). Two samples B19-1 and B19-5 were uncovered sufficiently along their lengths to expose one complete S-pattern, giving a low sinuosity index of 1.11 for B19-1 and 1.04 for B19-5 (sinuosity index = true length/straight length).

Table 4.1: Lemoenfontein burrow casts - basic dimensions

Field Number	Horizontal diameter (cm)	Vertical diameter (cm)	Aspect ratio	Height of central ventral ridge (cm)	Ramp angle (degrees)	Cross-sectional shape
B19-1	8,0	3,5	2,3	0,3	17	Reniform
B19-2	6,5	4,0	1,6	1,5	28	Reniform
B19-3	6,0	3,0	2,0	1,0	35	Reniform
B19-5	6,0	3,5	1,7	0,5	23	Reniform
B19-6	6,0	3,4	1,8	0,4	24	Reniform
B19-4	2,5	2,5	1,0		32	Circular
B19-7-1	5,8	4,0	1,5		25	Sub-circular
B19-7-2	6,9	6,5	1,1		25	Sub-circular
B19-7-3	6,0	4,0	1,5		25	Sub-circular
B19-8	3,0	2,2	1,4		22	Sub-circular
B19-9	4,0	2,7	1,5		35	Sub-circular

Surficial morphology of reniform burrow casts

The reniform burrow cast surfaces are sculpted with sharp-crested ridges of various sizes that are interpreted to be natural casts of the scratch marks left by the burrowing animal during the construction and occupation of the burrow. The larger and most distinctive are chevron-like parallel ridges that run from the distal (lower) dorsal midline along the sides towards the proximal end, traversing the lateral and ventral surfaces (Figure 4.1). Two samples: B19-1 and B19-5, best show these interpreted scratch marks. The ridges are typically 12 cm long, 2 to 5 mm apart and are angled at approximately 20° away from the long axis of the burrow shaft on the lateral surfaces (like UWMB 88600 of Sidor et al. (2008)). The ridges on the dorsal surfaces are less prominent. A second set of parallel ridges originate on the lateral walls of the burrow cast, approximately half-way up. These shorter ridges are more angled to the main axis (40° to 50°) and cross-cut the longer striations resulting in a rhomboid pattern of ridges on the lower lateral surfaces and the ventral surfaces of the burrow (Figure 4.1 C).

Specimen B19-5 appears to be penetrated on its dorsal surface by a burrow with a sub-circular cross-section of a lesser diameter at an angle that is more oblique with respect to the horizontal. This phenomenon has been noted by Abouessa et al. (2015) in their study of Upper Eocene crayfish burrows in Libya, where they point out that burrows are formed in stages according to changes in the water table. They note that it is possible for a new stage of burrows with smaller diameters to penetrate the larger and older burrows from a previous generation.

Reniform burrow fills

The Lemoenfontein reniform burrows are infilled with a very fine olive-grey (5Y 6/1) sandstone originating from a sandstone sheet 1.5 m above the calcareous nodular horizon and 20 cm below the pedogenic structural B-horizon. In specimen B 19-1, the trough on the ventral surface is much less pronounced than the other bi-lobed burrow casts from this locality (3 mm) and the lower part of the burrow fill contains fine grained sandstone with matrix-supported mudstone chips. This suggests a single infilling episode with some erosion of mudstone chips from the axial ridge on the burrow floor. As discussed above, the sandstone sheet was deposited on the palaeosurface during the event that filled the burrows. Burrow specimen B19-1 terminates approximately 30 cm below the nodular horizon. This suggest that the total vertical penetration depth of B 19-1 is approximately 1.8 m below the original floodplain surface.

4.4 Lemoenfontein sub-circular burrow casts

One burrow cast with a round cross-section and five casts with sub-circular cross-sections have been excavated (Figure 4.2).

Sub-circular burrow architecture

This burrow type penetrates the mudrocks at a steady inclination to at least 1m below the surface. It is an unbranching, single shaft and is straight to gently curved (curvilinear) in plan

view. The cross-sectional shape and area are nearly constant over the length of the shaft, except for the presence of isolated enlargement “chambers” in the burrow shaft (near the top of the exposed parts of the cluster of three burrows (B19-7-1/2/3)). The burrow entrance at the palaeo floodplain surface is not preserved. The excavated portion of the burrow shows no evidence of branching.

The basic dimensions, as recorded in the field and in the laboratory, are summarized in Table 4.1 and Appendix C. The shafts are at ramp angles that range from 25° to 35° (average 27.3°, SD 4.6°) as measured relative to the horizontal. The horizontal diameter of the burrow casts ranges from 2.5 to 6.9 cm (Average = 4.7 cm, SD = 1.6 cm). The vertical diameter ranges from 2.2 to 6.5 cm (Average of 3.7 cm, SD = 1.5 cm). The corresponding aspect ratio ranges from 1 to 1.5 (Average = 1.3, SD = 0.2).

Surficial morphology of sub-circular burrow casts

The surfaces of the three clustered burrow casts (B19-7-1/2/3) have knobby and hummocky textures with cm-scale protuberances (Figure 4.2). This type of surficial morphology is consistent with the knobby and hummocky surfaces of the burrow casts identified in Hasiotis and Mitchell (1993). The protuberances that result in the knobby surface are 2 – 4 mm wide and about 2 mm high.

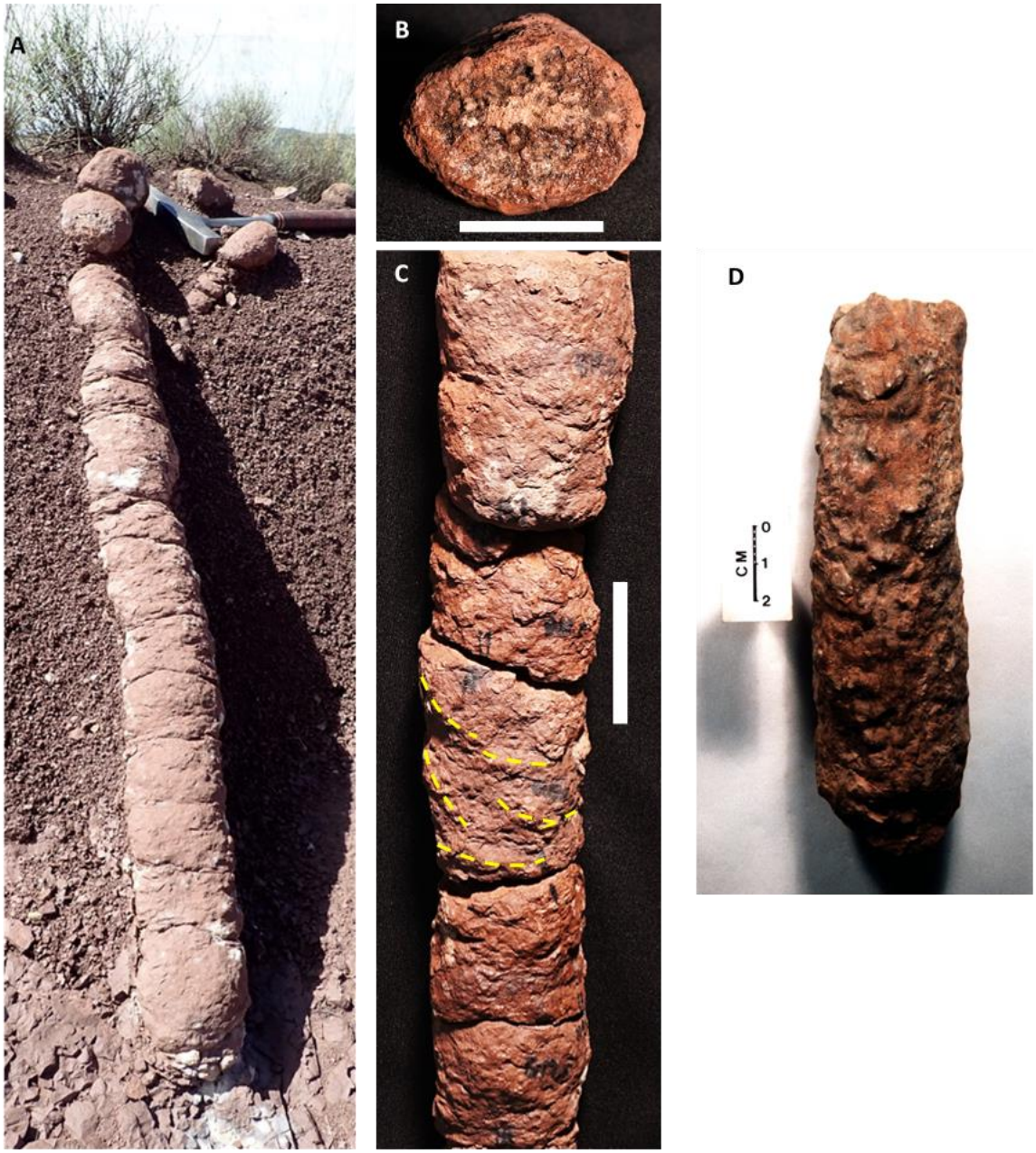


Figure 4.2: Sub-circular burrow cast.: (A) Burrow B19.7-2 with enlargement chamber near the top (total excavated length 80 cm). (B) Cross-section showing a diagenetic colour alteration halo. (C) Knobby and hummocky surficial morphology over printing sub-horizontal scrape marks (selected examples highlighted with yellow dashed lines). (D) Knobby and hummocky surficial burrow morphology from Hasiotis and Mitchell (1993, Fig. 6-E). Scale bar in B and C = 5 cm.

A second type of surficial morphology is present on specimen B19-10. In this case, cm-scale horizontal ridges representing scrape marks are present (refer to Figure 4.3). These are similar to but less distinctive than scrape marks on the surfaces of some of the burrow casts identified in Hasiotis and Mitchell (1993). The main horizontal scrape marks are produced by the chelae of crayfish during the construction of the burrow and are about 1 cm apart (~0.5 cm wide) on the Hasiotis and Mitchell (1993) specimen and about 1.2 cm apart (~0.6 cm wide) on specimen B19-10. Similar ridges are present on specimen B19-7-2. In this case the ridges are overprinted by the knobby and hummocky surface features (Figure 4.2).

The remaining sub-circular burrow specimens show similar features although some have smooth to irregular surfaces, but without any recognizable markings.

Burrow fill

The cluster of three sub-circular burrow casts (B19-1/2/3) is infilled with a moderate-brown (5YR 4/4) fine-grained sandstone. The well-cemented calcified sandstone is very resistant to weathering and has a greyish-brown diagenetic colour alteration halo around the burrow cast that has the appearance of a burrow lining. This halo is 2 – 5 mm thick. The infill of burrow casts B19-4 and B19-9 is the same very fine olive-grey (5Y 6/1) sandstone that also infilled the reniform burrows. For burrows B19-8 and B19-7, the colour of this fine sandstone infill is yellowish-grey (5Y 7/2).



Figure 4.3: Sub-circular burrow casts. (A) Burrow B19-10 with less prominent surface scrape marks or ridges transverse to the burrow axis (selected examples highlighted with white dashed lines). (B) Surficial burrow morphology from Hasiotis and Mitchell (1993 Fig. 6-B). Scale bar = 2 cm.

4.5 Qualitative analysis of Lemoenfontein burrow casts

As indicated in Table 4.1, there are two distinct types of burrows present at the same locality and in the same stratigraphic level and mudstone beds:

- reniform burrows with surficial morphologies that show longitudinal scratch marks and with horizontal diameters ranging in from 6 to 8 cm; and
- sub-circular burrows with a knobby and hummocky surficial morphology, ranging in main diameter from 2.5 to 6 cm.

Because these burrow types both occur at the same locality and in the same beds, it is important to clearly distinguish them from each other before any investigation of the potential burrow producers can be attempted. Hasiotis et al. (1999) performed an extensive observational and statistical analysis of putative Triassic crayfish burrows from Antarctica and was able to demonstrate that the burrows were in fact produced by tetrapods. This was achieved by comparing the architectural and surficial morphologies of the Antarctic burrows to Triassic crayfish burrows from the Canyonlands National Park in Utah (USA). The observational analysis identified that these burrows had the following in common:

- inclined shafts mostly at low angles (10° - 40°);
- longitudinal scratch marks that sometimes cross; and
- bases, consisting of two lobes separated by a trough running along the length of the ventral side of the burrow.

These features are considered sufficiently different from those observed in modern crayfish burrows to rule out crayfish as the burrow producers. Crayfish burrows are typically circular, sub-vertical with a surficial morphology that is knobby and hummocky, or show body impressions, scrape marks, and striae created by the various appendages of the crayfish. Mud liners may also be present. The statistical analysis focussed on the basic burrow dimensions and tested:

- the degree to which the Antarctic burrows were elliptical rather than circular (by plotting the larger burrow diameter against the smaller diameter);
- the flatness of the burrow shaft ramp angle; and

- the size of the burrow.

This analysis concluded that the Antarctic burrows are more elliptical, larger and at lower ramp angles than the Canyonlands crayfish burrows. They offered a caveat that crayfish burrows containing terminal living or mid-shaft level chambers and junctions can also be at low ramp angles.

The observational analyses of the architecture and surface morphology of the Lemoenfontein burrow casts presented previously conforms with the conclusions reached by Hasiotis et al. (1999). The architecture and surficial morphology of the reniform burrows correspond to the Antarctic tetrapod burrows, while those of the sub-circular burrows correspond to the Utah crayfish burrows. The basic measurable parameters of the Lemoenfontein burrows can be tested against the data presented in Hasiotis et al. (1999). By plotting the large (2) and small (1) diameters against each other, they derive a linear relationship of diameter 2 as a function of diameter 1 for the two types of burrows. These relationships are reproduced in Figure 4.4. The corresponding data for the two types of burrow casts from Lemoenfontein are also plotted on this graph.

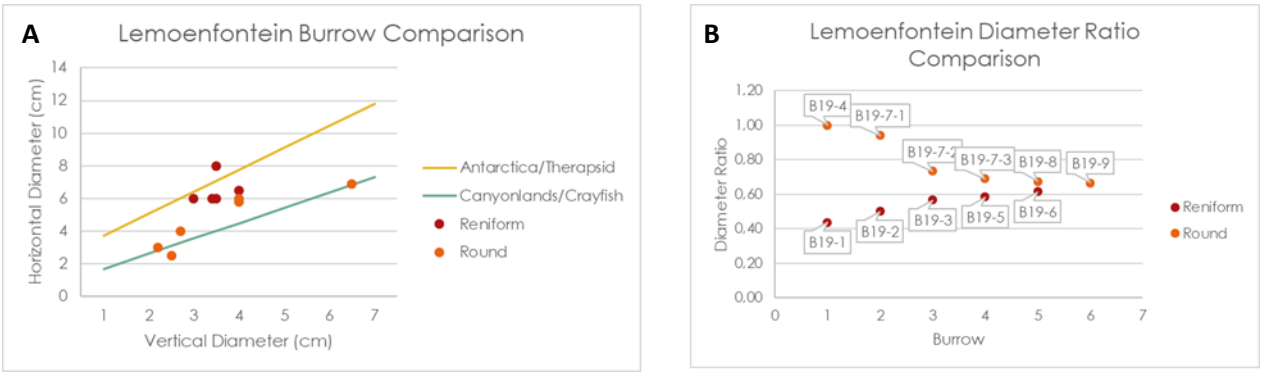


Figure 4.4: (A) Plot of horizontal to vertical diameter. (B) Comparison of diameter ratios for the two types of burrows.

The data are presented in two ways: (A) the large diameter is plotted against the small diameter; (B) the ratio of these two diameters is plotted for each burrow sample (sorted from large too small for the reniform burrows and small to large for the sub-circular burrows). Although there are not enough samples to do a quantitative statistical analysis, a remarkable qualitative correspondence can be observed. The reniform burrows cluster

around the Antarctic therapsid line and the sub-circular burrows follow the Canyonland crayfish line. The reniform burrows are consistently more oval than the sub-circular burrows and there is no overlap. This distinct lack of overlap is also confirmed by the diameter ratio plot. Hasiotis et al. (1999) found that all (except for one) of the crayfish burrows plotted on or above the lower linear curve. Most data points are on the curve and most of the remaining points are below the Antarctic therapsid line. Similarly, the Antarctic therapsid data points plotted above the Antarctic therapsid line, except for a few of points that plotted in between the two lines. The result for Lemoenfontein is very similar. All the sub-circular burrows plot cluster around the crayfish line (never above the Antarctic therapsid line) and the reniform burrows cluster around the Antarctic therapsid line (never below the Antarctic crayfish line).

Additional comparisons are possible using the data. These results are presented in Figure 4.5.

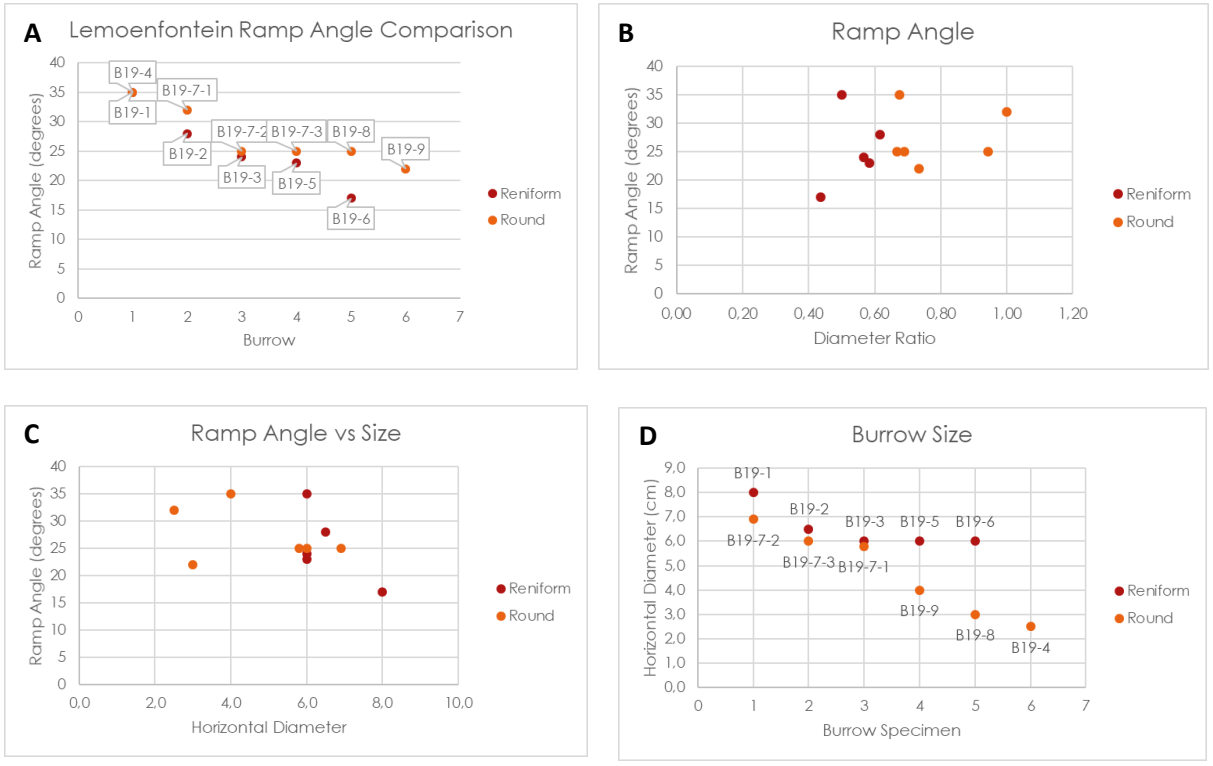


Figure 4.5: (A) Comparing ramp angles for the two types of burrows. (B) Plot of Ramp angle as a function of diameter ratio. (C) Plot of ramp angle versus burrow size. (D) Comparing burrow sizes for the two types of burrows.

The first test (Figure 4.5 A) compares the ramp angles of the reniform burrows to those of the sub-circular burrows. This is achieved by arranging the burrows of each type from large ramp angle to small ramp angle. The result shows that although there is some overlap for the largest pairs of ramp angles, the trend is for the sub-circular burrows to have a steeper angle than the reniform burrows. The second test (Figure 4.5 B) checks if there is any correlation between degree of ovality (diameter ratio) and ramp angle. The result is that the more oval a burrow is, the lower the ramp angle (except for the two highest reniform and sub-circular burrows – both at 35°). This agrees with an intuitive notion that due to compaction sub-horizontal burrows would tend to be more oval, while sub-vertical burrows would be more circular. Again, the reniform burrows are distinctly resolved from the sub-circular burrows in this case. The third test (Figure 4.5 C) checks if there is any correlation between ramp angle and burrow size (the horizontal diameter is used as a proxy for size). Again, the result suggests (except for the reniform and sub-circular burrows with the smallest ramp angles), that for both groups a larger burrow diameter corresponds to a smaller ramp angle. The fourth test (Figure 4.5 D) compares the burrow sizes of the reniform burrows to those of the sub-circular burrows (the horizontal diameter is used as a proxy for size). Both sets are arranged from large to small diameter. The trend is clear that the reniform burrows are always larger than the sub-circular burrows (except for a single largest sub-circular sample). All except one of the sub-circular burrows are smaller than 6 cm and all the reniform burrows are larger than 6 cm.

In summary:

- the reniform burrow diameter ratio is remarkably like the Antarctic Triassic tetrapod (likely therapsid) burrow data and the sub-circular burrows correspond to the modern Canyonland crayfish data;
- the sub-circular burrows are generally at a steeper angle than the reniform burrows;
- rounder burrows are steeper in ramp angle for both groups and there is no overlap between the two groups;
- smaller burrows tend to be steeper in ramp angle; and
- the reniform burrows are larger than the sub-circular burrows and the distinction between the two groups is approximately at 6 cm.

This result demonstrates a clear difference between the reniform and sub-circular burrows. Therefore, these two types are treated as distinct in the discussion that follows.

4.6 Reniform burrow discussion

A comparison of the characteristics of the Lemoenfontein reniform burrow casts to other known casts is provided in Table 4.2. In terms of the main characteristics of the architectural and surficial morphology, the reniform burrows from Lemoenfontein are consistent with *Reniformichnus katikatii* (Krummeck and Bordy, 2018), Therapsid Type L (Bordy and Krummeck, 2016; Hembree, 2010; Miller et al., 2001; Hasiotis et al., 1993) and Tetrapod Ichnogenus B (Sidor et al., 2008; Bordy and Krummeck, 2016). Specifically, the Lemoenfontein burrows have the following in common with these:

- the overall morphology consists of a simple, non-branching, low-sinuosity, inclined shaft with a bilobate base;
- the average burrow inclination of the Lemoenfontein burrows falls within the range of the *Reniformichnus* and Therapsid Type L burrows;
- a reniform cross-section;
- the average horizontal diameter is within the range of dimensions for Therapsid Type L and Tetrapod Ichnogenus B burrows (for *Reniformichnus* this measure is approximately double corresponding to Tetrapod Ichnogenus A (Sidor et al., 2008) or Therapsids Type G (Miller et al., 2001) burrows);
- an average aspect ratio within the range of these burrows; and
- longitudinal scratch marks along the burrow axis, with some overlap forming chevrons on the lateral to ventral sides.

Based on these corresponding characteristics, the Lemoenfontein reniform burrows are assigned to the ichnotaxon *Reniformichnus katikatii.* Using similar morphological considerations, Krummeck and Bordy (2016) assign the Antarctic Tetrapod Ichnogenus A and Therapsids Type G burrows to *Reniformichnus katikatii.* Ichnogenus A and Therapsids Type G have similar horizontal diameters to *Reniformichnus*. The Lemoenfontein burrows are closer

in size to Ichnogenus B and Therapsids Type L burrows but based on the exceedingly similar morphologies are also assigned to *Reniformichnus*. This conclusion is justified by the consensus reached in Bertling et al. (2006) that if a set of different traces share the same morphology, using size to distinguish at the inchnospecies, rank should be avoided, and size should not at all be used at higher ranks. Sidor et al. (2008) consider that the Ichnogenus B burrow casts from the Antarctic Lashly Formation to be "virtually identical" to burrow casts BP/1/5067 and SAM-PT-K10545 from the Burgersdorp formation of South Africa. Sample BP/1/5067 was collected by James Kitching from the same Lemoenfontein locality under consideration here (pers. comm., 1976; inscription on the actual specimen in the ESI collection).

Krummeck and Bordy (2016) also consider the tetrapod burrow casts described by Groenewald (1991) to be like *Reniformichnus.* Sidor et al. (2008) in turn consider that the *Langbergia* burrow casts described by Groenewald et al. (2001) from the lower Burgersdorp Formation are very much like the Ichnogenus B burrow casts from the Lashly Formation although the latter have a transverse diameter of about half the size (4 to 6 cm).

Table 4.2: Lemoenfontein burrow casts characteristics and comparison to similar burrow casts

Burrow Characteristic	This Study Reniform	This Study Sub-circular	*Reniformichnus*	Crayfish	Lungfish (Aestivation)	Therapsids (Type L)	Tetrapod (Ichnog B)
Architectural Morphology	Simple, single shaft. Asymmetrical bilobate base. Straight to low sinuosity.	Simple, single shaft varying from straight to gently curved.	Simple, single shaft. Straight to gently sinusoidal. Asymmetrical bilobate base.	Various: Single simple vertical shafts to straight or spiralling interconnected shafts.	Simple vertical cylindrical shaft	Tunnel steeply inclined at top of burrow to gently inclined downward. Rarely J-shaped, gently curving.	Placeholder ichnogenus for horizontal to gently inclined terrestrial burrows with bilobed ventral surface.
Orientation	Vertical shafts inclined at angles ranging from 17° to 35° (average 25°, SD 6)	Vertical shafts inclined at angles ranging from 22° to 32° (average 27°, SD 4.6)	Vertical shafts inclined at angles from 8° to 30° (average 20°, SD 9.0)	Vertical and horizontal	Vertical with deviation from vertical less than 5° - 8°	Predominantly sub-horizontal, 10° - 40°	Gently inclined
Cross-section	Reniform	Sub-circular (one specimen B19-4 is circular)	Reniform	Predominantly circular to elliptical	Circular to elliptical	Circular to elliptical, 50% of samples are reniform.	Reniform
Diameter (maximum)	6 - 8 cm (average 6.5 cm, SD 0.8 cm)	2.5 - 6 cm (average 4.8 cm, SD 1.8 cm)	10 - 15 cm (average 12.1 cm, SD 2.1 cm)	2.0 - 8.0 cm	1 - 10 cm	2.0 - 6.5 cm (mean 3.9 cm)	4.3 - 6.8 cm (average 5.3 cm, SD 0.81 cm)
Aspect ratio	1.6 - 2.3 (average 1.9, SD 0.2)	1.4 - 1.9 (average 1.4, SD 0.3)	1.7 - 3 (average 2.2, SD 0.5)	1.0 - 1.6 cm	1.0 - 2.6 (mean ~ 1.5)	1.0 - 2.6 cm (mean 1.4 cm)	1.3 - 2.2 (average 1.7, SD 0.27)
Curved burrow length	Burrows occur below the structural B horizon and extends through the underlying calcareous nodular horizon. Burrow entrances have eroded away. Exposed length from ~30 cm to ~100 cm.	Burrows occur below the structural B horizon Termination points not uncovered. Burrow entrances have eroded away. Exposed length from ~30 cm to ~100 cm.	Exposed length from 30 to 170 cm. Burrow entrances (apertures) at depositional surface are not preserved.	50 - 200 cm	10 - 50 cm (some > 100 cm)	Typically, 15 cm (maximum 50 cm)	Exposed length average 14.7 cm max 43.7 cm, total length likely > 50 cm.

Burrow Characteristic	This Study Reniform	This Study Sub-circular	*Reniformichnus*	Crayfish	Lungfish (Aestivation)	Therapsids (Type L)	Tetrapod (Ichnog B)
Terminal chamber	One burrow (B19-1) excavated to terminal. Terminal chamber tapers dorso-ventrally distally.	Enlargement chambers along the burrow vertical axis.	No terminal chamber	Yes, cross-sectionally expanded.	Cylindrical with a pseudo chambre or Flask Shaped with expanded bulbous chambre	Unknown	Present in one specimen (UWBM 88600). Lateral margins expand slightly distally. Dorsal and ventral surfaces taper towards dorso-ventral midline.
Burrow termination	Semi-rounded and flattened.	Unknown	Unknown	Rounded and enlarged	Semi rounded or bulbous	Unknown	Semi-rounded and flattened.
Branching	Absent	Absent	Absent	1 to 10 segments	Absent in aestivation burrows	Rare horizontal or vertical branching	Unknown
Number of surface openings	Although surface openings have eroded away, no evidence of multiple openings.	Although surface openings have eroded away, no evidence of multiple openings.	Entrances at the depositional surface are not preserved.	1 to 3	1, indistinct, grades into host rock	1 or more	Unknown
Surficial Morfology	Scratch marks initiate on upper surface, extend parallel to burrow axis from upper wall to side walls. Shorter cross cutting ridges extend from side walls to ventral wall.	Knobby and hummocky surfaces. Some evidence of millimetre scale semi-vertical striations and horizontal scrape marks.	Longer ridges and scratch marks parallel to burrow axis on upper and side walls, shorter cross cutting ridges on the ventral wall.	Knobby, hummocky surface with scratch marks and impressions of body parts.	Walls surfaces are smooth and well defined, some possess small bumps or horizontal to vertical striations.	Longitudinal ridges along the axis of the burrow are rare to common, rarely transverse, some overlapping ridges forming subtle chevrons	Longitudinal ridges/striations on ventral surface, angled at 20° to the horizontal on lateral surfaces.
Lining	None	Possible lining but likely a diagenetic or pedogenic halo around cast.	None	Mud pellet and mud lining	May be present in the form of packed mudstone containing scales and small bones.	Rare mud chip lining	Unknown

Burrow Characteristic	This Study Reniform	This Study Sub-circular	*Reniformichnus*	Crayfish	Lungfish (Aestivation)	Therapsids (Type L)	Tetrapod (Ichnog B)
Clusters	Isolated, not occurring in clusters.	Isolated except for one cluster of three casts (19-7-1/2/3) (~50 cm across)	Isolated, not occurring in clusters.	2 to 10 burrows per m of outcrop.	Dense clusters along a single stratigraphic horizon, a few cm's between.	1 burrow per 3.5 m of exposure (over 67 m)	Unknown
References	April 2019 Field Notes	April 2019 Field Notes	Krummeck and Bordy (2018)	Bordy and Krummeck (2016), Miller et al. (2001)	Bordy and Krummeck (2016), Hembree (2010), Miller et al. (2001), Hasiotis et al. (1993)	Bordy and Krummeck (2016), Hembree (2010), Miller et al. (2001), Hasiotis et al. (1993)	Sidor et al. (2008), Bordy and Krummeck (2016)

4.7 Sub-circular burrow discussion

Since there is a clear distinction between the reniform and the sub-circular burrows, a comparison of the characteristics of the sub-circular burrow casts is limited to crayfish and lungfish burrow casts (Table 4.2). Following the example of Bordy and Krummeck (2016) other significant continental burrowers, such as small soil arthropods, are not considered for comparison, due to the difference in burrow characteristics and size. Bordy and Krummeck (2016) also compare their burrow casts to those of lysorophian amphibians. These amphibian burrow casts are distinctly elliptical in cross-section and show a surficial morphology that consists of irregularly spaced nodes of variable size and no scratch marks. These characteristics do not correlate with the Lemoenfontein burrows and are therefore not considered further in this analysis.

Based on the characteristics recorded in Table 4.2, several comparisons are possible.

Architecture: The Lemoenfontein burrows consist of simple straight to slightly curving inclined shafts. Crayfish burrows can have this simple architecture but can also be more complex (Hasiotis and Mitchell, 1993). There can be branching, and the burrow orientation can vary from sub-vertical to horizontal - typically sub-vertical near the top, becoming more horizontal with increased depth. Lungfish aestivation burrows consist of simple vertical or sub-vertical shafts (Hasiotis et al. 1993). Lungfish nesting burrows can show more variation from branching with some horizontal segments (Hasiotis et al. 1993). In terms of these characters, the Lemoenfontein burrows are consistent with the lower and less vertical portions of crayfish burrows but not with the vertical orientation of lungfish aestivation burrows. The cross-section of both the crayfish and lungfish burrows is circular to elliptical with diameter ranges that would include the range for the Lemoenfontein burrows. Some Lemoenfontein burrows contain enlargement chambers near the top of the exposed length, but since the burrow entrances and upper portions of the shafts are not preserved, these enlargements were originally lower down the shafts. Crayfish burrows also have such enlargements chambers, and these are created to accommodate seasonal changes in the water table (Hasiotis and Mitchell, 1993; Abouessa et al., 2015). Lungfish aestivation burrows may terminate in a pseudo chamber, or it can be flask-shaped with an expanded bulbous

chamber (Hasiotis et al. 1993). The maximum excavated portion of the burrows of this study is approximately 80 cm long. Crayfish burrows can reach 5 m in length (Hasiotis et al. 1993), while lungfish burrow lengths do not exceed 0.5 m.

Surficial morphology: The sub-circular burrows show a clear knobby and hummocky surface (Figure 4.2). These surface features correlate well with the crayfish burrow surficial morphology as described by Hasiotis and Mitchell (1993); the knobs are of comparable size and the overall surface undulation is very similar. On the other hand, the walls of the lungfish burrows are generally smooth and well-defined. Some specimens show some small bumps, vague nodes or sub-horizontal scratch marks, but the overall surface does not have a distinct morphological variation as is the case for crayfish burrows (Hasiotis et al., 1993; Bordy and Krummeck, 2016).

Considering the overall burrow architecture and surficial morphology, the sub-circular burrows are more like crayfish burrows, being significantly different from lungfish burrows.

4.8 Potential burrow-makers

As demonstrated in the discussion above, there are two distinct types of burrows present at the same locality and in the same stratigraphic level and mudstone beds.

- Reniform burrows with a surficial morphology that corresponds closely to that of *Reniformichnus*, Ichnogenus B and the reniform versions of Antarctic Type L, ranging in horizontal diameter from 6 to 8 cm.
- Sub-circular burrows with a knobby and hummocky surficial morphology, ranging in main diameter from 2.5 to 6 cm.

Lemoenfontein reniform burrow trace makers

Miller et al. (2001) firmly assign Type G burrows from Antarctica to a tetrapod origin based on the close correspondence of their architectural and morphological characteristics to burrows from South African deposits of similar age that contain remains of their therapsid producers. However, no firm conclusion is reached about the Type L burrow producers since this grouping includes cross-sectional shapes that vary from oval to reniform, surficial morphology can be "bumpy/irregular" or have longitudinal scratch marks along the burrow axis and are considered small compared to confirmed adult tetrapod produced burrows. These contrasting surficial features were not used to distinguish between different burrow types. Based on these observations, Miller et al. (2001) assign the Type L burrows to either crayfish or tetrapods. Sidor et al. (2008) come to similar conclusions about the Type L burrows as well as the burrow casts from the Burgersdorp Formation (i.e., Lemoenfontein). Using the skull width of the procolophonid *Teratophon* (Specimen SAM-PK-K10174, skull width = 12.8 cm) as a proxy for minimum burrow major axis diameter, they rule it out as possible burrow producer as the width of sample SAM-PT-K10545 is only 5 cm. By contrast, Hasiotis et al. (2004) come to the firm conclusion that the Antarctic Type L burrows are of tetrapod origin because the burrow morphologies are "extremely similar" to burrows that were constructed by smaller mammal-like reptiles. This conclusion also suggests that mammal-like reptiles may have been present in the high-palaeolatitude portions of Pangea

and that they may have used burrowing to assist with hibernation in cold periods (Hasiotis et al., 2004).

In contrast to Miller et al. (2001), the interpretation is made here that these two types of burrows from Lemoenfontein were created by different burrow producers and are therefore considered to be distinct allowing an independent assessment of each type. This avoids the complication introduced by the contrasting surficial morphologies in Miller et al. (2001). However, it is remarkable that both types of burrows occur in similar aged sedimentary rock in two localities a large distance apart in Gondwana. For reference see Figure 6 A (reniform burrow cast with chevron shapes scratch marks) and Figure 6 B (oval burrow cast with knobby surface) in Miller et al. (2001).

A unique feature of the Lemoenfontein locality is that over 140 tetrapod skulls attached to curled-up skeletons or isolated skulls with articulated lower jaws from a variety of taxa have been collected from the same mudrock beds that host the burrows (over a confined surface area). Specimens ranging from juveniles to adults of procolophonids (*Teratophon spinigenis*, *Thelephon contritus*), trirachodontid cynodonts (*Trirachodon berryi*), probainognathian cynodonts *(Lumkuia fuzzi),* bauriid therocephalians (*Microgomhodon oligocynus*), rhynchosaurs (*Eohyosaurus wolvaardti*). Several of these taxa are associated with burrowing.

- It has been observed that procolophonids were burrowing animals (Colbert and Kitching, 1975; Sidor et al., 2008; Bordy and Krummeck, 2016; deBraga, 2003). Many of these citations referred to Kitching's verbal communication as reported by Groenewald (1991) about possible procolophonid fossil remains in a burrow.
- Groenewald et al. (2001) describe vertebrate burrow complexes from the Early Triassic and attribute these to *Trirachodon* (Note that the trirachodontid material from the *T-K* Subzone of the *Cynognathus* AZ has subsequently been recognized as the new taxon *Langbergia modisei* (Abdala et al., 2006; Smith et al., 2012)).
- A cast of a burrow infill (specimen number CGP/1/ 44 (previously numbered GSA 1/44)) was collected on the farm Moerbeidal 648 in the Rouxville district (Free State) in November 1997 by J. Neveling. Based on the presence of tetrapod bones visible on

the cross-sectional break in the burrow cast, this specimen was recently CT-scanned revealing an articulated skeleton of *Microgomphodon* in what appears to be the burrow terminal chamber (V. Fernandez, F. Abdala, and J. Neveling, pers. comm., August 2019), see Figure 4.6.

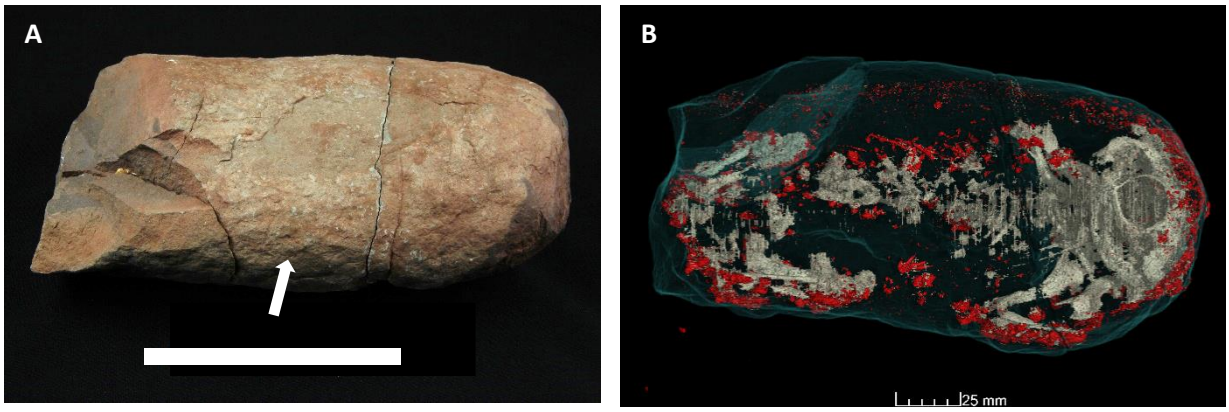


Figure 4.6: Microgomphodon in the burrow terminal chamber (pictures provided by V. Fernandez, August 2019). (A) Burrow chamber surface showing scratch marks (arrowed). (B) Micro CT scan showing the articulated Microgomphodon *skeleton. Scale bar = 10 cm.*

It is noteworthy that two procolophonid genera, one trirachodontid genus, and one bauriid genus, all of which have been associated with burrowing, all occur in the same mudstone strata as the burrow casts from this locality. The skull width of some of the representative specimens from the Lemoenfontein locality are summarised in Table 4.3.

Table 4.3: Skull width of the possible burrow makers

Genus	Specimen number	Maximum cranium width (cm)	Source
Microgomphodon	SAM-PK-K10160	6.3	Abdala et al. (2014)
Teratophon	SAM-PK-K10174	12.8	Iziko collection
Teratophon	L18-2	9.5	Iziko collection
Teratophon	L18-21	7.2	Iziko collection
Teratophon	L18-5	3.9	Iziko collection
?Teratophon	L18-8	3.6	Iziko collection
Thelephon	SAM-PK-K10172	6.5	Iziko collection
Thelephon	SAM-PK-K10162	4.2	Iziko collection
Trirachodon	SAM-PK-K10762	6.4	Iziko collection

Several authors have noted a strong correlation between burrow diameter and burrow producer body size (Anderson, 1982; White 2005, Catena and Hembree, 2014). Anderson (1981) points out that the minimum burrow radius must only be large enough to allow the animal free passage and that any increase in size beyond this increases the energy cost of burrowing significantly. White (2004) found that the reduction in burrow cross-sectional area is limited by morphological modifications to the body components needed for digging or excavation. Also, the need for animals to pass each other or turn around in a burrow results in larger burrow sizes depending on the whether the animals are colonial or not. Catena and Hembree (2014) analysed the burrowing behaviour of skinks. A skink burrows by penetrating the host medium with its triangular head, resulting in a burrow diameter that is only slightly larger than the skink's skull width (1.1 cm versus 0.9 cm). Depending on the burrowing style (excavation or penetration) or social behaviour of the burrow producers, the burrow cross-sectional area ratio to skull or body width varies; with excavating burrowers requiring a larger burrow cross-sectional area. The general conclusion is that the burrow diameter must at least be larger than the maximum cranial width of the producer.

The reniform burrow horizontal diameters from Lemoenfontein range from 6 to 8 cm while the skull width of the possible burrow producers varies from 3.6 to 12.8 cm. Due to the incomplete nature of the fossil record, larger burrows from this locality cannot be ruled out. One giant burrow terminal chamber (like Type G of Miller et al., 2001) has been recorded in mud rock beds higher up in the succession, see Figure 4.7. The large adult and subadult *Teratophon* specimens (SAM-PK-K10174, L18-2) can be ruled out as potential burrow makers for the typical Lemoenfontein reniform burrow that have a width smaller or equal to 8 cm. However as demonstrated in Figure 4.7, large burrows that could accommodate *Teratophon* with mature quadratojugal spine development, were probably also present but have not been preserved.



Figure 4.7: (A) Giant reniform burrow terminal chamber from the study locality. (B) Distinct reniform cross-section (width = 15 cm, mid-level height = 7.5 cm, maximum height 12.5 cm). Scale bar = 5 cm.

Although Krummeck and Bordy (2016) consider the tetrapod burrow casts described by Groenewald (1991) and those attributed to cynodonts, e.g., *Thrinaxodon* (Damiani et al., 2003), to be like *Reniformichnus* they do not definitively identify a burrow producer due to the absence of tetrapod remains with sizes that are consistent with the burrow diameters and the absence of fossil remains within the burrow casts. Using the same arguments, Sidor et al. (2008), also do not commit to a burrow maker for their tetrapod ichnogenus B, but state that these burrows are identical to the two burrow samples from Lemoenfontein that they used for comparison. Hasiotis et al. (2004) come to the firm conclusion that the Antarctic Type L burrows are also of tetrapod origin.

Burrow casts excavated in this study have extended the burrow lateral diameter range (6 to 8 cm) and many tetrapod body fossils of compatible skull size (3.6 to 8 cm) have been collected from the same host matrix as the burrows. To date, no skeletal remains have been found within any of the burrow casts collected in this study. However, many curled-up procolophonid skeletons from this locality do appear to have been trapped in confined spaces. This is investigated further in the taphonomy study in Chapter 6. Furthermore, since

the architecture and surface markings of the reniform burrow casts do not resemble burrows of other producers such as crayfish or lungfish (Table 4.2), these can be ruled out as burrow makers.

Miller et al. (2001) identify seven criteria that can be used to identify producers of terrestrial burrows. These criteria allow identification within three levels of confidence: Most reliable; Less reliable; and Least reliable. Consistent with Smith (1987) the first two most reliable criteria require the presence of the burrow maker (either in life position or skeletal fragments) within the burrow. The third most reliable criterion requires that the burrow resembles the burrow of a known producer in 1) size, 2) architecture and 3) surface markings (the fourth requires a resemblance in two of these three characteristics). As a result of the consensus reached by Bertling et al. (2006) that size should not be used as a criterion, criteria three and four can be combined by considering only architecture and surficial morphology. Therefore, based on these arguments, the reliable conclusion is made that the reniform burrows of this study are of tetrapod origin and that they were excavated by procolophonids, trirachodontids or bauriids whose skeletal remains occur in the same interval at the same locality.

Lemoenfontein sub-circular burrow trace makers

Hasiotis and Mitchell (1993), compared crayfish burrow casts from the Upper Triassic Chinle Formation to casts of modern crayfish burrows that were constructed under laboratory conditions, as well as under natural conditions in the field. This important study showed that the Triassic and modern crayfish employ the same burrowing techniques that result in very similar architectural and surface morphologies.

By studying the mechanisms used by modern crayfish for the construction, maintenance and habitation of the burrows and the surficial features that result from these activities, they were able to correlate the following:

- sub-horizontal cm-scale scrape marks and ridges are produced by the crayfish chelae (claws) while excavating and shaping the burrow;
- knobby and hummocky surficial features are created by the crayfish pereiopods (walking legs) during construction, maintenance and habitation of the burrows;
- sub-vertical mm-scale striations are produced by the crayfish telson (tail);
- various body impressions in the wetter regions of the burrows are possible, such as mm-scale striations made by the multiple abdominal pleopods (swimlettes); and
- mud- or lag-liners and chimney structures are also common.

Similarly, by comparing the architectural morphologies of modern and Triassic crayfish burrows, three types of burrowing signatures can be identified.

- Type I: Relatively complex architecture, several entrances leading to a main chamber, several shafts linking the main chamber to secondary chambers, depth less than 1 m. These burrows are inhabited by primary burrowers (spend most of their lives in the burrow), are not connected to open water, but are constructed in modern and palaeo floodplain environments where the water table is near the surface.
- Type II: Architecture of medium complexity, one or more entrances, a few branches, one chamber, depth less than 1 m. These burrows are inhabited by secondary burrowers (spend variable durations in the burrow), are connected to open water and

are constructed in modern and palaeo channel, point bar or levee deposits where the water table is at or above the surface.

- Type III (Long): Architecture relatively simple, one or more entrances, bifurcates at the water table with horizontal branches leading to possible chambers, sometimes show mid-length enlargement chambers (at wet season ground water level), depth can be from 0.5 to 5 m. These burrows are inhabited by primary burrowers (spend most of their lives in the burrow), are not connected to open water and are constructed in modern and palaeo floodplain environments where the water table is deep and fluctuating.
- Type III (Short): Architecture simple, sub-vertical or sub-horizontal shafts, with simple chamber, may have a simple U-shape with two entrances, less than 0.5 m in depth. These burrows are like burrows of Tertiary burrowing crayfish (spend most of their lives in open water) and are constructed in lacustrine, channel, or point bar deposits, where the water table is at or above the surface, burrowing only during dry season when water bodies dry out to mitigate desiccation or for reproduction.

The work of Hasiotis and Mitchell (1993) allowed the definition of a systematic ichnology for ancient terrestrial freshwater crayfish burrows. The surficial morphology of the burrow defines its ichnogenus, while its architectural morphology defines its ichnospecies (Hasiotis and Mitchell, 1993; Hasiotis and Honey, 2000). They adopted the following ichnotaxonomy:

- Ichnogenus – *Camborygma;*
- Ichnospecies (Type I) – *symplokonomos;*
- Ichnospecies (Type II) – *araioklados;*
- Ichnospecies (Type III long) – *eumekenomos; and*
- Ichnospecies (Type III short) – *litonomos.*

This method of characterising burrows provides an important tool for discerning burrow makers from each other (Hasiotis et al. 1993). The discovery that Triassic and Holocene terrestrial freshwater crayfish used the same burrowing methods, which resulted in identical burrow morphologies ((Hasiotis et al. 1993) allowed for a reliable identification of ancient crayfish burrows based on the correlation between architectural and surficial morphological

signatures. In other words, crayfish burrows can reliably be identified without the presence of crayfish body fossils. In fact, the presence of crayfish burrows is a good proxy for the presence of crayfish in the fossil record where there are no crayfish body fossils (Hasiotis et al., 2002; Hasiotis et al., 1998; Hasiotis et al., 1993; Hasiotis and Honey, 2000; Hasiotis, 2002; Bedatou et al., 2007; Baucon et al., 2014). This is important since crayfish body fossils are often not preserved (Hasiotis et al., 1998; Hasiotis, 2002). The absence of crayfish fossils from Gondwana has long been an enigma and Hasiotis (2002) predicted that evidence for the presence of crayfish could be obtained based on the re-examination of Mesozoic Gondwana sedimentary rocks for evidence of crayfish burrows. The morphologies of these burrows should be like the North American crayfish burrows. Subsequently, Early Cretaceous crayfish body and burrow fossils have been discovered in Australia (Martin et al., 2008) and Upper Eocene crayfish burrows have been described from Libya (Abouessa et al., 2015). In the Upper Permian and Lower Triassic of the Karoo Basin, Gastaldo and Rolerson (2008) described a new ichnogenus and ichnospecies, *Katbergia carltonichnus,* which they assign to a possible decapod crustacean burrow maker (burrow diameter 1 -2 cm). Smith and Botha-Brink (2014) also note the occurrence of *Katbergia* in the Early Triassic and suggests that the crustacean may be a callianassid-shrimp.

Based on the close correspondence of the quantitative form and qualitative parameters (major axis versus minor axis, diameter, size of knobs and ridges, spacing ridges on the hummocky and knobby surfaces) of the Lemoenfontein sub-circular burrows to the burrow surfaces described by Hasiotis (e.g. Hasiotis and Mitchel, 1993; Hasiotis et al., 1998; Hasiotis et al., 1993, Hasiotis and Honey, 2000; Hasiotis, 2002), the interpretation is made that these sub-circular burrows can be assigned to the ichnogenus *Camborygma.* This interpretation is supported by the sub-horizontal scrape marks and ridges present on some of these burrow casts.

Sedimentary features recorded in the burrow host matrix such as the structural B and calcareous nodular horizons point to a seasonal water table variation, with the dry season water table being at least 2 m below the floodplain palaeosurface at the time of burrowing. There is also sedimentary evidence pointing to a proximal flood plain setting (such as the

presence of the crevasse splay sandstone). The length of the exposed part of the sub-circular burrows is greater than 80 cm. This information and the architectural morphology of simple, long cylindrical shafts with mid-length expanded chambers (corresponding to the height of the wet season water table) suggests that these burrows could be assigned to the ichnospecies (Type III long) – *Camborygma eumekenomos.* This interpretation needs further qualification. The Triassic burrows from North American proximal and distal floodplain sedimentary rocks are predominantly vertical (Hasiotis and Mitchell, 1993; Hasiotis, 2002). The Lemoenfontein burrows are at ramp angles that range from 25° to 35°. However, crayfish burrows can be more horizontal where they attach to burrow chambers or shaft junctions (Hasiotis et al., 1999). The vertical nature of crayfish burrows is typical, but not as important as the surficial morphology for identification purposes (Hasiotis et al., 1998). Changes in burrow orientation from sub-vertical to oblique can also occur at the mid-way enlargement chambers (Abouessa et al., 2015). The cluster of three burrows (B19-7-1/2/3) that are preserved from just above the mid-way size enlargement, are at a ramp angle of 35° below this point and are consistent with the possibility of burrows changing angles below mid-way chambers.

The results of Hasiotis and Mitchell (1993) have been applied numerous times for the identification of ancient crayfish burrows and therefore to infer the presence of crayfish in palaeoenvironments where no crayfish body fossils have been preserved (e.g., Hasiotis et al., 1993; Hasiotis et al., 1998; Hasiotis and Honey, 2000; Hasiotis, 2002; Bedatou et al., 2007; Baucon et al., 2014). Authors have also used these methods to rule out crayfish as potential burrow makers (e.g., Hasiotis et al., 1999; Bordy and Krummeck, 2016). In other cases, crayfish burrows could be identified based on their architectural and surficial morphology in strata where the host matrix of the burrows also contained crayfish body fossils, further strengthening the link between the presence of the burrow and the crayfish as burrow maker (e.g., Hasiotis et al., 1998; Martin et al., 2008; Abouessa et al., 2015). In conclusion, by assigning the Lemoenfontein sub-circular burrows to the ichnotaxon *Camborygma eumekenomos,* the inference is made that the burrow maker was a continental freshwater crayfish, and that crayfish were present in the ancient flood plain environment of the Middle Triassic strata of the Burgersdorp Formation. This is the first potential identification of presence of ancient crayfish in the Karoo Basin of South Africa (Hasiotis, 2002).

Palaeoenvironmental significance of crayfish burrows

Crayfish burrows are of palaeohydrological and stratigraphic significance for the interpretation of ancient floodplain environments (e.g., Hasiotis and Micthell, 1993; Hasiotis et al. 1998; Hasiotis and Honey, 2000; Baucon et al., 2014; Abouessa et al., 2015). The crayfish behaviour is recorded in the burrow construction (Hasiotis et al., 1998) and the depth of the crayfish burrows corresponds to the lowest palaeo-water table during the dry season; with the location of the mid-level enlargement chambers indicating the shallow water table level during the wet season (Hasiotis et al., 1998; Hasiotis and Honey, 2000; Abouessa et al., 2015). An excellent schematic representation of these phenomena is provided in Abouessa et al. (2015) and is redrawn here considering the specific Lemoenfontein characteristics (Figure 4.8).

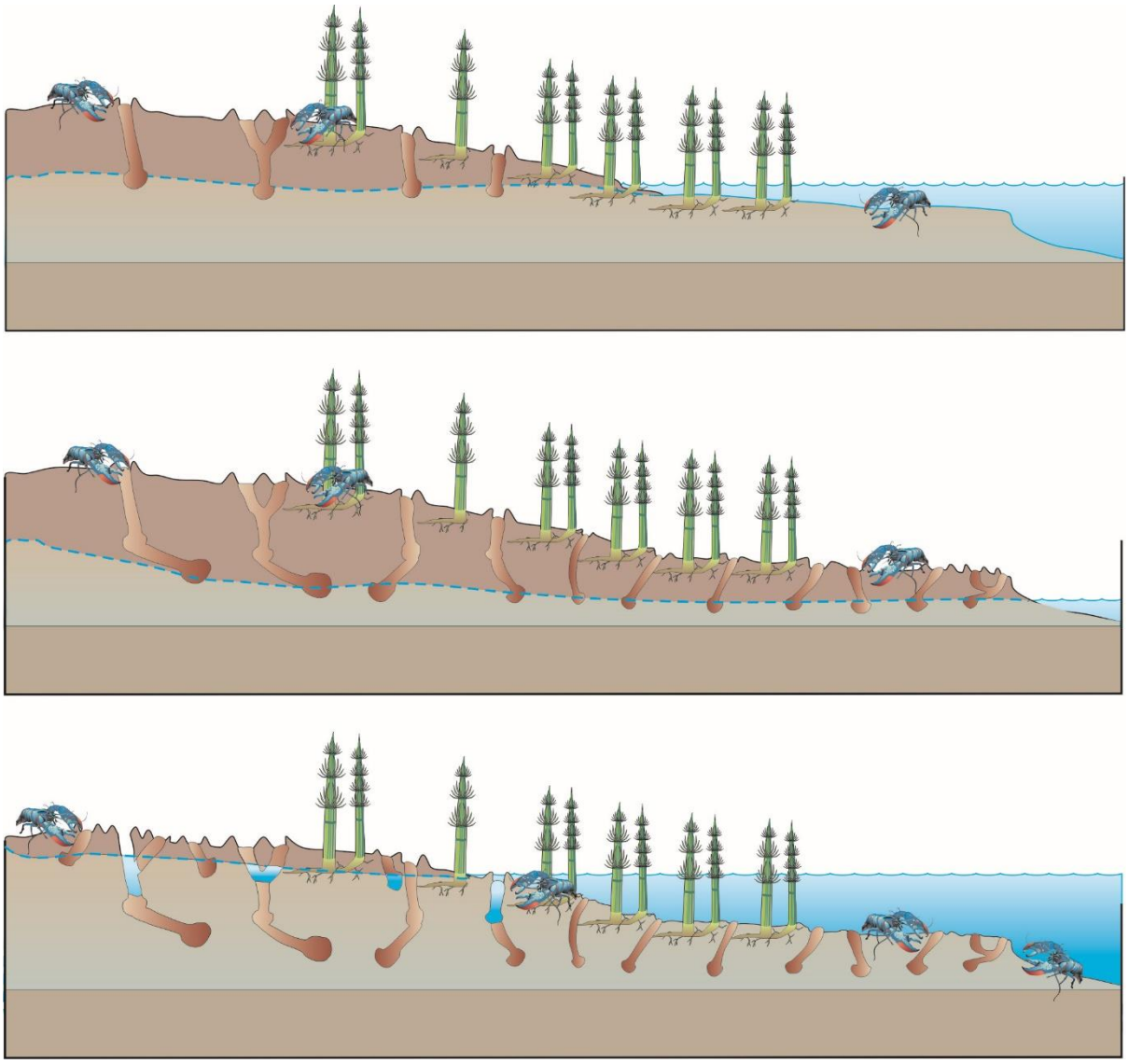


Figure 4.8: Schematic model of continental freshwater crayfish burrowing near a water source where there is a seasonal variation in the ground water table (based on Abouessa et al., 2015, Fig. 8). (A) Mid-season water level and burrow depth; (B) Dry season water level, older burrows are extended down to the new water level and new burrows are excavated all the way to the lowered water level, note the change in the burrow orientation from sub-vertical to oblique below the mid-level enlargements; (C) Wet-season water level, older burrows are partially filled in with mud or sand and can get penetrated by smaller new burrows. (This is a diagrammatic representation and the burrows and reedbeds are not to scale, the former has been enlarged for clarity).

Considering that the enlargement chambers of the Lemoenfontein burrows are located at the top of the approximately 80 cm exposed length, the interpretation can be made that the palaeoenvironment experienced seasonal fluctuation in the groundwater level and that this level varied by at least 80 cm between the dry and wet seasons. This conclusion is consistent with the evidence from the pedogenically altered sedimentary host rocks, i.e., the presence of a calcareous nodular horizon that is intersected by the crayfish and tetrapod burrows present at the study locality. The crayfish burrow makers lived in a continental environmental setting where the burrows had to be several meters deep to allow them to reach the water table for breathing purposes, while still be able to access the floodplain surface for feeding purposes. Note that the tetrapod burrows from Lemoenfontein terminate some 30 cm below the calcareous nodular horizon, but above the applicable seasonable water level.

The presence of a crevasse splay sandstone, a thin sheetwash fine-grained sandstone associated with the burrow infill of the tetrapod burrows and the fine sandstone infill of the sub-circular burrows, point to seasonal heavy down pours on the floodplain that led to sheet wash events and overbank depositional events.

4.9 Putative *Langbergia* burrow cast and its biostratigraphic significance

During the second formal field trip to the Lemoenfontein locality in 2020, a large bifurcating burrow cast was located about 1 m above the prominent sandstone base of the first upward-fining sedimentological sequence (Cycle 1), see Figure 4.9. This stratigraphic level is 7 m below the first mudstones that host the accumulation of tetrapod fossils and burrow casts. This burrow cast consists of two connected shafts that protrude out of the siltstone cliff in an inverted “V” shape. The shafts were excavated up to the point where they connect to each other. The angle between them is 120°. Both shafts terminate in an enlarged chamber. The left-hand shaft extends for 1.4 m from the T-junction at a ramp angle of 6°. It curves gently (low sinuosity), its horizontal diameter is 14.5 cm, and its vertical diameter is 8 cm. It has a reniform cross-section and shows several cm-scale striations longitudinally on the lateral and dorsal surfaces of the shaft. The right-hand shaft extends 85 cm from the T-junction to its

terminal enlargement at a ramp angle of 10° to the horizontal. Its cross-section is 16 cm wide by 11 cm high and it also has a reniform cross-section with longitudinal striations.

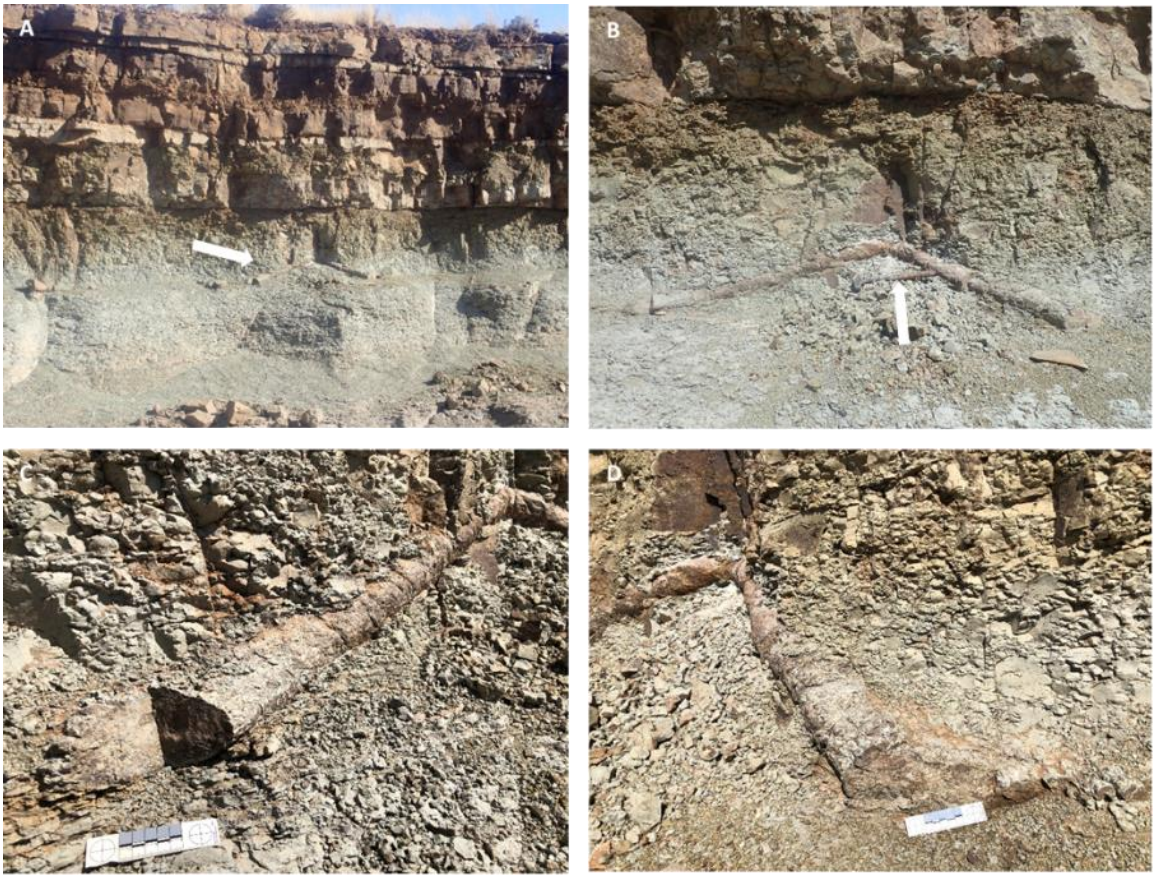


Figure 4.9: Large reniform burrow cast at 1 m of the Lemoenfontein stratigraphic section. (A) location in siltstone cliff face (arrowed). (B) View showing T-junction. Hammer length = 33 cm (arrowed). (C) Left shaft and terminal chamber. (D) Right shaft and terminal chamber. Ruler = 10 cm.

The fact that it contains a bifurcation or T-junction, has a low ramp angle and is significantly larger in cross-section (14.5 cm versus 8 cm) distinguishes this burrow cast from the *Reniformichnus* burrow casts described from the bonebed locality 7 m higher up in the succession. This burrow cast has an architectural and surficial morphology that is like the burrow cast complex described by Groenewald et al. (2001). They attributed these to *Trirachodon* as the burrow maker, but as pointed out in *Section 4.1*, trirachodontid material from the *L-G* Subzone of the *Cynognathus* AZ has subsequently been recognized as the new taxon *Langbergia* (Abdala et al., 2006). These burrows are reniform in cross-section and have the following dimensions:

- proximal burrow cast, 15.4 cm wide, 6.4 cm high;

- distal burrow cast, 10.9 cm wide, 4.5 cm high; and
- ramp angles, 1° to 23° (17° typical).

The burrow complex contains at least one bifurcation or T-junction, and the burrows show longitudinally scratch marks on the lateral and dorsal surfaces of the shafts.

The large bifurcating Lemoenfontein burrow cast cross-sectional shape and size, the low ramp angle, and the presence of the T-junction point to a general architectural and surficial morphology that is like that produced by the trirachodontid, *Langbergia* (see Figure 4.10 for a visual comparison).

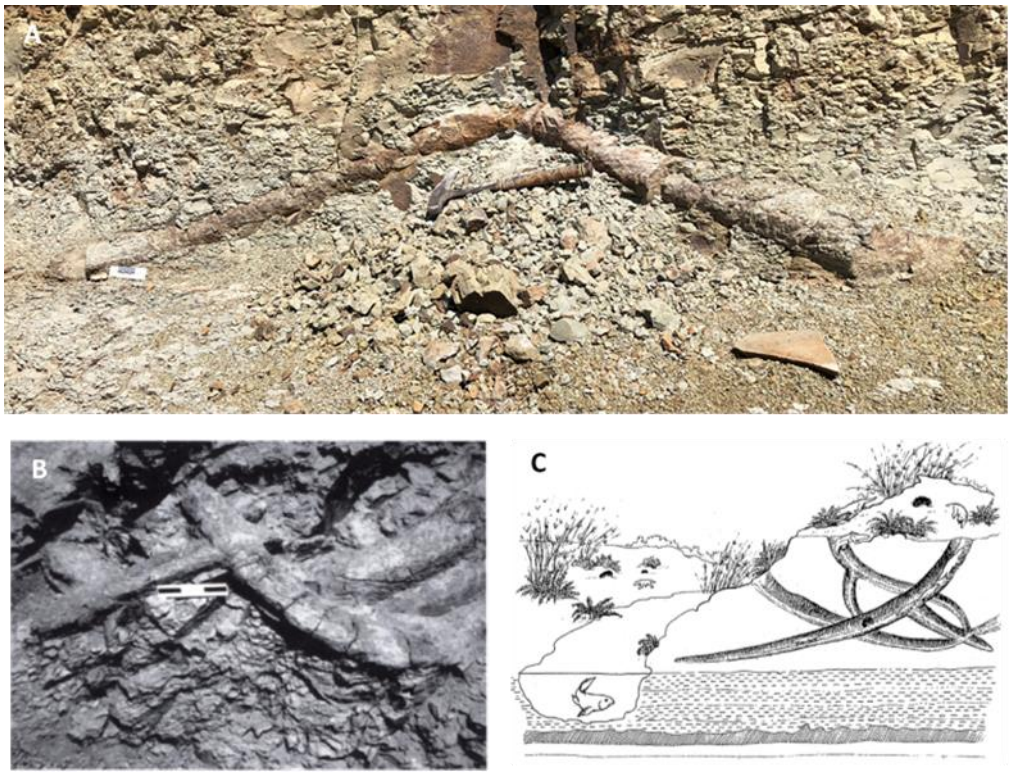


Figure 4.10: Comparison of the Lemoenfontein bifurcating burrow cast (A) with the Langbergia *burrow casts (B) and palaeoenvironmental reconstruction (C.) B and C are Figures 6 and 13 of Groenewald et al. (2001). Hammer length in A = 33 cm. Scale bar in B = 15 cm.*

This similarity is consistent with the interpretation in the stratigraphic analysis (Chapter 3) that the sandstone complex that forms the base of Cycle 1 is the Eldorado marker of Neveling (2004). Neveling found *Cynognathus* AZ, *L-G* Subzone taxa in the mudstones just above the

Eldorado sandstone on his section on the farm Klipplaatsdrif (J. Neveling, pers. comm., October 19, 2020; Neveling (2004)) and identified these mudstones with the top of the *L-G* Subzone. This interpretation has the biostratigraphic implication that the beds containing the bone accumulation at Lemoenfontein occur at the base of the *T-K* Subzone of the *Cynognathus* AZ. This interpretation is supported by the faunal analysis in Chapter 7 of the taxa present on Lemoenfontein.

5. CREVASSE SPLAY SURFACE ICHNOLOGY OF LEMOENFONTEIN

5.1 General description

The focus of the work now turns to the laterally extensive yellowish-grey (5Y 7/2), fine-grained tabular sandstone (Figure 5.1) that occurs at 12.9 m, approximately 3 m above the highest stratigraphic level of the saddle exposure that links the Lemoenfontein hill to the sandstone body that forms the base of the second stepped plateau. This sandstone is approximately 10 to 20 cm-thick and fan shaped. Its widest margin is approximately 100 m across from east to west. It points in a northwesterly direction, forming a semicircle around the hill with its narrow end extending towards the southeast for some 210 m. At its northwest margin, the sandstone is ripple cross-stratified. These are non-climbing ripples (in-phase), indicative of slow deposition of suspended and bedload sediment. The sandstone has rib-and-furrow structures on its top surface that indicate a paleocurrent direction of west-southwest. Its top surface is well bioturbated with small (±5 mm diameter) vertical, unlined, passively filled *Skolithos* burrows (Figure 5.1). This sandstone has a flat sharp bottom contact. It is interpreted as having been deposited by unconfined shallow sheet floods that also scoured the floodplain surface and, in the process, dislodged and transported pedogenic nodules and mud chips. In elongate patches close to the margin of the sandstone outcrop these have been deposited as clast supported intraformational mud-pebble and nodule conglomerate (Facies Se_i). The sandstone bed does not fine upwards and is interpreted to be a crevasse splay sand sheet that prograded and fanned-out from approximately east-southeast (proximal) to northwest (distal).

At about 90 m southeast from the centre of the hill (S 30° 36.943′, E 26° 37.372′, Elevation 1346 m), the underside of this 10- to 20 cm-thick crevasse splay sandstone records as sole marks several features of the underlying mudstone palaeosurface. These are interpreted in the discussion below to be current crescents, desiccation cracks, scratch digging and other traces. At this location, the sandstone body is structureless apart from the inclusion of small, isolated mud clasts that were dislodged by the flow from the underlying mud deposits. Here the sandstone is light grey (N7) in colour, fine-grained, well sorted and coarsens upward. It

contains black mineral and pinkish specs, the latter being indicative of feldspar. It thins distally towards the west and the interpretation is made that the crevasse splay flowed into a pond margin. The top surface in this portion of the splay deposit is also bioturbated by *Skolithos* burrows, approximately 5 mm in diameter.



Figure 5.1: (A) View of tabular crevasse splay sandstone that crops out at the Lemoenfontein study site. (B) Skolithos *vertical burrows opening onto sharp top surface of crevasse splay sandstone. Examples arrowed. Ruler in (A) = 10 x 10 cm, Scale bar in (B) = 15 cm.*

5.2 Current crescents

Prominently featured on the sole surface of this sandstone, are numerous horseshoe- or U-shaped, crescent-like structures. These features are widespread but appear to occur in randomly spaced clusters of three to five in a 10 by 10 cm area. They consist of horseshoe-shaped raised ridges around a central cylindrical depression (see Figure 5.2). The thickest part (approximately 2 to 5 mm) of the ridge is at the closed end of the "U", thinning out towards the open arms of the U-shape. The shapes range in size from 0.5 cm to 3.5 cm at the widest point with arm lengths of 1 to 4 cm. The inner cylinder diameter is typically one third of the maximum outer diameter and its depth is $1/7^{th}$ of the outer diameter. There is also a raised peg or pin in the centre of each inner cylindrical depression that is $1/5^{th}$ of the diameter of this cylinder. An important observation is that all these U-shaped traces are aligned with the tapered "arms" pointing in a westerly direction. The concave structures in the hyporelief are depressions on the epirelief of the underlying original floodplain palaeosurface. In rare cases, the shape is asymmetrical with one of the arms displaying a spiral geometry. These structures are interpreted as casts of crescent-shaped scour pits etched into the semi-consolidated muddy surface by turbulent water flow.

The sole surface also contains prominent longitudinal ridges that are approximately 2 cm wide forming irregular polygonal shapes (Figure 5.2 B). In some cases, these ridges dissect the horseshoe-shaped surface features. These ridges are interpreted as sand-filled desiccation cracks in hyporelief. Since they cross through existing crescent structures, it can be concluded that the horseshoe-shaped structures were formed before the palaeosurface dried, with this drying resulting in the formation of the mud cracks. The presence of mud cracks suggests the existence of seasonal rainfall and the presence of clay in the ancient vertisol.



Figure 5.2: (A) Cluster of aligned current crescents. Note Cynodontipus *traces in the foreground. (B) Desiccation crack dissecting current crescents. Foreground scale bar in A = 15 cm, Scale bar in B = 5 cm.*

Numerous fine-grained sandstone cylinders have also been collected from this locality (Figure 5.3). These cylinders have eroded from the crevasse splay sandstone. They range in diameter from approximately 1.5 to 5 cm, are several cm long, and display mm scale longitudinal ridges around outer surfaces resulting in a ribbed and furrowed surficial morphology. One of the larger examples of these (3 cm diameter) also shows a joint or node at one of its ends. Based on these characteristics, these cylinders are interpreted to be stem and possibly pith casts of sphenophytes or "horsetails". There is evidence of a possible periderm, but this is probably a diagenetic colour alteration halo around the cast. The stem casts are not laterally compressed, suggesting that they were formed and preserved in their vertical growth

position. Some stem compressions are also preserved in a horizontal orientation between the crevasse splay and the underlying mudrock (Figure 5.3 B). They occur on both the top and bottom surfaces of the crevasse splay sandstone and are approximately 0.5 to 4 cm in diameter and up to 30 cm or more in length. Significantly, there is a range of overlap in the size of the outer diameters of the stem casts and the inner diameters of the horseshoe shaped features describe above. This is compelling evidence that the upright stem provided the obstruction to flow that resulted in the crescentic scour pits.



Figure 5.3: (A) Stem casts preserved in 3-D. (B) Horizontal stem compressions on top surface of crevasse splay sandstone (arrowed). (C) Pith casts preserved as the central peg in each crescent. (D) Vertically preserved stem cast showing horizontal nodes and vertical ridges around the stem. Scale bar in A = 5 cm, scale bar in B = 10 cm, Scale bar in C= 4 cm, scale bar in D = 3 cm.

Clearwater scour around vertical cylinders is an area of study in the fields of civil or coastal engineering, particularly about flow induced scouring around the base of piers that support bridges and other structures (e.g., Zhoa et al., 2010; Jahangirzadeh et al., 2014; Yagci et al., 2017). The earlier of these studies are based on small scale flume tank experimental setups in laboratories, while the later studies are based on numerical analyses that are often tested against small scale laboratory based experimental results (see Figure 5.4 for typical

experimental and analyses results). Similar studies have also been performed for scours around isolated or groups of vegetation elements (e.g., Yagci et al., 2016). The main fluid flow mechanisms that cause the scour around the base of a vertical cylinder are known as "horsehoe" and "wake" vortices. The horseshoe vortex is created at the base of the cylinder on the upstream side by water stagnating against the cylinder shaft causing down flow. The resultant horseshoe vortex causes a ring-shaped vortex hole around the cylinder with its deepest part on the upstream side. The wake vertices are cause by vortex shedding on the downstream side of the cylinder and result in a characteristic scour flute in the flow direction downstream of the cylinder.

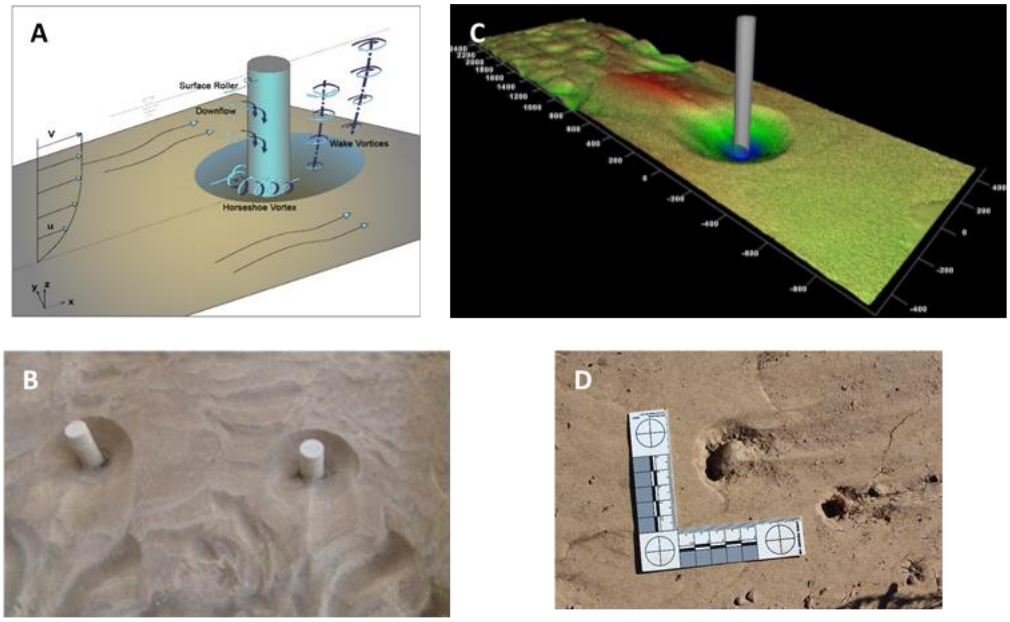


Figure 5.4: Typical examples of Horseshoe Vortex simulation and experimental results. Diagrams from (A) Jahangirzadeh et al. (2014), (B) Zhao et al. (2010), (C) Yagci et al. (2017). (D) Modern example of a scour around a sub-round pebble (picture taken after an overbank flood at the Lemoenfontein locality). Ruler in D = 10x10 cm.

As can be observed *qualitatively* in Figures 5.2 and 5.4, the scour holes caused by clear water flowing around a vertical cylinder are strikingly like the horseshoe shaped features on the sole surface of the Lemoenfontein crevasse splay sandstone (if viewed in hyporelief). The following observations are relevant:

- the horseshoe shaped crescents are aligned with all the flutes pointing in the same direction;
- the associated presence of sphenophyte stem casts preserved in their vertical growth position with diameters overlapping with the inner diameters of the crescents; and

- scours induced by horseshoe vortices in water flowing around vertical cylinders being like these crescents.

Based on these observations, a reliable interpretation can be made that the Lemoenfontein crescents were formed by clear water flowing through a stand of sphenophytes resulting in a horseshoe-shaped scour around the base of each plant stem. Furthermore, the pin or peg in the centre of each crescent can be interpreted as the cast of the pith or stem cavity of each plant. This interpretation is supported by Rex (1985) who investigated the formation of fossil plant pith casts by conducting laboratory experiments using a small flume tank. In one of the scenarios hollow plant stems were positioned vertically in a sediment bed. Scouring occurred rapidly around the base of the stems at flow rates as low as 15 – 20 cm/s leading to excavation of these stems. At very low speeds (4 – 5 cm/s) scouring on the upstream side of the stem led to deposition on the downstream side and thus preventing excavation. The filling of the vertical cavity resulted in horizontal laminated sediments within the stem. Based on this experimental setup, the interment of plant stems in the vertical growth position would only occur under very low flow rate conditions. In the case of Lemoenfontein, the plants were rooted and would therefore survive higher flow rates without being excavated, while some of the thinner stems could be bent over to lie horizontally.

The occurrence of sphenophytes in the Burgersdorp Formation is well documented (e.g., Anderson et al., 1999; Anderson and Anderson, 1985). Sphenophytes had a cosmopolitan distribution during the Middle to Late Triassic and often occurred as single homogenous and dense cultures on the margins of lakes or streams (Holmes, 2001). Specifically, Osborn et al. (2000) describe sphenophytes from the early Middle Triassic Fremouw Formation of Antarctica. It is interesting to note that burrow casts from the Lower Triassic Fremouw Formation, which are like the burrow casts from the Lemoenfontein locality, have also been described (Hasiotis et al., 1999; Miller et al., 2001). The presence of rooted sphenophytes at this locality provides further evidence for the interpretation that this was a palaeoenvironment consistent with a pond margin.

5.3 Scratch-digging traces

The most enigmatic trace features on the sole surface are numerous bilaterally symmetrical lobes displaying “scratch-like” traces consisting of sub-parallel ridges in hyporelief, (Figure 5.5). Broadly crescent- shaped in plan view, these features are approximately 4 cm long and 3.5 cm wide. The ridges are oblique to the axis of symmetry at the narrow end of the structure and fan out towards the wide end, where they run approximately parallel to the axis of symmetry. In some cases, the ridge network extends up to 10 cm forming a bilobate structure. The ridges are gently curving to straight and they cross the axis of symmetry at the narrow end of the structure creating a chevron pattern. Each ridge is approximately 2 cm long, spacing is 1.5 – 2.0 mm and the width is less than 1 mm with a sharp crest. The individual ridges are approximately 1 to 2 mm high and the maximum height of the overall bilobed structure is up to 5 mm. These structures appear to be randomly orientated on the splay sole surface.

The scratch structures bear superficial resemblance to the ichnogenus *Rusophycus* (see for example Bromley and Asgaard (1979) and Gibb and Pemberton (2016)) but lack the characteristic median groove. On the other hand, these scratch marks closely resemble the ichnotaxon *Cynodontipus* (Figure 5.6). *Cynodontipus* has been identified as tetrapod burrow attempt by Olsen et al. (2020). They use an apomorphic approach to identify the possible trace maker as follows:

- the bilobed nature of the longer traces along the bedding plane is indicative of bilateral symmetry;
- the traces appear to occur in sets with four to five subparallel scrapes with the same direction, depth and length, this being indicative of the number of claws on a tetrapod manus or pedes; and
- the sharpness of the scrapes indicates the presence of claws.

Using these arguments, they conclude that the traces can be attributed to Amniotes. They conclude that the crescentic opposing scrapes marks are abandoned burrow attempts created by the front feet of the animal. The longer horizontal scrapes were made by the

animal's hind legs as it burrowed along the bedding plane. The Lemoenfontein traces also show a bilobed nature (Figure 5.5 B) and occur as sharp subparallel scratches in groups of four to five (Figure 5.7).

Sues and Olsen (2015) propose a scenario where the tetrapod tried to burrow through a layer of sand and then terminated the burrow when it encountered a layer of dry mud under the sand that resisted further burrowing. In this example the scratch marks were also recorded on the sole surface of a sandstone bed. Some burrowing also continued horizontally within the bedding plain between the sand and mud. Sues and Olsen (2015) further propose that the simplest explanation for the burrow maker is the procolophonid *Hypsognathus* (referencing Groenewald (1991) as evidence that procolophonids were burrowers). *Hypsognathus* occurs in the same beds as these traces. Due to size variation in these burrow terminations, they leave the possibility open that other burrowing tetrapods may also have been responsible for the traces.

In a recent in-depth study, Bordy et al. (2019) describe similar tetrapod traces (although much larger) in the bedding plane between a sandstone block and an underlying massive mudstone (recorded on the sole surface of the sandstone) from the Burgersdorp Formation some 50 km from Lemoenfontein (see Figure 9 B of their study). Based on their morphology the traces from Lemoenfontein may be assigned to the ichnotaxon *Cynodontipus.*

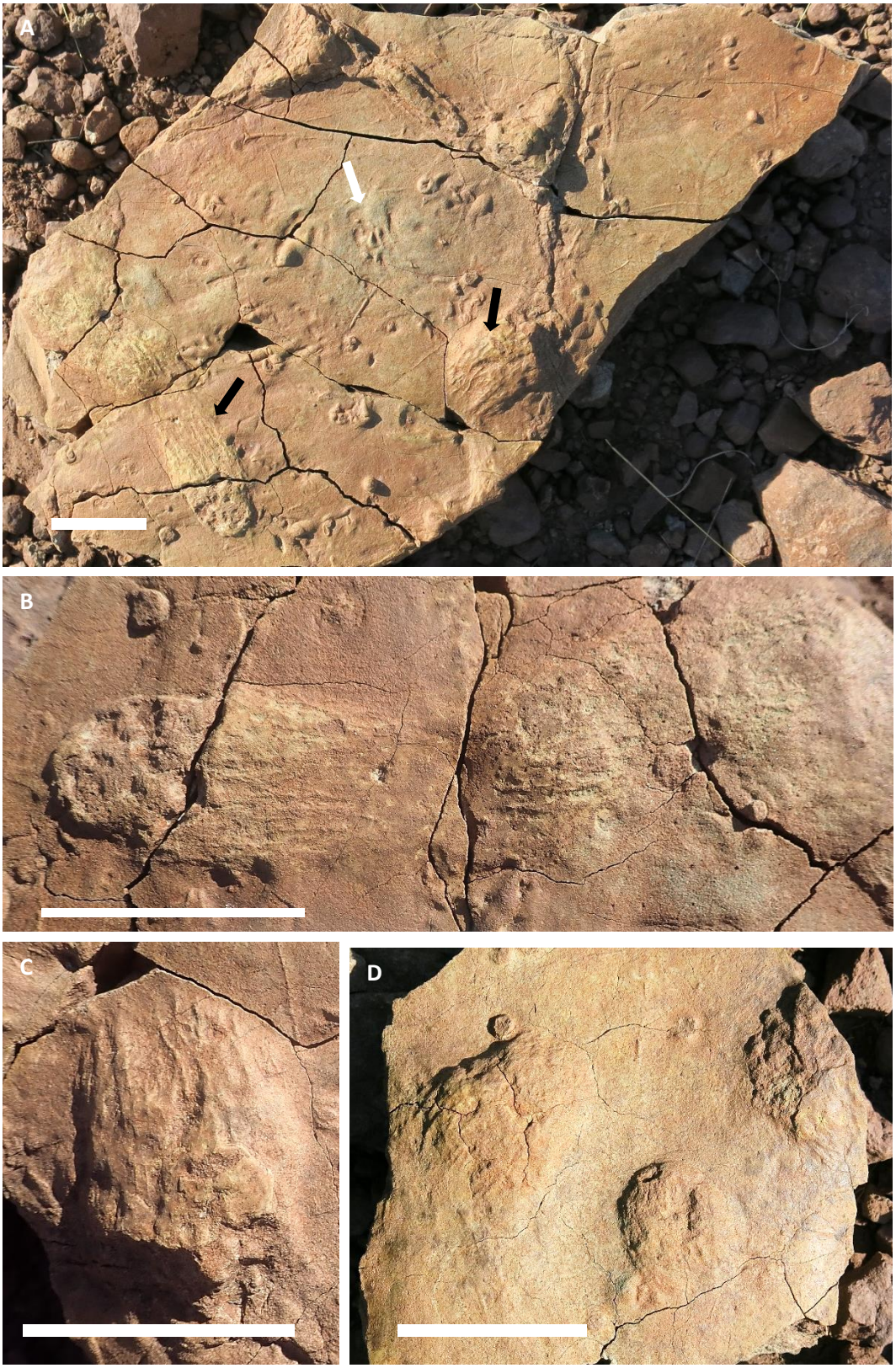


Figure 5.5: Lemoenfontein scratch-like traces. (A) Slab containing an elongated trace and a single crescentic trace (arrowed in black) and a possible Rhynchosauroides *footprint (arrowed in white). (B) Elongated trace showing a bilobed architecture. (C) Crescentic trace showing opposing scrapes. (D) Cluster of three crescentic traces. Scale bars = 5 cm.*

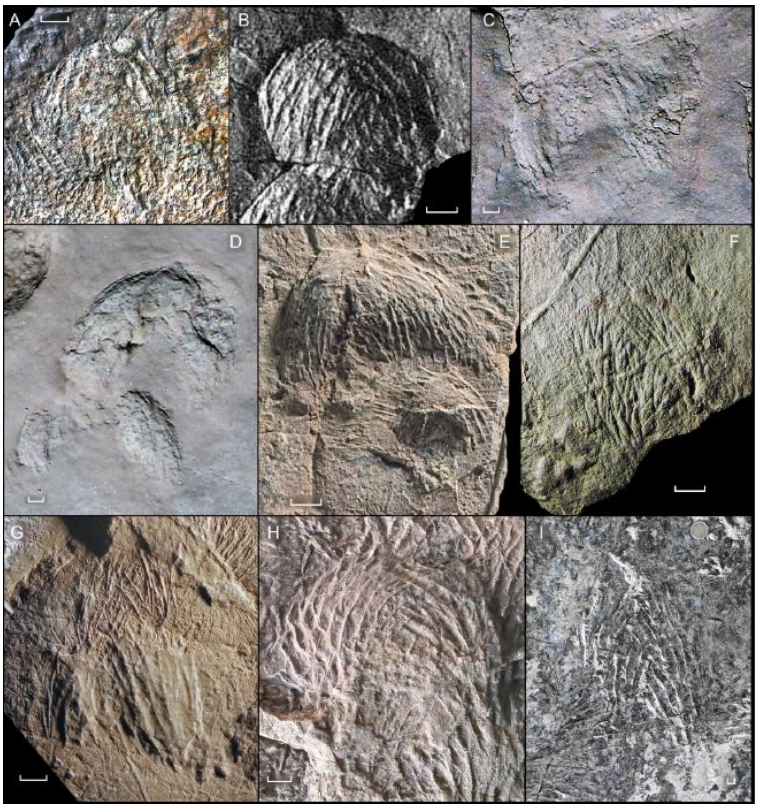


Figure 5.6: Examples of Cynodontipus *terminal burrow traces from Olsen et al. (2020), Figure 23. Scale bar = 1 cm.*

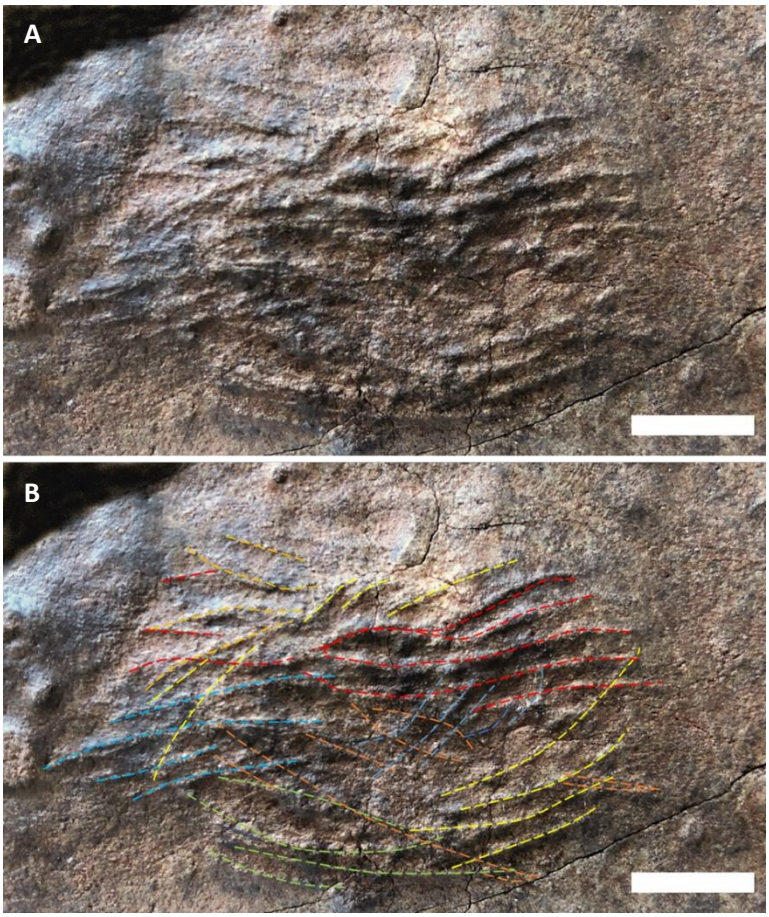


Figure 5.7: (A) Example of crescentic scrape marks from Lemoenfontein (B) Colour coded traces of scrape marks that occur in sets with four to five subparallel scrapes with the same direction, depth, and length, this being indicative of the number of claws on a tetrapod manus or pedes. Scale bar = 1 cm.

At Lemoenfontein, these bilobed scratch-digging structures occur in the same interval as tetrapod burrows (identified as *Reniformichnus*) as well as the tetrapod body fossils of the procolophonid, *Teratophon,* and other likely burrowing animals such as the cynodont *Trirachodon,* and the therocephalian, *Microgomphodon* (as discussed in Chapter 4). The simplest hypothesis is that these scratch marks were created by burrowing animals (such as *Teratophon*) before deposition of the splay sand on top of the dried-out mud. A more complex explanation is that the scratch digger penetrated the sand after deposition and terminated when the animal encountered the hard, dried out mud beneath. In some cases, burrowing extended for short distance (~ 10cm) in the interface between the sand and the mud. The overall width of these structures (~ 4 cm) is much smaller than the average width of the tetrapod burrows at this locality and this is consistent with what could be expected from an incomplete burrowing attempt. These burrow attempts occur with a density of three to five per square metre, suggesting that burrowing was common. The parsimonious interpretation is therefore that these features are abandoned burrow attempts or the terminations of *Reniformichnus* burrows, and that there is no need to invoke the ichnotaxon *Cynodontipus.*

Olsen et al. (2020) point out that the surfaces that contain *Cynodontipus* often also contain true footprints that were made before the mud or clay surface dried out and became recalcitrant. These resemble *Rhynchosauroides* (see Figure 14 in Olsen et al. (2020)). At Lemoenfontein at least two potential *Rhynchosauroides* prints have been observed (see Figure 5.5 A and Figure 5.8). Olsen et al. (2020) were unable to conclude whether the *Cynodontipus* traces at each locality were made by a single animal, multiple animals of the same taxon or a colony of animals of multiple taxa. At Lemoenfontein the *Cynodontipus* traces occur in the same beds that host tetrapod burrow casts and at least six taxa of possible burrowing animals. Also, several tetrapod skull specimens were preserved with a manus attached to the skull (SAM-PK10180, *Eohyosaurus* (rhynchosaur); SAM-PK10762, *Trirachodon*; SAM-PK-K10160, *Microgomphodon*). The Lemoenfontein data collected could be analysed to determine which taxon or taxa were most likely to have made the traces. This analysis is however beyond the scope of the current work. In Figure 5.8 A trace of the manus of *Eohyosaurus* (SAM-PK10180) is superimposed on traces of *Cynodontipus* and

Rhynchosauroides from Lemoenfontein. This demonstrates qualitatively that *Eohyosaurus* could have been one of the trace makers.

In summary, the Lemoenfontein crescentic structures are interpreted to be convex hyporelief casts of scratch-digging activity of an animal using multiple sharp appendages to penetrate the semi-consolidated muddy surface, the same surface that supported stands of reed-like plants and was later subject to subaerial exposure before being rapidly buried by a lobe of crevasse splay sand. The presence of these abandoned burrow attempts is indicative of an environment with a seasonal rainfall, where the water table periodically drops below the sediment surface allowing the clay or mud to dry out before these burrowing attempts were made (Olsen et al., 2020).

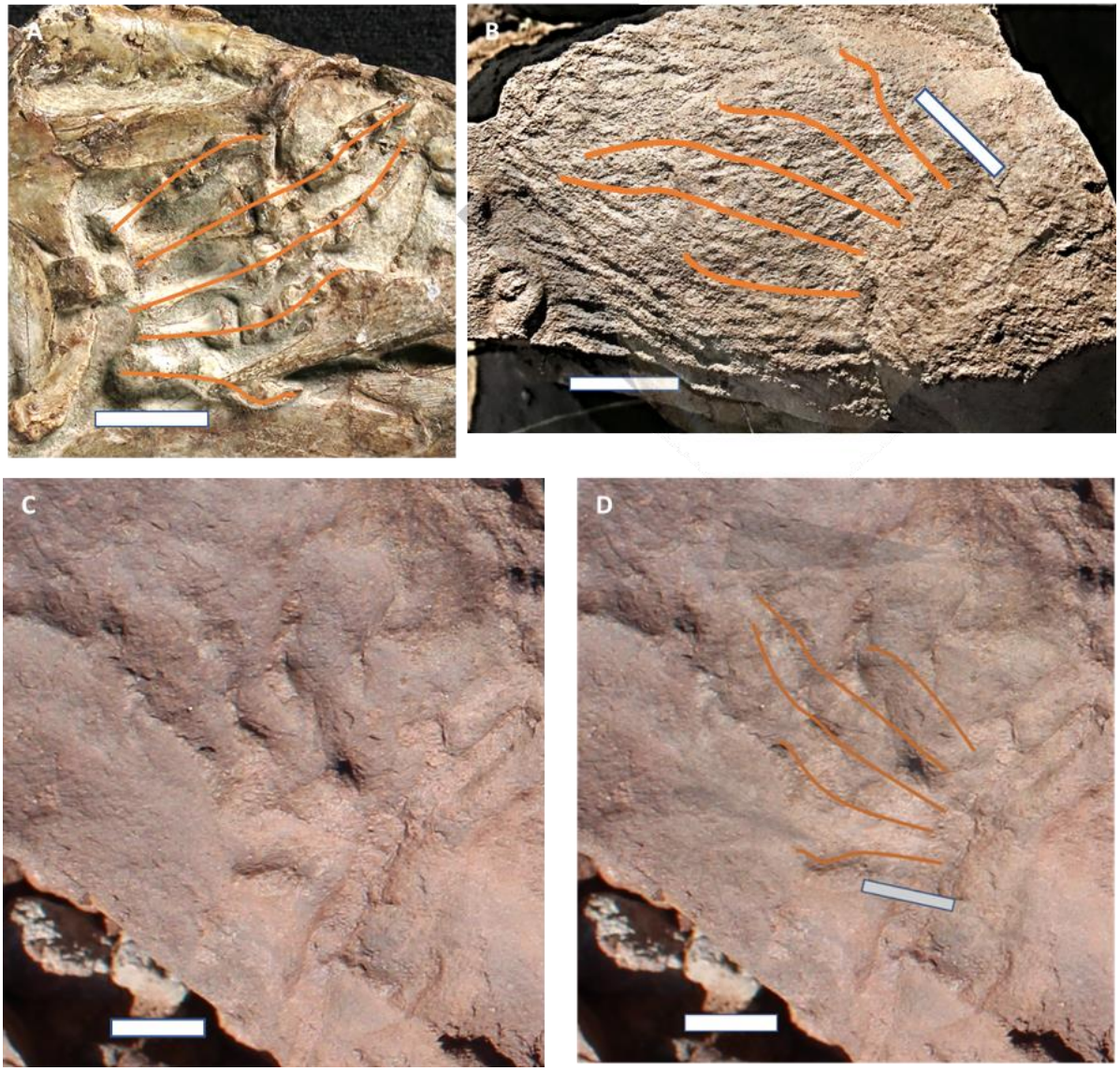


Figure 5.8: (A) Trace of the rhynchosaur manus (SAM-PK10180). (B) Superposition of this trace on a Cynodontipus *specimen from Lemoenfontein. (C) and (D) Superposition of this trace on a possible* Rhynchosauroides *print from Lemoenfontein. Scale bars = 1 cm.*

5.4 *Scoyenia* ichnofacies

The crevasse splay upper surface is bioturbated by *Skolithos* burrows, approximately 5 mm in diameter. Based on field observations of the vertical fracture planes of the sandstone, these burrows penetrate the sandstone bed all the way down to the underlying mudrock. Various gently curving to straight horizontal traces (concave in hyporelief) that vary from 1 to 4 mm wide and that are tenths of centimetres long also occur on the sandstone surface (Figure 5.9 A). These traces are interpreted to be meniscate backfilled feeding structures that lack striated walls in a soft ground setting (e.g., Buatois and Mángano, 2013, (Figure 10.8 A)). There is also a single enigmatic trace consisting of a series of subparallel concave scratches, each approximately 1.5 cm long and 1 mm wide appearing approximately 3 mm apart forming a stacked sequence 4.5 cm long (Figure 5.9 B). In some cases, these striae are orientated crosscut to each other. These structures are interpreted as firmground meniscate striated traces (e.g., Buatois and Mángano, 2013, (Figure 10.8 B)). Figure 10 A and B of Buatois and Mángano (2013) bears a close resemblance to these two types of traces from Lemoenfontein. Following Buatois and Mángano (2007) these traces are assigned to the *Scoyenia* ichnofacies occurring in a firmground freshwater environment in desiccated ponds and lake margins.

In addition to the *Scoyenia* traces, some of the sandstone slabs also show various worm, insect, and arthropod (*Diplichnites*) traces.

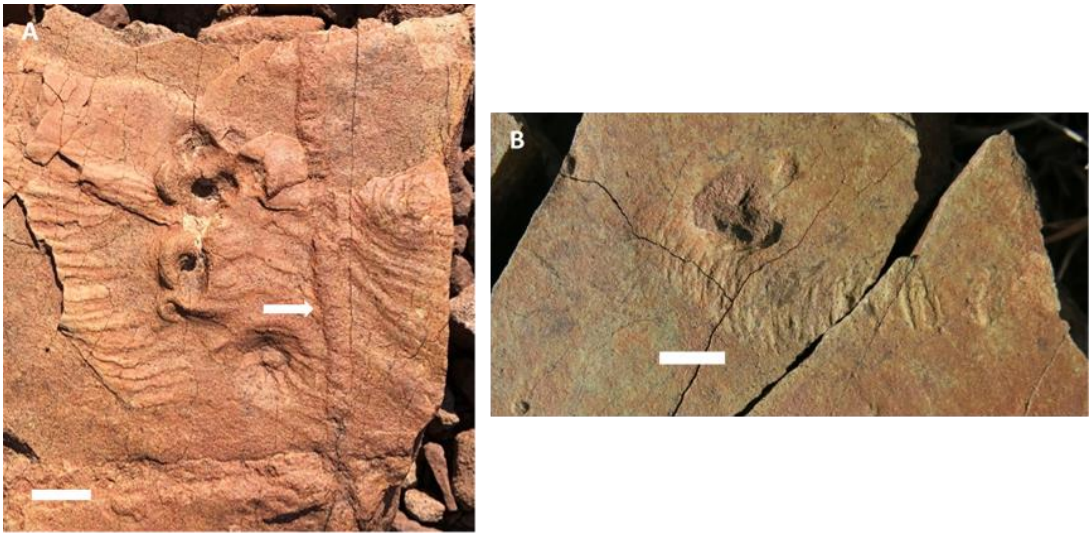


Figure 5.9: Scoyenia *ichnofacies. (A) Narrow softground meniscate feeding trace (arrowed). (B) Wide firmground striated meniscate traces. Scale bars = 1 cm.*

5.5 Sequence of deposition and trace events

The event scenario that can explain the overall combination of features that are observed on the crevasse splay sole surface is schematically presented in Figure 5.10.

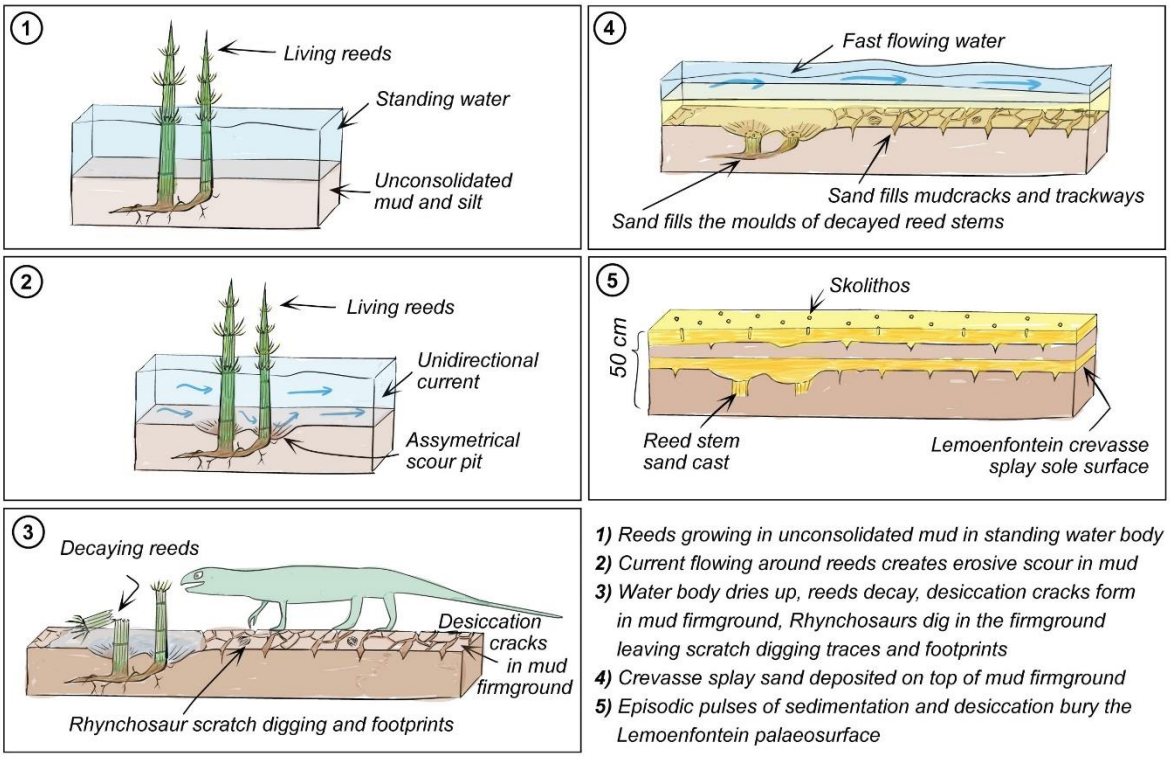


Figure 5.10: Sequence of events that allowed the Cynodontipus, Scoyenia, *and* Rhynchosauroides *traces to be made on the mud surface as well as the preservation of Sphenophyte stem casts. Drawing by Claire Browning (2021).*

- The setting is a floodplain pond or lake with a monoculture sphenophyte thicket growing around and in the shallow water margins.
- A periodic dry season shrinks the water body and exposes and area of muddy lake floor around the margins which drains but does not desiccate. This is followed by a downpour resulting in sheet flow emanating from the crevasse channel. This creates horseshoe-shaped scours around the bases of the horsetail stems as it flows into the lake.
- The flood water subsides while various *Scoyenia* ichnofacies traces are formed by insects and worms on the wet floodplain surface.
- Shortly after the mud has consolidated sufficiently to support the weight of small tetrapod, these sharp-clawed tetrapods regularly walked on and scratched pits and

furrows into the semi consolidated mud bed, leaving furrowing and footprint traces. (Perhaps this regular furrowing formed part of a foraging and feeding behaviour).

- The surface undergoes further desiccation in the dry season and mud cracks form, some transecting the current crescents. The surface hardens during the drying. The sharp-clawed tetrapods continue to attempt to scratch furrows and holes into the now recalcitrant mud bed, resulting in the formation of *Cynodontipus* traces.
- Another larger overbank crevasse splay event occurs depositing 10 to 20 cm of sand over this surface. This laminar flow does not scour the hard mud surface and the trace and desiccation cracks, and horseshoe scours are filled with fine sand and preserved. Some of the thinner horsetail stems are bent over and anchored in the bedding plane between the two surfaces.
- The vertical sphenophyte stems eventually die and decay. Subsequent deposition of fine sand first fills the hollow cores of the stems forming the pith casts that are preserved as the central peg in each crescent. After further decay some of the larger remaining cylindrical holes are infilled resulting in the vertically preserved stem casts.

6. VERTEBRATE TAPHONOMY OF LEMOENFONTEIN

6.1 Literature review of studies relevant to the taphonomic analysis of the Lemoenfontein bonebed

The literature survey for this project yielded a limited number of taphonomic studies on the sedimentary strata and vertebrate fauna of the main Karoo Basin of South Africa. These include the pioneering taphonomy study of the lower Beaufort Group floodplain deposits by Smith (1980), the extension of this work by Smith in his PhD thesis (1989), and a study of the sedimentology and vertebrate taphonomy of a reworked palaeosol of the *Tritylodon* Acme Zone in the Lower Jurassic Elliot Formation (Smith and Kitching, 1997). On the other hand, several taphonomic investigations have been performed on Karoo equivalent strata in Africa. Smith (2000) investigated the sedimentology and taphonomy of Late Permian vertebrate fossil localities in southwestern Madagascar and Smith and Swart (2002) studied the changing fluvial environments and vertebrate taphonomy in response to climatic drying in the Middle Triassic Omingonde Formation of central Namibia. Rogers et al. (2004) investigated the sedimentology and taphonomy of the upper Karoo-equivalent Mpandi Formation in the Tuli Basin of Zimbabwe. Finally, Smith et al. (2017) performed an extensive study of the taphonomy and palaeoenvironments of the Middle Triassic bone accumulations in the Lifua Member of the Manda Beds in Tanzania.

Some Triassic taphonomy studies have also been performed for other basins in Brazil, Argentina and Arizona in the United States of America. As discussed further in Chapter 8, Bertoni-Machado and Holz (2006) studied the taphonomy of an accumulation of disarticulated herbivorous and carnivorous cynodont skeletons along with a single non-cynodont specimen (Rhadinosuchidae) in the Middle Triassic Santa Maria Formation, located in the central region of the Rio Grande do Sul State in Brazil. Holz and Souto-Ribeiro (2000) documented the taphonomy of the South-Brazilian Triassic vertebrates in the Lower Triassic (Scythtian) Sanga do Cabral Formation. Rogers et al. (2001), reported on the Middle Triassic palaeoenvironment and taphonomy of the Chañares Formation tetrapod assemblage in northwestern Argentina, where the bone is preserved in volcanogenic concretions. Fiorillo et

al. (2000) performed a study of the taphonomy and depositional setting of the Late Triassic *Placerias* Quarry in the Chinle Formation of Arizona.

Behrensmeyer (1978) developed the framework for systematic taphonomic analyses of fossil terrestrial vertebrate occurrences based on long-term observations of recent mammal bones in the Amboseli Basin, southern Kenya. She found that distinctive weathering characteristics on the bones could be roughly correlated with time-since-death, but that they were also influenced by local conditions such as temperature, humidity, vegetation cover and soil chemistry. Based on the severity of environmentally induced damage to the bones, six weathering categories or stages were defined, with descriptive criteria that characterize each stage. This study also calibrated the time required to reach each stage of weathering. It was found that in the Ambesoli semi-arid open grassland setting, most bones decompose beyond recognition in 10 to 15 years, and that the bones of small animals and juveniles appear to weather more rapidly than those of large animals or adults. The continued study of recent bones in the Amboseli Basin (Behrensmeyer et al., 1979) discovered two significant biases in the potential for bone preservation. Firstly, the presence or absence of a species in a surface bone accumulation differ from the living species occurrences. Secondly, the relative species abundances in the bone accumulation differ from those in the living population. Both these biases are correlated with body size, since the bones of smaller animals (1 – 1000kg) are subjected to a greater degree of destruction. Small bones have a greater susceptibility to damage by mastication, trampling and weathering. This size bias resulting from primary surface processes will then be inherited by the buried bone assemblages. The following biostratinomic observations from the actuo-palaeontology study of Behrensmeyer et al. (1979) are deemed relevant to the taphonomic analysis of the Lemoenfontein bone accumulation:

- *if large bones were present in a bone assemblage, they would have had a better chance of preservation than smaller bones;*
- *therefore, their absence in a fossil assembly that consists mainly of small bones suggests that the large bones were probably not present in the first place; and*
- *if the small bones are complete and articulated, bone crunching mastication can be ruled out as a major taphonomic modifier.*

Smith (1989, 1993) extended Behrensmeyer's approach and applied his method of classification to 2500 *in-situ* fossils (mainly *Diictodon*) collected in the southwestern main Karoo Basin in the Adelaide Subgroup (Teekloof Formation). By using regular patterns of skeletal disarticulation, disassociation, and dispersion, he was able to identify eight taphonomic classes that can be grouped into three main groupings.

- Preserved at the site of death (A, B). Applies to skeletons entombed in burrows.
- Preserved near the site of death (C, D, E, F). Applies to skulls with various degrees of lower jaw disarticulation.
- Preserved far from the site of death (G, H). Applies to bone beds and isolated bones.

The eight classes correlated to residence time on the floodplain and degree of transportation and reworking. (The information contained in Table 2 of Smith (1993) is reviewed and expanded in Table 6.1 below).

Six factors that resist the disarticulation and dispersion of skeletons are identified here:

1. desiccation and mummification;
2. protection from scavengers;
3. protection from trampling;
4. large bone size and density;
5. rapid sedimentation (obrution); and
6. anchoring of carcasses by vegetation.

Similarly, nine environmental factors were identified that promote dispersal and disarticulation of carcasses:

1. carnivore mastication and ingestion of small animals;
2. carnivore scavenging and gnawing of larger carcasses;
3. trampling (edge of water hole or migration path);
4. complete bacterial decomposition of soft parts in permanently saturated environments;
5. decay causing detachment of bones from floating carcasses;
6. entrainment of small bones by shallow sheet floods;

7. reworking of carcasses in the main channel of rivers;
8. excessive weathering of bones in areas of slow sediment deposition; and
9. absence of vegetation that can anchor carcasses.

To interpret the taphonomic pathways for the *Diictodon* remains, the following additional factors were considered: attitude of the skull; the degree of perimineralisation (i.e., the development of a surface encrustation of calcium carbonate); weathering stage (as per Behrensmeyer, 1978); and bone colour.

Zoehfeld et al. (2013) reported on articulated curled-up skeletons of *Diplocaulus* and *Eryops* amphibians from Early Permian Red Beds of north Texas. The skeletons are curled-up such that the skulls contact the caudal vertebrae. The snouts of these skulls are angled upward by up to 15°. They conclude that the amphibians burrowed into the soft mud for aestivation purposes. The upward tilt of their skulls near the surface allowed them to breathe during the dry season. The accumulation of several specimens in the same area was due to the existence of a soft clay deposit that enabled burrowing. Several of the *Diplocaulus* skulls show bite marks and missing snouts. In one case the entire skull is absent. Their interpretation is that this is due to predation attempts by *Dimetrodon* to remove the amphibians from their aestivation chambers.

In a study considered relevant to the current project, Smith (2000) used field data on the sedimentology and vertebrate taphonomy of three separate Late Permian vertebrate fossil localities in southwestern Madagascar to reconstruct the sub- environments of the Sakamena axial rift valley lake. At the first of these localities, thick beds of microlaminated mudstone were deposited in a deep thermally stratified lake environment. These sediments contain at least three mass mortality horizons of an aquatic procolophonid reptile *Barasaurus*. The cause of the mass mortality is assigned to thermal shock associated with periodic de-stratification and poisoning from algal blooms. Soon after the mortality events, the carcasses sank to the bottom of the lake after release of stomach gasses. Sinking to the lakebed was likely sped up by their extra ballast of abdominal stones (the *Barasaurus* fossils contain clumps of rounded pebbles within the abdominal region). The carcasses settled, mostly

ventral-up, on the lakebed where they were fairly rapidly covered by clay-rich suspended load sediments with intermittent granular silt layers deposited by suspension/traction currents.

The fossil vertebrate skeletons from this Late Permian locality occur in calcareous nodules that take the shape of the skeletons around which the nodules formed in a similar manner as that recorded at the Triassic Lemoenfontein site (Figure 6.6). In the Permian rift valley lake deposits of Madagascar there are three distinct nodular horizons that were precipitated during at least 3 “micritization episodes” when low water levels prevented thermal stratification and allowed oxygenated waters to reach the anoxic lake bottom sediments. The nodules display reduction haloes around the skeletons. These haloes were formed by the release of hydrogen sulphide, formed by anaerobic bacterial decay of the soft tissues of the carcasses (Smith, 2000). During each “micritization episode” calcium carbonate was precipitated in the reduction halo around the skeletons. During this non-displacive post-burial mineralization the original siltstone micro-laminae were preserved within the nodule.

The classic Middle Triassic Chañares Formation tetrapod assemblage in northwestern Argentina (Rogers et al., 2001) yielded over 100 fossils of a diverse taxa that include cynodonts, archosaurs and dicynodonts with excellent bone preservation in volcanogenic concretions. The taphonomy points to a mass mortality event that killed both juveniles and adults of the various taxa. It resulted in an unusual concentration of carnivores and their prey in the same locality. There is also a bias against the preservation of large animals, probably due to a better ability of the large-bodied animals to survive the mortality event. The concentration and spatial orientation of the fossil skeletons is consistent with the marooning of floating carcasses on a strand line. It is proposed that volcanism may have caused a catastrophic flood that drowned the small-bodied animals. Bacterial decomposition of the carcasses triggered the formation of concretions around the bones, which in turn protected the fossils and led to the excellent state of preservation.

The Late Triassic *Placerias* Quarry in the Chinle Formation of Arizona is one of the most diverse Triassic vertebrate fossil localities in the world (Fiorillo et al., 2000). The taphonomy and depositional setting of this locality point to a low-energy depositional environment. The fossils from this locality originate in a mudstone layer that contain many carbonate nodules. This is interpreted to imply that bones accumulated in a soil with a high-water table. No definitive cause of death could be identified, however, using proposed climatic models for the Chinle Formation, the authors suggests that seasonal droughts were responsible.

6.2 Lemoenfontein: Spatial and stratigraphic distribution of fossil bones

The fossiliferous beds at this locality are exposed at three sites (Figure 6.1). The first (identified here as Gully 1), is an erosion gully that originates on the saddle, 80 m north of the centre of the Lemoenfontein hill and extends approximately 80 m to the east cutting into the flank of the saddle. This gully has a maximum depth of approximately 2 m near its middle section. Horizon 1 (calcareous nodular horizon) is exposed on both sides of the gully banks for approximately 40 m from the middle to the distal part of the gully. This gully yielded several *in-situ* tetrapod fossils, numerous *Reniformichnus* burrow casts and a single *Camborygma* burrow cast. The second (Bonebed 1) occurs on the lower part of the eastern flank exposures below the second ledge-forming sandstone approximately 210 m north of the Lemoenfontein hill. This gently sloping area extends approximately 60 m south to north and 20 m west to east. This area is has contributed by far the most tetrapod fossils found on Lemoenfontein to date. Bonebed 1 is bordered in the southeast by a small dolerite dyke. The third locality (Gullies 2 and 3), which delivered additional *in-situ* tetrapod fossils and *Camborygma* burrow casts consists of two gullies 85 m and 145 m north of the centre of Bonebed 1 (see Figure 6.1).

The tetrapod fossil bones at this site come from four consecutive fossiliferous layers. With reference to the stratigraphic log (Figure 3.4 detailed section) they are identified as follows:

- Bed 1 (BCk): A massively bedded dark reddish-brown (2.5YR 5/4) mudstone extending from 7.6 m to 9.2 m;

- Horizon 1: A continuous greyish red (5R 4/2) carbonate horizon consisting of coalescing nodules that occurs at 8.2 m within Bed 1;
- Bed 2 (BCt): A greyish-red (5R4/2) silty mudstone from 9.2 m to 23.5 m;
- Horizon 2 (Bg): A strongly developed but thin (10 to 15 cm) light olive grey (5Y6/1) silty mudstone bed occurs at 9.9 m within bed 2 that consists of elongated prismatic peds.

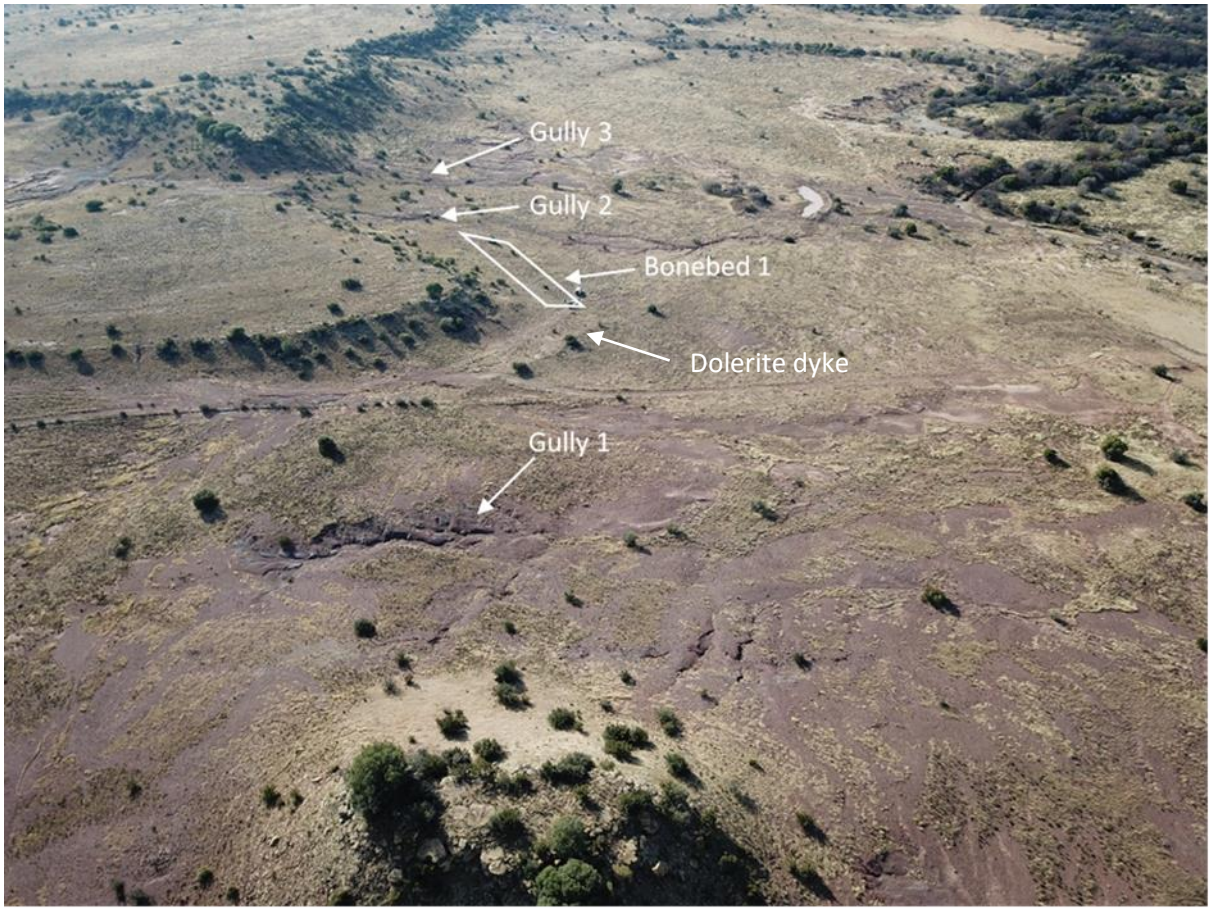


Figure 6.1: Drone image showing the Lemoenfontein hill in the foreground with the three exposures of the fossiliferous beds, Gully 1, Bonebed 1, and Gullies 2 and 3 in the distance.

6.3 Lemoenfontein: Taphonomic analysis of fossil bones

Taphonomic data recorded

The taphonomic features of the tetrapod fossils differ from locality to locality. In the following section, each locality is discussed individually. Where individual fossils show distinct taphonomic styles, they are discussed on a specimen-by-specimen basis. Where several fossils show the same style, they are described as a taphonomic group (refer to Table 6.1). For each collected specimen (see Appendix B), the following features are documented:

- skeletal articulation;
- pattern of association of disarticulated elements;
- host matrix and bedding features;
- attitude of fossils; and
- bone modification (breakage, borings, scratches, point compression, puncture marks etc.).

Based on the outcome of these assessments and following Behrensmeyer (1978) and Smith (1989), the fossils are assigned to a taphonomic class that reflects the degree of transport and the duration of the postmortem/preburial period (Table 6.1). Conclusions are derived about the environmental factors that may have resisted or promoted the disarticulation and dispersion of the skeletons.

Lemoenfontein Taphonomic classes

To allocate the tetrapod fossils from Lemoenfontein to taphonomic classes, the basic methodology as set out in Table 2 of Smith (1993) is adopted (see Table 6.1). This methodology is expanded by adding two types of descriptors: the first relates to physical characteristics and the second to interpretation based on these characteristics. This is like the use of modifiers to provide additional short-hand descriptors to master soil horizons (e.g., Bk horizon).

Physical characteristics descriptors

K Fossil bone encased in calcium carbonate nodule. The parsimonious explanation for this category is that a carcass became buried in mud shortly after death, and that the bacterial decay of its soft tissue resulted in a hydrogen sulphide halo around the carcass that in turn precipitated microcrystalline calcium carbonate (micrite) from the descending water of meteorological origin. The groundwater chemistry conditions were such that calcium carbonate was in solution.

C Surface of fossil bone coated by calcium carbonate. The parsimonious explanation for this category is that the burial of a carcass in mud after death was delayed long enough to allow the decay of most of its soft tissue. The decay of the remaining soft tissue (mainly collagen fibres in the bone matrix) resulted in the release of hydrogen sulphide in the vicinity of the bone surface leading to precipitation of a thin layer of calcium carbonate from the descending water of meteorological origin.

U Surface of fossil bone non-mineralized. In this case the bones were exposed for a long enough period to the atmosphere such that decomposition had progressed to completion and as such there was no bacterial decay after burial to promote the precipitation of calcium carbonate.

M Fossil bone encased in cemented mudrock. In some cases, the animals were embedded under conditions where “mature” calcium carbonate nodules did not form around the carcases, however, the mud or silt surrounding the carcass became preferentially cemented forming a pseudo-nodule.

S One or more skeletons in confined space. This descriptor considers characteristics such as the degree of skeletal disarticulation, physical orientation or the attitude of fossil, and the surficial or architectural morphology of the nodule (or pseudo-nodule) containing the skeletons. Indicates that the bones were buried whilst contained within a confined space that is just large enough to accommodate carcasses of the individual animals in close association.

F Fossil bone on floodplain surface. This descriptor is used instead of S if the fossil bone was buried while resting on the floodplain surface.

R Reworked fossils. This identifier is used for bones that underwent permineralisation following burial, but during subsequent denudation and erosion of the floodplain they became subaerially exposed, transported, abraded, re-deposited and buried. Typical evidence for this includes signs of post- permineralisation weathering, water wear (abrasion and polishing), or articulated skeletons that became broken into smaller elements where each element still contains articulated bones.

D Preburial modification. This descriptor is used to identify fossils that show physical damage such as tooth puncture and scrape marks, point compressions, serrated fractures, restricted crushed patches, borings etc. that occurred before the carcass became covered in mud.

Interpretation descriptors

The physical descriptors are modified by adding a subscript based on causative interpretations assigned to each physical characteristic.

b Fossil in burrow. Considers architectural morphology e.g., reniform cross-section, angle relative to horizontal, sinuosity, surficial morphology (scratch marks), physical orientation and attitude of fossil within nodule, stratification of infill, presence of a burrow liner.

t Fossils in burrow terminal chamber, aestivation hole or nest. Considers the same factors as for b, but specifically looks for the shape of a burrow terminal chamber or hole.

a Shelter sharing or aggregation of more than one individual. In addition to criteria for descriptors b and t, this interpretation also considers the close association of more than one skeleton of the same or different taxa in the same nodule. By implication, this descriptor also includes b and t.

g Skeleton preserved in floodplain gully/hollow. This descriptor identifies a scenario where one or more full or partial skeletons became buried in a confined space on the floodplain through hydraulic action.

f Bones buried on floodplain surface. This descriptor applies to a scenario where partially articulated and isolated bones, including skulls, are incrementally embedded where they died on the floodplain surface.

d Disarticulated skeleton but still associated due to desiccated skin. In this scenario a fossil skeleton remained on the dry floodplain surface for a long time and became disarticulated, but the bones were held in association by mummified skin and tendons.

m Pre-burial damage due to bone crushing mastication. This subscript is used if the interpretation can be made that puncture marks, point compressions, serrated fractures, crushed bone etc. are predator bite marks (such as tooth punctures).

A code consisting of four identifiers is used to allocate the Lemoenfontein fossils to taphonomic groups as follows:

- the first identifier corresponds to the taphonomic class (first column in Table 6.1);
- the second relates to the degree in which the fossil is coated in calcium carbonate (*K*, *C, U, M*);
- the third identifies whether the animal was trapped in a confined space, died on the floodplain surface, experienced desiccation or if the fossil underwent reworking (*S, F, R*); and
- the final identifier indicates if preburial damage is present or not (*D*).

The identifier for damage (*D*) is only assigned if damage is present. The codes for confined space (*S*) and preburial damage (*D*) are modified using subscripts corresponding to the interpretation descriptors.

Table 6.1: Taphonomic classes with characteristic descriptors (adapted from Smith (1989))

Taphonomic class			Physical characteristic descriptors	Interpretive descriptors	Transportation	Duration of postmortem/ pre-burial period
Preserved at site of death	A_x	Complete articulated skeleton. The skeletal attitude can take three forms: A_1 "spread-eagled" and taking the shape of the carcass, A_2 "curled-up" in 2-dimensional horizontal bedding plain, A_3 "curled-up" in 3-dimensional spiral.	*K, C, U, M, S, F*	*b, t, a, g, f, m*	No transportation	Very Short
	B	Complete or near complete skeleton with straight or reflexed spinal curvature.	*K, C, U, M, S, F*	*b, t, a, g, f, d, m*	Slightly rolled	Short
Preserved near site of death	C	Skull with articulating cervical vertebrae and lower jaw	*K, C, U, M, R, F*	*d, f, m*	Lag - short distance transport	Short
	D	Skull with displaced lower jaw	*K, C, U, M, R*	*m*		Long
	E	Skull without lower jaw	*K, C, U, M, R*	*m*		Long
	F	Lower jaw	*K, C, U, M, R*	*m*		Long
Preserved far from site of death	G	Accumulation of variety of small postcranial elements into "bone bed"			Long distance transport Reworked, winnowed and sorted	Very Long
	H	Isolated and/or fragmented ribs, limb bones and vertebrae			Long distance transport	Very Long

Perimineralisation and nodule formation

Most of the fossil vertebrate skeletons and skulls from Lemoenfontein occur in brown weathering calcareous nodules. These nodules are like those described in Smith (2000) in his sedimentological and taphonomic study of the aquatic procolophonoid reptile *Barasaurus* from Late Permian fossil localities in southwestern Madagascar. Like the *Barasaurus* nodules, some of the Lemoenfontein nodules also take the shape of the skeletons around which they formed (Figure 6.6). Anaerobic bacterial decay of the *Barasaurus* soft tissues released hydrogen sulphide into the surrounding sediments, forming reduction haloes. These reduction haloes resulted in the early precipitation of calcium carbonate (micrite) from the groundwater around the skeletons. The sharp outer boundaries of the nodules indicate that the precipitation of carbonate occurred incrementally over time as the decay of soft tissue progressed. This perimineralisation occurred soon after burial, but before compaction and provided the mechanical strength to prevent any significant compaction of the skeletons. It is also noted that those carcasses that were buried quickly, as well as instances of more than one overlapping carcass, were encased in more continuous and thicker micrite nodules than those that were buried slowly, where less organic material was left to form reduction haloes in the surrounding sediments.

In their study of a tetrapod assemblage in the Middle Triassic Chañares Formation, Rogers et al. (2001) also concluded that bacterial decomposition of carcasses triggered the formation of concretions around the bones, which in turn protected the fossils and led to the excellent state of preservation.

The phenomenon of bacterially-induced precipitation of calcium carbonates in or on decaying bone has been simulated in laboratory experiments (Carpenter, 2005; Daniel and Chin, 2010). In these experiments decaying bone samples and sterile bone samples were buried in river sand, simulating a fluvial environment. Water containing calcium carbonate was then allowed to percolate through the sand. In the case of Carpenter (2005), calcium carbonate precipitated on the decaying bone by 30 days and within the bones after 296 days.

However, Daniel and Chin (2010) found that sand grains were cemented to the bone in one week and completely covered the bone in six weeks. Permineralisation of internal cancellous bone occurred after 12 weeks. In both cases no permineralisation occurred in the sterile bones. These studies demonstrate that bacterially mediated calcite precipitation also occurs outside the decaying bones by cementing sand grains to the outside surface. This phenomenon is referred to as perimineralisation by Smith (2000). The conclusion is reached that early and simultaneous peri- and permineralisation of bone can play an important role in the preservation of bone until fossilisation/recrystallisation occurs.

It is not unreasonable to conclude that early bacterially induced calcite mineralisation of the bone cavities also provides some structural resistance to burial depth induced compaction. The occurrence of virtually un-compressed bones in the rock record must be an indication that early permineralization has happened. Accepting this fact would thus imply that bones that have become sterile by long term sub-aerially exposure before burial would not have bacterially mediated permineralisation and should therefore be significantly more compressed and would not be coated in calcium carbonate. The topic of how peri- and permineralisation of therapsid bones helps resist compaction is however a taphonomic investigation that is beyond the scope of this study.

6.4 Taphonomy of tetrapod fossils in Gully 1

Although Gully 1 does not have the same abundance and diversity of tetrapod fossils as Bonebed 1, the locality did deliver several significant fossils that are in close association (from both a stratigraphic level and horizontal spatial distribution perspective) with *Reniformichnus* and *Camborygma* burrow casts.

Teratophon SAM-PK-K10174 (Field number 117)

This specimen consists of a virtually complete, curled-up skeleton and skull, with an articulated lower jaw. It was found embedded in a dorsal up position in the Bed 1 (BCk-horizon) mudstone approximately 30 cm above Horizon 1 (carbonate horizon), see Figure 6.2. It occurs in the bed that contains the *Reniformichnus* burrow casts and one of these burrows occurs within 1 m of this specimen (Figure 6.2). Unlike many of the specimens from Bonebed 1, this specimen is not inside a calcareous nodule, however the mudrock at the interface with the bone surface is calcified. Mechanical preparation revealed that the bone surface displays many fine cracks (Figure 7.7 C). This may have been caused by the displacive precipitation of calcite at the bone/matrix contact. Otherwise, the fossil bone is in a very good state of preservation.

Following the criteria set out in Table 6.1, this specimen is allocated to Taphonomic Class $\mathbf{A_2}CF_f$, i.e., complete articulated skeleton in 2D "curled-up" attitude, surface-coated in calcium carbonate (*C*), no transportation, preserved at site of death on floodplain surface (F_f), and very short duration of postmortem/preburial period. Apart from its curled-up attitude and its association with *Reniformichnus* burrow casts, there is no strong taphonomic evidence that this specimen was preserved in an underground burrow. Also, based on the high degree of articulation the desiccation interpretation (*d*) is also ruled out. It is worth noting that the rib cage retained its original 3-dimensional shape to a certain extent.



Figure 6.2: Teratophon *(SAM-PK-K10174). (A)* In-situ *during excavation, showing association with* Reniformichnus*, and vertical position relative to the calcareous horizon. (B) Specimen post-excavation showing calcium carbonate surface coating. (C) Specimen post-preparation. Scale bar = 5 cm.*

Teratophon SAM-PK-K011599 (Field number L18-2)

This *Teratophon* specimen is encased in two connected nodules of cemented siltstone that have separated from each other (See Figure 6.3). The main "curled-up" articulated skeleton resides in a large nodule, while its skull is in a small nodule that attaches in life position to the cervical vertebrae of the spine along a clean break. The larger nodule also contains the

articulated skeleton of a second *Teratophon*. The two nodules became separated during recent storm-induced sheet flows that dislodged both from their embedded conjoined position. The skull was found about 1 m upstream from the nodule containing the skeleton, both about 1 m below the calcareous nodular horizon in the midline of the main channel of Gully 1 (see Figure 6.3 A). The larger oblate shaped skeleton nodule has a greater hydrodynamic resistance, but it was washed 1 m further downstream than the skull following recent heavy rainfall at the locality suggesting that it eroded out first. Both the skull and the nodule containing the main skeleton (and second specimen) were found dorsal-up. Based on the proximity of the two nodules and the fact that both were still in their original dorsal-up position, it is reasonable to assume that they did not tumble out of the flanks of the gully and that they were found close to their original embedded position in the midline of the channel in Bed 1 (BCk) (see Figure 6.3 A). The interpreted bottom surface is mostly flat and has the same colour as the underlying mudrock. The top surface is more convex and its displays a significant degree of gleying induced mottling. The dominant colour is weak-red (10R 4/3), while the mottling is greyish-blue (5PB 7/2) and light-grey (N 7). These colours correspond to the mottling observed in the beds of the sedimentological Cycle 0, described in Chapter 3. This type of low chroma mottling is consistent with a reduction of and removal of iron or manganese through gleying. Gleying is caused by the seasonal variation of groundwater levels in generally saturated clay-rich soil horizons.

This specimen occurs in the bed that contains *Reniformichnus* burrow casts that extend from above the calcareous horizon down to below this k-horizon. One of these burrows occurs within 1 m of this specimen (Figure 6.3). The vertical stratigraphic position of this fossil likely places it below the interpreted wet season palaeo-water table, and that could explain why it is not encased in a calcium carbonate nodule like most of the specimens that occur above the k-horizon. The degree of mottling is also consistent with the interpretation that this specimen originated below the calcareous nodular horizon, in the region of seasonal variation of the ground water table.

The nodule contains two medium sized articulated and curled-up *Teratophon* skeletons. Both skulls have quadratojugal processes, but these are not as prominently developed as those of specimen SAM-PK-K10174 (Figure 6.2). Based on the intermediate skull size and underdeveloped quadratojugal processes, the interpretation is made that these two specimens are sub-adults. The second specimen's skull is curled-in under the abdomen of the first. Two of the upper specimen's gastralia ribs lay on top of the second skull. This is a good indication that the top skeleton likely still had skin on to keep the gastralia in place when the second individual was already in position. The flexure of the vertebrae in the top specimen over the skull of the lower specimen suggests that they both died at around the same time and were subject to the same post-burial compaction without any transportation. This flexure supports a dorsal-up interpretation for this. It appears that the limbs of the lower specimen are at a high angle rather than lying flat, which may indicate that they were in a confined space. This confined space could be interpreted as a burrow, near surface hole or some form of surface hollow. One of the hind limbs of the upper specimen appears to penetrate the surface of the nodule, suggesting that the nodule surface does not correlate exactly with the boundary of the interpreted confined space. The nodule surface is smooth and does not show distinct scratch marks or striations. This could be due to an incomplete formation of a reduction halo around the specimens leading to an incomplete cementation of the mud surrounding the specimens in the confined space. However, the high degree of articulation of more than one individual together in behaviourally controlled aggregation that resembles huddling in a confined space, does provide compelling evidence that this may be an underground burrow terminal chamber or nest (e.g., Smith and Evans, 1995).

Mechanical preparation revealed that the bone surface displays many fine cracks. This is likely caused by the displacive precipitation of calcite at the bone/matrix contact. The fossil bone is in an excellent state of preservation. The skeletons of the specimens are uncompressed, and the rib cage of the upper specimen has retained its original three-dimensional shape. The bones must have experienced early permineralisation that provided resistance to compaction retaining the three-dimensional nature of the skeletons. Early permineralisation could have given the ribs the rigidity to combat compaction (i.e., crushing),

but the fact that the skeletons remained in life position without evidence of collapse must be related to the sheltered situation underground and rapid burial.

Following the criteria as set out in Table 6.1, these specimens are allocated to Taphonomic Class A_2MS_a, i.e., complete articulated skeleton in 2D "curled-up" attitude, encased in cemented mudstone *M*, in confined space that is interpreted to be a burrow terminal chamber, containing an aggregation of two individuals (S_a), no transportation, preserved at site of death below floodplain surface, and very short duration of postmortem/preburial period. It is important to note that although these specimens are not curled-up in a spiral 3-dimensional (A_3) shape, it is uncompacted as clearly visible in the 3-dimensional shape of the rib cage and the flexure of the vertebrae of the top specimen, as well as the high angle of the limbs of the lower specimen. This taphonomic style suggests that the two sub-adult *Teratophon* had their skin intact when they became arranged into this configuration, and that they were most likely both alive. An underground burrow setting is therefore the most likely scenario.

This is an important specimen that deserves a full analysis that is currently beyond the scope of this study, however a plausible taphonomic pathway (sequence of events) that led to the preservation style observed in this specimen can be hypothesized based on existing evidence.

- The *Teratophon* constructed the hollow or nest in the beginning of the dry season for thermoregulation or burrowed to have access to a more humid environment just above the saturated phreatic zone.
- This burrow is used as a shelter (possibly as a nest) for the duration of the dry season.
- Due to an extended drought or cold spell, the animals entered the shelter, went into a state of cold torpor, and subsequently died in their curled-up “torpor position” in the terminal chamber.
- A series of sheet floods at the end of the dry season resulted in sediment-laden water entering the burrow slightly disrupting the carcasses and incrementally burying them with transported mud aggregates (see sedimentology discussion, Chapter 3). The

upper reaches of the tunnel were then in-filled with mud aggregates during subsequent flood events for as long as it stays open.

- The bacterial decay of the soft tissue in buried carcasses led to the cementation of the mud around the skeletons (perimineralisation) in the burrow terminal chamber and around the skull at the chamber entrance. The bones also underwent early permineralisation that provided resistance to compaction and the 3-dimensional nature of the skeletons was retained. During the wet season, this specimen eventually ended up below the water table resulting in the interruption of the calcium carbonate precipitation in the host matrix and a "mature" calcium carbonate nodule is not formed. This also caused the characteristic mottling of the nodule's mudstone matrix.
- After deposition of clay aggregates in the burrow tunnel, compaction and the addition of suspended clay quickly destroys the aggregate structure of the sediments and as a result the portions of the burrow tunnel that are filled with mud aggregates are not easily distinguished from the host mudstone in weathered outcrops.

Several authors have studied different types of fossil aggregations such as multi-taxon shelter sharing (Abdala, 2006), mono-taxon social aggregation (Botha-Brink and Modesto, 2009), behavioural aggregations for reproduction (Maddin, 2020), or for thermoregulation or moisture retention during droughts (Smith and Evans 1995). Procolophonids, including *Teratophon,* had prominent pineal openings in their skulls. It is believed that the pineal organ in tetrapods had an important and precise function in achieving thermoregulation in ectotherms (Benoit et al., 2016). It is therefore likely that procolophonids were ectothermic (or at most poikilothermic). This leads to the most parsimonious explanation that this sub-adult *Teratophon* association was simply shelter-sharing for thermoregulation. Furthermore, the conclusion that curled-up skeletons of two sub-adults of the same taxon lying in contact with each other, is compelling evidence that they were buried at the same time in a confined space and without postmortem transportation. Thus, an underground burrow is the simplest explanation. It provides additional convincing evidence that procolophonids practiced a fossorial lifestyle. Several authors have proposed the same based on anatomical features of procolophonids, such as the existence of a spade–shaped skull, robust phalanges, and large

unguals (de Braga, 2003; MacDougall et al., 2013; Zaher et al., 2018), morphology and bone histology (Botha-Brink and Smith, 2012), by association with burrow casts (Groenewald, 1991, Botha-Brink and Smith, 2012), and other historical accounts (Kitching, pers. comm., 1990, as reported in Groenewald, 1991). Botha-Brink and Smith (2012) proposed that burrowing may have played an important role in their survival during the harsh post-extinction Triassic environment. Ivakhnenko (1979) also concluded that a skeleton of the procolophonid *Tichvinskia vjatkensis* was probably preserved in a burrow based on its a fully-articulated and curled-up nature (Sues, 2019).

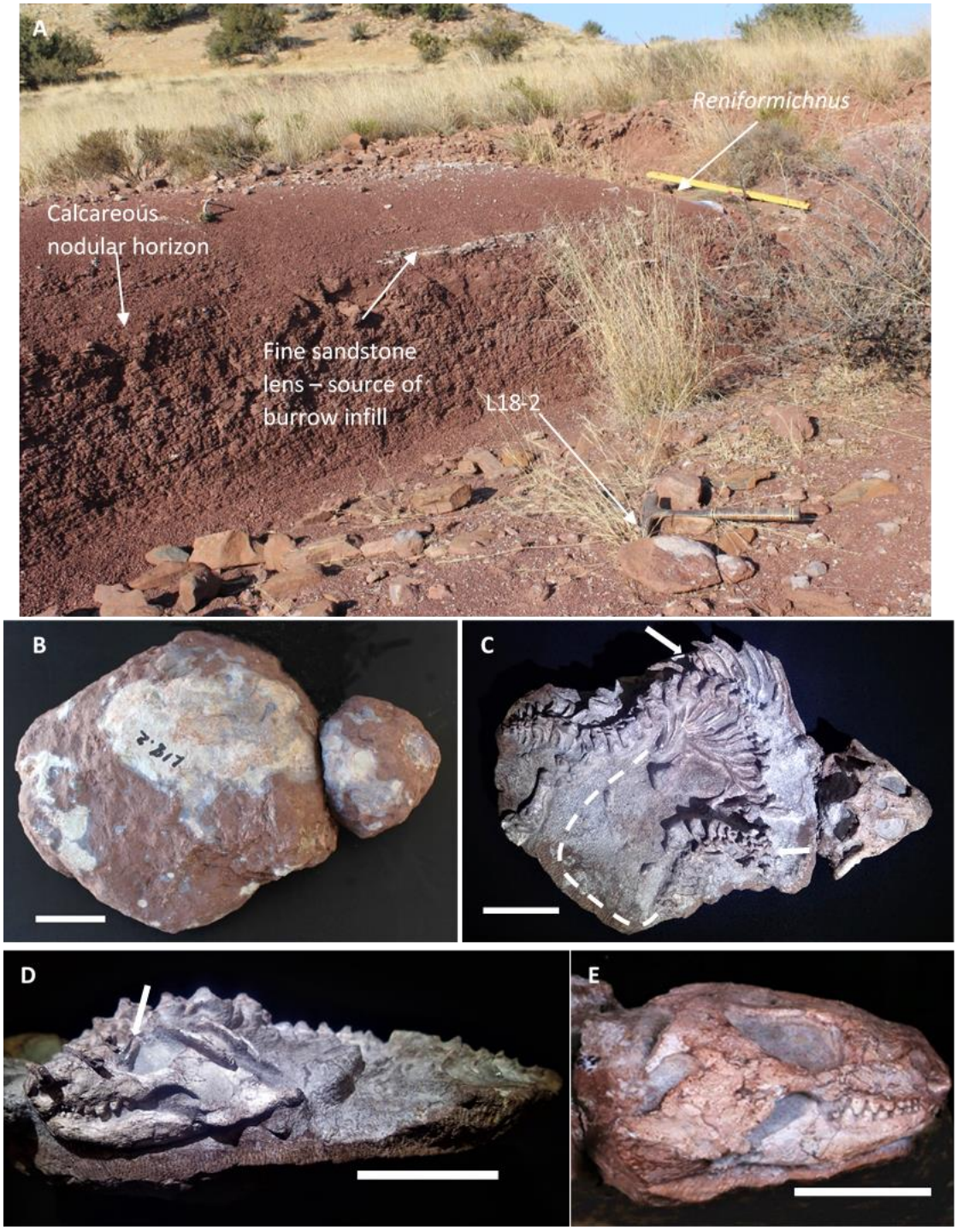


Figure 6.3: (A) L18-2 lying in the base of erosion gully in the orientation and attitude that it was found, which although apparently ex-situ *it is still considered to be in its original stratigraphic position. Note the association with* Reniformichnus *and its stratigraphic level relative to the calcareous horizon. (B) L18-2 before preparation showing the detached skull block and colour mottling attributed to hydromorphic gleying of the mudrock surrounding the specimen. (C) Specimen after mechanical preparation showing the presence of 2 fully articulated curled-up* Teratophon *skeletons, one on top of the other. Top arrow indicates position of the second skull. Dashed line traces the inferred still-covered articulated spine, and the bottom arrow indicates the string of articulated caudal vertebra attributed to the second specimen. (D) Lateral view of second* Teratophon *skull lying dorsal-up beneath the still articulated, but slightly dislodged, thoracic ribs of the top specimen. Note the position of two gastralia ribs (arrowed) that had also become slightly dislodged from the top specimen. This taphonomic style suggests that the two sub-adult* Teratophon *had their skin intact when they became arranged into this configuration, and that they were most likely both alive. An underground burrow setting is therefore the most likely scenario. (E) Right lateral view of uppermost specimen. The two skulls have small differences in shape and size that may be attributed to ontogeny or sexual dimorphism. All scale bars = 5cm.*

Teratophon Field number L18-1

This specimen consists of a large and complete procolophonid skull without a lower jaw. It was found embedded in a dorsal-up attitude in the Horizon 1 (carbonate horizon), see Figure 6.4. It occurs in the same bed that contains the *Reniformichnus* burrow casts. Although not in a carbonate nodule, the mudrock at the interface with the bone surface is calcified. Mechanical preparation revealed that the bone surface displays many fine cracks. This may have been caused by the displacive precipitation of calcite at the bone/matrix contact like that described from similar-aged deposits in south Brazil (Bertoni-Machado and Holtz 2006; Holtz and Souto- Ribeiro 2000), otherwise the fossil bone displays very good preservation.

Following the criteria set out in Table 6.1, this specimen is allocated to Taphonomic Class **E***CF*$_f$, i.e., Skull without a lower jaw, surface-coated in calcium carbonate (*C*), short distance transportation, preserved near site of death on floodplain surface (F_f), and long duration of postmortem/preburial period. Apart from its association with *Reniformichnus* burrow casts, there is no taphonomic evidence that this specimen was preserved in a burrow.

Teratophon Field number L19-1

This specimen consists of a partial procolophonid lower jaw. It was found embedded in left lateral-up attitude in dark reddish brown mudrock, see Figure 6.4. It occurs at the same location as L18-1 (*Teratophon* skull without lower jaw) in the calcareous nodular horizon (Horizon 1), that in turn occurs in the bed (Bed 1) that contains the *Reniformichnus* burrow casts. This specimen is not however coated in calcium carbonate.

The lower jaw is assigned to the taphonomic class **F***UF*$_f$, short distance transport and long duration of postmortem/preburial period.

Teratophon Field number L20-10

This specimen consists of an apparently complete skeleton and skull. It was found embedded in a dorsal-up position in the Bed 1 (BCk-horizon) mudstone approximately 30 cm above Horizon 1 (carbonate horizon; see Figure 6.4). It is in the same horizon as the curled-up *Teratophon* specimen, SAM-PK-K10174, some 20 m upstream near the top of the gully (there is a 10° dip in these beds towards the southeast). It occurs in the bed that contains the *Reniformichnus* burrow casts. Unlike many of the specimens from Bonebed 1, this specimen is not encased in a calcareous nodule, however the mudrock at the interface with the bone surface is cemented. This specimen is not yet prepared, and its identification is based on the distinct triangular shape of the skull.

Following the criteria set out in Table 6.1, this specimen is allocated to Taphonomic Class **B***MF*$_f$, i.e., Complete skeleton with straight spine (**B**), encased in cemented mudstone (*M*), no transportation, preserved at site of death on floodplain surface (F_f), and very short duration of postmortem/preburial period. Apart from its association with *Reniformichnus* burrow casts, there is no taphonomic evidence that this specimen was preserved in a burrow.

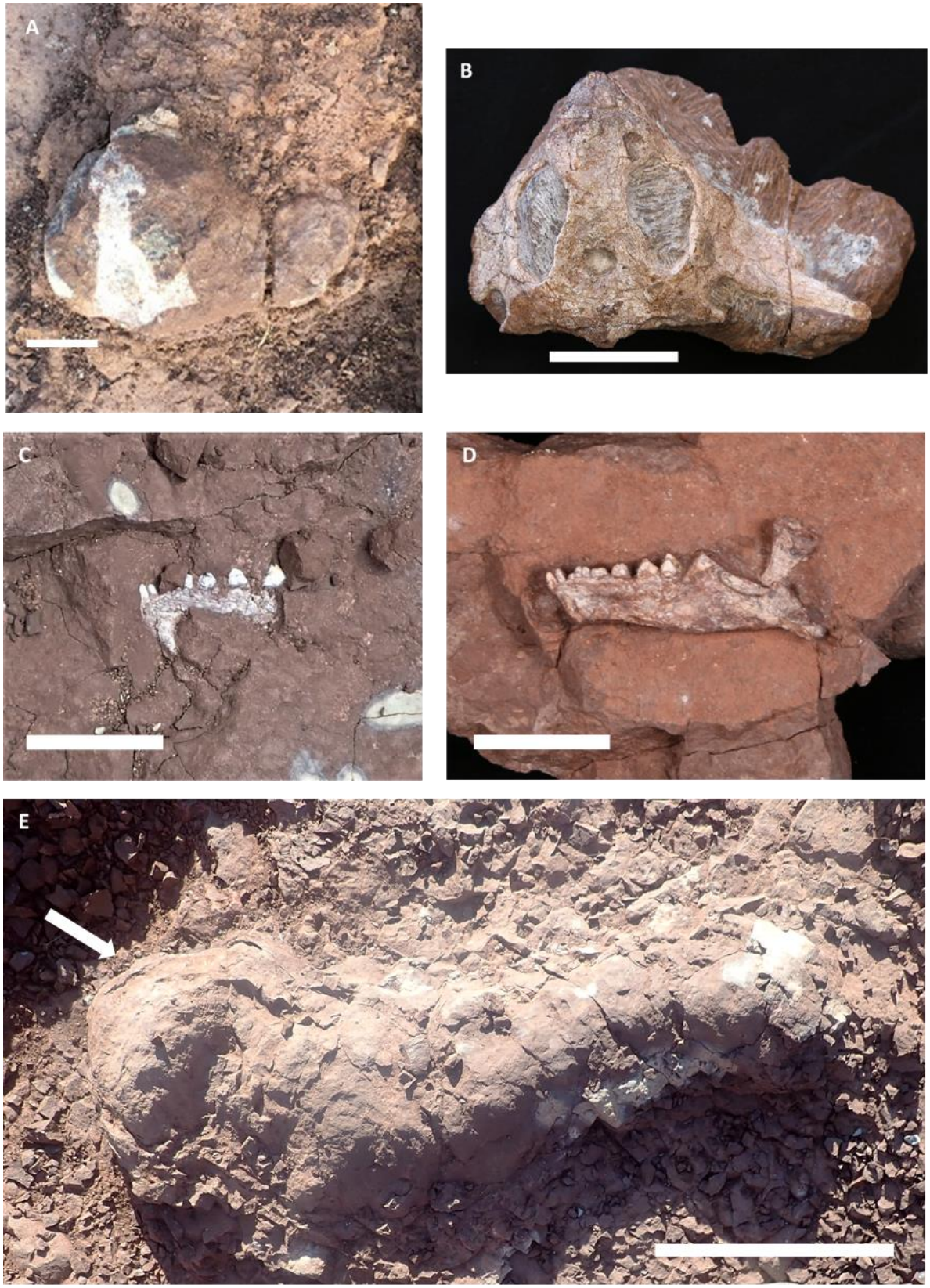


Figure 6.4: (A) Teratophon *(L18-1), skull embedded in calcareous nodular horizon. (B) L18-1 Specimen afer preparation. (C) L19-1* Teratophon *lower jaw embedded in calcareous nodular horizon. (D) L19-1* Teratophon *lower jaw after preparation. (E) In-situ* Teratophon *articulated skeleton (L20-10) coated in cemented mudstone. Identification based on triangular shape of skull (arrowed). Scale bars in A = 3 cm and B = 4 cm, scale bar in C and D = 2 cm, scale bar in E = 10 cm.*

Procolophonid SAM-PK-K10171

This specimen consists of a procolophonid skull with articulated lower jaw. It was found embedded in dorsal-up attitude in dark reddish-brown mudrock (2.5YR 5/4) with a thin lens of sandstone beneath. It occurs in the bed (Bed 1) that contains the *Reniformichnus* burrow casts about 50 cm above the calcareous nodular horizon (Horizon 1). This specimen is not coated in calcium carbonate. An uncoated partial procolophonid lower jaw was found in a lateral-up attitude embedded next to this specimen.

Following the criteria set out in Table 6.1, this specimen is allocated to Taphonomic Class **C***UF*$_f$, i.e., skull with articulating lower jaw, surface uncoated (*U*), short distance transportation, preserved near site of death on floodplain surface, and short duration of postmortem/preburial period. Apart from its association with *Reniformichnus* burrow casts, there is no taphonomic evidence that this specimen was preserved in a burrow. The lower jaw is assigned to the taphonomic class **F***UF*$_f$, short distance transport and long duration of postmortem/preburial period.

Gully 1 also yielded a few large *ex-situ* procolophonid skulls like L18-1 (downstream from it), as well as smaller procolophonid skulls encased in calcium carbonate nodules (these are very similar to the specimens from Bonebed 1 where a generic description is provided).

6.5 Taphonomy of tetrapod fossils in Bonebed 1:

Most of the more than 140 tetrapod fossils from the Lemoenfontein locality were found on the surface of Bonebed 1, originating from the 1.7 m thick mudrock sections of Bed 1 and Bed 2 that occur above Horizon 1 (calcium carbonate horizon at 8.2 m in Figure 3.4) up to and including Horizon 2 (structural B-horizon at 9.9 m in Figure 3.4). This sub-horizontal area extends approximately 60 m south to north and 20 m west to east. The fossils originating between Horizons 1 and 2 are encased in very hard brown-weathering calcium carbonate

nodules. Several fossils originate from within the structural B-horizon (Horizon 2), and these are thinly coated in light olive grey (5Y5/6) siltstone. Due to the large number of fossils collected, these are grouped according to the taphonomic style for discussion purposes and only representative examples are discussed.

Taphonomic Group 1: Isolated skull with articulated lower jaw

This group of specimens consists of isolated skulls with articulated lower jaws that are completely encased in calcium carbonate nodules that weather to greyish-brown (5YR6/2) and they make up most of the tetrapod fossils recovered from Bonebed 1. These nodules were found as "float" on the sloping surface that extends down from Horizon 2 to Horizon 1 (downsloping 1.7 m over 20 m). The specimens include procolophonids, rhynchosaurs, therocephalians and cynodonts (see Figure 6.5 for examples). Mechanical preparation of several specimens revealed that the bone surface displays many fine cracks. This was most likely caused by the displacive precipitation of calcite at the bone/matrix contact and within the bone itself. The bone preservation of most of these specimens is excellent. The specimens nearer to the dolerite dyke are slightly baked giving the bone a porcelain-like quality.

Following the criteria set out in Table 6.1, this group of specimens is allocated to Taphonomic Class CKF_f, i.e., skulls with articulating lower jaws, encased in calcium carbonate nodules (*K*), short distance transportation, preserved near site of death on floodplain surface, and short duration of postmortem/preburial period. These specimens were likely buried while lying on the floodplain surface and the additional interpretative descriptor F_f is assigned. Smith (1989) identified eight environmental factors that promote dispersal and disarticulation of carcasses. The first of these, carnivore mastication and ingestion of small animals, provides a plausible explanation for the presence of large numbers of skulls with articulated lower jaws, but with no postcranial elements present. Zaher et al. (2018) postulated that the quadratojugal spines of the procolophon, *Kapes bentoni*, were a possible adaptation that interfered with the ability of smaller predators to swallow it after being captured. Here, a plausible scenario is that a predator that is slightly larger than the prey would be able to devour the postcranial part of

the prey but would not be able to swallow the skull. Consistent with an interpretation by Bertoni-Machado and Holz (2006), this could explain the presence of isolated skulls (predominantly of *Teratophon*) at this locality. The sixth factor identified by Smith (1989), entrainment of small bones by shallow sheet floods, could also provide an explanation in cases where complete soft tissue decay of the carcasses has occurred, allowing the skulls to separate from the skeletons. In such a scenario the less transportable skulls are less likely to have been washed away than the lighter postcranial bones. However, most skulls have articulated lower jaws and are encased in calcium carbonate nodules, suggesting a short duration postmortem/preburial period and hence the complete decay of the soft tissue before burial is unlikely.

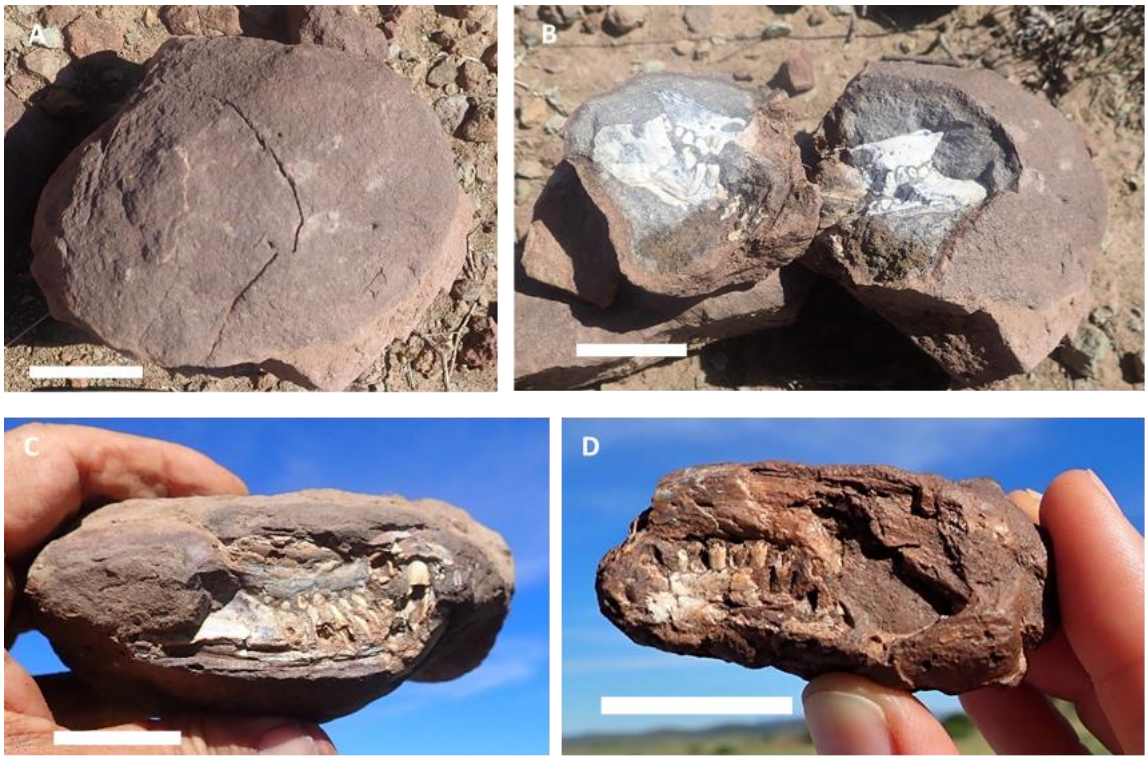


Figure 6.5: Examples of Taphonomic Group 1: Isolated skull with articulated lower jaw. (A) and (B) Microgomphodon *skull (L20-3), encased in carbonate nodule as found in the field. (B)* Trirachodon *skull (L19-17) encased in carbonate nodule as found in the field. (D) Very rare* Lumkuia *skull (L19-19) encased in carbonate nodule as found in the field. Scale bar in A, B and C = 3 cm, scale bar in D = 2 cm.*

Taphonomic Group 2: Articulated skeletons encased in nodules that take the shape of the carcass

This group of specimens consists of fossil vertebrate skeletons that occur in greyish brown-weathering (5YR6/2) calcareous nodules that take the shape of the skeletons around which

the nodules formed (Figure 6.6). Several nodules containing skulls with articulated lower jaws, cervical vertebrae or at least one articulated manus, show fresh breaks between the skull and the rest of the skeleton. Due to the shape of the nodule that generally follows the anatomy there is a naturally occurring narrow region between the skull and the skeleton and that leads to the skull and skeleton commonly separating from each other during natural exhumation and post-erosional transport. These specimens are also included with this taphonomic group. The representative *Microgomphodon* specimen, SAM-PK-K11601 (L18-6), was found embedded in Bed 1 above horizon 1 in a spread-eagled dorsal-up attitude, while the skulls with attached postcranial elements were found as float on the downsloping surface. The overall morphology and smooth surface texture of the nodule that contains the specimen SAM-PK-K11601, is like those that encase the aquatic procolophonoid reptile *Barasaurus* from Madagascar (Smith, 2000). A further similarity to the *Barasaurus* nodules, is that during recent weathering and exhumation, groundwaters flushing through cracks in the parts of the nodule containing the limbs, weather away the fossilised bone forming a natural mould of the original skeletal material (Smith, 2000). The specimens making up Taphonomic Group 2 include procolophonids, rhynchosaurs and a therocephalian, see Figure 6.6 for examples. Mechanical preparation of several specimens has revealed the bone surfaces to be crazed with many fine cracks. This may have been caused by the displacive precipitation of calcite at the bone/matrix contact.

Specimen (SAM-PK-K11601, L18-6) shows a high degree of articulation and excellent bone preservation (almost porcelain-like quality); however, it also shows damage to the snout (see Figure 6.6). The modification appears to be point compressions and they occur on both sides of the snout. To conclude that they are caused by carnivore teeth, the specimen needs to be Micro CT-scanned and analysed in detail. Such an investigation is beyond the scope of the current study. However, the following observations can be made:

- the compressed bone fragments appear to be still in the puncture hole which suggests that the damage happened whilst the skin was still on the animal;
- the compression appears to be restricted to the maxilla with a single puncture of the lower jaw.

To confirm that these are tooth punctures, confirmation is needed that the pits on both sides of the skull match. This is a unique specimen, not only because of its perfect preservation and that it is the first *Microgomphodon* with articulated postcrania but also that it shows possible tooth puncture marks on both sides of the snout, possibly the suffocating muzzle bite or feeding trace of an adult *Cynognathus.* A modern analogy of this style of killing prey, is the way in which lions attempt to suffocate their prey by either tightly gripping the prey's throat with their jaws, or by covering the prey's nostrils and mouth with their jaws, completely cutting off air flow (Schaller, 1972).

Following the criteria set out in Table 6.1, this group of specimens is allocated to Taphonomic Class BKF_fD_m, i.e., a complete or near complete skeleton with straight or reflexed spinal curvature, encased in a calcium carbonate nodule (*K*), short distance transportation, preserved near site of death on floodplain surface, and short duration of postmortem/preburial period. These specimens were likely buried while lying on the floodplain surface and the additional interpretative descriptor F_f can be assigned. The tentative additional interpretation D_m is made due to the possibility that the modification was due to bone crushing mastication.

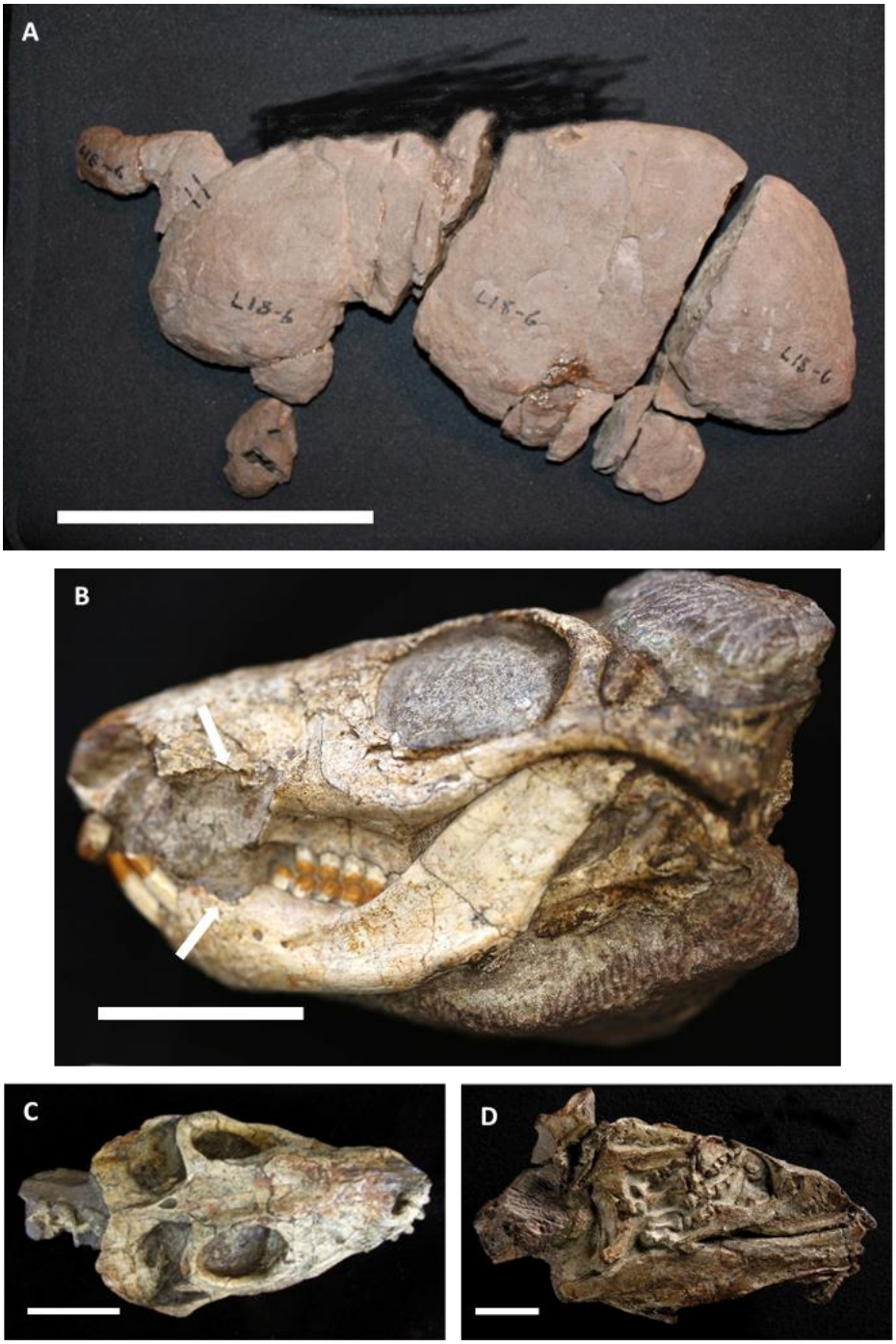


Figure 6.6: Examples of Taphonomic Group 2: Articulated skeletons encased in nodules that take the shape of the carcass. (A) Microgomphodon *(SAM-PK-K11601), skeleton encased in carbonate nodule that takes the shape of the carcass. This is the first* Microgomphodon *specimen with a fully articulated skeleton attached to the skull. (B) Left lateral view of SAM-PK-K11601 skull, showing possible preburial damage (arrowed) and excellent preservation quality of the bone. (C)* Microgomphodon oligocynus *(SAM-PK-K10160), skull with articulating cervical vertebrae and manus encased in carbonate nodule (articulated manus removed from nodule during preparation). (D)* Eohyosaurus wolvaardti*, SAM-PK-K10180, skull was encased in carbonate nodule before preparation. Note articulated right manus on temporal region. Scale bar in A = 15 cm, scale bar in B = 3 cm, scale bar in C and D = 2 cm.*

Taphonomic Group 3: Articulated skeletons curled-up in a 3-D spiral, encased in nodules

Several juvenile procolophonid specimens consisting of tightly curled-up articulated skeletons in small (approximately 10 cm across) calcareous nodules were collected lying dorsal up on the sloping surface beneath Horizon 2 in an area of approximately 10 m by 10 m (Figure 6.7). Specimen L18-23B is a typical example and consists of a tightly curled-up skeleton with the skull curled-in under the caudal vertebrae, with the ribs in their original 3-dimensional configuration. The attitude of these specimens suggests that they were buried whilst in a confined space (**S**). Mechanical preparation of the specimens revealed that the bone surface displays many fine cracks. This may have been caused by the displacive precipitation of calcite at the bone/matrix contact. Otherwise, the bone preservation is very good.

Following the criteria set out in Table 6.1, this group of specimens is allocated to Taphonomic Class $\mathbf{A_3}KS_t$, i.e., a complete curled-up skeleton in 3-dimensional spiral with skull curling in above the body (below the body in one case), encased in a calcium carbonate nodule (*K*), no transportation and very short duration of postmortem/preburial period. The additional interpretative descriptor S_t is assigned.

Following Zoehfeld et al. (2013) the interpretation is made that these procolophonids burrowed into soft mud for aestivation purposes. They curled-up in spirals with their skulls and nostrils near the surface of the mud. The soft mud consolidated around their bodies. The calcium carbonate nodule that developed after death, formed in the spiral shape of the carcass and retained a smooth outer surface, unlike what would be expected if the animal died in a burrow terminal chamber that subsequently became infilled with mud or sand.

Many of the procolophonid skulls from Lemoenfontein also show pre-burial damage to their snouts. It is possible that the nasal and premaxillary bones are particularly thin and loosely-sutured and this promoted early disarticulation. However, it is also possible that these curled-up, head-up aestivating procolophonids in their near surface holes promoted the rapid burial of the body yet left the snout exposed to the elements for much longer. Alternatively, like

Dimetrodon trying to remove the *Diplocaulus* amphibians from their aestivation chambers as described by Zoehfeld et al. (2013), it may be speculated that a large predator, such as *Cynognathus,* caused the damage whilst trying to remove the individuals from their chambers (incidentally *Diplocaulus* also has tabular horns very similar to *Teratophon*).

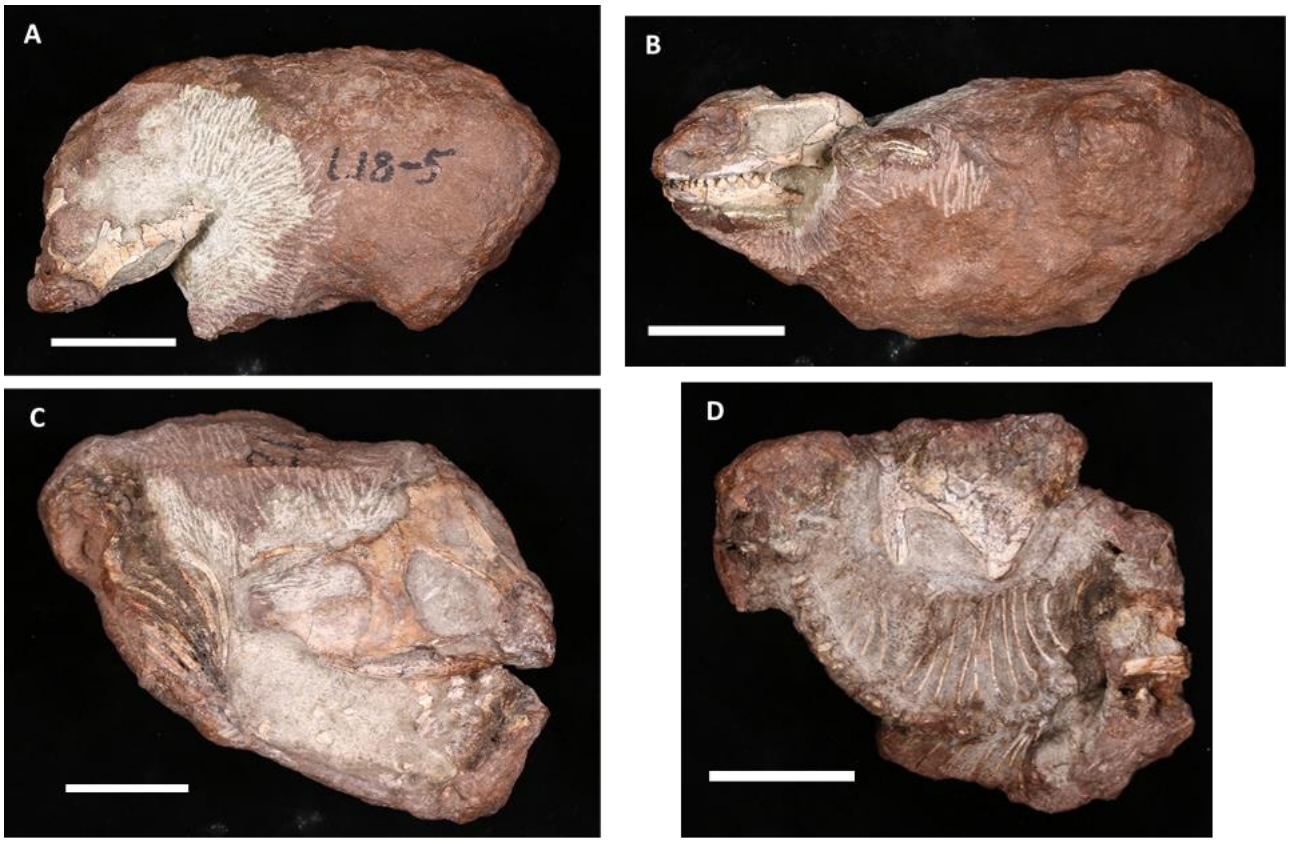


Figure 6.7: (A) Examples of juvenile Teratophon *articulated skeletons tightly curled-up and encased in carbonate nodules. (A) and (B) L18-5 dorsal and lateral views. (C)* Teratophon *(L19-21), note the position of the manus beneath the skull and 3-dimensional preservation of the articulated ribs in life position. (D)* Teratophon *(L19-23B), articulated juvenile skeleton. Scale bars = 3 cm.*

Taphonomic Group 4: Isolated skulls and articulated postcranial elements SAM-PK-10201 (Field numbers 122 A/B, and L19-2 to L19-8)

Twenty-four procolophonid skulls and one *Trirachodon* skull as well as articulated postcranial elements were recovered from the surface float just below, and within 1 m of, Horizon 2 (the structural Bg-horizon) from which they likely originated. These skulls and skeletal elements are thinly coated in the same light olive grey (5Y 6/1) siltstone that makes up the host matrix of the Bg-horizon (Figure 6.8.). Although the skulls have articulated lower jaws and the different postcranial elements are articulated there is no evidence of recent breaks that

could have led to the separation of the fossil skulls from their skeletons. This implies that the skulls became separated from the skeletons and the skeletons were broken-up before final burial. However, since some articulation has been retained, it is most likely that the permineralisation process had begun before these fossils were finally buried in a silt bed that was then pedogenically altered to a Bg-horizon. These fossils are not encased in calcium carbonate like most of the fossils from Bonebed 1, however since their original burial conditions were most likely the same, the surface precipitation of calcium carbonate (peri-mineralisation) must have been interrupted before any significant coating took place. The fossil bone is white as opposed to the usual brown of the coated bone and does not show the fine cracks present on the surfaces of those bones encased in the nodules. The quality of bone preservation is very good.

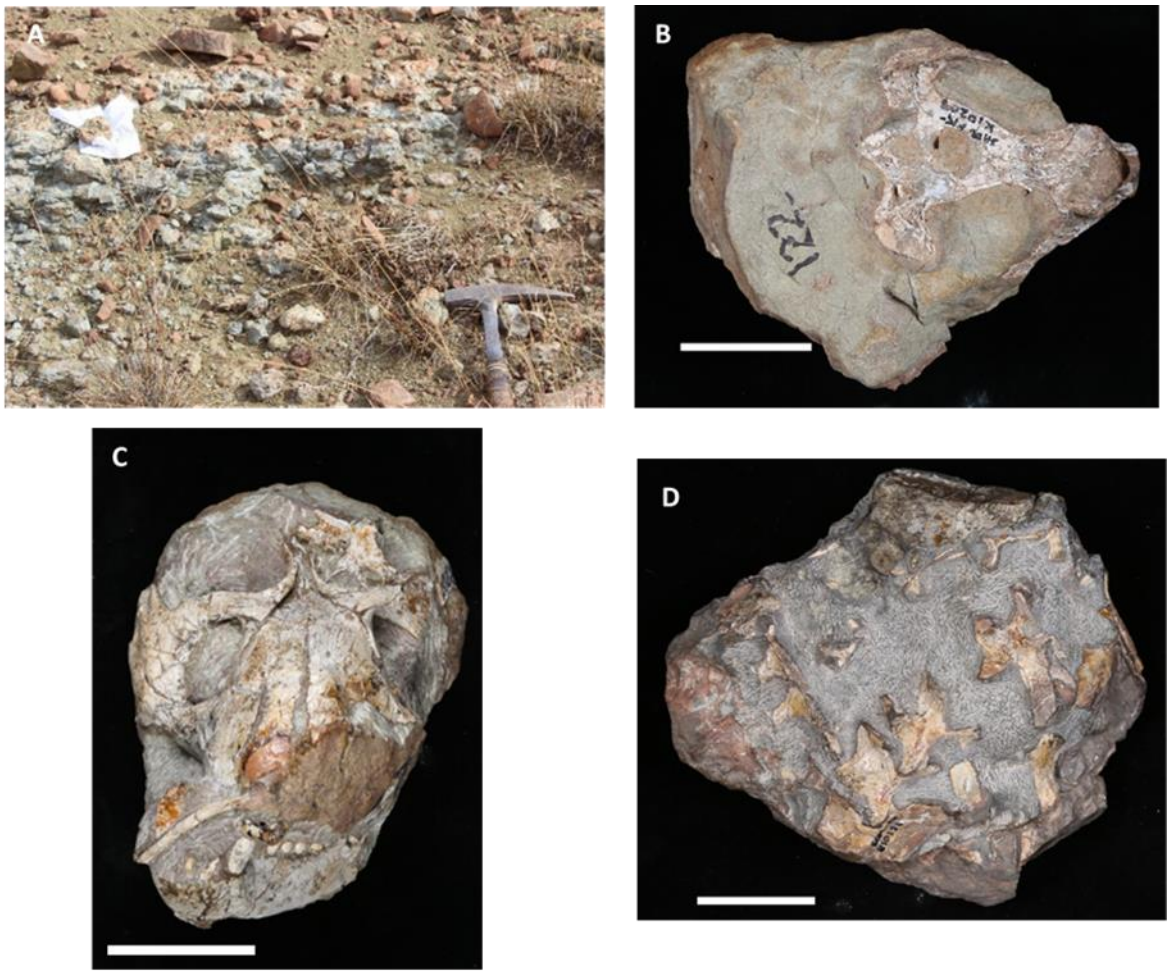


Figure 6.8: (A) Structural Bg-horizon, source of numerous isolated, reworked, and articulated skulls and postcranial elements. (B) Procolophonid skull, SAM-PK-K10208. (C) Trirachodon *skull SAM-PK-K10207, note evidence of reworking in that the snout has been weathered off and "re-sealed" after final burial with an iron-rich crust. (D) semi-articulated postcranial elements. Scale bars = 3 cm.*

The unusual concentration of skulls and skeletal elements in the Bg-horizon needs further investigation. Bown and Kraus (1981) studied an unusual concentration of disarticulated vertebrate fossils in palaeosols in the Willwood Formation of northwest Wyoming. These palaeosols are identified as remnant, clay eluviated, A-horizons. Based on the degree of weathering and disarticulation of the bones, they conclude that the fossils were short-term lag accumulations with attrition being the dominant concentrating mechanism. The Lemoenfontein scenario is different from that of the Willwood Formation palaeosols in that some of the fossil elements are articulated and the bone surface does not show signs of long postmortem exposure to the elements. In the sedimentology section of this study (Chapter 3), it is pointed out that the period of rapid floodplain deposition was followed by a long period of thousands of years with no significant sedimentation. This period of stasis allowed the formation of cm-scale coalescing Stage III carbonate nodules within the BC-horizon and the formation of the strongly developed Bg-horizon. Since the formation of the Stage III calcareous horizon takes an order of magnitude longer than the formation of the peds in the B-horizon, the peds underwent erosion during the period of non-deposition on the soil surface. A plausible mechanism that can explain the Lemoenfontein scenario is that these fossils were initially buried in the A-horizon above the developing B-horizon shortly after mortality, and that they underwent initial permineralisation and attained structural integrity. During the period of depositional stasis and regional degradation of the floodplain, a secondary form of attrition-based accumulation occurred during which the fossils were concentrated in the A-horizon and then progressively lowered to the top of the more resistant Bg-horizon.

Following the criteria set out in Table 6.1, this group of specimens is allocated to Taphonomic Class **B***MR*, i.e., articulated skeletons (**B**) that underwent some peri-mineralisation following burial (*M*), but that became subaerially exposed, relocated, reworked and re-embedded during subsequent down wasting of the floodplain. These bones underwent little transport and had a short postmortem preburial period. Since these fossils underwent reworking (*R*), the additional interpretative qualifiers cannot be assigned with any confidence.

6.6 Taphonomy of tetrapod fossils in Gullies 2 and 3:

Like Gully 1, Gullies 2 and 3 also cut through palaeosol Horizons 1 and 2 and Beds 1 and 2, but unlike the sloping Bonebed 1, the energy of the channelled flood water flow is high. Consequently, any uncoated fossil bone that gets uncovered in the walls and floor quickly gets undercut, entrained and washed away. Similarly, the fossils encased in calcium carbonate nodules also get transported downstream by the flow. One such example is specimen SAM-PK-K10160, *Microgomphodon oligocynus,* (Figure 6.6 B) that was collected from the lower margin of Gully 3. As a result, the Gullies 1/2/3 do not have the same abundance and diversity of tetrapod fossils as Bonebed 1. Gullies 2/3 also delivered some specimens that are thinly coated in the light olive grey (5Y6/1) siltstone that makes up the host matrix of the Bg-horizon. One specimen from Gully 2 merits an individual description.

Trirachodon SAM-PK-K10163 (Field number 98)

This specimen consists of a skull and most likely a complete articulated postcranial skeleton (still need full preparation). It was found lying dorsal-up in fissile dark reddish-brown mudstone on the northern side of Gully 2 in Bed 1. It was lying at approximately a 25° angle to the horizontal, with the skull at the lower end with its snout pointing down and to the right of the main body axis such that it could be described as in a posterio-right-lateral-up attitude. The entire skeleton is encased in calcium carbonate (Figure 6.9). As with all the specimens in the nodules, the bone surface displays many fine cracks. This may have been caused by the displacive precipitation of calcite at the bone/matrix contact. Overall, the preservation quality is very good.

Based on the cylindrical shape of the nodule (i.e., not spread-eagled), the angle at which it was found with the skull at the lower end, as well as the orientation of the skull, it can be concluded that this specimen was in in a confined space. Recognising that trirachodontids have been interpreted as burrowers (Groenewald, 2001), the simplest explanation is that this specimen died in an underground tunnel and may possibly have drowned in the same flood event that buried it in mud.

Following the criteria set out in Table 6.1, this specimen is allocated to Taphonomic Class BKS_b, i.e., complete articulated skeleton with straight spine (*B*), encased in calcium carbonate (*K*), no transportation, preserved at site of death in a confined space (S_b) that may have been a burrow tunnel, and a very short duration of postmortem/preburial period.

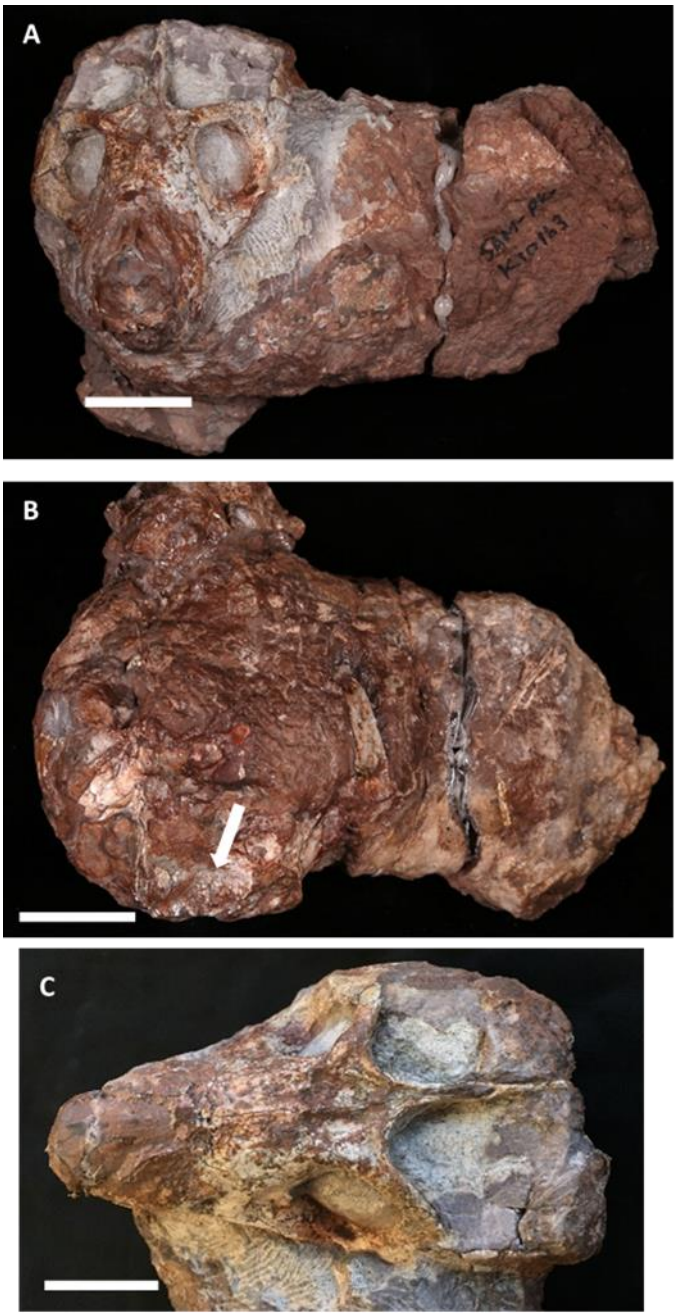


Figure 6.9: Trirachodon *SAM-PK-K10163 (A) Ventral view of the anterior half of the burrow tunnel-shaped nodule containing skull and skeleton showing the orientation of the skull that is downwards and to the right. Note the presence of the maxillary platform that is characteristic of* Trirachodon*. (B) Dorsal view of the cylindrical nodule as found in the field (left squamosal arrowed). (C) Dorsal view of skull. Scale bars = 3 cm.*

6.7 Taphonomic insights

The systematic taphonomic analysis of the Lemoenfontein tetrapod fossils resulted in the recognition of the following taphonomic classes (since it was only possible to prepare representative samples of the large number of specimens, the number counts presented below are indicative in some cases):

- A_2CF_f: complete articulated skeleton curled-up in a horizontal two-dimensional orientation, thinly coated in calcium carbonate (*C*), probably buried while lying on floodplain surface (F_f), no transport and very short postmortem/preburial period, single specimen;
- A_2MS_a: complete articulated skeletons in two-dimensional curled-up attitude, encased in cemented mudstone (*M*), in confined space (S_a) that is interpreted to be a burrow terminal chamber or nest, containing an aggregation of two sub adults, no transportation, preserved at site of death below floodplain surface, and very short duration of postmortem/preburial period, single specimen;
- A_3KS_t: complete curled-up articulated skeleton in 3-dimensional spiral with skull curling in over the body, encased in a calcium carbonate nodule (*K*), no transportation and very short duration of postmortem/preburial period, in a confined space (S_t), probably in aestivation hole, five specimens;
- BKF_f: complete or near complete skeleton with straight or reflexed spinal curvature, encased in a calcium carbonate nodule (*K*), short distance transportation, preserved near site of death on floodplain surface (F_f) and short duration of postmortem/preburial period, five specimens;
- BKS_b: complete articulated skeleton with straight spine, encased in calcium carbonate (*K*), no transportation, preserved at site of death in a confined space (S_b) that may have been a burrow tunnel, and a very short duration of postmortem/preburial period, two specimens;
- BMR: articulated skeletons that underwent permineralisation following burial, coated in cemented mudrock (*M*), but that became subaerially exposed, relocated, reworked (*R*) and re-embedded during subsequent down wasting of the floodplain, 24 specimens;

- C*CF$_f$*: skull with articulating lower jaw and with some postcranial material, surface-coated in calcium carbonate (*C*), short distance transportation, preserved near site of death on floodplain surface (*F$_f$*), and short duration of postmortem/preburial period, less than five specimens;
- C*KF$_f$*: skulls with articulating lower jaws, encased in calcium carbonate nodules (*K*), short distance transportation, preserved near site of death on floodplain surface (*F$_f$*), more than 50 specimens;
- C*UF$_f$*: skull with articulating lower jaw, surface uncoated (*U*), short distance transportation, preserved near site of death on floodplain surface (*F$_f$*), and short duration of postmortem/preburial period, less than five specimens;
- E*CF$_f$*: skull without a lower jaw, surface-coated in calcium carbonate (*C*), short distance transportation, preserved near site of death on floodplain surface (F$_f$), and long duration of postmortem/preburial period, single specimen.
- F*UF$_f$*: uncoated (*U*) partial lower jaw, preserved near site of death on floodplain surface (*F$_f$*), short distance transport and long duration of postmortem/preburial period, less than five specimens; and

Most of the tetrapod fossils are encased in calcium carbonate nodules. The articulated nature of the skeletons, as well as skulls with articulating lower jaws, indicate that these fossils underwent little or no postmortem transport and that they were buried at the time of death or very shortly thereafter. This is consistent with the insight from the sedimentological investigation that the climate was seasonal and that periodic flood events occurred that deposited thick beds of mud aggregates. As a result, the carcasses still retained most of their soft tissue at the time of burial. Bacterial decay of the soft tissue and ligaments led to the formation of hydrogen sulphide in haloes around the decaying carcasses. These haloes rapidly resulted in precipitation of calcium carbonate leading to the permineralisation of the bone as well as perimineralisation of the bone surface and surrounding mudrock. This rapid permineralisation provided the structural strength to the skeletons that was able to resist deformation due to compaction. Due to this, many specimens were preserved with their rib cages in the life position (3-dimensional shape).

A further consequence of the calcium carbonate encasement of the skeletons and skulls is that these hard nodules are very resistant to post-exhumation weathering. There is a preferential preservation bias for fossils encased or coated in calcium carbonate. Most of these nodules were found floating on the surface in Bonebed 1. Since gullies 1, 2 and 3 cut through the same mudrock beds as Bonebed 1, there should be no reason why these gullies do not contain the same density of fossil bearing nodules as Bonebed 1. However, since Bonebed 1 is gently dipping and has not been gullied, the nodules that erode out of these beds do not get significantly transported by present day run-off. Instead, they largely remain in their relative horizontal positions and the secondary concentration mechanism results as the surface is eroded. The presence of a small dolerite dyke along the eastern margin of Bonebed 1 prevented gully formation through erosion and contributed to conditions conducive for the formation of a secondary modern lag concentration. It also resulted in some degree of baking of the specimens within the 10 m metamorphic aureole where the bone has a porcelain-like quality which further enhanced the resistance to weathering once exposed. On the other hand, the high energy flow in the gullies results in the smooth, sub-spherical, boulder sized nodules washing downstream and into the main channel of the spruit.

In summary, the precipitation of calcium carbonate is an important factor in the taphonomic pathway following the burial of the carcass up to the present-day occurrence on the modern landscape:

- it leads to a rapid peri-mineralisation of the bone, and in this way improve the likelihood of fossilisation;
- it provides early diagenetic structural strength to the bones so that they can resist compaction, leading to the preservation of the elements in- the- round and in life position;
- it provides resistance to weathering and improves survival of the specimens on the present-day landscape, which in turn results in a secondary lag concentration mechanism; and

- it likely also results in an anthropogenic collecting bias through prospectors developing a preferential search image for boulder-sized brown weathering nodules that could potentially contain complete skeletons.

Very few uncoated fossil remains were found. These are limited to embedded lower jaw fragments and they show signs of a long duration of postmortem/preburial period. The fact that they have no calcium carbonate coating suggests that complete bacterial decomposition of the soft tissues took place before they were buried. They are generally very fragile and would quickly disintegrate following their exhumation. This susceptibility to weathering likely explains why there is a general lack of uncoated bone fragments in the collections from this locality.

For comparison, the detailed taphonomic classes recognised for the Lemoenfontein fossils can be grouped into the broader classes of Smith (1993).

- A: Preserved at site of death, complete articulated skeleton, seven specimens.
- B: Preserved at site of death, complete or near complete skeleton with straight or reflexed spinal curvature, 31 specimens.
- C: Preserved near site of death, skull with articulating lower jaw and (or) cervical vertebrae, approximately 60 specimens.
- D: Preserved near site of death, skull with displaced lower jaw, absent.
- E: Preserved near site of death, skull without lower jaw, single specimen.
- F: Preserved near site of death, lower jaw, less than five specimens.
- G: Preserved far from site of death, accumulation of variety of small postcranial elements into “bone bed”, absent.
- H: isolated and/or fragmented ribs, limb bones and vertebrae, absent.

This comparison with Smith’s (1993) broader grouping recognises five of his taphonomic classes at Lemoenfontein. Class C contains the most specimens, followed by Class B. This consistency suggests that a methodology for defining taphonomic classes for the tetrapod fossils in the Karoo Basin, that relies on more than one indicator in a hierarchical structure,

would be beneficial. The first order indicator would capture the generic disarticulation class (e.g., Smith (1993)), with additional indicators capturing the unique features of the taphonomy of each site, thus ensuring that all the specific taphonomic pathways are recorded.

The results of the taphonomic investigation provides insights into the behaviour of the animals on the ancient floodplain. The presence of several complete, fully-articulated juvenile and adult skeletons in attitudes that suggest that they were buried in confined spaces, leads to an interpretation that the animals were buried within holes or underground tunnels that they themselves excavated. This interpretation is strengthened by the presence of two sub-adult *Teratophon* in the same large nodule that has the architectural morphology of a burrow terminal chamber (or nesting hole), as well as the co-occurrence of the tetrapod burrow casts of *Reniformichnus* in the same beds that host the vertebrate fossils. Because of the seasonal nature of the palaeoclimate, the animals burrowed underground, or scratched-out near surface holes in search of shade and moisture, most likely for thermoregulation. Since the curled-up skeletons are in their "life positions" they either died while in a state of aestivation or cold torpor and were buried shortly after death, or they were killed and buried in the same event. If the animals drowned on the floodplain surface whilst alive or in an active state, they would not have retained the curled-up attitude. Even if they were in a burrow, they would have attempted to escape leading to a different physical orientation. The specimen with the multiple skeletons also shows that procolophonids practiced shelter-sharing. One explanation for the presence of many isolated small skulls with articulated lower jaws is that the animals fell victim to predation or scavenging by small carnivores. The possible presence of the extremely rare probaignognathian cynodont, *Lumkuia*, at this locality is consistent with this. The co-occurrence of procolophonids, therocephalians, cynodonts and rhynchosaurs in the same locality suggests that a diverse fauna with possibly the same feeding habit colonised the floodplain at this site. This is explored further in Chapter 7.

The taphonomic study also provides insights into the palaeoenvironment that existed at the time that the fossils were buried. The articulated nature of many of the skeletons indicate that they were buried at or near their site of death and that this occurred at or shortly after death. This can be explained if there were periodic floods that quickly deposited thick layers of mud aggregates resulting in obrution. The evidence pointing to the burrowing behaviour of the animals suggests that significant temperature and rainfall variation occurred between the seasons, and that these animals used this mechanism for thermoregulation. Both juvenile and adult procolophonids occur at this locality, suggesting that the environment was not stressed, for example, the animals did not accumulate around an ever-shrinking water hole in a drought. Under such conditions, the smaller skeletons would be trampled, and they would undergo disarticulation and breakage.

An order of magnitude estimation can be made of the density of fossils preserved in the mudrock beds that made up Bonebed 1 before present day down wasting. Considering the collection of approximately 100 fossils in a volume of 2 040 m^3 (1.7 m thick, 20 m width and 60 m long), a minimum density of 1 fossil per 20 m^3 (0.05 fossils per m^3) is obtained. This translated to a concentration on the surface after down wasting of about 8 fossils every 100 m^2 (10 m by 10 m patch). This is clearly significantly higher than the surface density of fossils occurrences that is typical of Subzone *T-K* of the *Cynognathus* AZ. This leads to the conclusion that this area of the floodplain must have been colonised for an extended period by a concentration of small tetrapods. Due to the location of this palaeosurface near a pond margin (consequently with a shallow water table), its periodic flooding and deposition of thick beds of mud aggregates, the burrowing behaviour of the animals, as well as conditions that allowed the precipitation of calcium carbonate around the carcasses leading to higher probabilities of fossilisation, the record of their existence is well preserved.

A final taphonomic insight is offered by the absence of the typical preservation style of bones in *Cynognathus* AZ, *T-K* Subzone. The common, almost ubiquitous, presence at many *Cynognathus* AZ sites of articulated skeletons or isolated long bones, vertebrae, ribs, skull elements or tusks of the large dicynodont *Kannemeyeria* are significantly absent at this locality. Also, no large predator (i.e., *Erythrosuchus or Cynognathus*) remains were preserved

at this locality. At other *Cynognathus* AZ sites these bones are typically uncoated or coated only in a thin layer of calcium carbonate. One possible explanation is that the larger animals either were not present in this environment, or that they were able to escape the flooding events that led to the burial of the smaller animals (for example see Rogers et al., 2001). Based on Behrensmeyer et al. (1979), the following interpretation was proposed in the introduction to this taphonomic discussion:

"If large bones were present in a bone assembly, they would have had a better chance of preservation than smaller bones. Therefore, their absence in a fossil assembly that consists mainly of small bones, points to the fact that the large bones were probably not present in the first place."

Following the taphonomic assessment of the Lemoenfontein site it is concluded that the evidence supports a similar interpretation.

7. VERTEBRATE PALAEONTOLOGY OF LEMOENFONTEIN

7.1 Overview of the *Cynognathus* AZ biostratigraphy

The rocks of the Beaufort Group preserve a largely continuous sedimentary record covering the period from the Middle Permian to the Middle Triassic (Hancox and Rubidge 2001, Rubidge 2005). The abundant tetrapod fossil record has allowed an eight-fold biostratigraphic subdivision (Rubidge, 1995) that has recently been revised and updated to seven assemblage zones with nine subzones (Smith et al., 2020). It also provides extensive data for the study of terrestrial vertebrate evolution and records the changes that occurred in the terrestrial fauna below and above PTB extinction event at 252 Ma (Smith, 1995; Bowring et al., 1998; Smith and Botha, 2005; Botha and Smith, 2006; Smith et al., 2011; Shen et al., 2011; Smith and Botha-Brink, 2014). The richness of the vertebrate and ichnofossil record, as well as its excellent preservation, has contributed to an understanding of the palaeoenvironment, as well as the behaviour of the fauna that occupied it (Smith, 1995; Groenewald, 1991; Groenewald et al., 2001; Damiani et al., 2003; Abdala et al., 2006; Abdala and Ribeiro, 2010).

The Triassic strata of the Beaufort Group consist of the Early Triassic *Lystrosaurus declivis* AZ (*L. declivis* AZ) and the Early to Middle-Triassic *Cynognathus* AZ, and correspond litho-stratigraphically to the uppermost Palingkloof Member (lower *L. declivis* AZ) of the Balfour Formation, the overlying Katberg Formation (middle to upper *L. declivis* AZ) and Burgersdorp Formation (*Cynognathus* AZ) (Rubidge et al., 1995; Hancox et al., 2020; Smith et al., 2020).

The *Cynognathus* AZ has been subdivided into three subzones based on differences in spatial and temporal distribution of faunal types. Until recently, these subzones were informally identified as subzones A, B and C – with subzone C being the stratigraphically uppermost and temporally youngest (Hancox et al., 1995; Shishkin et al., 1995; Hancox and Rubidge, 2001; Neveling, 2002; Damiani and Hancox, 2003; Neveling, 2004; Abdala et al., 2005; Catuneanu et al., 2005; Neveling et al., 2005).

Extensive field-based research and taxonomic revisions of the *Cynognathus* AZ fauna over the last 20 years allowed Hancox et al. (2020) to formalise these subzones as follows:

- *Langbergia-Garjainia (L-G)* Subzone (former subzone A);
- *Trirachodon-Kannemeyeria (T-K)* Subzone (former subzone B); and
- *Cricodon-Ufudocyclops (C-U)* Subzone (former subzone C).

A concise summary of the ages, faunas and the index taxa of each subzone has been extracted from Hancox et al. (2020) and Smith et al. (2012). Several recent updates to the list provided in Smith et al. (2012) are noted in the paragraphs following this summary. The lowermost Subzone *L-G* of the *Cynognathus* AZ is Lower Triassic (Olenekian) in age, whereas the middle and upper parts of the biozone are considered to be of Middle Triassic (Anisian) age (Shishkin, Rubidge, and Hancox 1995; Hancox 1998, 2000; Hancox et al. 2020).

Lower *Cynognathus* AZ (*Langbergia-Garjainia* Subzone) (Olenekian)

The L-G Subzone is characterised by the co-occurrence of *Langbergia* and *Garjainia.* Its tetrapod fauna includes:

- the amphibians *Bathignathus, Kestrosaurus, Parotosuchus* and *Trematosuchus;*
- the archosauromorph *Garjainia;*
- the cynodont *Cynognathus,* the trirachodontid cynodont *Langbergia*;
- the therocephalian *Microgomphodon*;
- the indeterminate *Palacrodon;* and
- an indeterminate parareptile.

Middle *Cynognathus* AZ (*Trirachodon-Kannemeyeria* Subzone) (Early Anisian)

Until recently, the informal subzone B of the *Cynognathus* AZ was characterised by the combined presence of *Xenotosuchus africanus, Kannemeyeria simocephalus,* and *Erythrosuchus africanus* (Hancox et al., 1995; Shishkin et al., 1995). Following the recent formalisation of the *Cynognathus* AZ subzones (Hancox et al., 2020) the *T-K* Subzone is now characterised by the combined presence of *Trirachodon* and *Kannemeyeria*.

Its tetrapod fauna includes:

- the amphibians *Batrachosuchus, Jammerbergia, Laidleria, Microposaurus, Vanastega, Xenotosuchus*;
- the archosauromorphs *Erythrosuchus, Euparkeria, Howesia, Mesosuchus,* and *Eohyosaurus;*
- the cynodonts *Cynognathus, Lumkuia, Bolotridon, Diademodon, Trirachodon,* and *Cricodon;*
- the anomodonts *Kannemeyeria* and *Kombuisia;*
- the therocephalians *Bauria, Microgomphodon;*
- the parareptiles *Teratophon, Thelephon, Thelerpeton, Theledectes, and Myocephalus;* and
- the indeterminate *Palacrodon.*

Uppermost *Cynognathus* AZ (*Cricodon-Ufudocyclops Subzone*) (Late Anisian)

Historically this subzone (Hancox 1998; Hancox and Rubidge 1994, 1996, 1997) was based on the presence of the dicynodonts *Angonisaurus* and *Shanisiodon* and the possible presence of *Dolichuranus* (Hancox 1998), the cynodont *Cricodon* (Abdala, Hancox, and Neveling 2005) and the amphibian *Paracyclotosaurus* (Hancox et al., 2000). The newly formalised *C-U* Subzone is characterised by the dominance of cynodonts, notably *Cricodon,* and its co-occurrence with the dicynodont *Ufudocyclops* (Hancox et al., 2020). Its tetrapod fauna includes:

- the large amphibian *Paracyclolotosaurus;*
- the cynodonts *Cynognathus, Diademodon, Cricodon* and the newly described *Impidens (hancoxi),* Tolchard et al. (2021); and
- the anomodonts *Shanisiodon* and *Ufudocyclops.*

The therocephalians *Sesamodon* from the *L-G* Subzone (Smith et al., 2012) and *Herpetogale* from the upper Omingonde Formation in Namibia have been synonymised with *Microgomphodon* (Abdala et al., 2014). Abdala et al. (2014) also extend the biostratigraphic range of *Microgomphodon* in the main Karoo Basin from the *L-G* Subzone into the *T-K* Subzone based on a unique specimen from the Lemoenfontein locality that is under

consideration in this study. One of the hypotheses of this project is that the sedimentary strata hosting the Lemoenfontein bonebed are at the transition between the *L-G* Subzone and *T-K* Subzone. The authors (Abdala et al., 2014) also point out that either *Microgomphodon* has not yet been found in the *C-U* Subzone, or that this subzone is younger than the upper Omingonde Formation. Furthermore, *Bauria* only occurs in the *T-K Subzone* (Abdala et al., 2014; Hancox et al., 2020).

The fossil fauna at Lemoenfontein is dominated by procolophonids. At least two genera are present and the holotype of *Teratophon* originates from this locality. Therefore, it is important to note that Modesto and Damiani (2003) declared the parareptile *Thelegnathus browni* a *nomen dubium* and re-assigned the four previously identified *Thelegnathus* species from the *T-K* Subzone to new genera as follows: *Thelerpeton oppressus, Theledectes perforates, Thelephon contritus* and *Teratophon spinigenis*.

A new genus of basal rhynchosaur, *Eohyosaurus wolvaardti,* from the *Cynognathus* AZ *T-K* Subzone of South Africa has been described by Butler et al. (2015). The holotype specimen (SAM-PK-K10159) and a second potential paratype specimen (SAM-PK10180) were discovered by the author at the Lemoenfontein locality in 2000 and 2003, respectively.

Two dicynodont skulls from the *Cynognathus* AZ *C-U* Subzone, that were previously assigned to the Tanzanian taxon *Angonisaurus*, have recently been referred to a newly described kannemeyeriiform dicynodont, *Ufudocyclops mukanelai* (Kammerer et al., 2019). This referral removes the presence of *Angonisaurus* from the *C-U* Subzone, along with its correlative significance with respect to the Manda Beds of Tanzania.

The *L-G* Subzone in the lower Burgersdorp Formation is the only biozone of the entire Beaufort Group that does not contain any dicynodonts (J. Hancox, pers. comm., November 10, 2018) and is dominated by aquatic or semi-aquatic taxa (Hancox et al., 2010).

7.2 Systematics of the Lemoenfontein fauna

1. *Eohyosaurus wolvaardti* (Butler et al. 2015)

Material: This taxon is represented at the Lemoenfontein locality by two skulls, SAM-PK-K10159 (Holotype) and SAM-PK10180 (Figure 7.1).

Remarks: Two rhynchosaur species that have previously been found in the *Trirachodon-Kannemeyeria* Subzone are *Mesosuchus browni* and *Howesia browni*. The new *Eohyosaurus wolvaardti* holotype from Lemoenfontein increases the number of rhynchosaur species in this subzone to three. In the absence of direct evidence, the presence of multiple tooth rows on the lingual as well as occlusal surfaces of the transversely expanded maxilla and dentary, it is likely that *Eohyosaurus* was predominantly herbivorous, like the other two *T-C* Subzone rhynchosaurs (R. Butler, pers. comm., November 24, 2020).



Figure 7.1: (A) Right lateral and (B) left lateral views of the rhynchosaur, Eohyosaurus wolvaardti*, SAM-PK-K10159, (holotype, from Butler et al., 2015). Right lateral (C), dorsal (D) and left lateral (E) photos of prepared skull of SAM-PK10180,* Eohyosaurus wolvaardti*. Note articulated right manus lying across the temporal fenestra on the right side. Scale bars = 2 cm.*

2. Trirachodon berryi (Seeley, 1895)

Material: This taxon is represented in the Lemoenfontein fauna by thirteen skulls (SAM-PK-K010157, SAM-PK-K010158, SAM-PK-K010161, SAM-PK-K010163, SAM-PK-K010164, SAM-PK-K010165, SAM-PK-K010166, SAM-PK-K010176, SAM-PK-K010207, SAM-PK-K010411, SAM-PK-K010762, L19-17, L20-12), one of which is attached to an articulated skeleton (SAM-PK-K010163), (Figure 7.2).

Remarks: *Trirachodon* and *Langbergia* are important biostratigraphic index fossils as their occurrence characterise the existence of the *T-K* and *L-G* subzones, respectively. To place the Lemoenfontein locality at the base of the *T-K* subzone it is important that the gomphodont cynodonts from this locality be identified with confidence as *Trirachodon.* According to Abdala et al. (2006), the following characteristics are key in distinguishing *Trirachodon* from *Langbergia*.

- The *Trirachodon* postcanine gomphodont teeth are expanded perpendicular to the long axis of the maxilla and are oval in cross-section. The gomphodont postcanines of the dentary are similar in morphology to those in the maxilla. Like *Langbergia*, the long axis of the lower gomphodont postcanines are oblique to the long axis of the mandible. The *Langbergia* postcanine gomphodont teeth are circular to ovoid (subcircular), with the long axis orientated labiolingually.
- The maxilla in *Trirachodon* curves sharply inward to form a platform lateral to the postcanine teeth. The maxilla in *Langbergia* "curves gently at its ventral margin, reaching the row of postcanines. In contrast, the maxilla in *Trirachodon* curves sharply inward to form a platform lateral to the postcanine teeth" (Abdala et al., 2006).

Due to the articulated lower jaws of the Lemoenfontein gomphodont cynodont skulls, the occlusion surfaces of the postcanine teeth are not visible. The main feature that identifies these specimens as belonging to the genus *Trirachodon* is the presence of a prominent maxillary platform. It is not easy to record the presence of the maxillary platform in lateral view photographs of these specimens, however, in ventral view the existence of the platform can be seen distinctly (see Figure 7.3). One specimen, L19-17, could not be prepared fully on its left lateral side (the right side being damaged) and this introduced the possibility of it belonging to the genus *Langbergia*. However, close visual inspection revealed the presence of a platform as can be seen in the ventral view in Figure 7.3.

According to Hendrickx et al. (2019), the labiolingual expansion of the upper and lower postcanine teeth in gomphodont cynodonts, resulted in crown-to-crown occlusion of these teeth. This specialisation suggests that gomphodonts (including *Langbergia* and *Trirachodon*) were "omnivorous or possibly exclusively herbivorous animals, feeding on hard plant material". *Langbergia* and *Trirachodon* have also been identified as being omnivorous by Smith et al. (2012).

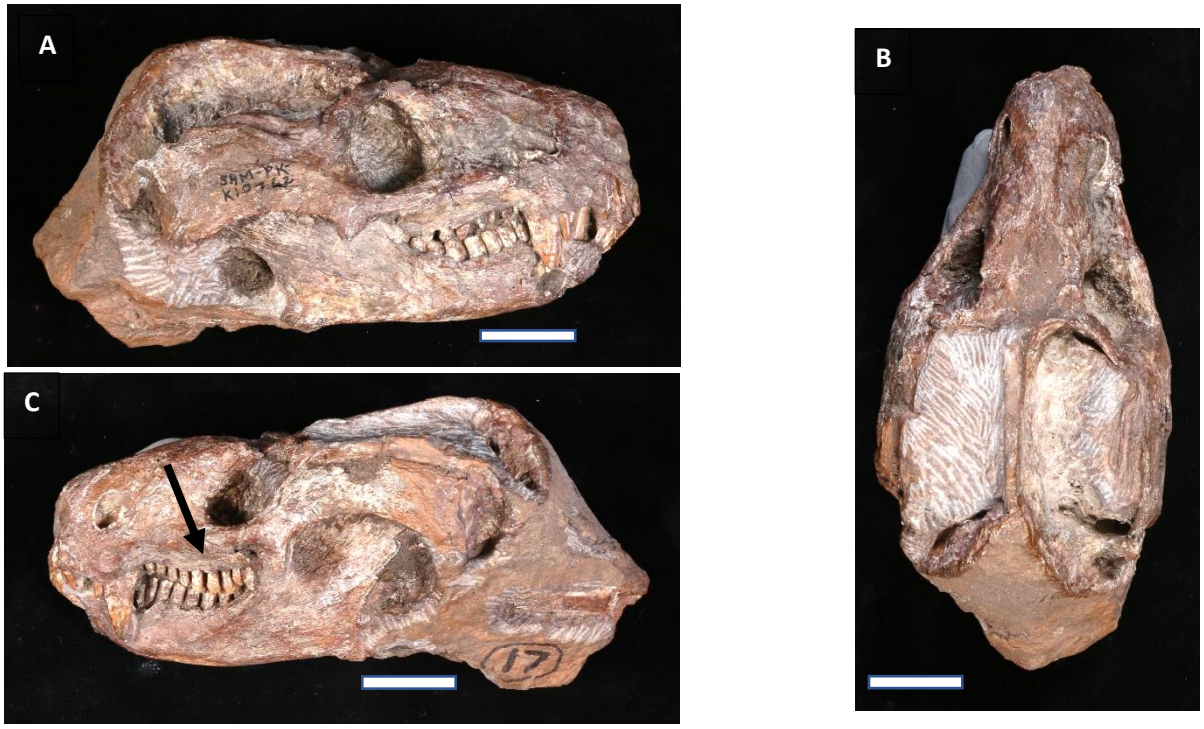


Figure 7.2: (A) Right lateral, (B) dorsal and (C) left lateral photos of prepared skull of SAM-PK-K10762, Trirachodon berryi *from the Lemoenfontein locality. Note prominent maxillary platform (arrowed). Scale bar = 2 cm.*

Two species of *Trirachodon* have been recognized: *Trirachodont berryi* and *Trirachodon kannemeyeri* (Seeley, 1895; Sidor and Hopson, 2018; Hendrickx et al., 2019). Sidor and Hopson (2018) considered *Trirachodon kannemeyeri* to be a sister taxon of *Cricodon metabolus* and transferred the species *kannemeyeri* to the genus *Cricodon (Cricodon kannemeyeri*). The distinction is based on the following apomorphic dental characters:

- symmetry and degree of labiolingual expansion of the upper gomphodont postcanine teeth;
- presence, absence, shape, and size of cingular cuspules; and

- the presence or absence of one or two, three-cusped, sectorial teeth at the rear of the upper postcanine tooth row.

Hendrickx et al. (2019) point out that the presence or absence of the sectorial teeth in *Trirachodon berryi* is the most important differentiating character. In the *Trirachodon* specimens from Lemoenfontein, the sectorial teeth are absent in one of the larger skulls (specimen SAM-PK-K10762, skull length = 10 cm, Figure 7.2 A and C) but they are present in the smaller skull (specimen L20-12, skull length = 7 cm, Figure 7.3 D). Also, the larger skull has more upper postcanine gomphodont teeth (nine gomphodont, Figure 7.2 C) than the smaller skull (five gomphodont, two sectorial, Figure 7.3 D). Hendrickx et al. (2019) propose that these differences are due to ontogenetic variations, with *Trirachodon kannemeyeri* being a younger ontogenetic version of *Trirachodon berryi.* In adult *Trirachodon berryi* the last sectorial teeth are replaced by two to three gomphodont teeth, accounting for the additional number of upper postcanines. The coexistence of both "species" at Lemoenfontein, with the smaller skulls like *Trirachodon kannemeyeri* and the larger skulls like *Trirachodon berryi* is consistent with the proposal that these differences are due different degrees of ontogenetic development. However, some of the smaller *Trirachodon* skulls (e.g., SAM-PK-K10176, skull length = 7 cm and SAM-PK-K10157, skull length = 8.5 cm) do not show any obvious sectorial teeth. The Lemoenfontein trirachodontid material, consisting of 13 specimens identified so far, with skull sizes ranging from small to large will allow an ontogenetic study of this taxon. This detailed investigation is beyond the scope of the current study. In the absence of the results of such a study, specimen L20-12 (Figure 7.3 D) is assigned to the formally recognized *Cricodon kannemeyeri* (Hancox et al., 2020). This adds a seventh taxon to the Lemoenfontein fauna.



Figure 7.3: (A) Ventral view of Langbergia modisei*, holotype specimen NMQR 3255 (from Abdala et al., 2006). Note the absence of a prominent maxillary platform (arrowed). (B) Ventral view of partially prepared skull of L19-17,* Trirachodon *and (C) ventral view of prepared skull of SAM-PK10762,* Trirachodon berryi *from the Lemoenfontein locality. Note prominent maxillary platforms in B and C (arrowed). (D) Lateral view of L20-12,* Cricodon*, showing sectorial postcanines (arrowed). Scale bar = 2 cm.*

3. *Lumkuia cf. fuzzi* (Hopson and Kitching, 2001)

Material: This taxon is represented by a single skull (L19-19, Figure 7.4).

Remarks: To date the Family Lumkuiidae has been represented by a single specimen (holotype, BP/1/2669) consisting of a skull and postcranial material that was found near the Lumku Mission close to the town of Lady Frere in the Eastern Cape Province of South Africa. The *Cynognathus* AZ in the vicinity of Lady Frere consists of the *T-K* Subzone (Hopson and Kitching, 2001, Hancox et al., 2020). *Lumkuia fuzzi* is the earliest and most primitive probainognathian cynodont. The find of an additional specimen from Lemoenfontein is the first new discovery in many decades of a probainognathian cynodont in the main Karoo Basin, and it is therefore an important contribution. It is the only carnivore from the locality (note the sectorial postcanines in Figure 7.4).

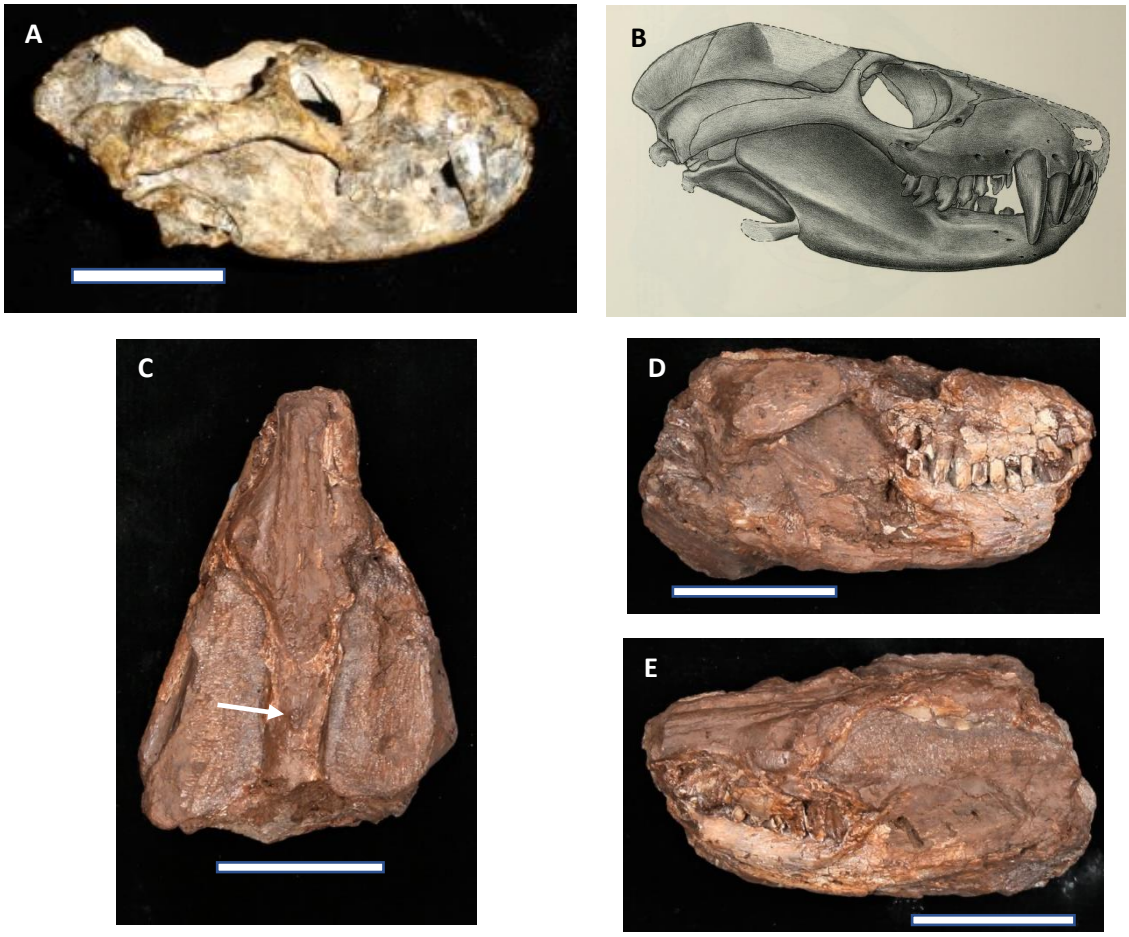


Figure 7.4: (A) and (B) Right lateral views of the prepared skull of the holotype of Lumkuia fuzzi, *Specimen BP/1/2669 (Picture in A by C. Kammerer (2018), drawing in B from Hopson and Kitching, 2001). (C) Dorsal view showing possible parietal foramen endocast (arrowed), (D) right lateral view and (E) left lateral view of the new prepared skull of* Lumkuia, *Specimen L19-19. Scale bar = 2 cm.*

Postscript: L19-19 characters indicating *Lumkuia*: overall skull length (5.4 cm), size and number of sectorial postcanines (seven), shape of the snout, maxilla posterior to the post-canine series, the dentary. The skull roof and possible sagittal crest have been weathered away, exposing a possible endocast of the parietal foramen (arrowed in Figure 7.4 C). Most postcanines have lost the large central cusps (that curl posteriorly in *Lumkuia*), giving the appearance of straighter post-canines like those of *Cistecynodon* (Brink and Kitching, 1953). A parietal foramen is absent in the holotype of *Lumkuia*. In a study of *Massestognathus* Abdala and Giannini (2000) identified, for the first time, the ontogenetic reduction and eventual loss of the parietal foramen in a cynodont. Possibly specimen L19-19 displays the same ontogenetic phenomenon. However, the possibility that L19-19 is a new *Lumkuia* species cannot be ruled out. A definitive identification will require additional preparation exposing the palate and/or micro-CT scanning so at this time the most parsimonious identification of L19-19 is *Lumkuia*.

4. Microgomphodon oligocynus (Seeley, 1895)

Material: This taxon is represented in the Lemoenfontein fauna by four specimens: three isolated skulls (SAM-PK-K10160, L20-3, SAM-PK-K010762) and a skull with a fully- articulated skeleton (SAM-PK-K11601) (Figure 7.5).

Remarks: Specimen, SAM-PK-K10160, consists of a skull with lower jaw in occlusion, four cervical vertebrae, and a manus. SAM-PK-K10160 is exceptionally well preserved, with most sutures of the skull observable. Based on the completeness and excellent preservation of SAM-PK-K10160, the therocephalians *Sesamodon, Herpetogale, Watsoniella* and *Melinodon*, have been synonymised with *Microgomphodon* (Abdala et al., 2014). It also extends the biostratigraphic range of *Microgomphodon* in the main Karoo Basin from the *L-G* Subzone to the *T-K* Subzone. Although this specimen was not defined as a paratype, it is the best preserved bauriid specimen to date (Abdala et al., 2014) and it will be the future reference specimen for *Microgomphodon.*

Specimen L18-6 is equally well preserved and represents the first skull attached to a fully articulated skeleton of *Microgomphodon.* As discussed in the section on taphonomy, it also shows pre-burial carnivore induced damage to the left side of the snout.

The *Microgomphodon* postcanines are oval in cross-section. The upper postcanines occlude with those of the lower jaw and they have cusps that interlock. Based on the occluding nature of the postcanine teeth *Microgomphodon* is considered to have been herbivorous (Smith et al., 2012).



Figure 7.5: (A) Microgomphodon oligocynus *(SAM-PK-K10160), dorsal, left lateral and ventral views of the skull with articulating cervical vertebrae and manus that was encased in carbonate nodule (articulated manus removed from nodule during preparation), Image from (Abdala et al., 2014). (A)* Microgomphodon *(SAM-PK-K11601), skeleton encased in carbonate nodule that takes the shape of the carcass. This exceptional specimen is the first* Microgomphodon *specimen with a fully articulated skeleton attached to the skull. (C) Dorsal view of its skull. (D) Right lateral view of its skull. Scale in A bar = 1 cm, Scale bars in B, C and D = 3 cm.*

5. Teratophon spinigenis (Modesto and Damiani, 2003)

Material: The first *Teratophon* specimen, holotype BP/1/4299, was discovered at Lemoenfontein by James Kitching in 1973. This specimen consists of a cranium without teeth and mandible. In 2003 Roger Smith found a second specimen (PK-K010174, Figure 7.6 A) consisting of a skull and articulated skeleton. As part of this study a third significant specimen, SAM-PK-K011599 (L18-2), was found in 2018 by the author (Figure 7.6 B). This specimen consists of a large nodule containing a sub-adult skull and curled-up articulated skeleton along with a second sub adult skull and skeleton that curls in underneath the first. The teeth in the first skull are well preserved and clearly visible. During field trips in 2019 and 2020 numerous additional *Teratophon* specimens were discovered covering an ontogenetic range from small juvenile skulls with curled-up skeletons to isolated large adult skulls (see Appendix B for a full list). One more fully articulated adult specimen was also found in 2020 (L20-10, still to be prepared).

Remarks: Modesto and Damiani (2003) re-assigned the previous four *Thelegnathus* species from the *T-K Subzone to* four new genera as follows: *Thelerpeton oppressus, Theledectes perforates, Thelephon contritus* and *Teratophon spinigenis*. The distinguishing characteristic of *Teratophon* is the presence of large quadratojugal processes that extend posterolaterally (Modesto and Damiani, 2003). These processes are like those of *Procolophon trigoniceps* (but significantly larger) and as such Modesto et al. (2002) consider a close relationship between these two genera.

In the *Teratophon* specimens from Lemoenfontein the length of the quadratojugal processes increase significantly with increasing skull size (Figure 7.7). This allows an interpretation that these specimens represent an ontogenetic range of *Teratophon* from small juveniles (Figure 7.7 A), sub-adults (Figure 7.7 B) to large adults (Figure 7.7 C)

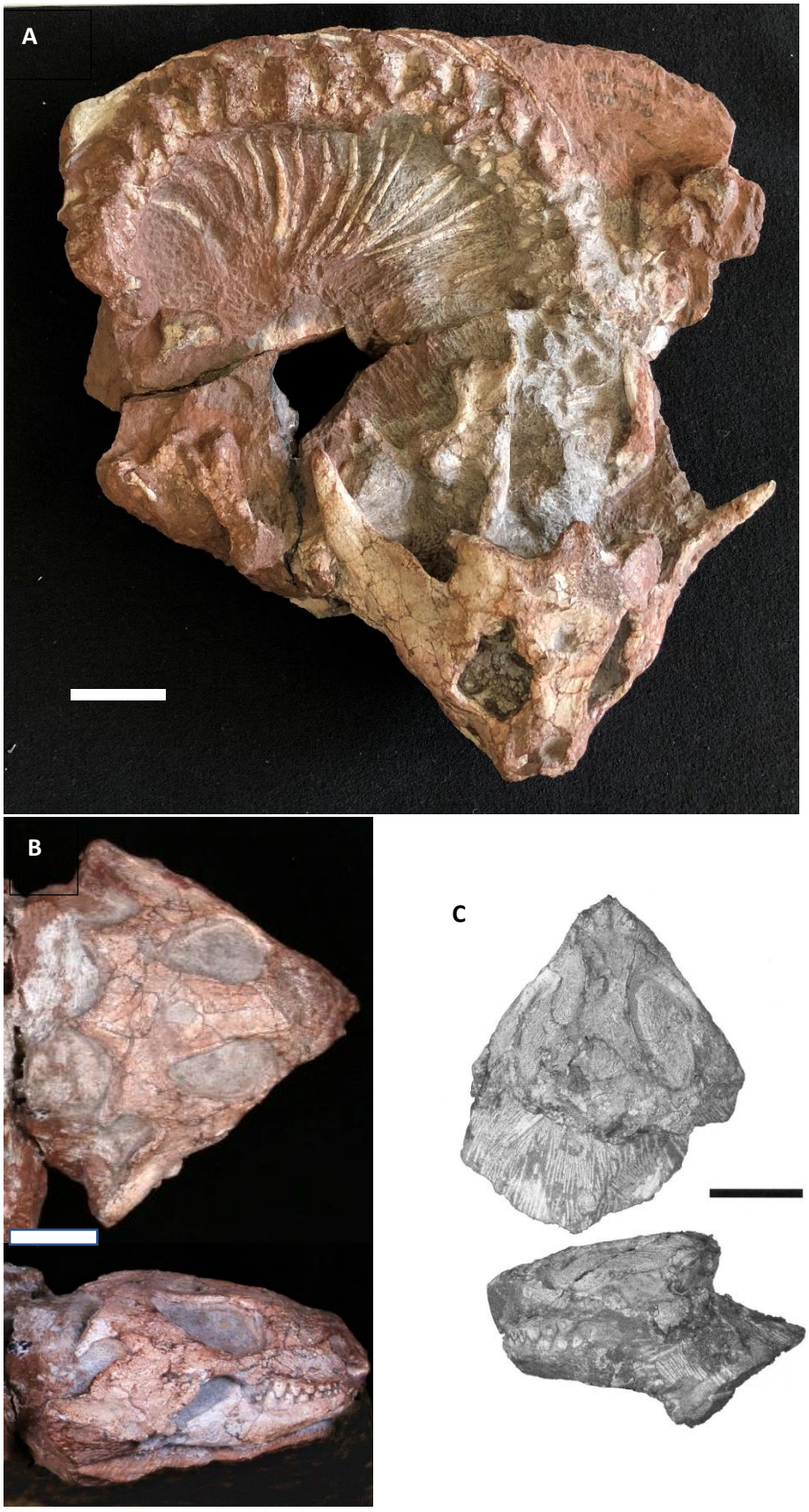


Figure 7.6: (A) Teratophon spinigenis *(SAM-PK-K010174). (B) Dorsal and right lateral view of* Teratophon spinigenus *(skull of L18-2). (C) Dorsal and left lateral views of the holotype of* Thelerpeton oppressus *(BP/1/4538, from Modesto and Damiani (2003)). Scale bar = 2 cm.*

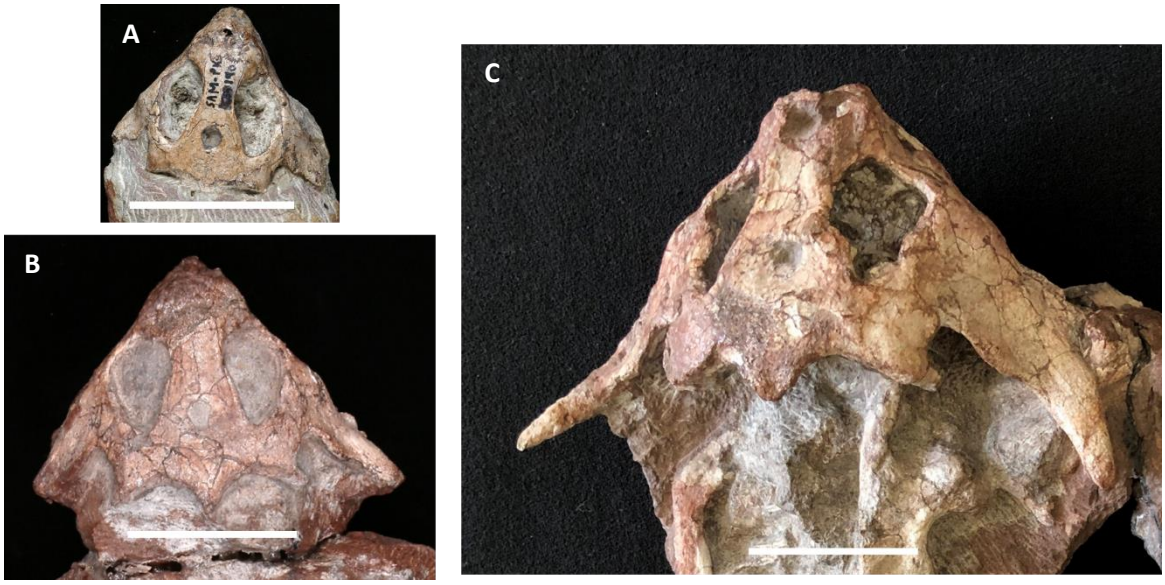


Figure 7.7: Ontogenetic range of Teratophon *skull sizes from Lemoenfontein. (A) Juvenile (SAM-PK-K10190). (B) Sub-adult (SAM-PK-K011599, L18-2). (C) Adult (SAM-PK-K010174). Scale bars = 4 cm.*

According to Modesto and Damiani (2003) and Gow (1977), *Thelerpeton oppressus,* can be distinguished from the remaining three genera by the presence of "bulbous marginal teeth with the crowns pinched up to present a small occlusal area, and dentary dentition that is undercut labially by a continuous, longitudinal sulcus". The upper and lower teeth interlock in a "gear like" fashion (see Figure 7.6 C). The species name "*oppressus*" is derived from the Latin *apprimo* = crush and represents powerful crushing teeth (Gow, 1977). The orbits in *Thelerpeton* extend posteriorly beyond the pineal opening.

The excellent state of preservation of the skull of the new specimen (L18-2), in general, and its teeth in particular, now allows a comparison of *Teratophon* and *Thelerpeton* (see Figure 7.6 B). Visual inspection shows that the teeth of *Teratophon* are also bulbous with a similar pinch that leads to a "gear like" interlocking with a reduced occlusal area. The lower jaw teeth also appear to be undercut by a longitudinal groove, and the orbits also extend posteriorly beyond the pineal opening.

The main difference between *Teratophon* and *Thelerpeton* is the presence or absence of quadratojugal spines. However, in the juvenile *Teratophon* specimens from Lemeonfontein the quadratojugal spines are not yet fully developed and are like those of the *Thelerpeton* holo- and paratypes. These skulls are also similar in size (Figure 7.8). Apart from these similarities there are also some differences. The shaped of the orbits of *Thelerpeton* narrows posteriorly, while those of *Teratophon* remain more oval. Also, the snout of *Teratophon* appears to curve downwards over the anterior part of the lower jaw in some of the smaller specimens (Figure 7.8 D).



Figure 7.8: Comparison of juvenile Teratophon *to* Thelerpeton. *(A) and (B)* Thelerpeton *paratype (BP/1/4586), dorsal and right-lateral views, respectively. (C) and (D) Juvenile* Teratophon *(SAM-PK-K10190), dorsal and right-lateral views, respectively. Scale bars = 4 cm.*

Thus, considering the following, an investigation could be undertaken to determine if there is any relationship between *Thelerpeton* and the juvenile *Teratophon* from Lemoenfontein:

- the new and significantly larger *Teratophon* sample size (and ontogenetic range) that resulted from this study;
- the similarity in the bulbous teeth of *Teratophon* and *Thelerpeton*;
- the orbits that extend posteriorly beyond the pineal opening in both *Teratophon* and *Thelerpeton*; and
- the under developed quadratojugal spines in the juvenile *Teratophon* skulls that are of similar skull size as *Thelerpeton*.

These common characteristics suggest that *Teratophon* and *Thelerpeton* may well belong to the same genus, particulary since at Lemoenfontein, *Teratophon* skulls with a range of quadratojugal spine sizes are present in close association. This detailed investigation is beyond the scope of the current study.

The same siltstone bed that delivered the embedded *Teratophon* specimens also yielded, in close association, several large isolated *in-situ* skulls that appear similar to *Teratophon*, except that the quadratojugal processes are absent. It is possible that they may have been lost before burial or that they were not present at all, perhaps due to them being a sexually dimorphic character of *Teratophon*. As a preliminary test of these hypotheses two specimens were selected for preparation, L18-1 and SAM-PK-K10172. It was found that L18-1 is indeed *Teratophon* based on the presence of the prominent right quadratojugal horn that was uncovered during preparation (Figures 6.4 A, B and Figure 7.9). The left horn had clearly been broken off (probably pre-burial). The quadratojugal horns are completely absent in specimen SAM-PK-K10172 and it could be identified as *Thelephon* (Figures 7.9 and 7.10) based on the presence of a marginal tooth that is almost twice as expanded mediodistally as the neighbouring teeth (See item 6, below). The preliminary conclusion is that the absence of quadratojugal spines cannot be attributed a sexually dimorphic character of *Teratophon.* A

detailed investigation that is beyond the scope of the current study is required to verify this observation.

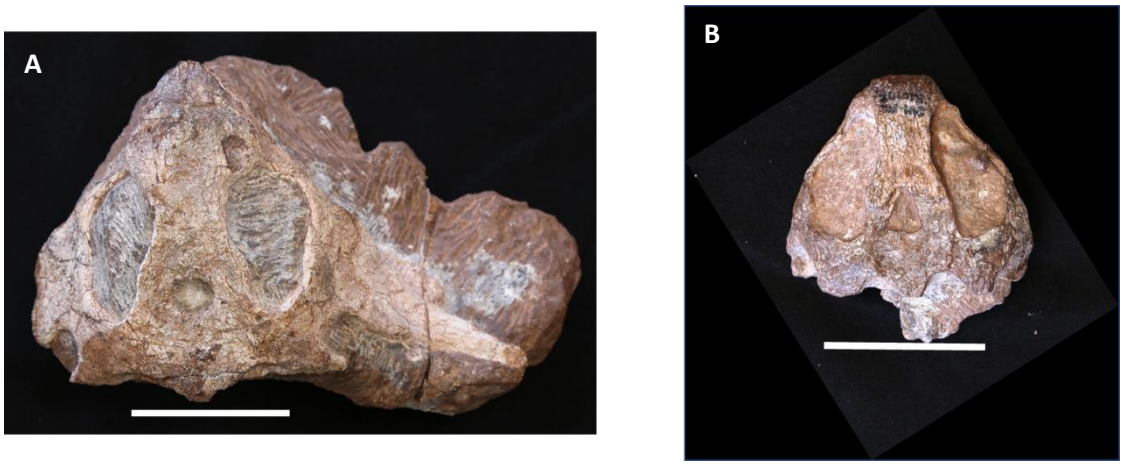


Figure 7.9 (A) Teratophon *specimen 18-1 showing prominent right quadratojugal horn after preparation. (B) Thelephon specimen SAM-PK-K10172. Scale bars = 4 cm.*

The teeth of most advanced procolophonids are labio-lingually widened and they are considered to be herbivorous (Gow, 1977). Gow (1977) speculates that the reason for the sporadic occurrence of procolophonids in the fossil record is that they were “upland” animals reducing the probability of preservation in the fossil record. As such they faced little competition during much of the Permian and Triassic from the large lowland anomodont herbivores until the appearnce of the bauriamorphs and gomphodonts. Gow (1977) considers that the large bulbous, sharp-tipped molars of *Thelegnathus opressus* (now *Thelerpeton opressus)* have evolved to crush hard seeds. He was unable to comment on the teeth of *Thelegnathus spinigenus* (now *Teratophon spinigenus)* due to the absence of preparable specimens at the time of publication in 1977. At the Lemoenfontein locality, the procolophonids were preserved in overbank floodplain mudrocks and occur in the same beds as the gomphodonts, rhynchosaurs and bauriids. No body fossils of large anomodonts are preserved at the Lemoenfontein locality.

6. Thelephon contritus (Modesto and Damiani, 2003)

Material: The genus, *Thelephon,* is represented by four identified specimens from the Lemoenfontein locality (SAM-PK-K010162, SAM-PK-K010168, PK-K010215, SAM-PK-K10172).

Remarks: The main characteristic that identifies *Thelephon contritus* is the "presence of a marginal tooth that is almost twice as expanded mediodistally as the neighbouring teeth" (Modesto and Damiani, 2003), See Figure 7.10. Note that two different procolophonid genera co-existed at this locality. Gow (1977) suggests that *Thelegnathus contritus* (now *Thelephon contritus*) was a foliage feeder due to the presence of "pounding" teeth like in *Procolophon*. The *Thelephon* specimens are significantly smaller than those of *Teratophon* from this locality.

Theledectes perforates, although not present at Lemoenfontein*,* is distinguished from the other three genera by multiple rows of marginal teeth. The molars are more like piercing teeth and could have been used to feed on the soft outer layers around certain hard seeds.

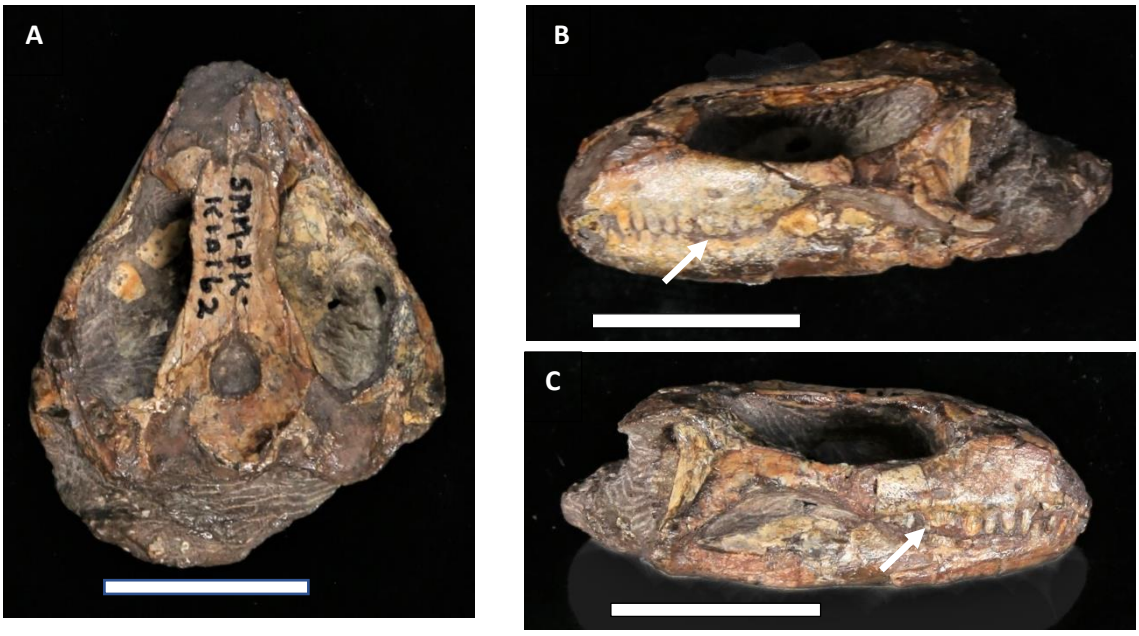


Figure 7.10: (A) Dorsal view, (B) left lateral view, and (C) right lateral views of Thelephon contritus *(PK-K010162). Note the expanded marginal teeth in B and C (arrowed). Scale bar = 2 cm.*

7.3 Discussion of the Lemoenfontein fauna

The relative occurrence frequency of the different genera from Lemoenfontein are presented in graphic form in Figure 7.11 for 115 of the specimens that could be identified to family or genus level. The fauna is dominated by procolophonids (74%). This is made up with 57% of specimens currently assigned to the family procolophonidae but not yet allocated to genus level, 12% to *Teratophon* and 5% to *Thelephon*. Cynodonts that have not been allocated to genus level contribute 8%. The gomphodont cynodont *Trirachodon* makes up 11%, and the trirachodontid cynodont *Cricodon*, 1%. The remaining genera consist of the therocephalian, *Microgomphodon*, 3%, the carnivore, *Lumkuia*, 1%, and the rhynchosaur, *Eohyosaurus*, 2%.

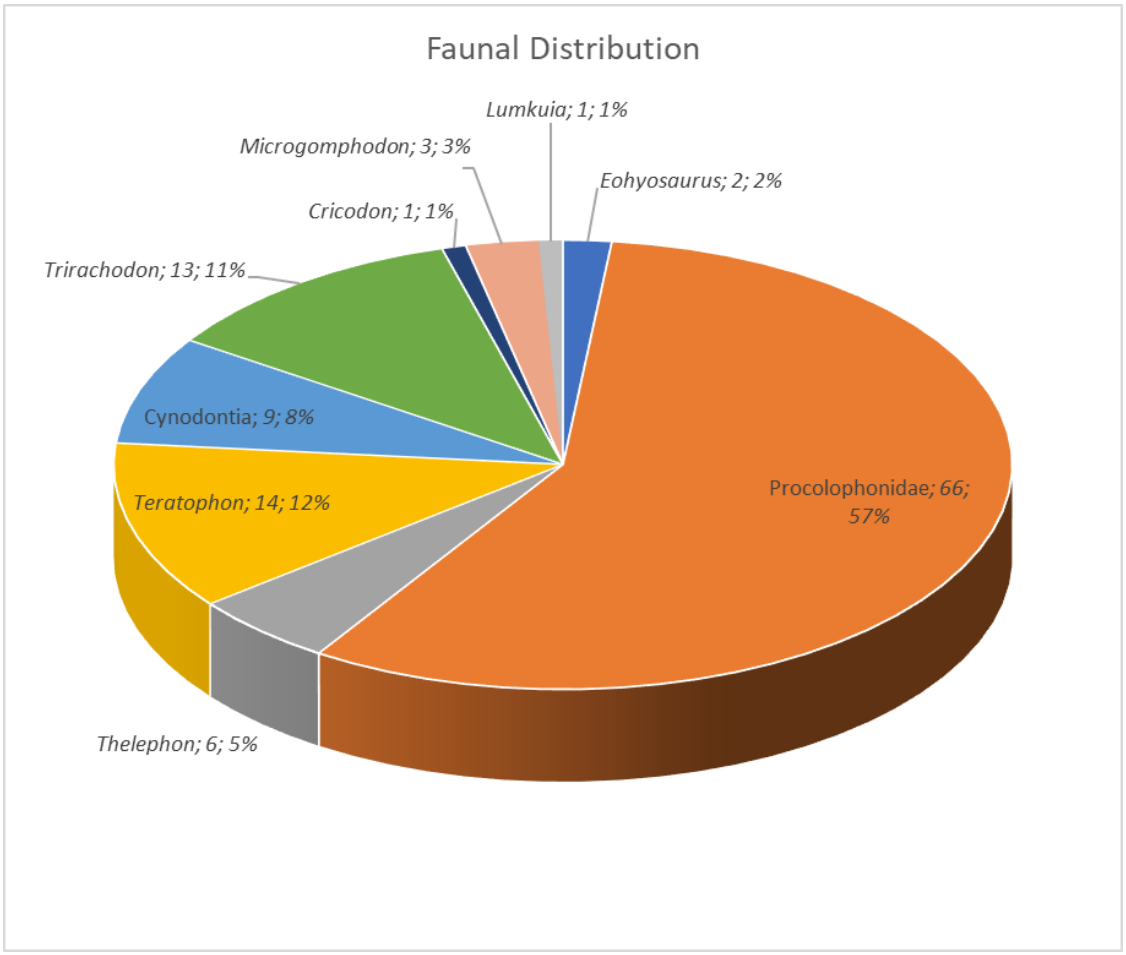


Figure 7.11: Relative frequency of the fossils of different genera collected from the Lemoenfontein locality.

The single *Lumkuia* skull is the only carnivore body fossil found at this locality. However, as discussed in the Taphonomy Section, several specimens display pre-burial damage to the skulls that can be attributed to carnivory. Although no fossils of large carnivores, such as

Cynognathus, have been found, it could be inferred that they were present and active at the time. As postulated under the taphonomy discussion, the presence of a large number of isolated skulls that were separated from the carcasses before burial could be due to the action of small carnivores such as *Lumkuia* that could feed on the bodies but were unable to crush or swallow the skulls.

The remaining genera that are present were all herbivorous except for the gomphodont cynodonts that may have been omnivorous. These genera all display some form of teeth adaptation for dealing with tough fibrous material:

- *Eohyosaurus* – presence of multiple tooth rows on the lingual as well as occlusal surfaces of the transversely expanded maxilla and dentary;
- *Trirachodon and Cricodon* – presence of oval postcanine gomphodont teeth that are expanded perpendicular to the long axis of the jaws;
- *Microgomphodon* – postcanines are oval in cross-section and the upper postcanines occlude with those of the lower jaw with interlocking cusps;
- *Teratophon* – molars are bulbous, labio-lingually expanded, with pinched tips that lead to interlocking with a reduced occlusal area (like those of *Thelerpeton oppressus* that have evolved to crush hard seeds);
- *Thelephon contritus* – a foliage feeder due to the presence of "pounding" teeth.

In a description of the Middle Triassic procolophonid, *Kapes bentoni*, Zaher et al. (2018) accept the view of Gow (1977) that the labiolingually expanded posterior teeth indicate herbivory consisting of fibrous plant material and suggest that this diet may also have included arthropods (Sues et al. 2000) or invertebrates with hard exoskeletons (deBraga 2003; Cisneros 2008). Based on the presence of freshwater crayfish burrow casts at the Lemoenfontein site, it is possible that these crayfish formed part of the *Teratophon* diet and that this may have played a role in the presence of the procolophonids in an overbank pond-margin environment.

Zaher et al. (2018) also suggest that the presence of the quadratojugal horns in *Kapes bentoni* played a defence role in making the animal appear larger to potential predators, or that it would make it harder to swallow for smaller predators (perhaps this supports the explanation for the many isolated skulls at Lemoenfontein). The presence of *Teratophon* skulls with a range of quadratojugal horn sizes that vary proportional to skull size at the study locality represents an ontogenetic development sequence.

Despite the intense collecting pressure that this locality was subjected to over many years and particularly during the 2019 and 2020 field trips, no fossil remains of any large dicynodont were found (except for a single possible archosauriform vertebra, SAM-PK-K10181). The presence of fossil remains of *Kannemeyeria* is ubiquitous in the *T-K* Subzone and it does occur higher up in the stratigraphy on Lemoenfontein. The *L-G* Subzone is the only biozone of the entire Beaufort Group that does not contain any dicynodonts (J. Hancox, pers. comm., November 10, 2018), and this suggests that the fossil fauna at Lemoenfontein was preserved before the appearance of the large herbivorous dicynodont *Kannemeyeria,* and that the sedimentary rocks at this locality were deposited during the transition from the *L-G* Subzone to the *T-K* Subzone. Furthermore, the abrupt increase in Mean Annual Precipitation (MAP) recognised by Retallack (2021) (also see Chapter 3) is coincident with the transition between the *L-G* and *T-K* Subzones that heralds the arrival of the large herbivorous dicynodont *Kannemeyeria* into the Karoo Basin. It is possible, therefore, that with the increase in rainfall (and water table) on the Karoo floodplains there was enough perennial vegetation on the riverbanks and around permanent standing water bodies to support these new large-bodied browsers.

It is worth noting that all the fossilised tetrapod remains from this locality are of small animals – less than 30 cm in total length. Several authors have pointed out that the faunal recovery after the Permian-Triassic Mass Extinction event in the Karoo Basin was only fully developed by the Middle Triassic (e.g., Roopnarine et al., 2018; Irmis and Whiteside, 2012). The reduction of animal body size is a regular feature after a mass extinction events (Huttenlocker, 2014) and is known as the “Lilliput effect”.

The Lilliput effect can be caused by:

- size reductions within the same taxa following the event;
- extinction of large taxa; and
- post event radiation of small taxa (Huttenlocker, 2014).

Huttenlocker (2014) performed a statistical analysis of body size changes in cynodonts and therocephalians in the Karoo Basin from the Late Permian into the Early Triassic and found that there was indeed a size reduction - probably driven by the extinction of large taxa. Apart from *Garjainia,* the terrestrial taxa from the *L-G* Subzone are all small in body size and probably burrowers; *Garjainia* was a piscivore and was probably also aquatic (J. Hancox, pers. comm., November 23, 2020). It is also interesting to note that following the End Permian mass extinction there was a general Lilliput effect except for the apparently piscivorous *Proterosuchus* with a lifestyle like *Garjainia* (R. Smith, pers. comm., December 5, 2020). This apparent presence of the Lilliput effect at the Lemoenfontein locality again suggests that the fauna was still in a recovery phase, and hence the beds represent the transition from the *L-G* Subzone to the *T-K* Subzone.

The intense exploration of this locality revealed that it is most unusual and that its rocks record a very diverse faunal record. In an area of approximately one hectare, a variety of well-preserved fossils of several different taxa were found. This led to the identification of this locality as a hyper-concentration of fossils due mainly to the sedimentary and environmental setting. The fossil taxa from this bonebed have several features in common, such as specialized dentition (pointing to herbivory), small body size and a high degree of skeletal articulation and preservation. To date, the collection includes two holotypes, one potential paratype and an additional specimen of a taxon previously known from only one specimen. Along with the body fossils, at least three different types of interpreted burrow cast geometries have also been identified at this field site.

8. LEMOENFONTEIN PALAEOENVIRONMENTAL RECONSTRUCTION AND THE ORIGIN OF BONE ACCUMULATION

8.1 Overview of bonebed definition, classification, and genesis.

A generic conceptual framework for the genesis and analysis of vertebrate skeletal concentrations is provided by Rogers et al. (2007). This framework clarifies the terminology by introducing operational definitions based on the dynamics of vertebrate hard part accumulation. It also introduces a scheme for categorising bonebeds generically. A bonebed is defined as a "relative concentration of vertebrate hard parts preserved in a localized area or stratigraphically limited sedimentary unit (e.g., a bed, horizon, or stratum) and derived from more than one individual". Two types of bone concentrations are recognized: *macrofossil* bonebeds where most bioclasts (>75%) of either isolated elements or entire skeletons are >5 cm in maximum dimension, and *microfossil* bonebeds where >75% of the bones are ≤5 cm in maximum dimension.

The bonebeds are further categorized based on whether their origin is *biogenic* or *physical* (Rogers et al., 2007). *Biogenic* concentrations are produced by biological agents or events. These biological agents can be *intrinsic*, i.e., the concentration results from the behaviour or activity of the individuals that are preserved in the assembly, or *extrinsic*, i.e., the concentration results from feeding behaviour or collecting activity of other animals. *Physical* concentrations are produced by physical processes and are also divided into two general categories. *Hydraulic* concentrations result from the action of surface flows (water, wind, sediment), whereas *sedimentologic* concentrations reflect the dynamics of the sedimentary budget (obrution, starvation, erosion). Once a concentration has occurred it can be subjected to different post-concentration agents: direct permanent burial, reworking and/or overprinting and dispersal and/or destruction.

Animal behaviour is the key element that produces *intrinsic* biogenic bone concentrations. The behaviour may be "perilous in life", such as colonial nesting habits, or "gregarious in death", such as fatal spawning events. The behaviour could also be forced upon the animals

by environmental hazards or perturbations such as stranding/miring, flooding/drowning, wildfire, drought, poisoning/disease and severe short-term meteorological events.

Although predators are the most important agents that can produce *extrinsic* biogenic concentrations through spatially-focused carnivory, nonpredatory animals such as porcupines can also concentrate vertebrate hard parts by their habitual bone collecting activities.

Hydraulic concentrations of vertebrate hard parts form during the transport and deposition of bones by unidirectional surface flows (wind, water, sediment) or bidirectional wave activity. Factors such as the volume, density and velocity of the flow medium, the number of hard parts coming into the system and the trapping mechanisms determine to what extent a concentration will develop. Bioclasts can enter the system from multiple entry points along the flow, from a pre-existing concentration, or from beached carcasses along a strand line.

Three types of sedimentologic concentrations are defined (Rogers et al., 2007). The first, an *obrution assemblage*, combines ecology and sedimentology. Living animals initially behaviourally congregate; then an obrution event causes mass mortality and captures the concentration. In this instance, death and burial occur in the same catastrophic sedimentation event (e.g., ashfall, mudslide, burrow collapse, sediment laden overbank flood). The second, an *attritional assemblage*, forms when there is very slow sediment input (sediment starvation) over many seasons so that due to time averaging, bones become more concentrated relative to the amount of sediment. By definition, these bones will likely undergo a greater degree of subaerial weathering. The third, a *residual lag assemblage*, is formed by erosion of matrix from an attritional assemblage (by wind or water flow), leaving a lag accumulation of the larger, denser, and least-transportable skeletal elements.

Once a vertebrate hard part assemblage has formed, different taphonomic pathways can either maintain or modify the original accumulation and thus its ecological representation or signal. Rogers et al. (2007) identify four distinct pathways. Path A leads to the permanent burial of the unaltered assemblage and maintains the original ecological signal. Path B is when mortality occurs in areas of sediment starvation (or during extended periods). The original bone assemblage thus receives an attritional overprint. Biological (path C) and

physical (path D) agents can create a secondary impact on a mass death assembly by reworking, transporting, sorting and ultimately re-concentrating.

In this context, Rogers et al. (2007) caution as follows: *"If a relative concentration of vertebrate skeletal debris exhibits a taphonomic signature that does not readily correspond to one of our major formative categories, it should be viewed as a clear warning to consider a suite of more complex formative scenarios."*

A concise summary of these principles and definitions by Rogers et al. (2007) is provided in Tables 8.1 and 8.2 below.

Table 8.1: Summary of the various biogenic and physical bone accumulation mechanisms. Specific examples and influencing factors of these mechanisms are also provided. Summary based on Rogers et al., 2007.

Macrofossil or Microfossil Bonebed									
Main Concentrating Agent	Biogenic				Physical				
Type	Intrinsic		Extrinsic		Hydraulic		Sedimentologic		
Subtype	Behaviour perilous in life, or gregarious in death	Behaviour induced by environmental hazards	Spatially-focused carnivory	Nonpredatory Post-mortem habitual collecting	Surface flows	Wave activity	Obrution assemblage (Catastrophic Sedimentation Event)	Attritional assemblage	Residual lag assemblage (Erosional Exhumation)
Examples	death during gestation, death during parturition, gregarious nesting/birthing, death upon spawning, rutting	stranding/miring flooding/drowning wildfire drought poisoning/disease severe short-term weather	serial predation bone-rich faeces/regurgitation	predator/ porcupine lair packrat midden ant chaff heap	wind, water, sediment	strandline deposits	ashfall, mudslide, burrow collapse, sediment laden overbank flood	sedimentation starvation	Erosion of matrix from an attritional assemblage (by wind or water flow) leaving lag
Additional influencing factors					flow energy, trapping mechanism, bioclasts amount	floating or submerged carcasses	combines ecology and sedimentary geology, Death and burial occur in the same event	time averaging, greater degree of weathering	lag of the larger or denser non-transportable bones.
Variations					multiple entry points along the flow, or from a pre-existing concentration				
Post concentration agents	direct permanent burial, reworking and/or overprinting, and dispersal and/or destruction.								

Table 8.2: Summary of the possible post concentration taphonomic pathways and their resultant signatures. Summary based on Rogers et al., 2007.

Post Concentration Taphonomy Pathways				
Paths	A	B	C	D
Description	Permanent burial of the unaltered assemblage	Mass mortality event during conditions of sediment starvation	Biological Agent	Physical Agent
Resultant Signature	Maintains the original signal	Original signal modified by attritional overprint.	Extrinsic biogenetic	Hydraulic overprint
Mechanism example			Ultimately reconcentrated in bone collector's lair	reworking, transportation, sorting, winnowed and ultimately reconcentrated.
Multiple Agents	If a relative concentration of vertebrate skeletal debris exhibits a taphonomic signature that does not readily correspond to one of the major formative categories, it should be viewed as a clear warning to consider a suite of more complex formative scenarios.			

8.2 Triassic Karoo Bone Accumulations

Literature review of studies relevant to the sedimentologic and taphonomic analyses of the Lemoenfontein bone accumulation.

The occurrence of different types of tetrapod bone accumulations in the Beaufort Group rocks has been documented by a number of authors in the form of bonebeds (e.g., Smith and Botha, 2005; Kitching ,1963; Viglietti et al., 2013), fossil "pockets" (Kitching, 1963), multi-specific aggregation (Abdala et.al, 2006), mono-specific aggregations (Smith and Evans, 1995, 1996; Watson, 1957; Gow, 1972; deBraga, 2003; Reisz and Laurin, 1991; Reisz and Scott, 2002; Ewer, 1965; Damiani et al., 2003; Smith and Botha, 2005) as well as accumulations in burrow complexes (Groenewald, 2001).

Behaviour-related interpretations have been assigned to several mono-taxon aggregations of more than one articulated skeleton in mutual contact. Late Permian examples include the diapsid *Youngina* (Smith and Evans, 1995, 1996) and the millerettid *Milleropsis* (Watson, 1957; Gow, 1972). Early Triassic examples include the procolophonids *Procolophon* (deBraga, 2003) and *Owenetta kitchingorum* (Reisz and Laurin, 1991; Reisz and Scott, 2002), and are commonly found for the cynodont *Thrinaxodon* (Brink, 1965; Damiani et al., 2003; Smith and Botha, 2005; Fernandez et al., 2013). While for the Middle Triassic, Ewer (1965) reported on the pre-death aggregation of several individuals of the archosaur *Euparkeria*.

Further evidence of behaviourally driven therapsid aggregations of several individuals of the same taxon is provided by the *Trirachodon* burrow complexes of the Burgersdorp (Driekoppen) Formation (Groenewald, 2001). The presence of 18 to 20 *Trirachodon* skeletons at "Locality 2" within numerous burrow terminal chambers is interpreted to be evidence of multiple cohabitation. This interpretation, as well as sedimentary evidence, suggests that the cohabitating community was trapped in the burrow complex during a catastrophic flood event. (Note that the trirachodontid material from the *Cynognathus* AZ *L-G* Subzone has subsequently been recognized as the new taxon *Langbergia modisei* (Abdala et al., 2006; Smith et al., 2012)).

Abdala et al. (2006) also assigned a behaviourally-driven shelter-sharing interpretation to a *multi-taxa* aggregation from the Early Triassic *Lystrosaurus declivis* AZ of articulated skeletons of a cynodont *Galesaurus planiceps,* a procolophonoid *Owenetta kitchingorum,* as well as a diplopod millipede.

Examples of drought-induced aggregations of several individuals of the same taxon forming true bone-on-bone bonebeds occur in the Lower Triassic Katberg Formation (Smith and Botha, 2005; Botha and Smith, 2006). These *compact* bonebeds occur in an approximately 8-metre-thick stratigraphic interval dubbed the "*Lystrosaurus* abundant zone" (Smith and Ward, 2001). The first of these mono-taxon bonebeds (SAM-PK-K855) was uncovered during the 2004 field season (Viglietti et al., 2013). It consists of several (±10) disarticulated and mixed up sub-adult *Lystrosaurus declivis* skeletons in a single 220 x 110 cm mudrock block. During subsequent field seasons another five *Lystrosaurus* bonebeds were found (Botha and Smith, 2006). The primary interpretation is that these animals died around a drying and shrinking flood plain pond during a prolonged drought (Smith and Botha, 2005). Following the drought, heavy downpours created sheet wash events that disarticulated and relocated the desiccated carcasses into floodplain depressions creating a mud clast, nodular conglomerate that cemented the disarticulated bones together. Subsequent detailed sedimentological and isotopic studies of the *Lystrosaurus* bonebed discussed above (SAM-PK-K855), point to an additional concentration mechanism at play during the Early Triassic (Viglietti et al., 2013). The sedimentology results for this block show no evidence of transportation, while the isotope data show evidence of seasonal cool weather. The primary concentration mechanism and cause of death was due to the palaeoclimate, i.e., a drought leading to the animals congregating and dying around a shrinking pond. However, the absence of evidence for a transportation mechanism and the evidence for cold weather suggest a secondary thermoregulatory huddling behaviour to explain the close association of the animals, i.e., the animals congregated together due to cold temperatures before dying of hunger or thirst.

In the Joe Gqabi (Burgersdorp) district, Kitching (1963) reported compact bonebeds in the *Cynognathus* AZ on two farms, Nooitgedacht and Winnaarsbaken. Two bonebeds occur on Winnaarsbaken. The first consists of an abundance of fragmented amphibian (*Xenotosuchus*)

and lungfish (*Ptychoceratodus*) remains and a few isolated cynodont teeth in an elongate scour. This bonebed is 25 cm thick and runs for more than 1.2 m (Kitching, 1963). The second contains isolated cynodont teeth and fragmentary post cranial elements. On the farm Nooitgedacht a large 12 square metre bone bed occurs in red to grey-green shales with thin sandstone bands. A sample block, 60 cm by 60 cm by 25 cm thick yielded over 500 jaw, skull, skeletal fragments and isolated teeth of *Diademodon* and *Cynognathus* (Kitching, 1963). Additional bonebeds consisting of fragmentary *Kannemeyeria* and amphibian remains have also been recorded on this farm. At Lady Frere in the Chris Hani district, several bonebeds have been recorded (Kitching, 1963). The first is close to the Lumku mission station, on the banks of the Cacadu River. Here, a 30 cm thick bone bed immediately below a 1.2 m sandstone horizon, contains an abundance of fragmentary cynodont remains. The second and third are on the Matyantya Mountain, where a blue-green mudstone exposure some 40 cm thick yielded fragmentary remains of small cynodonts, while a maroon-coloured mudstone about 3.5 m long and 50 cm thick yielded *Kannemeyeria* remains only. These bonebeds are all localized in area, stratigraphically limited and consist of crushed and fragmentary remains of many individuals. This points to a physical (i.e., hydraulic) or a sedimentological (residual lag) concentrating agent (Rogers and Kidwell., 2007).

A particularly rich and diverse bone accumulation occurs on the farm Driefontein (Free State province) in the *L-G* Subzone of the *Cynognathus* AZ (Hancox et al., 2010). Seventeen macrofaunal taxa have been identified (six amphibians, four fish, three therapsids, one procolophonid and three archosauromorphs). A diverse microvertebrate fauna, dominated by various reptile and fish remains, has also been discovered at this site. Similar Early Triassic microvertebrate remains have been found at only two other sites worldwide (Hancox et al., 2010).

At several localities in the Triassic of the main Karoo Basin, bone accumulations also occur in the form of scattered bonebeds or “fossil pockets” (Kitching, 1963; Damiani et al., 2003; Botha-Brink et al., 2014). Instead of the fossils being in close contact, such as in the bonebed (SAM-PK-K855) discussed above, the specimens are distributed over a limited surface area. Kitching (1963) defined a fossil “pocket” as “a limited area to which there is confined a

number of fossil specimens individually preserved and not sparsely and sporadically distributed". Typically, this area is limited to several square metres (Kitching, 1963). Examples of both mono-taxon and multi-taxon scattered bonebeds occur. Compact bonebeds are a more common phenomenon than scattered bonebeds in the *Cynognathus* AZ (Kitching, 1963).

Kitching (1963) first drew attention to the occurrence of scattered bonebeds in the Middle Triassic exposures in the Joe Gqabi (Burgersdorp) district. The first of these is located on the farm Cragievar eight kilometres south of Burgersdorp. In a locality next to the Wonderboomspruit, there is an exceptionally large concentration (in an area approximately 2 square metres) of mudrock nodules varying in colour from reddish-brown to grey that yielded some twelve almost complete cynodont skulls with parts of skeletons, as well as a complete *Bauria cynops* skull. At another locality on the nearby farm Winnaarsbaken (Kruger), north of the homestead, there is a hill containing a horizontally restricted nodular horizon in a mudrock exposure some 50 m long. Similar in nature to the nodules on Cragievar, these nodules contain complete skulls, some with portions of skeletons, or skeletal elements alone of the genus *Trirachodon.* Kitching makes the following significant observation: *"Particularly interesting is the occurrence of numbers of very immature, almost embryo-like specimens, but up to date none of these has been extracted from the matrix".* A similarly unusual fossil "pocket" occurs in the commonage of the town Lady Frere, where several fossil specimens, individually preserved, have been collected from a very limited exposure of hard blue-grey mudstone overlain by a maroon to grey-green shale (Kitching, 1963). When this locality was first discovered it yielded three *Diademodon* specimens, a *Sesamodon* skull (synonymised with *Microgomphodon* by Abdala et al., 2014) with skeleton, an *Inusitatodon* (synonymised with *Trirachodon* by Hopson & Kitching, 1972) and an immature *Kannemeyeria*.

A more extended form of fossil accumulation also occurs in the Triassic deposits of the main Karoo Basin. These bone accumulations are less concentrated and are less constrained from a sedimentological (temporal) and geographical point of view than the bonebeds discussed so far, but they still represent an unusual richness and diversity as compared to the background

(referred to here as a *Hyper-Accumulation*, also see Section 8.6). The fossils typically accumulated over time in subsequent sedimentary beds in a semi-constrained area such as around a small floodplain pond or lake. Triassic examples include fossil rich exposures surrounding small, isolated hills or "koppies" as reported by Damiani et al. (2003) and Botha et al. (2014). The fossils from these localities show a high degree of articulation and excellent preservation quality. Note that these authors report on the diversity and richness of the fauna from these localities, but do not identify these sites as bonebeds and do not specifically provide insights that explain these unusual accumulations. Lower Triassic *Lystrosaurus* AZ exposures on the farm Barendskraal, near Middelburg in the Eastern Cape Province, have delivered a diverse fauna of at least nine different species (Damiani et al., 2003). Typical fossiliferous *Lystrosaurus* AZ exposures are usually dominated by ubiquitous *Lystrosaurus* fossils. In this regard, the Barendskraal locality is atypical, as *Lystrosaurus* fossils are not as abundant. Another fossil rich locality (although somewhat larger in surface area than Barendskraal) occurs on the farm Nooitgedacht 68 in the Bethulie District (Botha-Brink et al., 2014). This locality contains strata that record a complete Permian Triassic Boundary (PTB) sequence. It has yielded at least 14 vertebrate species and as such is one of the richest PTB sites in the main Karoo Basin.

An additional example of a multi-taxon fossil accumulation, the well-known Harrismith Commonage in the north-eastern Free State, has yielded a diverse fauna consisting of 13 species, dominated numerically by *Lystrosaurus,* but also including three cynodonts *Galesaurus planiceps, Platycraniellus elegans* and *Thrinaxodon liorhinus* (Kitching, 1977; Damiani et al., 2003) and three temnospondyls *Micropholis stowi* (Schoch and Rubidge, 2005), *Lydekkerina huxleyi* and *Broomulus dutoiti* (Kitching, 1977; Damiani et al., 2003). '*Broomulus dutoiti*' is now regarded as a junior synonym of *Lydekkerina huxleyi* (Jeannot et al., 2006).

8.3 Lemoenfontein fossil accumulation

The Lemoenfontein locality records a diverse faunal record consisting of six different genera and it is dominated by procolophonids. More than 140 identifiable tetrapod fossils were found in an area of approximately one hectare. This led to the identification of this locality as a hyper-concentration of fossils. The abundance and spatial distribution of these fossils are plotted on aerial photographs of the locality using their GPS coordinates and overlaying them on Google Earth images in Figures 8.1 A and B, respectively. The size of each circle in (A) is proportional to the number of specimens assigned to the same GPS coordinate. During the field work undertaken as part of the current study, all specimens that occurred within approximately 1 m radius were assigned to the same GPS coordinate (for fossils collected in 2003 this measure was approximately 5 m). In (B) each white dot represents an individual tetrapod fossil in Gully 1, Bonebed 1 and Gullies 2 and 3. The linear alignment of the fossils in Gully 1 is due to individual skulls that have washed downstream. The first five specimens in the uppermost part of Gully 1 where found embedded and this is also the host bed for those specimens that have washed downstream. It is clear from Figure 8.1 that there is a hyper-concentration of fossils at this locality, in the sense defined by Kitching (1963), i.e., the specimens are distributed over a limited surface area and are individually preserved. Unlike the typical occurrence style of the *Cynognathus* AZ, they are not sparsely and sporadically distributed.

One of the main objectives of this study is to develop an understanding of which mechanisms, biogenic or physical, may have contributed to the accumulation of fossils at the Lemoenfontein site. Various insights have been gained about the depositional environment and the behaviour of the fauna that inhabited this environment. These insights are now used to reconstruct the once living *Cynognathus* AZ *T-K* Subzone ecosystem and its sedimentary and environmental setting.



Figure 8.1: (A) Spatial abundance of tetrapod fossils in Bonebed 1. The size of each circle correlates to the number of specimens assigned to the same GPS coordinate. (B) Spatial distribution of tetrapod fossils covering Gully 1, Bonebed 1 and Gullies 2 and 3. Each white dot represents an individual specimen (Black rectangle corresponds to the area in (A)).

8.4 Reconstruction of the once living *Cynognathus* AZ *T-K* Subzone ecosystem

The insights gained from the investigation of the Lemoenfontein sedimentology, the crevasse splay sole surface, the burrow casts, the taphonomy and the fauna are now summarised and then combined to interpret how the palaeo environmental and the behavioural factors contribute to the hyper-concentration of tetrapod fossils at the Lemoenfontein locality.

Sedimentological interpretations

- The palaeoclimate was semi-arid, with strong seasonal variation in rainfall and warm to hot average annual temperature. Such conditions resulted in clustering of vegetation around permanent and semi-permanent water bodies on the floodplain, with seasonally fluctuating water table. The fluctuating temperature and rainfall regimes also encouraged underground burrowing by both vertebrates and invertebrates at this time.
- The palaeoclimate also resulted in seasonal overbank flood events that led to the rapid deposition of mud aggregates on the floodplain.
- Avulsion events rapidly changed the course of the meandering river channel, changing proximal floodplain settings into distal settings with little or no floodplain deposition for long periods of time.

Crevasse splay sole surface interpretations

- The setting is a floodplain pond with a monoculture sphenophyte thicket growing around and in the shallow water margins. These reedbeds around semi-permanent ponds provide sheltered habitats for prey species and as such become “hotspots” for biological activity.
- Periodic dry seasons shrink these water bodies exposing areas of muddy lake floor around the margins which eventually desiccate forming mud cracks. Local downpours result in sheet flows emanating from crevasse channels.

- The flood water subsides while various *Scoyenia* ichnofacies traces are formed by insects (larvae and beetles) and worms on the wet floodplain surface.
- Small sharp-clawed tetrapods regularly attempt to burrow through the semi-consolidated mud beds. This burrowing possibly formed part of a feeding behaviour.

Burrow cast interpretations

- The reniform burrows of this locality are of tetrapod origin and they were excavated by procolophonids, trirachodontids or bauriids, whose skeletal remains occur in the same interval at the same locality.
- The crayfish burrow makers lived in a continental, environmental setting where the burrows had to be several metres deep to allow them to reach the water table for respiration, while still being able to access the floodplain surface for feeding purposes.
- The presence of a crevasse splay sandstone, a thin sheetwash fine-grained sandstone associated with the burrow infill of the tetrapod burrows, and the fine sandstone infill of the sub-circular burrows, point to seasonal heavy downpours on the floodplain that led to sheet wash events and overbank depositional events.
- By assigning the Lemoenfontein sub-circular burrows to the ichnotaxon *Camborygma,* the inference is made that the burrow maker was a continental freshwater crayfish. This is the first potential identification of presence of ancient crayfish in the main Karoo Basin of South Africa.
- The crayfish behaviour is recorded in the burrow construction (Hasiotis et al., 1998) and the depth of the crayfish burrows corresponds to the lowest palaeo-water table during the dry season; with the location of the mid-level enlargement chambers indicating the highest water table level during the wet season.

Taphonomic interpretation of the bone accumulation

The taphonomic investigation provides insights into mechanisms that resulted in the hyper-concentration of fossil skeletons.

- The high degree of articulation of the skeletons indicate that these fossils underwent little or no post-mortem transport and that they were buried at the time of death or very shortly thereafter during periodic flood events that deposited thick beds of mud aggregates.
- Calcium carbonate precipitation led to a rapid perimineralisation of the bone, and in this way improved the likelihood of fossilisation. It provided early diagenetic structural strength to the bones so that they could resist compaction, leading to the preservation of the elements in-the-round and in life position. It also provides resistance to weathering and improves survival of the specimens on the present-day landscape, which in turn results in a modern secondary lag concentration mechanism.
- Several fossils underwent permineralisation following burial, but became subaerially exposed, relocated, reworked and re-embedded during subsequent down wasting of the floodplain in the structural B horizon.
- The hyper-concentration of fossils suggests that this area of the floodplain must have been colonised for an extended period by a concentration of small tetrapods.

The taphonomic investigation also provides insights into the behaviour of the animals on the ancient floodplain.

- The presence of several complete, fully-articulated juvenile and adult skeletons in attitudes that suggests that they were behaviourally aggregated and buried in confined spaces, suggests that the animals were burrowers. This interpretation is strengthened by the presence of two fully articulated subadult *Teratophon* skeletons in the same large nodule and suggests that behavioural aggregation of multiple individuals of the same species occurred. Because of the seasonal nature of the palaeoclimate, the animals burrowed underground, or scratched out near surface holes in search of shade and moisture, most likely for thermoregulation.
- The animals may have died while in a state of estivation or cold torpor and were buried shortly after death or they were killed and buried in the same event.

- The presence of many isolated small skulls with articulated lower jaws suggests that the animals fell victim to selective predation or scavenging by small carnivores. This is reinforced by the direct presence of the genus *Lumkuia*. The presence of pre-burial damage to otherwise perfectly preserved skeletons or skulls points to predation by large carnivores.
- The presence of juvenile, sub-adult and adult procolophonids suggests that the environment was not stressed. The animals did not accumulate around an ever-shrinking water hole during a drought.
- The common presence of remains of the large dicynodont *Kannemeyeria* at many *Cynognathus* AZ *T-K* Subzone sites is absent. No large predator (i.e., *Erythrosuchus, Cynognathus*) remains were preserved at this locality. The larger animals were either not present in this environment or they were able to escape the flooding events that led to the burial of the smaller animals.

Faunal community interpretations

- The only carnivore present is the small probainognathian cynodont *Lumkuia*. Several specimens display pre-burial damage to the skulls that can be attributed to carnivory. Although no fossils of large carnivores, such as *Cynognathus*, have been found, it could be inferred that they were present and active at the time.
- The remaining genera that are present in the bone concentration are all regarded as herbivorous except for the gomphodont cynodonts that may have been omnivorous. The genera that display teeth adapted for feeding on tough fibrous material include *Eohyosaurus, Trirachodon, Cricodon, Microgomphodon, Teratophon,* and *Thelephon.*
- Crayfish possibly formed part of *Teratophon* diet, and it is here proposed that this may be a contributing factor for the dominance of procolophonid remains in this floodplain lake-margin environment.
- No fossil remnants of large dicynodonts occur, suggesting that the fossil fauna was preserved before the appearance of the large dicynodont *Kannemeyeria* in this part of the basin, and that the sedimentary succession thus records the transition from the *L-G* Subzone to the *T-K* Subzone.

- All the fossilised tetrapod remains from this locality are of small animals. The apparent presence of the Lilliput effect at the Lemoenfontein locality suggests that the fauna was still in the post end-Permian extinction recovery phase which further supports the pre-*T-K* Subzone interpretation.

Palaeoenvironmental reconstruction

The palaeoenvironment and once-living ecosystem at the base of the *Cynognathus* AZ *T-K* Subzone can be reconstructed by integrating the evidence from the various investigations. The general palaeoenvironmental setting of Lemoenfontein is consistent with a meandering river and floodplain system. The main drivers of the environmental conditions that led to the bone accumulation are third order events such as river avulsions and fifth order events such as periodic floods. The avulsion events changed the course of the meandering river flow, changing proximal floodplain settings into distal settings with little or no floodplain deposition for long periods of time, while the palaeoclimate also resulted in seasonal overbank flood events that led to the rapid deposition of mud aggregates on the floodplain. The climate was semi-arid, with seasonal rainfall causing a periodic rise and fall of the water table. The seasonality also led to significant changes in the ambient temperature. There is evidence of seasonal downpours that caused sheetwash deposits of silt and fine sandstone on the floodplain surface. Seasonal drying also occurred as evidenced by the presence of mudcracks. No fossil or other evidence of prolonged droughts have been found. The fossil evidence points to an environment that was not under stress, i.e., the animals did not die around an ever-decreasing pond (absence of evidence of trampling) and the full ontogenetic range of sizes are present.

Evidence from the sedimentology, crevasse splay traces and *Camborygma* burrows suggests that the local setting of the Lemoenfontein locality is that of a pond margin in a proximal to distal placement relative to the main river channel. A monoculture sphenophyte thicket grew around and in the shallow water margins. These reedbeds around semi-permanent ponds acted as hotspots for biological activity.

One such pond (the Lemoenfontein site) was colonized for an extended period by a diverse population of largely herbivorous tetrapods with specialised dentition to browse the fibrous reedbeds surrounding the pond. Some smaller omnivorous species likely fed on insects, worms and molluscs based on invertebrate traces of *Scoyenia* ichnofacies formed on the wet floodplain surfaces. This post-extinction late recovery fauna was small in overall body size and colonised the floodplain during an interval before the first appearance of the large dicynodont *Kannemeyeria*. As a result, they did not face competition from large herbivores and could fully-exploit the available fodder. The relatively shallow water table around the pond also provided an ideal habitat for freshwater crayfish to flourish. The apparently most abundant procolophonid, *Teratophon*, may have used the crayfish as a food source. The crayfish accessed the groundwater for breathing and procreating by burrowing, whilst feeding on the flood plain surface (likely at night). To cope with the seasonality that led to temperature extremes, dry periods, and fluctuating water table, many of these tetrapods burrowed underground or scratched out near surface holes in search of shade and moisture for thermoregulation. At least one specimen consisting of two subadult *Teratophon* in the same confined space indicates that underground aggregation behaviour occurred.

The presence of the concentration of small herbivores around the pond margin also attracted the attention of large carnivores such as *Cynognathus* (which occurred during the entire *Cynognathus* AZ). Several of the otherwise perfectly preserved complete skeletons show signs of carnivore (teeth) induced damage, particularly around the snout region of the skulls. These large carnivores roamed the floodplain in search of food and these pond margin ecological hotspots probably provided a ready source of prey. The presence of the small carnivore, *Lumkuia*, also suggests that these animals also inhabited the ecological niche around the pond on a long-term basis to selectively prey or scavenge on the small tetrapods and/or crustaceans.

In addition to predation, death due to other non-biological agents also occurred. Seasonal overbank flood or obrution events that rapidly deposited thick layers of mud aggregates on

the floodplain played an important role in drowning some of the small animals and at the same time burying their carcasses and increasing their preservation potential. The animals may have died while in a state of estivation or cold torpor as many were buried in near surface holes or in burrows. These seasonal floods depositional events also incrementally buried carcases that may have died from causes other than drowning. This mechanism provides a plausible explanation for the many articulated curled-up skeletons preserved at Lemoenfontein.

A schematic reconstruction of the palaeoenvironment and once living ecosystem at the base of the *Cynognathus* AZ *T-K* Subzone at the Lemoenfontein locality is provided in Figure 8.2.

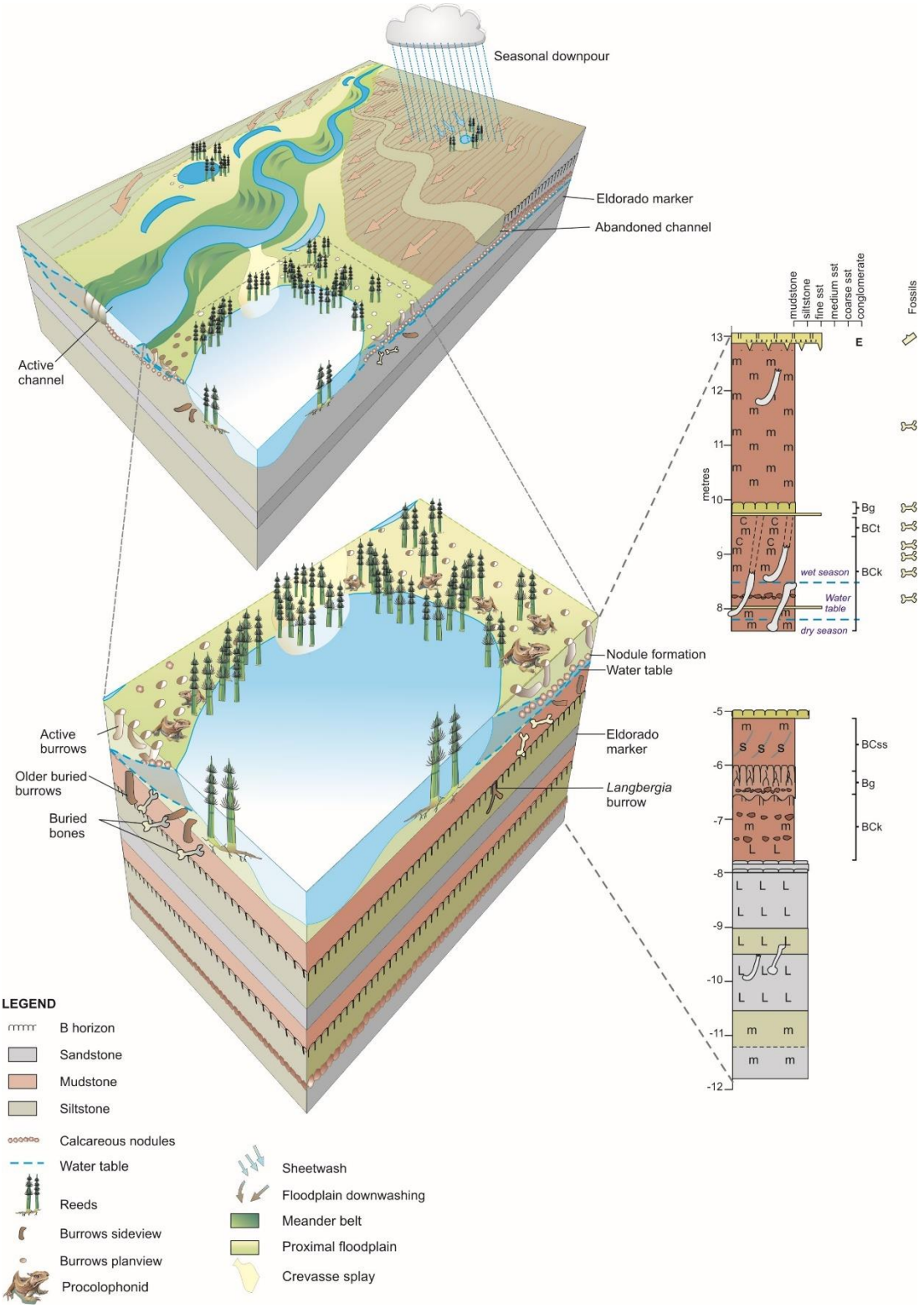


Figure 8.2: Schematic palaeoenvironmental reconstruction of the once-living ecosystem at the base of the Cynognathus *AZ* T-K *Subzone at the Lemoenfontein locality. The landscape was dominated by a floodplain dotted with seeps and standing water bodies that became the preferred habitat of small herbivorous and carnivorous cynodonts, archosaurs, therocephalians and procolophonids. These semi-permanent ponds were surrounded by sphenophyte reed beds that acted as source of food. The stratigraphic sequence has been simplified from that of Lemoenfontein. Active and older buried burrows and bones are indicated. Also, areas of down wasting of the floodplain following the abandonment of previously active channels as well as areas of floodplain deposition due to sediment laden overbank flood events is also presented schematically.*

8.5 Origin of bone accumulations at Lemoenfontein

The focus now changes to developing the most parsimonious explanation for the concentration of fossil bones on Lemoenfontein. The palaeoenvironment that formed semi-permanent ponds surrounded by an abundant food source is the first concentration agent. This physical agent allowed the animals to concentrate on the lake margins and colonise them for a long period of time. The animals were adapted to feeding on fibrous plant material, to burrow, and to enter states of torpor or estivation for thermal regulation. This adaptation resulted in animal behaviour that acted as a further intrinsic biogenic concentrating agent (see Table 8.1). Another behaviour related agent, predation by small predators resulted in the accumulation of many isolated skulls with articulated lower jaws. Predation by large predators provided some carcases where the prey was abandoned before it could be eaten. These predatory related taphonomic styles are extrinsic biogenic.

Seasonal sheet floods occurred, drowning the animals on the surface or in their burrows and the same flood covered them in a thick layer of mud aggregates (obrution events). This explains the unusual accumulation of curled-up articulated skeletons between the calcareous nodular horizon and the B horizon. These regular increments of mud aggregates deposited on the floodplain surface also ensured that animals that died from other causes were completely covered within a few years (less than five years) after death. These overbank floods acted as physical sedimentological agents for bone accumulation and combined ecology and sedimentary geology, with death and burial occurring in the same event. Although these physical hydromorphic events were not the primary concentration agents (which was biogenic), they did lead to an increased probability of fossilisation and preservation in articulation.

The next physical agent that ensured that the carcasses survived the full taphonomic journey through fossilization to being collected on the modern-day landscape is the early diagenetic peri- and permineralisation of the bones by calcium carbonate precipitation that encased the skeletons and skulls in hard calcium carbonate nodules. It provided early diagenetic structural

strength to the bones so that they could resist compaction, leading to the preservation of the elements in-the-round and in life position. These nodules are also resistant to weathering and ensure survival of the specimens on the present-day landscape, which in turn has led to a secondary lag concentration. In Bonebed 1, the formation of surface erosion gullies was prevented by the presence of a small dolerite dyke downslope to the east. This prevented the secondary lag deposited specimens from being washed away and destroyed downstream during present day thunderstorms.

During an extended period of non-sedimentation on the floodplain due to an avulsion-controlled re-direction of the contributing river channel floodplain, down wasting caused an attritional concentration of reworked skulls and post cranial elements on the newly-exposed resistant Bg horizon. This is an additional physical-sedimentological concentration agent (see Table 8.1) that resulted in the accumulation of many isolated skulls and partially articulated postcranial elements near the top of Bonebed 1.

At Lemoenfontein, it is concluded that the primary bone accumulation agent was due to intrinsic biogenic behaviour (Table 8.1), while several different physical agents combined to ensure a higher-than-average probability of fossilisation and preservation even to the present day. There are several key contributors.

- Palaeoenvironmental and sedimentological conditions allowed semipermanent ponds surrounded by thickets of sphenophyte to form on the floodplain (physical accumulation agent).
- Small tetrapods and freshwater crayfish congregated around these food rich biological activity hotspots on the floodplain. These animals burrowed and scratched out near surface holes for thermal regulation and estivation (intrinsic biogenic-behavioural accumulation agent).
- Selective predation played a role in establishing certain taphonomic styles (extrinsic biogenic accumulation agent).

- Seasonal flood events that deposited thick layers of mud drowned the animals and covered them at the instant of death or shortly thereafter (physical-sedimentological accumulation agent).
- Precipitation of calcium carbonate that encased the bones in nodules increased their probability of fossilisation and resistance to weathering (physical-sedimentological accumulation agent).
- During a period of floodplain depositional stasis, attritional accumulation of reworked fossils occured on the B horizon (physical-sedimentological accumulation agent).
- The present-day landscape surface undergoes down wasting resulting in the modern secondary lag concentration of the weathering resistant nodules containing fossils (physical-sedimentological accumulation agent).

8.6 Comparison to other bone accumulations in the Triassic strata of the Karoo Basin

Based on the literature survey of bone accumulations in the Triassic strata of the main Karoo Basin, and considering examples from similar aged basins elsewhere, several types of fossil accumulations are considered relevant to understanding the Lemoenfontein occurrence.

- *Multitaxic Aggregations:* Shelter-sharing, the behaviour-driven occurrence of two or more partially or fully-articulated skeletons of different taxa in mutual contact, typically in a confined place of shelter or burrow terminal chamber. The concentrating agent is intrinsic biogenetic, and behaviour driven (Rogers et al., 2007).
- *Monotaxic Aggregations:* Shelter-sharing, the behaviour-driven occurrence of two or more partially or fully-articulated skeletons of the same taxon in mutual contact, typically in a confined place of shelter or burrow terminal chamber. The concentrating agent is intrinsic biogenetic, and behaviour driven (Rogers et al., 2007).
- *Compact Bonebed:* A relative concentration vertebrate hard parts of more than one individual of the same or different taxa in physical contact preserved in a localized area or stratigraphically limited sedimentary unit. Typically, the fossil bones occur in a single block and were concentrated by a physical transportation mechanism or an intrinsic behaviourally driven response to a harsh environmental condition (Rogers et al., 2007).
- *Scattered Bonebed:* A relative concentration vertebrate hard parts of more than one individual of the same or different taxa individually preserved in a localised area or stratigraphically limited sedimentary unit. Typically, this area is limited to a few square meters and fossils occur in individual mud nodules. (This corresponds to Kitching's historical "fossil pocket" definition). The concentration is possibly due to a physical transportation mechanism, an intrinsic behaviourally driven response to a harsh environmental condition, intrinsic behaviourally driven colonial nesting habits, or an extrinsic biogenetic agent such as spatially-focused carnivory (Rogers et al., 2007).
- *Burrow Complex:* This is a behaviour-driven accumulation where several tetrapod burrow casts occur in proximity with many containing the semi-articulated remains of the same species. This would be classified as an intrinsic biogenetic agent (Rogers et al., 2007).

- *Attritional Accumulation:* Bonebeds that are less constrained from a sedimentological (temporal) and a geographical area point of view, but still represent an unusual richness and diversity as compared to the background. Typically, the fossils accumulated over time (time-averaged) in areas of low sediment accretion rates in a relatively constrained area and as a result show more weathering and disarticulation. This qualifies as a physical sedimentologic accumulation (Rogers et al., 2007).

- *Hyper-Accumulation:* An additional extended form of fossil accumulation also occurs in the Triassic deposits of the main Karoo Basin. These bone accumulations are less concentrated and are less constrained from a sedimentological (temporal) and a geographical point of view than conventional bonebeds, but represent an unusual richness and diversity as compared to the background. Typically, the fossils show excellent preservation and a high degree of articulation. The bones accumulated in cycles over time in subsequent sedimentary beds in a semi-constrained area, possibly around a small floodplain pond or lake. Such accumulations can be explained by combinations of concentrating agents (Rogers et al., 2007). For example, an initial concentration occurs due to an intrinsic biogenetic agent such as the gregarious and fossorial behaviour of the animals. This concentration in life is then followed by a concentration in death due to an environmental upset condition (i.e., drought). Following soon after the death of the animals, a physical sedimentological obrution (sediment laden overbank flood event or crevasse splay event) then covers the carcasses. Alternatively, an intrinsic biogenetic concentration due to the gregarious and fossorial behaviour of the animals is directly followed by a physical obrution (sediment laden overbank flood event or crevasse splay event) leading to a catastrophic sedimentation event that entombs the gregarious animals and trap some in their burrows.

It is concluded that the Lemoenfontein bone accumulation in the main Karoo Basin is most like the *Hyper-Accumulation* type of bonebed, that by its definition above, also contains elements of *Monotaxic Aggregations* and *Burrow Complex* forms of bone accumulation.

8.7 Comparison to the Lifua Member of Tanzania and the Santa Maria Formation of Brazil

Outside of the Karoo Basin, six productive Middle Triassic multi-taxon bone accumulations have been discovered in the Kingori and Lifua members of the Manda Beds of the Songea Group (Ruhuhu Basin) in Tanzania (Smith et al., 2017). Smith et al. (2017) identify two main taphonomic styles in the Lifua Member. In the Kingori/Lifua transition the bone accumulation was induced by crevasse splay events. Animals were initially trapped in the crevasse channel, followed by subsequent crevasse splay events that reworked the bones over several seasons resulting in secondary bone concentrations downstream. In the middle to upper Lifua Member, the bone accumulation occurred around distal floodplain pond margins. Significant evidence of groundwater fluctuation points to an environment where ponds and springs were a common occurrence on the floodplain with the sedimentology and taphonomy pointing to an increasing mean annual temperature and a seasonal rainfall regime. Increased vegetation growth around the ponds led to an associated increase in the number and diversity of tetrapods (small cynodonts and archosaurs) that were adapted to feed on these plants. This implies a climatic control over the distribution of bone accumulation sites. Hancox (1998) proposed a similar climactic and depositional environment transition from the *Cynognathus* AZ *T-K* Subzone to *C-U* Subzone.

The mechanism for bone accumulation at Lemoenfontein correlates strongly with that of the middle to upper Lifua Member. Both locations involve accumulation of small and diverse tetrapods adapted to feed on plants around floodplain ponds. The climate was seasonal in both cases and groundwater fluctuation occurred.

Elsewhere in Gondwana, in the Middle Triassic Santa Maria Formation, located in the central region of the Rio Grande do Sul State in Brazil near the city of Santa Cruz do Sul, a special accumulation of disarticulated therapsid skeletons dominated by herbivorous and carnivorous cynodonts along with a single non-cynodont specimen (*Rhadinosuchidae*) was discovered (Bertoni-Machado and Holz, 2006). The accumulation was in a form of a large

number (< 100) of isolated bones distributed chaotically in a mudrock block 10 m wide and 20 m long (5 m thick). The presence of calcareous rhizoliths and carbonate nodules in the block gave rise to the interpretation that the bones accumulated on a playa lake margin. Seasonal variation in rainfall resulted in a changing lake shoreline due to ground water level variation. The bone accumulation consists mainly of disarticulated and disassociated skulls and lower jaws. Large bones occur along-side very small bones in an irregular fashion. The authors interpret this taphonomic style to point to a biogenic concentration mechanism, i.e., selective predation.

There are similarities between the agents for bone accumulation at Lemoenfontein and those at the Santa Maria Formation. Both locations involve accumulation of diverse herbivorous tetrapods and a single carnivorous tetrapod around floodplain lakes. The climate was seasonal in both cases and groundwater fluctuation occurred resulting in a changing lake shoreline. The bone accumulation at both localities consists mainly of disassociated skulls. At the Santa Maria formation the main bone accumulation agent is selective predation, whilst at Lemoenfontein, selective predation is one of several biogenic and physical accumulation agents.

9. CONCLUSIONS

The detailed conclusions derived from the investigation of the sedimentology, pedogenesis, crevasse splay sole surface, burrow casts, taphonomy, and the fauna of the Lemoenfontein locality have already been summarised and integrated into the taphonomic pathways of Chapter 8. This allowed for a plausible interpretation explaining how the palaeoenvironmental and the behavioural factors contributed to the hyper-concentration of tetrapod fossils. This concluding chapter is therefore devoted to a summary of the more general outcomes of this study.

- The palaeoenvironmental setting of Lemoenfontein is that of a meandering river and floodplain system. The climate was semi-arid, with seasonal rainfall causing a periodic rise and fall of the water table. Frequent sediment-laden overbank floods led to periods of rapid deposition of mud aggerates on the proximal parts of the floodplain, while river avulsions resulted in extended periods with little or no deposition elsewhere on the floodplain. This sedimentological evidence leads to the conclusion that the local accumulation of sediments (and ultimately of bones) at this site was mainly controlled by third order geomorphic events (e.g., avulsions), fourth order events (e.g., periodic erosion of the floodplain surface) and fifth order climatic events (e.g., seasonality, periodic overbank flood events), rather than first and second order allogenic causes.
- Evidence from the sedimentology, palaeopedology and ichnology suggests that the local setting of the Lemoenfontein locality is that of a lake or pond margin, in a proximal to distal placement relative to the main river channel. A monoculture sphenophyte thicket grew around, and in, the shallow water margins of the water body. These reedbeds around semi-permanent ponds acted as “hotspots” for biological activity.
- The Lemoenfontein site was colonized for an extended period by a diverse population of largely herbivorous tetrapods, with dentitions adapted to browse the fibrous reedbeds surrounding the pond. These animals, including the procolophonids, burrowed and scratched out near surface holes for thermal regulation and estivation.

- The primary bone accumulation agent was intrinsic animal behaviour i.e., the animals habitually congregated around the pond margins, while several different physical agents combined to ensure a higher-than-average probability of fossilisation and preservation from death and burial up to the present-day weathering and erosion.
- The presence of *Trirachodon* and the absence of *Langbergia* places the Lemoenfontein fossil fauna in the *T-K* Subzone. However, since the fauna at Lemoenfontein was preserved before the appearance of the large dicynodont *Kannemeyeria,* Lemoenfontein is considered to be at the base of the *T-K* Subzone. This conclusion preserves the integrity of the three-fold subdivision of the *Cynognathus* AZ.

During this investigation, several opportunities for further research have been identified. The *Teratophon* fossil skeletons range from small juveniles to large adults; this will allow for an ontogenetic study of this taxon.

The rich and diverse nature of the fauna yielding two holotypes, and only the second specimen of *Lumkuia*, merits further preparation and CT-scanning of all the specimens collected, as well as continued field work at the site. There is a compelling possibility that additional taxa may be identified.

One of the specimens consists of a complete and fully articulated skeleton of *Microgomphodon* and there is evidence of predator induced damage to the skull. Since this is the first articulated postcranial skeleton of this taxon, it needs to be described in a dedicated study. Several other specimens show predator induced pre-burial damage; this provides an additional theme for future study.

The large nodule containing two articulated, overlapping sub-adult *Teratophon* skeletons requires CT-scanning and detailed description.

Finally, the possibility that the fauna is still part of the post extinction recovery fauna and the possible “Lilliput” effect needs to be placed in the context of a detailed comparison of body sizes with the underlying *L-G* Subzone fauna.

This study of the Lemoenfontein hyper-accumulation of fossil bones contributes to our general understanding of bone accumulation mechanisms and in doing so generates information that will help to more accurately reconstruct the palaeoenvironments and palaeoecology of similar fossil bone accumulations elsewhere in the Triassic Karoo (such as on the farms Winnaarsbaken and Cragievar) as well as other known procolophonid fossils clusters such as “*Procolophon* Hill” in the “Tussen die Riviere” nature reserve near Bethulie. A similar procolophonid dominated skeleton accumulation also occurs on Kitching ridge in Antarctica (Colbert and Kitching, 1975). These accumulations that occur in two latitudinally (climatically) separate parts of Gondwana merit future work to determine if these accumulations reflect intrinsic (procolophonid behaviour) or extrinsic (procolophonid palaeohabitats) taphonomic factors. These results from South Africa are also comparable with similar studies that are already underway in neighbouring countries and the other Gondwanan continents. Eventually we should be able to draw a detailed palaeogeographic map with tetrapod species distributions covering all the Middle Triassic palaeoecosystems of western Gondwana.

REFERENCES

Abdala, F., Giannini, N.P., 2000. Gomphodont cynodonts of the Chañares Formation: the analysis of an ontogenetic sequence. Journal of Vertebrate Paleontology, vol. 20, pp. 501–506.

Abdala, F., Hancox, P.J. and Neveling, J., 2005. Cynodonts from the uppermost Burgersdorp Formation, South Africa, and their bearing on the biostratigraphy and correlation of the Triassic *Cynognathus* Assemblage Zone. Journal of Vertebrate Paleontology, vol. 25, pp. 192-199.

Abdala, F., Cisneros, J.C. and Smith, R.M.H., 2006. Faunal aggregation in the Early Triassic Karoo Basin: earliest evidence of shelter sharing behaviour among tetrapods? PALAIOS, vol. 21, pp. 507–512.

Abdala, F., Neveling, J. and Welman, J., 2006. A new trirachodontid cynodont from the lower levels of the Burgersdorp Formation (Lower Triassic) of the Beaufort Group, South Africa and the cladistic relationships of Gondwanan gomphodonts. Zoological Journal of the Linnean Society, vol. 147, pp. 383–413.

Abdala, F. and Smith, R.M.H., 2009. Gondwana Middle Triassic cynodonts and the Namibian connection. Journal of Vertebrate Palaeontology, vol. 29, pp. 873-851.

Abdala, F. and Ribeiro, A.M., 2010. Distribution and diversity patterns of Triassic cynodonts (Therapsida, Cynodontia) in Gondwana. Paleogeography, Paleoclimatology, Paleoecology, vol. 286, pp. 202–217.

Abdala, F., Jashashvili, T., Rubidge, B.S. and Van den Heever, J., 2014. New Material of *Microgomphodon oligocynus* (Eutherapsida, Therocephalia) and the Taxonomy of Southern African Bauriidae. Early Evolutionary History of the Synapsida. Vertebrate Paleobiology and Paleoanthropology, pp. 209-231.

Abouessa, A., Duringer, P., Schuster, M. and Pelletier, J., 2015. Crayfish fossil burrows, a key tool for identification of terrestrial environments in tide-dominated sequence, Upper Eocene, Sirt Basin, Libya. Journal of African Earth Sciences, vol. 111, pp. 335-348.

Alonso-Zarza, A.M., 2003. Palaeoenvironmental significance of palustrine carbonates and calcretes in the geological record. Earth-Science Reviews, vol. 60, pp. 261–298.

Andersen, D.C., 1982. Belowground herbivory: the adaptive geometry of geomyid burrows. The American Naturalist, vol. 119, No. 1, pp. 18-28.

Anderson, J.M. and Anderson, H.M., 1985. Palaeoflora of Southern Africa: Prodromus of South African Megafloras, Devonian to Lower Cretaceous. Rotterdam, Balkema, pp. 423.

Anderson, J.M., Anderson, H.M., Archangelsky, S., Bamford, M., Chandra, S., Dettmann, M., Hill, R., McLoughlin, S. and Rosler, O., 1999. Patterns of Gondwana plant colonisation and diversification. Journal of African Earth Sciences, vol. 28, pp. 145–167.

Arakel, A.V. and McConchie, D., 1982. Classification and genesis of calcrete and gypsite lithofacies in paleodrainage systems of inland Australia and their relationship to carnotite mineralisation. Journal of Sedimentary Petrology, vol. 52, pp. 1149–1170.

Baucon, A., Ronchi, A., Felletti, F. and Neto de Carvalho, C., 2014. Evolution of Crustaceans at the edge of the end-Permian crisis: Ichnonetwork analysis of the fluvial succession of Nurra (Permian–Triassic, Sardinia, Italy). Palaeogeography, Palaeoclimatology, Palaeoecology, vol. 410, pp. 74–103.

Behrensmeyer, A.K., 1978. Taphonomic and ecologic information from bone weathering. Paleobiology, vol. 4, pp. 150-162.

Behrensmeyer, A.K, Western, D. and Dechant Boaz, D.E., 1979. New Perspectives in Vertebrate Paleoecology from a Recent Bone Assemblage. Paleobiology, vol. 5, No. 1, pp. 12-21.

Benoit, J., Abdala, F., Manger, P.R. and Rubidge, B.S., 2016. The sixth sense in mammalian forerunners: Variability of the parietal foramen and the evolution of the pineal eye in South African Permo-Triassic eutheriodont therapsids. Acta Palaeontologica Polonica, vol. 61 (4), pp. 777–789.

Bertling, M., Braddy, S., Bromley, R., Demathieu, G.R., Genise, J., Mikuláš, R., Nielsen, J.K., Nielsen, K.S.S., Rindsberg, A.K., Schlirf, M. and Uchman, A., 2006. Names for trace fossils: A uniform approach. Lethaia, vol. 39, pp. 265–286.

Bertoni-Machado, C.B. and Holz, M., 2006. Biogenic fossil concentration in fluvial settings: an example of a cynodont taphocoenosis from the Middle Triassic of southern Brazil. Revista Brasileria de Paleontologia, vol. 9, pp. 273–282.

Bedatou, E., Melchor, R.N., Bellosi, E. and Genise, J.F., 2008. Crayfish burrows from Late Jurassic–Late Cretaceous continental deposits of Patagonia: Argentina. Their palaeoecological, palaeoclimatic and palaeobiogeographical significance. Palaeogeography, Palaeoclimatology, Palaeoecology, vol. 257, pp. 169–184.

Bordy, E.M., Hancox, P.J. and Rubidge, B.S., 2004. Basin development during the deposition of the Elliot Formation (Late Triassic-Early Jurassic), Karoo Supergroup, South Africa. South African Journal of Geology, vol. 107, pp. 395–410.

Bordy, E.M., Hancox, P.J. and Rubidge, B.S., 2005. The contact of the Molteno and Elliot formations through the main Karoo Basin, South Africa: a second order sequence boundary. South African Journal of Geology, vol. 108, pp. 349-362.

Bordy, E.M., Sztanó, O., Rubidge, B.S. and Bumby, A., 2011. Early Triassic vertebrate burrows from the Katberg Formation of the south-western Karoo Basin, South Africa: Lethaia, vol. 44, pp. 33–45.

Bordy, E. M. and Krummeck, W. D., 2016. Enigmatic Continental Burrows from The Early Triassic Transition of The Katberg and Burgersdorp Formations in the Main Karoo Basin, South Africa, PALAIOS, vol. 31, pp. 389–403.

Bordy, E.M., Sztanó, O., Rampersadh, A., Almond, J. and Choiniere, J.N., 2019. Vertebrate scratch traces from the Middle Triassic Burgersdorp Formation of the main Karoo Basin, South Africa: Sedimentological and ichnological assessment, Journal of African Earth Sciences vol. 160, 103594.

Botha, J. and Chinsamy, A., 2004. Growth and life habits of the Triassic cynodont *Trirachodon*, inferred from bone histology. Acta Palaeontologica Polonica, vol. 49 (4), pp. 619-627.

Botha, J. and Smith, R.M.H., 2006. Rapid Vertebrate Recuperation in the Karoo Basin of South Africa Following the End-Permian Extinction. Journal of African Earth Sciences, vol. 45, pp. 502–514.

Botha-Brink, J. and Modesto, S.P., 2009. Anatomy and relationships of the Middle Permian varanopid *Heleosaurus scholtzi* based on a social aggregation from the Karoo Basin of South Africa. Journal of Vertebrate Paleontology, vol. 29, pp. 389-400.

Botha-Brink, J. and Smith, R.M.H., 2012. Palaeobiology of Triassic procolophonids, inferred from bone microstructure. Comptes Rendus Palevol, vol. 11, pp. 419–433.

Botha-Brink, J., Huttenlocker, A.K. and Modesto, S.P., 2014. Vertebrate Paleontology of Nooitgedacht 68: A *Lystrosaurus maccaigi*-rich Permo-Triassic Boundary Locality in South Africa, Early Evolutionary History of the Synapsida. Vertebrate Paleobiology and Paleoanthropology, pp. 289—304.

Bown, T.M. and Kraus, M.J., 1981. Vertebrate fossil-bearing paleosol units (Willwood Formation, Lower Eocene, northwest Wyoming, U.S.A.): implications for taphonomy, biostratigraphy, and assemblage analysis. Palaeogeography, Palaeoclimatology, Palaeoecology, vol. 34, pp. 31—56.

Bowring, S.A., Erwin, D.H., Jin, Y.G., Martin, M.W., Davidek, K. and Wang, W., 1998. U/Pb zircon geochronology and tempo of the end-Permian mass extinction. Science, vol. 280, pp. 1039–1045.

Brink, A.S., 1965. On two new specimens of *Lystrosaurus*-Zone cynodonts. Palaeontologia Africana, vol. 9, pp. 107–122.

Brink, A.S., Kitching, J.W., 1953. On some new *Cynognathus* Zone specimens. Palaeontologia Africana, vol. 1, pp. 29–48.

Bromley, R. and Asgaard, U., 1979. Triassic freshwater ichnocoenoses from Carlsberg Fjord, East Greenland. Palaeogeography, Palaeoclimatology, Palaeoecology, vol. 28, pp. 39—80.

Butler, R.J., Ezcurra, M.D., Montefeltro, F.C., Samathi, A. and Sobral G., 2015. A new species of basal rhynchosaur (Diapsida: Archosauromorpha) from the early Middle Triassic of South Africa, and the early evolution of Rhynchosauria. Zoological Journal of the Linnean Society, vol. 174 (3), pp. 571–588.

Buatois, L.A. and Mángano, G.M., 2007. Invertebrate Ichnology of Continental Freshwater Environments. In Trace Fossils: Concepts, Problems, Prospects (Chapter 17). Elsevier B.V., pp. 285–323.

Buatois, L.A. and Mángano, G.M., 2013. Ichnology of continental environments. In Ichnology Organism-Substrate Interactions in Space and Time (Chapter 10). Cambridge Books Online, Cambridge University Press, pp. 197-216.

Carpenter, K., 2005. Experimental investigation of the role of bacteria in bone fossilization: Neues Jahrbuch für Geologie und Paläontologie Monatshefte, pp. 83–94.

Catena, A.M. and Hembree, D.I., ·2014. Biogenic Structures of Burrowing Skinks: Neoichnology of *Mabuya multifaciata* (Squamata: Scincidae). In Experimental Approaches to Understanding Fossil Organisms, D. I. Hembree et al. (eds.), Topics in Geobiology 41, Chapter 14, pp. 344-369.

Catuneanu, O., Beaumont, C. and Waschbusch, P., 1997. Interplay of static loads and subduction dynamics in foreland basins: Reciprocal stratigraphies and the “missing” peripheral bulge. Geology, vol. 25 (12), pp. 1087-1090.

Catuneanu, O., Hancox, P.J. and Rubidge, B.S., 1998. Reciprocal Flexural Behaviour and Contrasting Stratigraphies: A New Basin Development Model for the Karoo Retroarc Foreland System, South Africa. Basin Research, vol. 10, pp. 417-439.

Catuneanu, O., Wopfner, H., Eriksson, P.G., Cairncross, B., Rubidge, B.S., Smith, R.M.H. and Hancox P.J., 2005. The Karoo basins of south-central Africa. Journal of African Earth Sciences, vol. 43, pp. 211–253.

Cisneros, J.C., 2008. New basal procolophonid reptile from the Katberg formation (Lower Triassic) of the South African Karoo. Palaeoworld, vol. 17, pp. 126–134.

Colbert, E.H. and Kitching, J.W., 1975. The Triassic reptile *Procolophon* in Antarctica. American Museum Novitates, vol. 2566, pp. 1–23.

Colombera, L., Mountney, N.P. and McCaffrey, W.D., 2013. A quantitative approach to fluvial facies models: Methods and example results. Sedimentology, vol. 60 issue 6, pp. 1526-1558.

Crompton, A.W., 1955. On some Triassic cynodonts from Tanganyika. Proceedings of the Zoological Society, London, vol. 125, pp. 617–669.

Cruickshank, A.R. I., 1965. On a specimen of the anomodont reptile *Kannemeyeria latifrons* (Broom) from the Manda Formation of Tanganyika, Tanzania. Proceedings of the Linnean Society of London, vol. 176, pp. 149–157.

Damiani, R., Neveling, J., Modesto, S. and Yates, A., 2003. Barendskraal, a diverse amniote locality from the *Lystrosaurus* Assemblage Zone, Early Triassic of South Africa. Palaeontologia Africana, vol. 39, pp. 53–62.

Damiani, R., Modesto, S., Yates, A. and Neveling, J., 2003. Earliest evidence of cynodont burrowing. Proceedings of the Royal Society B, vol. 270, pp. 1747–1751.

Daniel, J.C. and Chin, K., 2010. The role of bacterially mediated precipitation in the permineralization of bone. PALAIOS, vol. 25, pp. 507–516.

deBraga, M., 2003. The postcranial skeleton, phylogenetic position, and probable lifestyle of the Early Triassic reptile *Procolophon trigoniceps*. Canadian Journal of Earth Sciences, vol. 40, pp. 527–556.

De Wit, M.J. and Ransome, I.G.D., 1992. Regional inversion tectonics along the southern margin of Gondwana. In: De Wit, M.J., Ransome, I.G.D. (Eds.), Inversion Tectonics of the Cape Fold Belt, Karoo and Cretaceous Basins of Southern Africa. Balkema, Rotterdam, pp. 15–21.

Dilkes, D.W., 1995. The rhynchosaur *Howesia browni* from the Lower Triassic of South Africa. Palaeontology, vol. 38, pp. 665–685.

Dingle, R.V., Siesser, W.G. and Newton, A.R., 1983. Mesozoic and Tertiary geology of Southern Africa. viii+, pp. 375, Balkema, Rotterdam.

Duncan, R.A., Hooper, P.R., Rehacek, J., Marsh, J.S. and Duncan, A.R., 1997. The Timing and Duration of the Karoo Igneous event, Southern Gondwana. Journal of Geophysical Research, vol. 102, pp. 18127-18138.

Ewer, R., 1965. The anatomy of the thecodont reptile *Euparkeria capensis*. Philosophical Transactions of the Royal Society, Series B, vol. 248, pp. 379–435.

Fernandez, V., Abdala F., Carlson K.J., Cook D.C., Rubidge B.S., et al., 2013. Synchrotron Reveals Early Triassic Odd Couple: Injured Amphibian and Aestivating Therapsid Share Burrow. PLoS ONE 8(6): e64978.

Fiorillo, A.R., Padian, K. and Musikasinthorn, C., 2000. Taphonomy and Depositional Setting of the *Placerias* Quarry (Chinle Formation: Late Triassic, Arizona). PALAIOS, vol. 15, pp. 373–386.

Fourie, H. and Rubidge, B.S., 2007. The postcranial skeletal anatomy of the therocephalian *Regisaurus* (Therapsida: Regisauridae) and its utilization for biostratigraphic correlation. Palaeontologia Africana, vol. 42, pp. 1–16.

Gastaldo, R.A. and Rolerson, M.W., 2008. *Katbergia* gen. nov., a new trace fossil from the Late Permian and Early Triassic of the Karoo Basin: Implications for paleoenvironmental conditions at the P/Tr extinction event. Palaeontology, vol. 51, pp. 215–229.

Gibb, S. and Pemberton, S.G., 2017. *Rusophycus* by Any Other Name Is Still *Rusophycus carleyi.* Ichnos, vol. 24(1), pp. 19-26.

Gile, L.H., Peterson, F.F. and Grossman, R.B., 1965. The K horizon: a master horizon of carbonate accumulation. Soil Science, vol. 97, pp. 74– 82.

Gile, L.H., Hawley, J.W. and Grossman, R.B., 1981. Soils and geomorphology in the Basin and Range area of southern New Mexico—Guidebook to the Desert Project: New Mexico Bureau of Mines and Mineral Resources Memoir, vol. 39, p. 222.

Goudie, A.S., 1983. Calcrete. In: Goudie, A.S., Pye, K. (Eds.), Chemical Sediments and Geomorphology. Academic Press, London, pp. 93– 131.

Gow, C.E., 1972. The osteology and relationships of the Millerettidae (Reptilia: Cotylosauria). Journal of Zoology, vol. 167, pp. 219–264.

Gow, C.E., 1977. New procolophonids from the Triassic *Cynognathus* Zone of South Africa. Annals of the South African Museum, vol. 72, pp. 109–124.

Groenewald, G.H., 1991. Burrow casts from the *Lystrosaurus–Procolophon* Assemblage–Zone, Karoo Sequence, South Africa. Koedoe–African Protected Area Conservation and Science, vol. 34, pp. 13–22.

Groenewald, G.H., 1996. Stratigraphy of the Tarkastad Subgroup, Karoo Supergroup, South Africa. Unpublished PhD thesis, University of Port Elizabeth, South Africa, p. 145.

Groenewald, G.H., Welman, J. and Maceachern, J. A., 2001. Vertebrate Burrow Complexes from the Early Triassic *Cynognathus* Zone (Driekoppen Formation, Beaufort Group) of the Karoo Basin, South Africa. PALAIOS, vol. 16(2), pp.148-160.

Hancox, P.J. and Rubidge, B.S., 1994. A new dicynodont therapsid from South Africa: implications for the biostratigraphy of the Upper Beaufort (*Cynognathus* Assemblage Zone). South African Journal of Science, vol. 90, pp. 98–99.

Hancox, P. J., Shiskin, M.A., Rubidge, B.S. and Kitching, J.W, 1995. A threefold subdivision of the *Cynognathus* Assemblage Zone (Beaufort Group, South Africa) and its palaeogeographical implications. South African Journal of Science, vol. 91, pp. 143–144.

Hancox, P.J. and Rubidge, B.S., 1996. The first specimen of the Mid-Triassic dicynodont *Angonisaurus* from the Karoo of South Africa: implications for the dating and biostratigraphy of the *Cynognathus* Assemblage Zone, Upper Beaufort Group. South African Journal of Science, vol. 92, pp. 391–392.

Hancox, P.J. and Rubidge, B.S., 1997. The role of fossils in interpreting the development of the Karoo Basin. Palaeontologia Africana, vol. 33, pp. 41-54.

Hancox, P.J., 1998. A stratigraphic, sedimentological and palaeonvironmental synthesis of the Beaufort-Molteno contact in the Karoo Basin. PhD thesis, University of the Witwatersrand, Johannesburg, South Africa.

Hancox, P.J., 2000. The continental Triassic of South Africa. Zentralblatt für Geologie und Paläontologie Teil 1, 1998, Heft 11-12, pp. 1285-1324.

Hancox, P.J. and Rubidge, B.S., 2001. Breakthroughs in the biodiversity, biogeography, biostratigraphy and basin analysis of the Beaufort group. Journal of African Earth Sciences, vol. 33, pp. 563-577.

Hancox, J., Neveling, J. and Rubidge, B., 2010. Life in an Early Triassic lake: new developments at the Driefontein site, Burgersdorp Formation (*Cynognathus* Assemblage Zone), South Africa. Proceedings of the 16th Conference of the PSSA, Howick, Umgeni Valley Nature Reserve, pp. 41-42.

Hancox, P.J., Neveling, J. and Rubidge, B.S., 2020. Biostratigraphy of the *Cynognathus* Assemblage Zone (Beaufort Group, Karoo Supergroup), South Africa. South African Journal of Geology, vol. 123.2, pp. 217-238.

Hasiotis, S.T. and Mitchell, C.E., 1993. A comparison of crayfish burrow morphologies: Triassic and Holocene paleo- and neoichnological evidence, and the identification of their burrowing signatures: Ichnos, vol. 2, pp. 291–314.

Hasiotis, S.T., Mitchell, C.E. and Dubiel, R.F., 1993. Application of morphologic burrow interpretations to discern continental burrow architects: lungfish or crayfish? Ichnos, vol. 2, pp. 315–333.

Hasiotis, S.T., Kirkland, J.I. and Callison, G., 1998. Crayfish fossils and burrows, Upper Jurassic Morrison Formation, western Colorado: evolutionary and paleohydrologic implications. Modern Geol., Part 1, vol. 22, pp. 481-491.

Hasiotis, S.T., Miller, M. F., Isbell, J., Babcock, L E. and Collinson, J.W., 1999. Triassic trace fossils from Antarctica: burrow evidence of crayfish or mammal-like reptiles? Resolving crayfish from tetrapod burrows. Freshwater Crayfish, vol. 12, pp. 71–81.

Hasiotis, S.T. and Honey, J., 2000. Paleocene continental deposits and crayfish burrows of the Laramide Basins in the Rocky Mountains: paleohydrologic and stratigraphic significance. Journal Sedimentary Research, vol. 70, pp. 127-139.

Hasiotis, S.T., 2002. Where is the Fossil Evidence for Gondwanan Crayfish? Gondwana Research (Gondwana Newsletter Section), vol. 5, No. 4, pp. 872-878.

Hasiotis, S.T., Wellner, R.W., Martin, A.J., Demko, T.M. and Taylor, P., 2004. Vertebrate burrows from Triassic and Jurassic continental deposits of North America and Antarctica: Their paleoenvironmental and paleoecological significance. Ichnos, vol. 11, pp. 103–124.

Hembree, D.I., 2010. Aestivation in the fossil record: evidence from ichnology: Progress in Molecular and Subcellular Biology, vol. 49, pp. 245–262.

Hendrickx, C., Abdala, F., and Choiniere, J.N., 2019. A proposed terminology for the dentition of gomphodont cynodonts and dental morphology in Diademodontidae and Trirachodontidae. PeerJ 7:e6752 DOI 10.7717/peerj.6752.

Hiller, N. and Stavrakis, N., 1984. Permo-Triassic fluvial systems in the southeastern Karoo Basin, South Africa. Palaeogeography, Palaeoclimatology, Palaeoecology, vol. 45, pp. 1-21.

Holmes, W.B.K., 2001. Equisetalean Plant Remains from the Early to Middle Triassic of New South Wales, Australia. Records of the Australian Museum, vol. 53, pp. 9–20.

Holz, M. and Souto-Ribeiro, A., 2000. Taphonomy of The South-Brazilian Triassic Vertebrates. Revista Brasileira de Geociências, vol. 30(3), pp. 491-494.

Hopson, J.A. and Kitching, J.W., 1972. A revised classification of cynodonts (Reptilia; Therapsida). Palaeontologia Africana, vol. 14, pp. 71–75.

Hopson, J.A. and Kitching, J.W., 2001. A probainognathian cynodont from South Africa and the phylogeny of nonmammalian cynodonts. Bulletin of the Museum of Comparative Zoology, vol. 156, pp. 5-35.

Huttenlocker, A.K., 2014. Body size reductions in nonmammalian eutheriodont therapsids (Synapsida) during the end-Permian mass extinction. PloS ONE vol. 9, e87553.

Irmis, R.B., Whiteside, J.H., 2012. Delayed recovery of non-marine tetrapods after the end-Permian mass extinction tracks global carbon cycle. Proceedings of the Royal Society, vol. B 279, pp. 1310–1318.

Ivakhnenko, M.F., 1979. Permian and Triassic procolophons of the Russian Platform. Trudy Paleontologicheskogo Instituta Akademii Nauk SSSR, vol. 164, pp. 1-80. [[Russian].

Jahangirzadeh, A., Basser, H., Akib, S., Karami, H., Naji, S., et al. (2014). Experimental and Numerical Investigation of the Effect of Different Shapes of Collars on the Reduction of Scour around a Single Bridge Pier. PLoS ONE vol. 9 (6): e98592.

Jeannot, A.M., Damiani, R. and Rubidge, B.S., 2006. Cranial anatomy of the Early Triassic stereospondyl *Lydekkerina huxleyi* (Tetrapoda: Temnospondyli) and the taxonomy of South African lydekkerinids. Journal of Vertebrate Paleontology, vol. 26 (4), pp. 822–838.

Johnson, M.R., 1976. Stratigraphy and sedimentology of the Cape and Karoo Sequences in the Eastern Cape Province. Unpublished PhD thesis, Rhodes University, Grahamstown, pp. 336.

Johnson, M.R., 1984. The geology of the Queenstown area. Explanation to 1: 250 000 geology Sheet 3126, Queenstown. Council for Geoscience, Pretoria, p. 21.

Johnson, M.R. and Hiller, N., 1990. Burgersdorp Formation. South African Committee for Stratigraphy, Catalogue of South African Lithostratigraphic Units 2. Council for Geoscience, Pretoria, pp. 9-10.

Johnson, M.R., van Vuuren, C.J., Visser, J.N.J., Cole, D.I., Wickens, H.de V., Christie, A.D.M., Roberts, D.L. and Brandl, G., 2006. Sedimentary rocks of the Karoo Supergroup. In: M.R. Johnson, C.R. Anhaeusser and R.J. Thomas, (Editors.), The Geology of South Africa, Geological Society of South Africa and Council for Geoscience, pp. 461-499.

Kammerer, C.F., Viglietti, P.A., Hancox, J., Butler, R.J. and Choiniere, J.N., 2019. A new kannemeyeriiform dicynodont (*Ufudocyclops mukanelai*, gen. et sp. nov.) from Subzone C of the *Cynognathus* Assemblage Zone, Triassic of South Africa, with implications for biostratigraphic correlation with other African Triassic faunas. Journal of Vertebrate Paleontology, vol 39, pp. 1-18.

Kammerer, C.F. and De los Angeles Ordoñez, M., 2021. Dicynodonts (Therapsida: Anomodontia) of South America. Journal of South American Earth Sciences, vol. 108, 103171.

Karpeta, W.P. and Johnson, M.R., 1979. The geology of the Umtata area. Explanation to 1: 250 000 geology Sheet 3128, Umtata. Council for Geoscience, Pretoria, p.16.

Keyser, A.W. and Brink, A.S., 1977–1978. A new bauriamorph (*Herpetogale marsupialis)* from the Omingonde Formation (Middle Triassic) of South West Africa. Annals of the Geological Service, vol. 12, pp. 91–105.

Kitching, J.W., 1963. Notes on some fossil pockets and bone beds in the *Cynognathus* zone in the Burgersdorp and Lady Frere districts. Palaeontologia Africana, vol. 8, pp. 113 – 118.

Kitching, J.W., 1977. The distribution of the Karroo vertebrate fauna. Memoirs of the Bernard Price Institute Palaeontological Research, University Witswatersrand, vol. 1, pp. 1–131.

Kitching, J.W., 1995. Biostratigraphy of the *Cynognathus* Assemblage Zone. In Rubidge, B.S. (ed.) Biostratigraphy of the Beaufort Group (Karoo Supergroup). South African Committee for Stratigraphy, Biostratigraphic Series No. 1. Council for Geoscience, Pretoria. pp. 13-17

Krummeck, D.W. and Bordy, E.M., 2018. *Reniformichnus katikatii* (New Ichnogenus and Ichnospecies): Continental Vertebrate Burrows from the Lower Triassic, Main Karoo Basin, South Africa: ICHNOS, vol. 25, NOS. 2–3, pp.138–149.

Li, J. and Zhang, J., 2017. Sequence Stratigraphy of Fluvial Facies: A New Type Representative from Wenliu Area, Bohai Bay Basin, China, Seismic and Sequence Stratigraphy and Integrated Stratigraphy - New Insights and Contributions, Gemma Aiello, IntechOpen.

Li, Y., Zhang, W., Aydin, A., and Deng, X., 2018. Formation of calcareous nodules in loess–paleosol sequences: Reviews of existing models with a proposed new "per evapotranspiration model". Journal of Asian Earth Sciences, vol. 154, pp. 8-16.

Lucas, S.G., 1998. Global Triassic tetrapod biostratigraphy and biochronology. Palaeogeography, Palaeoclimatology, Palaeoecology, vol. 143, pp. 347–384.

MacDougall, M.J., Modesto, S.P. and Botha-Brink, J., 2013. The postcranial skeleton of the Early Triassic parareptile *Sauropareion anoplus*, with a discussion of possible life history. Acta Palaeontologica Polonica, vol. 58, pp. 737–749.

Machette, M.N., 1985. Calcic soils of the southwestern United States. In: Weide, D.L. (Ed.), Soils and Quaternary Geology of the Southwestern United States. Geological Society of America Special Paper, vol. 203, pp. 1–21.

Mack, G.H. and Cole, D.R., Trevinõ, L., 2000. The distribution and discrimination of shallow, authigenic carbonate in the Pliocene–Pleistocene Palomas Basin, southern Rio Grande rift. Geological Society of America Bulletin, vol. 112, pp. 643–656.

Mack, G.H. and James, W.C., 1994. Paleoclimate and global distribution of paleosols: Journal of Geology, vol. 102, pp. 360–366.

Maddin, H.C., Mann, A., and Hebert, B., 2020. Varanopid from the Carboniferous of Nova Scotia reveals evidence of parental care in amniotes. Nature Ecology & Evolution, vol. 4, pp. 50–56.

Marriott, S.B. and Wright, V.P., 1993. Palaeosols as indicators of geomorphic stability in two Old Red Sandstone alluvial suites, South Wales. Journal of the Geological Society, London, vol. 150, pp. 1109-1120.

Marsicano, C.A., Irmis, R.B., Mancuso, A.C., Mundil, R. and Chemale F., 2016. The precise temporal calibration of dinosaur origins. Proceedings of the National Academy of Sciences of the United States of America, vol. 113, pp. 509–513.

Martin, A.J., Rich, T.H., Poore, G.C.B., Schultz, M.B., Austin, C.M., Kool, L. and Vickers-Rich, P., 2008. Fossil evidence in Australia for oldest known freshwater crayfish of Gondwana. Gondwana Research, vol. 14, issue 3, pp. 287-296.

Miall, A.D., 1985. Architectural-Element Analysis: A New Method of Facies Analysis Applied to Fluvial Deposits. Earth-Science Reviews, vol. 22, pp. 261-308.

Miall, A.D., 1996. The Geology of Fluvial Deposits. Springer Press, p. 575.

Miall, A.D., 2014. Fluvial Depositional Systems. Springer Geology, Springer International Publishing, Switzerland. Chapter 2.

Miller, M.F., Hasiotis, S.T., Babcock, L.E., Isbell, J.L. and Collinson, J.W., 2001. Tetrapod and large burrows of uncertain origin in Triassic high paleolatitude floodplain deposits, Antarctica. PALAIOS, vol. 16, pp. 218–232.

Modesto, S.P. and Damiani R.J., 2003. Taxonomic status of *Thelegnathus browni* Broom, a procolophonid reptile from the South African Triassic. Annals of Carnegie Museum, vol. 72 (1), pp. 53–64.

Modesto, S. P. and Botha-Brink, J., 2010. A burrow cast with Lystrosaurus skeletal remains from the Lower Triassic of South Africa. PALAIOS, vol. 25, pp. 274–281.

Neveling, J., 2002. The Biostratigraphy and Sedimentology of the Contact Area between the *Lystrosaurus* and *Cynognathus* Assemblage Zones (Beaufort Group: Karoo Supergroup). Unpublished PhD thesis, University of the Witwatersrand, South Africa, p. 232.

Neveling, J., 2004. Stratigraphic and sedimentological investigation of the contact between the *Lystrosaurus* and the *Cynognathus* Assemblage Zones (Beaufort Group: Karoo Supergroup). Council for Geoscience, Pretoria, Bulletin, 137, p. 164.

Neveling, J., Hancox, P.J. and Rubidge, B.S., 2005. Biostratigraphy of the lower Burgersdorp Formation (Beaufort Group; Karoo Supergroup) of South Africa – implications for the stratigraphic ranges of early Triassic tetrapods. Palaeontologia Africana, vol. 41, pp. 81-87.

Olsen, P.E., Et-Touhami, M. and Whiteside, J.H., 2020. *Cynodontipus* is an amniote burrow, not a hairy synapsid track. Journal of Vertebrate Paleontology, in press.

Osborn, J.M., Phipps, C.J., Taylor, T.N. and Taylor, E.L., 2000. Structurally preserved sphenophytes from the Triassic of Antarctica: reproductive remains of *Spaciinodum.* Review of Palaeobotany and Palynology, vol. 111, pp. 225–235.

Ottone, E.G., Monti, M.M., Marsicano, C.A., de la Fuente, M.S., Naipauer, M., Armstrong, R. and Mancuso, A.C., 2014. A new Late Triassic age for the Puesto Viejo Group (San Rafael depocenter, Argentina): SHRIMP UPb zircon dating and biostratigraphic correlations across southern Gondwana. Journal of South American Earth Sciences, vol. 56, pp.186–199.

Reisz, R.R. and Laurin, M., 1991. *Owenetta* and the origin of turtles: Nature, vol. 349, pp. 324–326.

Reisz, R.R. and Scott, D., 2002. *Owenetta kitchingorum*, *sp. nov.,* a small parareptile (Procolophonia: Owenettidae) from the Lower Triassic of South Africa: Journal of Vertebrate Paleontology, vol. 22, pp. 244–256.

Retallack, G.J., 1994. The environmental factor approach to the interpretation of paleosols, *in* Amundson, R., et al., eds., Factors of soil formation: A fiftieth anniversary retrospective: Soil Science Society of America Special Publication, vol. 33, pp. 31–64.

Retallack, G.J., 1988. "Field recognition of paleosols" in Paleosols and Weathering Through Geologic Time: Principles and Applications. Geological Society of America, Special Paper 216.

Retallack, G.J., 2000. Depth to pedogenic carbonate horizon as a paleoprecipitation indicator: comment. Geology 28, pp. 572– 573.

Retallack, G.J., 2005. Pedogenic carbonate proxies for amount and seasonality of precipitation in paleosols. Geology vol. 33, pp. 333–336.

Retallack, G.J., 2021. Multiple Permian-Triassic life crises on land and at sea. Global and Planetary Change, vol. 198, 103415. pp 1-8.

Rex, G., 1985. A laboratory flume investigation of the formation of fossil stem fills. Sedimentology, vol. 32, pp. 245-255.

Rogers, R.R., 1990. Taphonomy of three dinosaur bone beds in the Upper Cretaceous Two Medicine Formation of northwestern Montana. PALAIOS, vol. 5, pp. 394–413.

Rogers, R.R., Arcucci, A.B., Abdala, F., Sereno, P.C., Forster, C.A. and May, C.L., 2001. Paleoenvironment and Taphonomy of the Chañares Formation Tetrapod Assemblage (Middle Triassic), Northwestern Argentina: Spectacular Preservation in Volcanogenic Concretions. PALAIOS, vol. 16, pp. 461–481.

Rogers, R.R., Rogers, K.C., Munyikwa, D., Terry, R.C. and Singer, B.S., 2004. Sedimentology and taphonomy of the upper Karoo-equivalent Mpandi Formation in the Tuli Basin of Zimbabwe, with a new 40Ar/39Ar age for the Tuli basalts. Journal of African Earth Sciences, vol. 40, pp. 147–161.

Rogers, R.R. and Kidwell S.M., 2007. A conceptual framework for the genesis and analysis of vertebrate skeletal concentrations. In: Bonebeds: Genesis, Analysis, and Paleobiological Significance. R.R. Rogers, D.A. Eberth, and A. Fiorillo (eds.), The University of Chicago Press, Chicago 60637. pp. 1–5.

Royer, D.L., 1999. Depth to pedogenic carbonate horizon as a paleoprecipitation indicator? Geology, vol. 27, pp. 1123–1126.

Roopnarine, P.D., Angielczyk, K.D., Weik, A. and Dineen, A., 2019. Ecological persistence, incumbency and reorganization in the Karoo Basin during the Permian-Triassic transition. Earth-Science Reviews, vol. 189, pp.244-263.

Rubidge, B.S., 1995 (Editor.), Biostratigraphy of the Beaufort Group (Karoo Supergroup). South African Commission for Stratigraphy, Biostratigraphic Series, 1, pp. 1-45.

Rubidge, B.S., 2005. Re-uniting lost continents—fossil reptiles from the ancient Karoo and their wanderlust. South African Journal of Geology, vol. 108, pp. 135–172.

Rust, B.R. and Nanson, G.C., 1989. Bedload transport of mud as pedogenic aggregates in modern and ancient rivers. Sedimentology vol. 36 (2), pp. 291–306.

Rutherford A.B., Rubidge B.S. and Hancox P.J., 2015. Sedimentology and palaeontology of the Beaufort Group in the Free State province supports a reciprocal foreland basin model for the Karoo supergroup, South Africa. South African Journal of Geology, vol. 118.4, pp. 355–372.

Schaller, G. B., 1972. The Serengeti lion: A study of predator–prey relations. Chicago: University of Chicago Press, pp. 244, 263–267.

Scheiber-Enslin, S. E., Ebbing, J. and Webb, S. J., 2015. New depth maps of the Main Karoo Basin, used to explore the Cape Isostatic Anomaly, South Africa. South African Journal of Geology, vol. 118.3, pp. 225–248.

Shen, S., Crowley, J.L., Wang, Y., Bowring, S.A., Erwin, D.H., Sadler, P.M., Cao, C., Rothman, D.H., Henderson, C.H., Ramezani, J., Zhang, H., Shen, Y., Wang, X., Wang, W., Li, W., Tang, Y., Liu, X., Liu, L., Zeng, Y., Jiang, Y. and Jin, Y., 2011. Calibrating the End-Permian Mass Extinction. Science, vol. 334, pp. 1367-1372.

Schoch, R.R. and Rubidge, B.S., 2005. The amphibamid *Micropholis stowi* from the *Lystrosaurus* Assemblage Zone of South Africa. Journal of Vertebrate Paleontology, vol. 25, pp. 502–522.

Seeley, H.G., 1895. On the structure, organization and classification of the fossil Reptilia III. On *Trirachodon.* Philosophical Transactions of the Royal Society of London B, vol. 186, pp. 48–57.

Shipman, P. 1975. Implications of drought for vertebrate fossil assemblages. Nature 257, pp. 667–668.

Shishkin, M.A., Rubidge, B.S. and Hancox, P.J., 1995. Vertebrate biozonation of the Upper Beaufort Series of South Africa—a new look on correlation of the Triassic biotic events in Euramerica and southern Gondwana. In: Sixth Symposium on Mesozoic Terrestrial Ecosystems. China Press, Beijing, pp. 39–41.

Shone, R.W., 1978. Giant *Cruziana* from the Beaufort Group. Transactions of the Geological Society of South Africa, vol. 81, pp. 327-329.

Sidor, C.A., Miller, M.F. and Isbell, J.L., 2008. Tetrapod burrows from the Triassic of Antarctica. Journal of Vertebrate Paleontology, vol. 28, pp. 277–284.

Sidor, C.A. and Hopson, J.A., 2018. *Cricodon metabolus* (Cynodontia: Gomphodontia) from the Triassic Ntawere Formation of northeastern Zambia: patterns of tooth replacement and a systematic review of the Trirachodontidae. Journal of Vertebrate Paleontology, vol. 37 (6, Supplement), pp.39–64.

South African Committee for Stratigraphy (S.A.C.S.), 1980. Stratigraphy of South Africa, part 1 (compiled by L.E. Kent). Lithostratigraphy of the Republic of South Africa, Southwest Africa/Namibia, and the Republics of Bophuthatswana, Transkei and Venda. Handbook Geological Survey South Africa, vol. 8, p. 690.

Smith, R.M.H., 1980. The lithology, sedimentology and taphonomy of floodplain deposits of the Lower Beaufort (Adelaide Subgroup) Strata near Beaufort West. Transactions of the Geological Society of South Africa, vol. 83, pp. 399-413.

Smith R.M.H., 1987. Helical Burrow Casts of Therapsid Origin from the Beaufort Group (Permian) of South Africa, Palaeogeography, Palaeoclimatology, Palaeoecology, vol. 60, pp. 155-170.

Smith, R.M.H., 1989. Fluvial facies, vertebrate taphonomy and palaeosols of the Teekloof Formation (Permian) near Beaufort West, Cape Province, South Africa. PhD thesis, University of Cape Town, South Africa.

Smith, R.M.H., 1990. Alluvial Paleosols and Pedofacies Sequences in the Permian Lower Beaufort of the Southwestern Karoo Basin, South Africa. SEPM Journal of Sedimentary Research, vol. 60, pp. 258-276.

Smith, R.M.H., 1993. Vertebrate Taphonomy of Late Permian Floodplain Deposits in the Southwestern Karoo Basin of South Africa. PALAIOS, Vol. 8 (1), pp. 45-67.

Smith, R.M.H., 1995. Changing fluvial environments across the Permian-Triassic boundary in the Karoo Basin, South Africa and possible causes of tetrapod extinctions. Palaeogeography Palaeoclimatology, Palaeoecology, vol. 117, pp. 81-104.

Smith, R.M.H. and Evans, S.E., 1995. An aggregation of juvenile Youngina from the Beaufort Group, Karoo Basin, South Africa. Palaeontologia Africana, vol. 32, pp. 45–49.

Smith, R.M.H. and Evans, S.E., 1996. New material of Youngina: Evidence of juvenile aggregation in Permian diapsid reptiles: Palaeontology, vol. 39, pp. 289–303.

Smith, R.M.H. and Kitching, J.W., 1997. Sedimentology and vertebrate taphonomy of the Tritylodon Acme Zone: a reworked palaeosol in the Lower Jurassic Elliot Formation, Karoo Supergroup, South Africa. Palaeogeography, Palaeoclimatology, Palaeoecology, vol. 131 pp. 29-50.

Smith, R.M.H., 2000. Sedimentology and taphonomy of Late Permian vertebrate fossil localities in southwestern Madagascar. Palaeontologia Africana, vol. 36, pp. 25-41.

Smith, R.M.H. and Ward, P.D., 2001. Pattern of vertebrate extinctions across an event bed at the Permian–Triassic boundary in the Karoo Basin of South Africa. Geological Society of America, vol. 29, pp. 1147–1150.

Smith, R.M.H. and Swart, R., 2002. Changing fluvial environments and vertebrate taphonomy in response to climatic drying in a Mid−Triassic rift valley fill: The Omingonde Formation (Karoo Supergroup) of Central Namibia. PALAIOS, vol. 17 (3), pp. 249–267.

Smith, R.M.H. and Botha, J., 2005. The recovery of terrestrial vertebrate diversity in the South African Karoo Basin after the end-Permian extinction. Comptes Rendus Palevol, 4, pp. 555–568.

Smith, R. M. H. and Botha-Brink J., (2009). Burrowing as a Survival Strategy in the earliest Triassic Karoo Basin, South Africa. Abs. Society of Vertebrate Palaeontology Annual Meeting, Bristol, England Journal of vertebrate Palaeontology vol. 29: 183A.

Smith, R.M.H., Rubidge, B.S. and Van der Walt, M., 2012. Therapsid Biodiversity Patterns and Paleoenvironments of the Karoo Basin, South Africa. In: Chinsamy-Turan (Ed) Forerunners of Mammals. Indiana University Press, pp. 31-62.

Smith, R.M.H and Botha-Brink, J., 2014. Anatomy of a mass extinction: Sedimentological and taphonomic evidence for drought-induced die-offs at the Permo-Triassic boundary in the main Karoo Basin, South Africa. Palaeogeography, Palaeoclimatology, Palaeoecology, vol. 396, pp. 99–118.

Smith, R.M.H., Sidor, C.A., Angielczyk, K.D., Nesbitt, S.J. and Tabor, N.J., 2017. Taphonomy and paleoenvironments of Middle Triassic bone accumulations in the Lifua Member of the Manda Beds, Songea Group (Ruhuhu Basin), Tanzania. Journal of Vertebrate Paleontology, vol. 37:sup1, pp. 65-79.

Smith, R.M.H., Rubidge, B.S., Day, M.O. and Botha, J., 2020. Introduction to the tetrapod biozonation of the Karoo Supergroup. South African Journal of Geology, vol. 123.2, pp. 131-140.

Stanistreet, I.G. and Turner, B.R., 1979. Discussion of ''Giant Cruziana from the Beaufort Group'': Transactions of the Geological Society of South Africa, vol. 82, pp. 371–375.

Stiles, C.A., Mora, C.I. and Driese, S.G., 2001. Pedogenic iron-manganese nodules in Vertisols: a new proxy for paleoprecipitation? Geology vol. 29, pp. 943-946.

Sues, H.D. and Olsen, P.E., 2015. Stratigraphic and temporal context and faunal diversity of Permian-Jurassic continental tetrapod assemblages from the Fundy rift basin, eastern Canada. Atlantic Geology, vol. 51, pp. 139-205.

Sues, H.D., 2019. The Rise of Reptiles: 320 Million Years of Evolution. Johns Hopkins University Press, Baltimore, pp29-30.

Tabor, N.J. and Myers, T.S., 2015. Paleosols as Indicators of Paleoenvironment and Paleoclimate. Annual Review of Earth and Planetary Sciences, vol. 43, pp. 333–361

Tabor, N.J., Myers, T.S. and Michel, L.A., 2017. Sedimentologist's Guide for Recognition, Description, and Classification of Paleosols. Terrestrial Depositional Systems, pp. 165-208.

Temp-Muller, R., de Araujo, H.I., Schiller Aires, A.S., Roberto-da-Silva, L. and Dias-da-Silva, S., 2015. Biogenic control on the origin of a vertebrate monotypic accumulation from the Late Triassic of southern Brazil. Geobios, vol. 48, pp. 331–340.

Tolchard, F., Kammerer, C.F., Butler, R.J., Hendrickx, C., Benoit, J., Abdala, F. and Choiniere, J. N., 2021. A new large gomphodont from the Triassic of South Africa and its implications for Gondwanan biostratigraphy. Journal of Vertebrate Paleontology. DOI: 10.1080/02724634.2021.1929265.

Van der Walt, M., Day, M. and Rubidge, B.S., 2010. A new GIS based biozone map of the Beaufort Group (Karoo Supergroup). South Africa. Palaeontologia Africana, vol. 45, pp.1-6.

Viglietti, P.A., Smith, R.M.H. and Compton, J., 2013. Origin and palaeoenvironmental significance of *Lystrosaurus* bonebeds in the earliest Triassic Karoo Basin, South Africa. Palaeogeography, Palaeoclimatology, Palaeoecology, vol. 392, pp. 9–21.

Visser, J.N.J. and Dukas, B.A., 1979. Upward fining fluviatile megacycles in the Beaufort Group north of Graaff Reinet, Cape Province. Transactions of the Geological Society of South Africa, vol. 82, pp. 149–154.

Watson, D.M.S., 1957. On *Millerosaurus* and the early history of the sauropsid Reptiles. Philosophical Transactions of the Royal Society, series B, vol. 240, pp. 325–400. White, C.R., 2005. The allometry of burrow geometry. Journal of Zoology, London, vol. 265, pp. 395–403.

Wopfner, H., 2002. Tectonic and climatic events controlling deposition in Tanzanian Karoo basins. Journal of African Earth Sciences, vol. 34, pp. 167–177.

Wright, V.P., 1990. Estimating rates of calcrete formation and sediment accretion in ancient alluvial deposits. Geological Magazine, vol.127, pp. 259-271.

Yagci, O., Celik, M.F., Kitsikoudis, V., Kirca, V.S.O., Hodoglu, C., Valyrakis, M., Duran, Z., and Kaya, S., 2016. Scour patterns around isolated vegetation elements, Advanced Water Research, vol.97, pp. 251–265.

Yagci, O., Yildirim, I., Celik, M.F., Kitsikoudis, V., Duran, Z. and Ozgur Kirca, V.S., 2017. Clear water scour around a finite array of cylinders. Applied Ocean Research, vol. 68, pp. 114–129.

Zaher, M., Coram, R.A. and Benton, M.J., 2018. The Middle Triassic procolophonid *Kapes bentoni*: computed tomography of the skull and skeleton. Papers in Palaeontology, pp. 1–28.

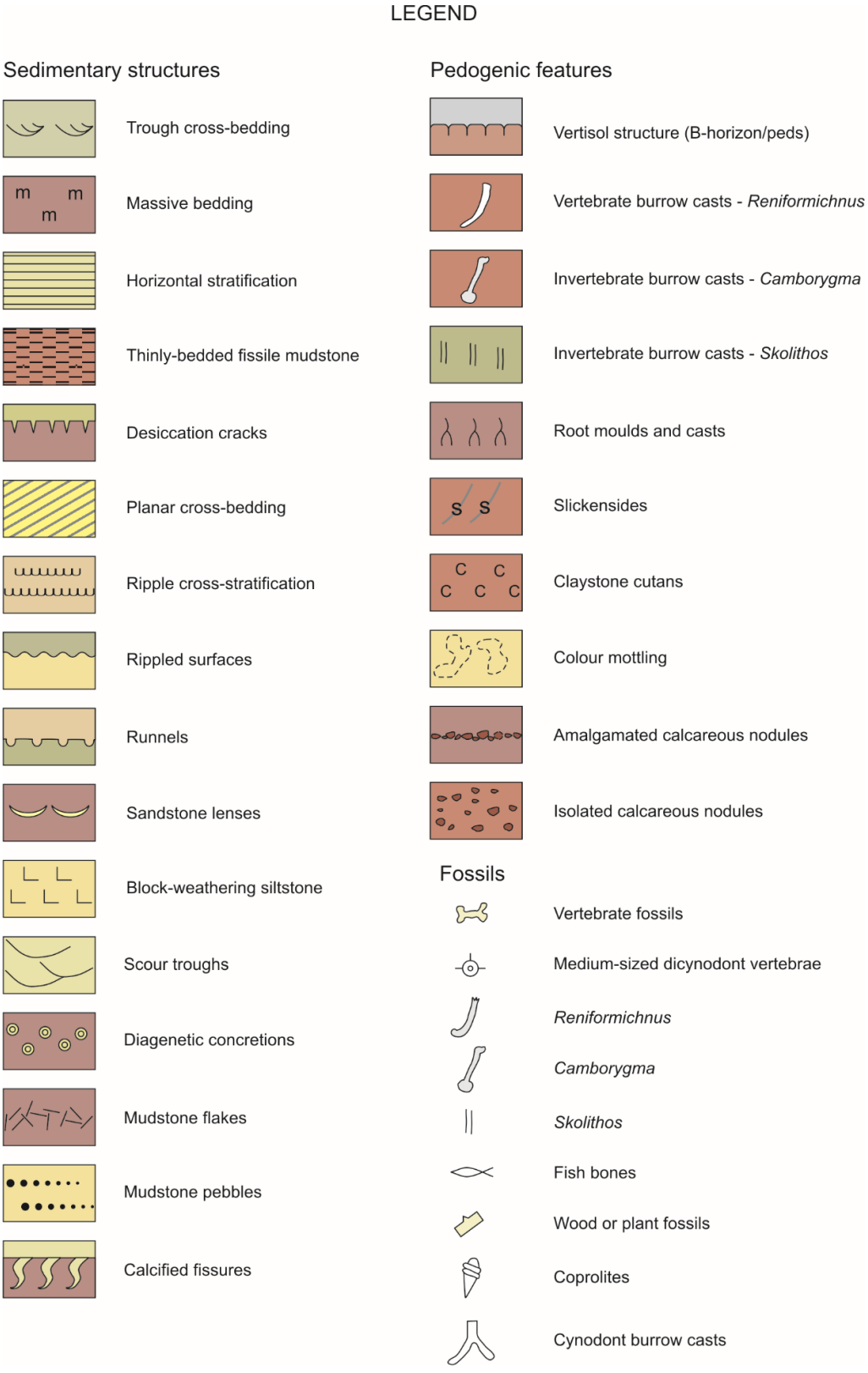
Zoehfeld, K.W., Bakker, R.T., Flis, C.J., Pettersson, C.B. and Bell, T. H., 2013. Burrows and break-ins on the Texas Permian delta: stacked aestivating amphibians and attacks by D*imetrodon.* Geological Society of America Abstracts with Programs, vol. 45, no. 7, p.324.

Zhao, M., Cheng, L. and Zang, Z., 2010. Experimental and numerical investigation of local scour around a submerged vertical circular cylinder in steady currents. Coastal Engineering, vol. 57, pp.709–721.

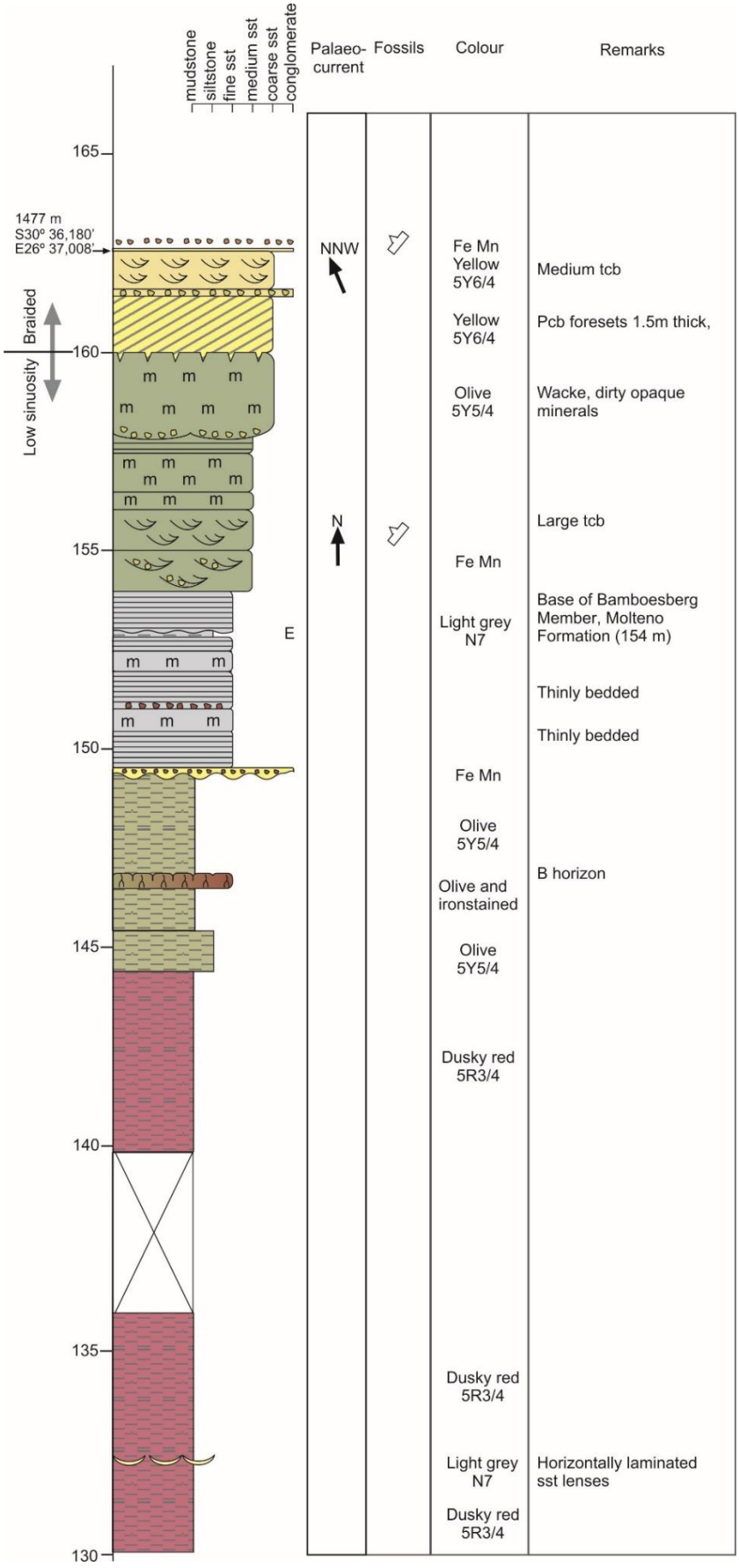
Zwoliński, Z., 1992. Sedimentology and geomorphology of overbank flows on meandering river floodplains. Geomorphology, vol. 4, pp. 367-379.

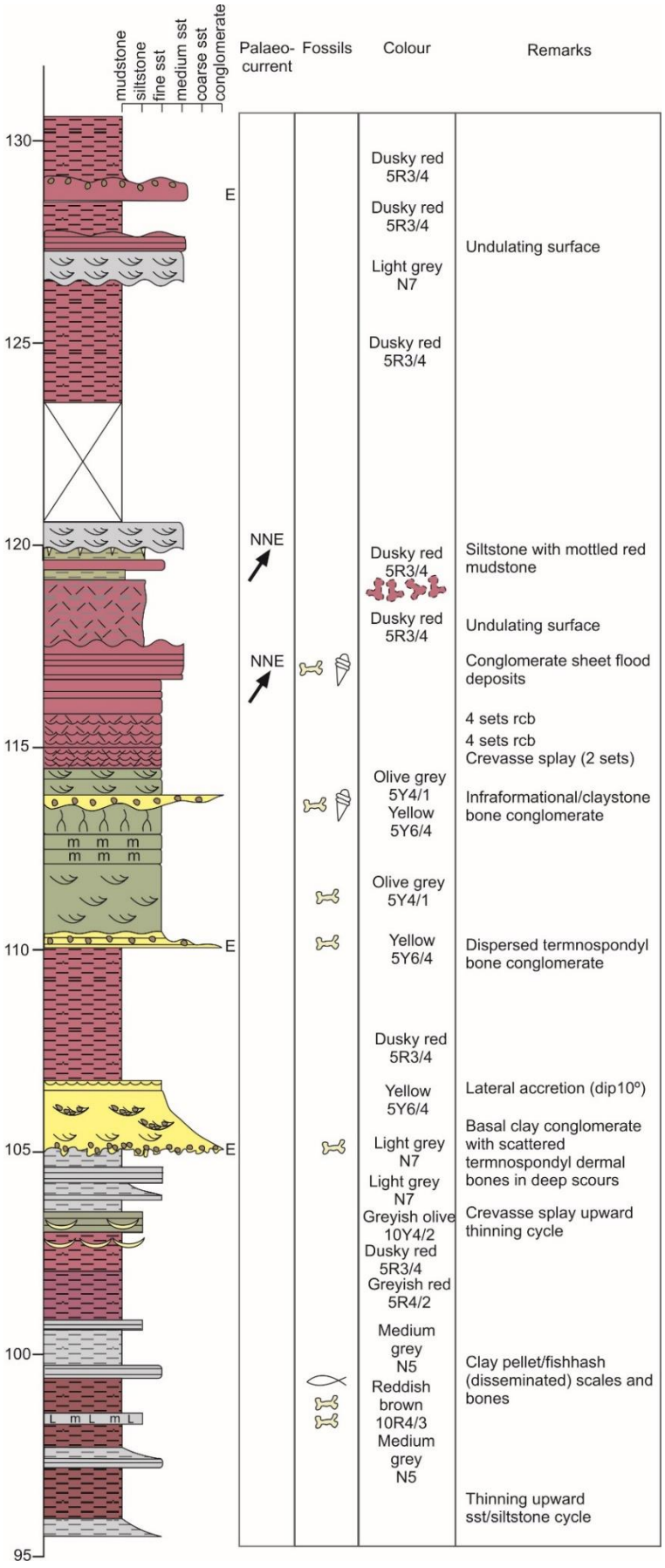
APPENDIX A: LITHOSTRATIGRAPHIC LOG

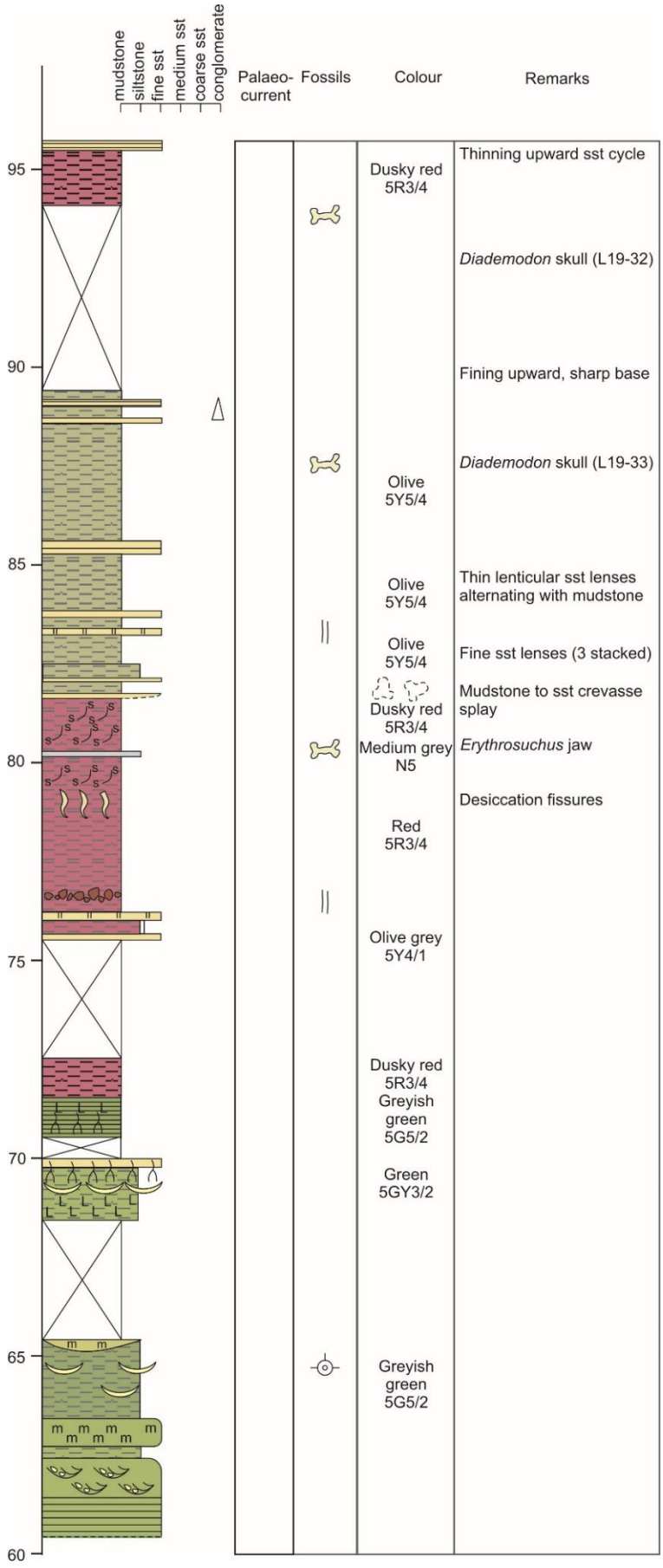
A.1 Legend

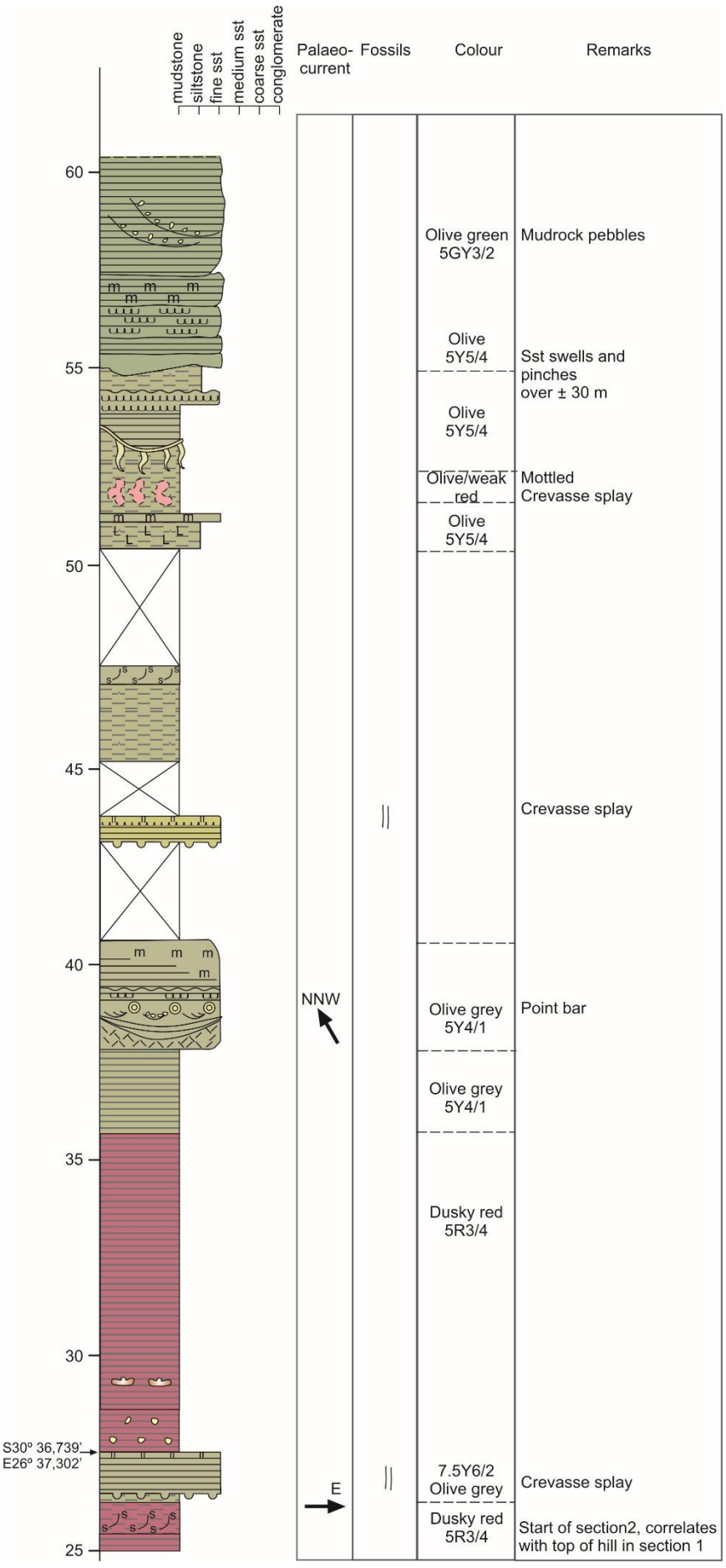


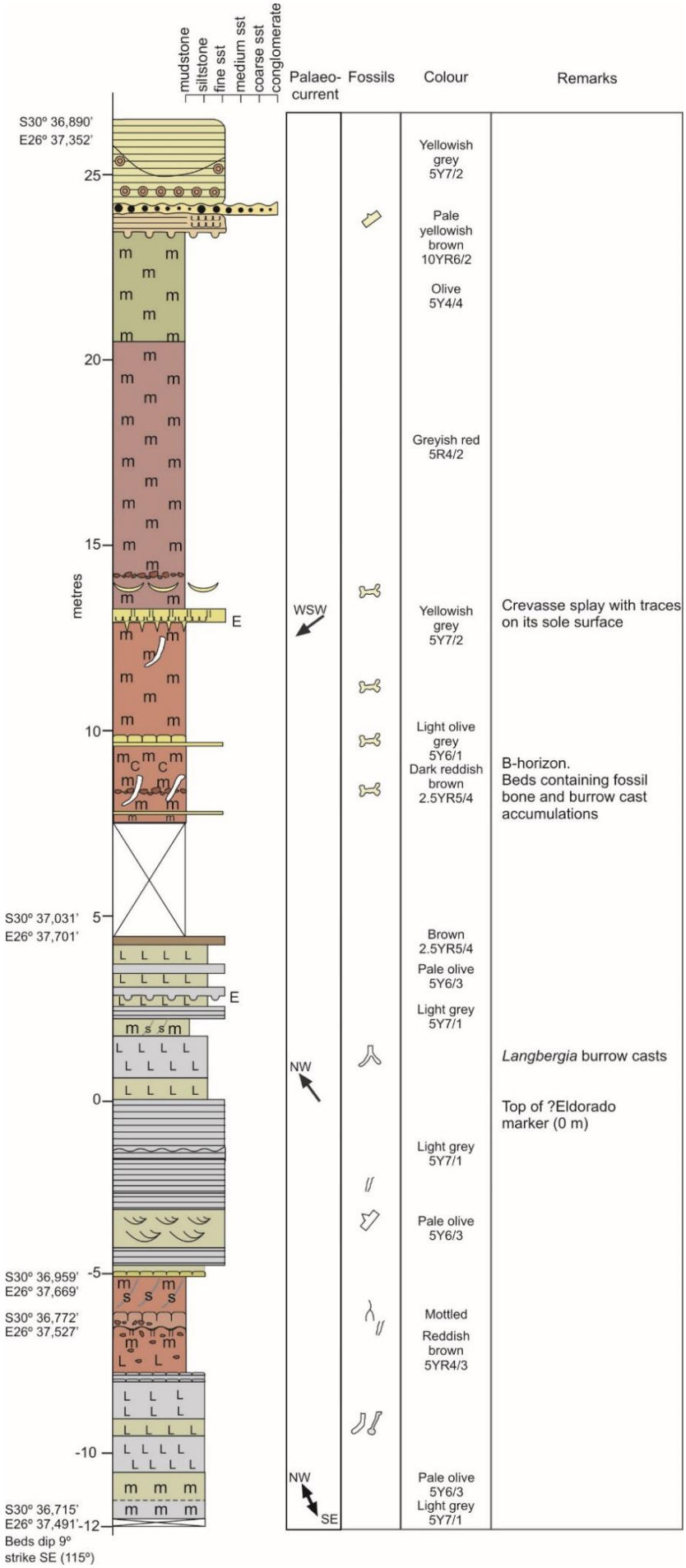
A.2 Lithostratigraphic log




mudstone
siltstone
fine sst
medium sst
coarse sst
conglomerate
Palaeo-current
Fossils
Colour
Remarks
130
125
120
115
110
105
100
95
E
NNE
NNE
E
E
m
L
Dusky red 5R3/4
Dusky red 5R3/4
Light grey N7
Dusky red 5R3/4
Undulating surface
Siltstone with mottled red mudstone
Dusky red 5R3/4
Undulating surface
Conglomerate sheet flood deposits
4 sets rcb
4 sets rcb
Crevasse splay (2 sets)
Olive grey 5Y4/1
Yellow 5Y6/4
Infraformational/claystone bone conglomerate
Olive grey 5Y4/1
Yellow 5Y6/4
Dispersed termnospondyl bone conglomerate
Dusky red 5R3/4
Yellow 5Y6/4
Lateral accretion (dip10°)
Basal clay conglomerate with scattered termnospondyl dermal bones in deep scours
Light grey N7
Light grey N7
Greyish olive 10Y4/2
Dusky red 5R3/4
Greyish red 5R4/2
Crevasse splay upward thinning cycle
Medium grey N5
Reddish brown 10R4/3
Medium grey N5
Clay pellet/fishhash (disseminated) scales and bones
Thinning upward sst/siltstone cycle


mudstone
siltstone
fine sst
medium sst
coarse sst
conglomerate
Palaeo-current
Fossils
Colour
Remarks
95
90
85
80
75
70
65
60
Dusky red 5R3/4
Thinning upward sst cycle
Diademodon skull (L19-32)
Fining upward, sharp base
Diademodon skull (L19-33)
Olive 5Y5/4
Olive 5Y5/4
Thin lenticular sst lenses alternating with mudstone
Olive 5Y5/4
Fine sst lenses (3 stacked)
Mudstone to sst crevasse splay
Dusky red 5R3/4
Medium grey N5
Erythrosuchus jaw
Desiccation fissures
Red 5R3/4
Olive grey 5Y4/1
Dusky red 5R3/4
Greyish green 5G5/2
Green 5GY3/2
Greyish green 5G5/2


mudstone
siltstone
fine sst
medium sst
coarse sst
conglomerate
Palaeo-current
Fossils
Colour
Remarks
60
55
50
45
40
35
30
25
S30° 36,739'
E26° 37,302'
NNW
E
Olive green 5GY3/2
Mudrock pebbles
Olive 5Y5/4
Sst swells and pinches over ± 30 m
Olive 5Y5/4
Olive/weak red
Mottled Crevasse splay
Olive 5Y5/4
Crevasse splay
Olive grey 5Y4/1
Point bar
Olive grey 5Y4/1
Dusky red 5R3/4
7.5Y6/2 Olive grey
Crevasse splay
Dusky red 5R3/4
Start of section2, correlates with top of hill in section 1


mudstone
siltstone
fine sst
medium sst
coarse sst
conglomerate
Palaeo-current
Fossils
Colour
Remarks
S30° 36,890'
E26° 37,352'
25
20
15
10
5
0
-5
-10
-12
metres
E
E
WSW
NW
NW
SE
Yellowish grey 5Y7/2
Pale yellowish brown 10YR6/2
Olive 5Y4/4
Greyish red 5R4/2
Yellowish grey 5Y7/2
Crevasse splay with traces on its sole surface
Light olive grey 5Y6/1
Dark reddish brown 2.5YR5/4
B-horizon.
Beds containing fossil bone and burrow cast accumulations
S30° 37,031'
E26° 37,701'
Brown 2.5YR5/4
Pale olive 5Y6/3
Light grey 5Y7/1
Langbergia burrow casts
Top of ?Eldorado marker (0 m)
Light grey 5Y7/1
Pale olive 5Y6/3
S30° 36,959'
E26° 37,669'
S30° 36,772'
E26° 37,527'
Mottled
Reddish brown 5YR4/3
S30° 36,715'
E26° 37,491'
Beds dip 9°
strike SE (115°)
Pale olive 5Y6/3
Light grey 5Y7/1

APPENDIX B: TETRAPOD FOSSIL DATABASE

Accession Number	Field Number	Genus	Species	Description	Collector Surname	Collector Name	Date Collected	Latitude	Longitude	Preparation
	L19-10	?Cynodont	indet.	Skull with articulated lower jaw	Browning	Claire	01/04/2019	-30,613013	26,622696	Unprepared
	L19-13	?Cynodont	indet.	Post-crania	Wolvaardt	Frederik	01/04/2019	-30,612817	26,62285	Unprepared
	L19-16	?Cynodont	indet.	Small skull encased in nodule	Smith	Roger	01/04/2020	-30,612700	26,622800	Unprepared
	L19-37	?Cynodont	indet.	Vertebra plus two skulls	Browning	Claire	04/04/2019	-30,611750	26,622317	Unprepared
	L19-45	?Cynodont	indet.	Post-crania	Wolvaardt	Frederik	02/04/2019	-30,612817	26,622850	Unprepared
	L20-01	?Cynodont	indet.	Skull	Browning	Claire	08/09/2020	-30,612800	26,622733	Unprepared
	L20-14	?Pocolophonid	indet.	Skull encased in nodule	Browning	Claire	11/09/2020	-30,612250	26,622533	Unprepared
	L19-38	?Procolophind	indet.	Skull	Wolvaardt	Frederik	02/04/2019	-30,612817	26,622850	Unprepared
	L19-39	?Procolophind	indet.	Skull	Wolvaardt	Frederik	02/04/2019	-30,612817	26,622850	Unprepared
	L19-40	?Procolophind	indet.	Skull	Wolvaardt	Frederik	02/04/2019	-30,612817	26,622850	Unprepared
	L19-41	?Procolophind	indet.	Snout	Wolvaardt	Frederik	02/04/2019	-30,612817	26,622850	Unprepared
SAM-PK-K10184	128	?Procolophonid	indet.	Possible skull with articulated skeleton	Wolvaardt	Frederik	16/06/2003	-30,612917	26,622817	Unprepared
	L19-03	?Procolophonid	indet.	Post-crania	Smith	Roger	01/04/2019	-30,612967	26,622667	Unprepared
	L19-07	?Procolophonid	indet.	Post-crania	Browning	Claire	01/04/2019	-30,612967	26,622667	Unprepared
	L19-08	?Procolophonid	indet.	Post-crania	Browning	Claire	01/04/2019	-30,612967	26,622667	Unprepared
	L19-09	?Procolophonid	indet.	Post-crania	Browning	Claire	01/04/2019	-30,612967	26,622667	Unprepared
	L19-12	?Procolophonid	indet.	Skull with articulated lower jaw	Browning	Claire	02/04/2019	-30,612800	26,622733	Unprepared
	L20-08	?Temnospondyl	indet.	Skull and lower jaw	Smith	Roger	10/09/2020	-30,612933	26,622950	Unprepared

Accession Number	Field Number	Genus	Species	Description	Collector Surname	Collector Name	Date Collected	Latitude	Longitude	Preparation
SAM-PK-K10181	125	Archosauriform	indet.	Possible vertebra	Wolvaardt	Frederik	16/06/2003	-30,612917	26,622817	Unprepared
	L20-12	*Cricodon*	*kannemeyeri*	Small skull with articulated lower jaw	Wolvaardt	Frederik	11/09/2020	-30,612167	26,622483	Partially prepared
SAM-PK-K10179	123	Cynodont	sp.	Skull with possible lower jaw	Wolvaardt	Frederik	16/06/2003	-30,613010	26,622693	Unprepared
SAM-PK-K10187	129	Cynodont	sp.	Skull with lower jaw	Stummer	Hedi	16/06/2003	-30,612700	26,622800	Unprepared
SAM-PK-K10200		Cynodont	sp.	Internal casts of palate	Smith	Roger	16/06/2003	-30,612950	26,622917	Unprepared
SAM-PK-K10219	86	Cynodont	sp.	Partial skull - coronoid process	Wolvaardt	Frederik	00/12/2000	-30,614826	26,621862	Unprepared
	L19-14	Cynodont	sp.	Large block with skull and skeleton	Wolvaardt	Frederik	02/04/2020	-30,612700	26,622800	Unprepared
	L19-20	Cynodont	sp.	Partial skull with lower jaw	Wolvaardt	Frederik	01/04/2019	-30,612317	26,622583	Unprepared
	L19-32	Cynodont	sp.	Large skull ?*Diademodon*	Smith	Roger	30/03/2019	-30,603567	26,620400	Unprepared
	L19-44	Cynodont	sp.	Partial skull with lower jaw	Browning	Claire	02/04/2019	-30,612817	26,622850	Unprepared
	L19-15	Cynodont	sp.	Skull in nodule	Smith	Roger	01/04/2019	-30,612700	26,622800	Unprepared
	L19-33	*Diademodon*	sp.	Skull without lower jaw	Browning	Claire	03/04/2019	-30,602333	26,620233	Partially Prepared
SAM-PK-K10159	85	*Eohyosaurus*	*wolvaardti*	Holotype - Skull with lower jaw	Wolvaardt	Frederik	00/12/2000	-30,612899	26,622750	Partially Prepared
SAM-PK-K10180	124	*Eohyosaurus*	*wolvaardti*	Skull with lower jaw and manus	Wolvaardt	Frederik	16/06/2003	-30,612850	26,622800	Fully prepared and CT scanned
	L20-15	*Erythrosuchus*	sp.	Lower jaw fragment with teeth	Hancox	John	02/04/2019	-30,604229	26,620030	Unprepared
	L20-11	Indet.	indet.	Accumulation of small bones in	Smith	Roger	11/9/2020	-30,612150	26,622183	Unprepared

Accession Number	Field Number	Genus	Species	Description	Collector Surname	Collector Name	Date Collected	Latitude	Longitude	Preparation
				possible burrow terminus						
	L19-48	Indet.	sp.	Very small skull snout with lower jaw	Browning	Claire	04/04/2019	-30,612850	26,622800	Unprepared
	L19-49	Indet.	sp.	Nodule with postcrania showing fine ribs	Browning	Claire	04/04/2019	-30,612850	26,622800	Unprepared
	L19-19	*Lumkuia*	*fuzzi*	Skull with articulated lower jaw	Schneiderhan	Eva	01/04/2019	-30,612383	26,622600	Prepared
SAM-PK-K10160	95	*Microgomphodon*	*oligocynus*	Skull with lower jaw	Wolvaardt	Frederik	00/12/2000	-30,611580	26,622517	Fully Prepared
SAM-PK-K011601	L18-6	*Microgomphodon*	*oligocynus*	Complete articulated skeleton and skull	Wolvaardt	Frederik	10/07/2018	-30,612899	26,622748	Skull prepared
	L20-03	*Microgomphodon*	*oligocynus*	Snout of skull in nodule	Smith	Roger	10/09/2020	-30,612899	26,622749	Unprepared
NMQR-03671	JB080843	Procolophonid	sp.	Small skull	Botha	Jennifer	23/08/2008	-30,612783	26,622883	
NMQR-03667	JB080839	Procolophonid	sp.	Skull in situ	Botha	Jennifer	23/08/2008	-30,612783	26,622883	
NMQR-03669	JB080841	Procolophonid	sp.	Back of skull	Botha	Jennifer	23/08/2018	-30,612783	26,622883	
SAM-PK-K10156	82	Procolophonid	sp.	Skull with lower jaw	Wolvaardt	Frederik	00/12/2000	-30,612900	26,622749	Slightly Prepared
SAM-PK-K10167	103	Procolophonid	sp.	Skull	Wolvaardt	Frederik	00/12/2000	-30,612219	26,622391	Unprepared
SAM-PK-K10169	107	Procolophonid	sp.	Anterior skull and lower jaw	Wolvaardt	Frederik	24/10/2002	-30,612189	26,621979	Partially Prepared
SAM-PK-K10170	108	Procolophonid	sp.	Snout?	Wolvaardt	Frederik	24/10/2002	-30,612178	26,621977	Unprepared
SAM-PK-K10171	110	Procolophonid	sp.	Skull with lower jaw	Wolvaardt	Frederik	16/06/2003	-30,614216	26,622121	Unprepared
SAM-PK-K10173	116	Procolophonid	sp.	Skull with lower jaw	Smith	Roger	16/06/2003	-30,614200	26,622524	Partially Prepared

Accession Number	Field Number	Genus	Species	Description	Collector Surname	Collector Name	Date Collected	Latitude	Longitude	Preparation
SAM-PK-K10175	118	Procolophonid	sp.	Skull with lower jaw	Stummer	Hedi	16/06/2003	-30,614315	26,622971	Unprepared
SAM-PK-K10177	121	Procolophonid	sp.	Skull with possible lower jaw	Wolvaardt	Frederik	16/06/2003	-30,612901	26,622749	Unprepared
SAM-PK-K10182	126	Procolophonid	sp.	Skull with lower jaw	Wolvaardt	Frederik	16/06/2003	-30,612917	26,622817	Unprepared
SAM-PK-K10188	130	Procolophonid	sp.	Skull with lower jaw	Wolvaardt	Frederik	16/06/2003	-30,612700	26,622800	Unprepared
SAM-PK-K10189	131	Procolophonid	sp.	Skull with lower jaw	Wolvaardt	Frederik	16/06/2003	-30,615437	26,622767	Partially Prepared
SAM-PK-K10190	132	Procolophonid	sp.	Skull with lower jaw	Stummer	Hedi	16/06/2003	-30,612783	26,622883	Partially Prepared
SAM-PK-K10192	134	Procolophonid	sp.	Skull with lower jaw	Wolvaardt	Frederik	16/06/2003	-30,612700	26,622800	Unprepared
SAM-PK-K10193	135	Procolophonid	sp.	Skull with lower jaw	Stummer	Hedi	16/06/2003	-30,612917	26,622800	Partially Prepared
SAM-PK-K10194	136	Procolophonid	sp.	Skull with lower jaw	Wolvaardt	Frederik	16/06/2003	-30,612917	26,622817	Partially Prepared
SAM-PK-K10195	137	Procolophonid	sp.	Skull with lower jaw	Wolvaardt	Frederik	16/06/2003	-30,612767	26,622767	Partially Prepared
SAM-PK-K10196	138	Procolophonid	sp.	Skull	Smith	Roger	16/06/2003	-30,613017	26,622900	Unprepared
SAM-PK-K10197	139	Procolophonid	sp.	Skull with horns	Stummer	Hedi	16/06/2003	-30,612950	26,622833	Unprepared
SAM-PK-K10198	141	Procolophonid	sp.	Skull with lower jaw	Wolvaardt	Frederik	16/06/2003	-30,612917	26,622817	Slightly Prepared
SAM-PK-K10199	142	Procolophonid	sp.	Skull with lower jaw	Wolvaardt	Frederik	16/06/2003	-30,612917	26,622900	Slightly Prepared
SAM-PK-K10201	122	Procolophonid	sp.	Skull with lower jaw	Smith	Roger	16/06/2003	-30,613016	26,622690	Partially Prepared
SAM-PK-K10202	122	Procolophonid	sp.	Skull with lower jaw	Smith	Roger	16/06/2003	-30,613019	26,622693	Partially Prepared
SAM-PK-K10203	122	Procolophonid	sp.	Skull with possible lower jaw	Smith	Roger	16/06/2003	-30,613016	26,622693	Unprepared
SAM-PK-K10204	122	Procolophonid	sp.	Post crania	Smith	Roger	16/06/2003	-30,613013	26,622693	Partially Prepared
SAM-PK-K10205	122	Procolophonid	sp.	Nodule with bone	Smith	Roger	16/06/2003	-30,613013	26,622693	Unprepared

Accession Number	Field Number	Genus	Species	Description	Collector Surname	Collector Name	Date Collected	Latitude	Longitude	Preparation
SAM-PK-K10206	122	Procolophonid	sp.	Nodule with bone	Smith	Roger	16/06/2003	-30,613013	26,622693	Unprepared
SAM-PK-K10208	122	Procolophonid	sp.	Nodule with bone	Smith	Roger	16/06/2003	-30,613016	26,622693	Unprepared
SAM-PK-K10209	122	Procolophonid	sp.	Skull with lower jaw	Smith	Roger	16/06/2003	-30,613013	26,622693	Unprepared
SAM-PK-K10210	122	Procolophonid	sp.	Skull with lower jaw	Smith	Roger	16/06/2003	-30,613013	26,622693	Partially Prepared
SAM-PK-K10211	122	Procolophonid	sp.	Post crania	Smith	Roger	16/06/2003	-30,613016	26,622696	Partially Prepared
SAM-PK-K10212	122	Procolophonid	sp.	Skull with lower jaw	Smith	Roger	16/06/2003	-30,612667	26,622683	Partially Prepared
SAM-PK-K10213	122	Procolophonid	sp.	Nodule with bone	Smith	Roger	16/06/2003	-30,613016	26,622696	Unprepared
SAM-PK-K10214	122	Procolophonid	sp.	Partial skull	Smith	Roger	16/06/2003	-30,613013	26,622693	Unprepared
	L18-3	Procolophonid	sp.	Small skull with articulated lower jaw and some post-crania	Wolvaardt	Frederik	10/07/2018	-30,614563	26,622987	Unprepared
	L18-5	Procolophonid	sp.	Small skull with articulated lower jaw and possible post crania	Wolvaardt	Frederik	10/07/2018	-30,612932	26,622748	Partially prepared
	L19-02	Procolophonid	sp.	Skull with articulated lower jaw	Browning	Claire	01/04/2019	-30,612967	26,622667	Unprepared
	L19-04	Procolophonid	sp.	Skull with articulated lower jaw	Browning	Claire	02/04/2019	-30,612967	26,622667	Unprepared
	L19-05	Procolophonid	sp.	Skull with articulated lower jaw	Browning	Claire	02/04/2019	-30,612967	26,622667	Unprepared
	L19-06	Procolophonid	sp.	Skull with articulated lower jaw	Browning	Claire	01/04/2019	-30,612967	26,622667	Unprepared

Accession Number	Field Number	Genus	Species	Description	Collector Surname	Collector Name	Date Collected	Latitude	Longitude	Preparation
	L19-11	Procolophonid	sp.	Small skull with articulated lower jaw	Wolvaardt	Frederik	02/04/2019	-30,612932	26,622702	Unprepared
	L19-18	Procolophonid	sp.	Skull	Smith	Roger	01/04/2019	-30,612600	26,622650	Unprepared
	L19-23	Procolophonid	sp.	Skull with curled up skeleton (3D) (?*Teratophon*) (previously L19-23A)	Wolvaardt	Frederik	01/04/2019	-30,612933	26,622950	Unprepared
	L19-24	Procolophonid	sp.	Small skull				-30,613017	26,622967	Unprepared
	L19-25	Procolophonid	sp.	Small skull	Hancox	John	02/04/2019	-30,613017	26,622900	Unprepared
	L19-26	Procolophonid	sp.	Skull with lower jaw	Wolvaardt	Frederik	02/04/2019	-30,613017	26,622900	Unprepared
	L19-27	Procolophonid	sp.	Small curled up skeleton (possibly no skull)	Woods	Ian	02/04/2019	-30,613000	26,622883	Partially Prepared
	L19-30	Procolophonid	sp.	Skull with lower jaw	Wolvaardt	Frederik	02/04/2019	-30,612100	26,621683	Unprepared
	L19-36	Procolophonid	sp.	Complete skull with lower jaw	Hancox	John	04/04/2019	-30,611750	26,622317	Unprepared
	L19-42	Procolophonid	sp.	Skull (same locality as L19-45)	Wolvaardt	Frederik	02/04/2019	-30,612817	26,622850	Unprepared
	L19-43	Procolophonid	sp.	Skull (snout only) (same locality as L19-45)	Wolvaardt	Frederik	02/04/2019	-30,612817	26,622850	Unprepared
	L20-02	Procolophonid	sp.	Spiralled skeleton in nodule (?*Teratophon*)	Smith	Roger	08/09/2020	-30,612931	26,622747	Unprepared
	L20-04	Procolophonid	sp.	Skull and skeleton in nodule	Wolvaardt	Frederik	09/09/2020	-30,612917	26,622983	Unprepared

Accession Number	Field Number	Genus	Species	Description	Collector Surname	Collector Name	Date Collected	Latitude	Longitude	Preparation
	L20-05	Procolophonid	sp.	Skull completely encased in nodule (?*Teratophon*)	Browning	Claire	10/09/2020	-30,612833	26,623033	Unprepared
	L20-06	Procolophonid	sp.	Skull completely encased in nodule (?*Teratophon*)	Wolvaardt	Frederik	10/09/2020	-30,612783	26,623033	Unprepared
	L20-07	Procolophonid	sp.	Skull and curled up skeleton in nodule (?*Teratophon*)	Wolvaardt	Frederik	10/09/2020	-30,612800	26,623017	Unprepared
	L20-09	Procolophonid	sp.	Juvenile curled up skeleton encased in nodule (?*Teratophon*)	Wolvaardt	Frederik	10/09/2020	-30,612900	26,622749	Unprepared
	L20-13	Procolophonid	sp.	Skull with lower jaw (?*Thelephon*)	Wolvaardt	Frederik	11/09/2020	-30,612167	26,622483	Unprepared
	L18-7	Procolophonid	sp.	Skull with articulated lower jaw	Wolvaardt	Frederik	10/07/2018	-30,612900	26,622748	Unprepared
	L18-8	Procolophonid	sp.	Skull with articulated lower jaw	Wolvaardt	Frederik	10/07/2018	-30,612900	26,622748	Partially Prepared
	L18-9	Procolophonid	sp.	Several badly weathered partial skulls	Wolvaardt	Frederik	10/07/2028	-30,612900	26,622748	Unprepared
	L19-34	Procolophonid	sp.	Small skull without lower jaw	Browning	Claire	04/04/2019	-30,612850	26,622800	Unprepared
	L19-46	Procolophonid	sp.	Skull with lower jaw	Wolvaardt	Frederik	01/04/2019	-30,612783	26,622883	Unprepared
	L19-47	Procolophonid	sp.	Small skull without lower jaw	Browning	Claire	04/04/2019	-30,612850	26,622800	Unprepared

Accession Number	Field Number	Genus	Species	Description	Collector Surname	Collector Name	Date Collected	Latitude	Longitude	Preparation
	L19-31	Temnospondyl	sp.	Bone fragments in basal conglomerate, with tiny phalanx	Smith	Roger	31/03/2019	-30,603700	26,619100	Unprepared
BP/1/4299		*Teratophon*	*spinigenis*	Holotype - Very large skull without lower jaw	Kitching	James	00/07/1973	30.6	26.6	Fully prepared
BP/1/4300		*Teratophon*	*spinigenis*	Paratype - Very large skull	Kitching	James	00/07/1973	30.6	26.6	Fully prepared
BP/1/4587		*Teratophon*	*spinigenis*	Paratype - Large almost complete skull with well-developed cheek spines	Kitching	James	00/01/1976	30.6	26.6	Fully prepared
BP/1/4588		*Teratophon*	*spinigenis*	Paratype - Large almost complete skull with well-developed cheek spines	Kitching	James	00/01/1976	30.6	26.6	Fully prepared
SAM-PK-K10174	117	*Teratophon*	*spinigenis*	Skull with lower jaw	Smith	Roger	16/06/2003	-30,614178	26,622222	Fully Prepared
SAM-PK-K10183	127	*Teratophon*	*spinigenis*	Skull with possible lower jaw	Wolvaardt	Frederik	16/06/2003	-30,613000	26,622883	Partially Prepared
	L18-1	*Teratophon*	*spinigenis*	Skull without lower jaw		Frederik		-30,614200	26,622168	Partially prepared
SAM-PK-K011599	L18-2	*Teratophon*	*spinigenis*	Two curled up articulated skeletons in the same nodule	Wolvaardt	Frederik	10/07/2018	-30,614246	26,622363	Partially prepared
	L18-4	*Teratophon*	*spinigenis*	Large skull without lower jaw. Palate detail visible.	Wolvaardt	Frederik	10/07/2018	-30,614207	26,622743	Fully prepared

Accession Number	Field Number	Genus	Species	Description	Collector Surname	Collector Name	Date Collected	Latitude	Longitude	Preparation
	L19-01	*Teratophon*	*spinigenis*	Left mandible	Smith	Roger	31/3/9019	-30,614183	26,622167	Prepared
	L19-21	*Teratophon*	*spinigenis*	Skull with partial skeleton and manus	Wolvaardt	Frederik	01/04/2019	-30,612900	26,623017	Prepared
	L19-22	*Teratophon*	*spinigenis*	Small partial skull with skeleton in nodule with knobby surface	Wolvaardt/ Smith	Frederik/R oger	02/04/2019	-30,612850	26,623083	Partially Prepared
	L20-10	*Teratophon*	*spinigenis*	Large skull with articulated skeleton	Wolvaardt	Frederik	10/09/2020	-30,614200	26,622133	Unprepared
	L19-50	*Teratophon*	*spinigenis*	Skull with curled up skeleton (3D)	Wolvaardt	Frederik	01/04/2019	-30,612933	26,622950	Prepared
SAM-PK-K10162	97	*Thelephon*	*contritus*	Skull with lower jaw	Wolvaardt	Frederik	00/12/2000	-30,611580	26,622524	Partially Prepared
SAM-PK-K10168	106	*Thelephon*	*contritus*	Skull with lower jaw	Wolvaardt	Frederik	24/10/2002	-30,611704	26,622035	Partially Prepared
SAM-PK-K10172	115	*Thelephon*	*contritus*	Skull with lower jaw	Wolvaardt	Frederik	16/06/2003	-30,612800	26,622733	Prepared
SAM-PK-K10215	122	*Thelephon*	*contritus*	Skull with lower jaw	Smith	Roger	16/06/2003	-30,613013	26,622693	Partially Prepared
	L19-28	*Thelephon*	*contritus*	Skull with articulated lower jaw	Wolvaardt	Frederik	02/04/2019	-30,612950	26,622833	Partially prepared
	L19-29	*Thelephon*	*contritus*	Skull with articulated lower jaw	Wolvaardt	Frederik	02/04/2019	-30,612100	26,621683	Unprepared
SAM-PK-K10157	83	*Trirachodon*	sp.	Skull with lower jaw	Wolvaardt	Frederik	00/12/2000	-30,612901	26,622750	Partially Prepared
SAM-PK-K10158	84	*Trirachodon*	sp.	Skull	Wolvaardt	Frederik	00/12/2000	-30,612901	26,622750	Partially Prepared
SAM-PK-K10161	96	*Trirachodon*	sp.	Skull with lower jaw	Wolvaardt	Frederik	00/12/2000	-30,611580	26,622531	Nearly Fully Prepared
SAM-PK-K10163	98	*Trirachodon*	sp.	Skull	Wolvaardt	Frederik	00/12/2000	-30,612248	26,622325	Partially Prepared
SAM-PK-K10164	99	*Trirachodon*	sp.	Skull	Wolvaardt	Frederik	00/12/2000	-30,618056	26,623250	Unprepared

Accession Number	Field Number	Genus	Species	Description	Collector Surname	Collector Name	Date Collected	Latitude	Longitude	Preparation
SAM-PK-K10165	100	*Trirachodon*	sp.	Skull	Wolvaardt	Frederik	00/12/2000	-30,618056	26,623250	Unprepared
SAM-PK-K10166	101 (&102)	*Trirachodon*	sp.	Skull	Wolvaardt	Frederik	00/12/2000	-30,613461	26,622223	Unprepared
SAM-PK-K10176	120	*Trirachodon*	sp.	Skull with lower jaw	Wolvaardt	Frederik	16/06/2003	-30,612900	26,622748	Partially Prepared
SAM-PK-K10207	122	*Trirachodon*	sp.	Skull with lower jaw	Smith	Roger	16/06/2003	-30,613016	26,622696	Partially Prepared
SAM-PK-K10411	107	*Trirachodon*	sp.	Lower jaw fragment with teeth	Wolvaardt	Frederik	24/10/2002	-30,612174	26,621969	Unprepared
SAM-PK-K10762	L1	*Trirachodon*	sp.	Skull with lower jaw	Wolvaardt	Frederik	09/03/2008	-30,612222	26,622472	Partially Prepared
	L19-17	*Trirachodon*	*berryi*	Skull with articulated lower jaw and manus	Smith	Roger	01/04/2019	-30,612667	26,622683	Partially Prepared
	L19-35	*Trirachodon*	sp.	Weathered skull with partial lower jaw	Woods	Ian	04/04/2019	-30,611750	26,622317	Unprepared
SAM-PK-K10191	133	Tetrapod	indet.	Skull with lower jaw	Smith	Roger	16/06/2003	-30,613017	26,622900	Unprepared

APPENDIX C: BURROW CAST DATA

Field ID	Horizontal Diameter (cm)	Vertical Diameter (cm)	Aspect Ratio	Height of Central Ventral Ridge (cm)	Ramp Angle (Degrees)	Cross Sectional Shape	Latitude	Longitude	Comment
B19-1	8,0	3,5	2,3	0,3	17	Reniform	-30,614133	26,622400	Burrow cast starts above calcareous nodular horizon and terminates in a sandy silt stone bedding plain below this horizon. Flattened terminal chambre present. Collected and Picture taken. Exposed true length 55.5 cm. Straight length 50cm. Sinuosity index 1.11.
B19-2	6,5	4,0	1,6	1,5	28	Reniform	-30,614283	26,621933	Sample collected; photo taken.
B19-3	6,0	3,0	2,0	1,0	35	Reniform	-30,614200	26,622367	Sample collected; photo taken.
B19-5	6,0	3,5	1,7	0,5	23	Reniform	-30,614167	26,622167	Burrow cast originates above calcareous nodular horizon. Intersected from above by smaller diameter round burrow. Collected and picture taken. Exposed true length 56 cm. Straight length 54 cm. Sinuosity index 1.04.
B19-6	6,0	3,4	1,8	0,4	24	Reniform	-30,614167	26,622167	Picture taken, not collected.
B19-4	2,5	2,5	1,0		32	Circular	-30,614133	26,622217	Burrow terminates in sheet sandstone above calcareous nodular horizon. Sample collected; photo taken.
B19-7-1	5,8	4,0	1,5		25	Sub-circular	-30,612183	26,622017	Cluster of three burrows in northern erosion gully. Sample from main burrow collected and photo taken. B19-7-1/2/3 all have a local enlargement chamber at the same stratigraphic level at the top of the exposed burrow.
B19-7-2	6,9	6,5	1,1		25	Sub-circular	-30,612183	26,622017	Photo taken, collected. Enlargement chamber horizontal diameter = 7.5 cm, vertical diameter = 6.1 cm.
B19-7-3	6,0	4,0	1,5		25	Sub-circular	-30,612183	26,622017	Photo taken.
B19-8	3,0	2,2	1,4		22	Sub-circular	-30,611383	26,621817	Photo taken.
B19-9	4,0	2,7	1,5		35	Sub-circular	-30,611517	26,622017	Collected; photo taken.